PROJECT CARDINAL

The detailed design of the Mars lander for a Mars 2030 settlement mission



Final Report

July 3, 2018

by

Kathleen Blyth	4446526
Allard de Boeij	4490142
Kevin Eppenga	4370996
Eoghan Gilleran	4443101
Lina Hosking	4429680
James Murdza	4467558
Tim Nachtergaele	4291662
Slaven Stoyanov	4430964
Domas Syaifoel	4436024
Michael Westheim	4355636

Tutor: Coaches:

Dr. A. Cervone,
Ir. N. van Hoorn,
Ir. V. Liu

TU Delft
TU Delft, NLR
TU Delft

TUDelft

Contents

No	omenclature	vi		5.7 Thermal	. 91
1	Executive Overview	1		5.8 Attitude Determination and Control $$. $$.	. 94
_		_		5.9 Navigation and Guidance Systems	. 96
2	Introduction	5		5.10 Hardware Block Diagrams	. 98
3	Project Overview	6		5.11 Embarkment and Disembarkment	. 104
	3.1 Project Description	6		5.12 Iteration, Safety Factors and Margins	. 105
	3.2 Trade-Off Summary for MEV Subsystems	8		5.13 General Approach to Sensitivity Analysis $$.	. 106
	3.3 Preliminary Design of Mission Vehicles	11		5.14 Contingency Management	. 106
	3.4 Functional Analysis	13	6	Design Overview	107
	3.5 Operations and Logistics	17		6.1 Configuration & Layout	. 107
	3.6 Market Analysis	18		6.2 System Characteristics	. 109
4	Project Management	22		6.3 RAMS Analysis	. 112
	4.1 Resource Budgets	22		6.4 Compliance Matrix	. 116
	4.2 Cost Breakdown	24	7	Post-DSE Activities	125
	4.3 Technical Risk Assessment	27		7.1 Project Design and Development Logic	. 125
	4.4 Verification and Validation Procedures	30		7.2 Project Gantt Chart	
	4.5 Sustainable Development Strategy	32		7.3 Production Plan	
5	Subsystem Design	35		7.4 Verification and Validation Procedures	. 132
	5.1 Propulsion	35	8	Conclusions and Recommendations	133
	5.2 Astrodynamics, Aerodynamics & Control	45		8.1 Conclusions	. 133
	5.3 Structures	68		8.2 Recommendations	
	5.4 Life Support	83	ъ.		136
	5.5 Communications	85	Вi	Bibliography	
	5.6 Power	87	Α	Requirements	137

Nomenclature

List	of Abbreviations	LMO	Low Mars Orbit
$ar{G}$	No Go	LOX	Liquid Oxygen
ADCS	Attitude Determination and Control System	LSS	Life Support System
ATV	Automated Transfer Vehicle	MCF	Mars Centred Inertial reference frame
BFR	Big Falcon Rocket	MEK	Mars Expeditionary Complex
C/N	Signal to Noise ratio	MEV	Mars Excursion Vehicle
CFRP	Carbon Fibre Reinforced Polymer	MIU	Mission Interface Unit
CMG	Control Moment Gyro	MLI	Multi Layer Insulation
\mathbf{CO}_2	Carbon dioxide	MMH/N	NTO Hydrazine
CVRs	Conservative voltage reducers	MOI	Moment Of Inertia
DARE	Delft Aerospace Rocket Engineering	MRO	Mars Reconnaissance Orbiter
	Dry Heat Microbial Reduction	N_2	Nitrogen
DHS	Data Handling and Control	NASA	National Aeronautics and Space Administration
DSE	Design Syntheses Exercise	NTR	Nuclear Thermal Rocket
DSN	Deep Space Network	\mathbf{o}_2	Dioxygen
DSPS	Deep Space Positioning Network	PMSE	Project Management and Systems Engineering
EEV	Earth Excursion Vehicle	R&D	Research and Development
EI	Entry Interface	RAMS	Reliability, Availability, Maintainability and Safety
ESA	European Space Agency	RCS RP-1	Reaction Control System
EUR	Euro	RTG	Rocket propellant 1
EVA	Extra Vehicular Activity		Radioisotope Thermoelectric Generator Sparse Nonlinear Optimiser
FBS	Functional Breakdown Structure	STA	Shuttle Training Aircraft
FFD	Functional Flow Diagram	SWOT	Strengths, Weaknesses, Opportunities, and Threats
GCH ₄	Gaseous Methane	TPS	Thermal Protection System
GDP	Gross Domestic Product	TRL	Technology Readiness Level
GNC	Guidance Navigation and Control	TT&C	Telemetry, Tracking, and Command
GOX	Gaseous oxygen	TWTA	Travelling Wave Tube Amplifier
GVA	Gross Value Added	USD	United States Dollar
G	Go	V&V	Verification and Validation
\mathbf{H}_2	Dihydrogen	VHP	Vapour Hydrogen Peroxide
IBDM	International Berthing and Docking Mechanism	More	on eletrone
ISO	International Organisation for Standardisation		enclature
ISRO	Indian Space Research Organisation	α	Absorbtivity[-]
ISRU	In Situ Resource Utilisation	α	Conical expansion angle
ISS	International Space Station	β	Ballistic coefficient [-]
ITV	Interplanetary Transfer Vehicle	β Λ ₹,	Contraction angle
JAXA	Japan Aerospace Exploration Agency	$\Delta \vec{x}_1$ $\Delta \vec{x}_2$	Final impulse burn [km/s]
LCH ₄	Liquid Methane	Δx_2 ΔT	Temperature difference [K]
LEO	Low Earth Orbit	Δt	Time interval [s]
LH ₂	Liquid Hydrogen	ΔV	Velocity increment
L11 2	inquia riyurogon	△ v	velocity increment[III/8]

CONTENTS iv

ΔV_{inc1}	ΔV for dog-leg manoeuvre [km/s]	θ_e	Wall angle exit [deg]
ΔV_{inc2}	ΔV to perform inclination change 2 at Earth [km/s]	θ_p	Wall angle[deg]
ΔV_{inc}	Velocity increment of plane change $[m/s]$	\vec{v}_1	Velocity of the vehicle at the initial orbit [km/s]
ΔV_{tot}	Total ΔV impulsive burn [km/s]	\vec{v}_2	Velocity of the vehicle at the final orbit [km/s]
ϵ	Emessivity	\vec{v}_{1-2}	Velocity of the vehicle at the beginning of the chase
ϵ	Expansion ratio		manoeuvre[m/s]
ϵ_c	$Contraction\ ratio \ $	\vec{v}_{2-2}	Velocity vector at the end of the chase manoeuvre [m/s]
η_{amp}	$Amplifier \ efficiency \ \dots \qquad [-]$	A	Area
η_{en}	Total engine efficiency	A	MEV effective surface area [m ²]
Γ	Ratio of specific heat capacities	A^*	Throat area [m²]
γ	Ratio of specific heats	$A_{\mathcal{S}}$	Surface area of vehicle [m ²]
γ_{ent}	Flight path angle at entry interface[deg]	a_1	Semi-major axis initial orbit[km]
γ_e	Flight path angle at entry interface[deg]	a_1 a_2	Semi-major axis final orbit[km]
κ	Thermal conductivity [WK/m]	A_C	Chamber cross-sectional area
λ	Wave length [m]		Effective area [m²]
ř	Position state vector [km]	A_e	
$\vec{\mathbf{v}}$	Velocity state vector[km/s]	A_{ins}	Insulated area[m]
μ	Gravitational parameter [m ³ /s ²]	A_{solar}	Area of solar panel
	Dynamic viscosity	A_{sun}	Area in sunlight [m ²]
μ_{v} Φ	Landing angle [deg]	A_{total}	Total area of ship[m ²]
		B	Bandwidth[Hz]
Ψ	Angle change from initial entry to landing [deg]	B	Planet's magnetic Field[T]
ψ	Angle change of Mars in relation to the initial conditions	b	Width[m]
ψ_{qmax}	Maximum heat flux[W/m ²]	C	Bit rate[bps]
	Maximum heat flux[W/m²]	C	Entry characteristic coefficient
ψ_q		C	Speed of light[m/s]
ρ	Density Martian atmosphere at max Q[kg/m³]	c	Centroid coordinate[m]
ρ	Density of the air for Earth max Q[kg/m³]	$C_{d(f)}$	Base drag[N]
$ ho_0$	Sea level density at Mars [kg/m³]	$C_{D(fb)}$	Body drag MEV[N]
ρ_{atm}	Atmospheric density [kg/m³]	C_d	Drag coefficient[-]
ρ_{ent}	Density at entry altitude [kg/m³]	C_{eng}	Engine cost [Manyears]
$ ho_F$	Fuel density [kg/m³]	$C_{f(fb)}$	Friction coefficient MEV body[-]
ρ_{Ox}	Oxidiser density [kg/m ³]		ain Maintenance cost[USD]
σ	Maximum stress [Pa]	C_{ma}	Mission cost for the MEV [Manyears]
σ	Stefan-Boltzmann constant $[W/(m^2K)]$	C_{MEV}	MEV cost[Manyears]
σ	Stress[Pa]	c_{pa}	Centre of pressure[m]
σ_1	Hoop stress [Pa]	c_{ps}	Centre of solar pressure[m]
σ_2	Axial stress[Pa]	C_{RCS}	RCS thruster cost [Manyears]
σ_{ax}	Axial stress	C_{ref}	Refurbishment cost [Manyears]
σ_{bendir}	Bending stress[Pa]	C_{unit}	Unit production cost[Manyears]
σ_{x}	Stress along x	cg	Centre of gravity[m]
σ_{γ}	Stress along y	D D	Residual dipole of the vehicle[A m ²]
τ_{xy}	Shear stress in the x-y plane [Pa]	d	Distance between r and t
θ	Apparent sidereal time	D*	Throat diameter [m]
θ	Maximum deviation of Z- axis[deg]	d_h	Maximum body diameter [m]
θ	True anomaly defined by user	D_c	Chamber diameter [m]
θ_e	Entry true anomaly	d_d	Diameter of rocket base [m]
$\circ e$	Linu y dide diformary[-]	u_d	Diameter of focker base[III]

CONTENTS v

D_e	Exit diameter [m]	L*	Characteristic Length	[m]
E	Modulus of elasticity[Pa]	L/D	Lift over drag ratio	[-]
e_1	Eccentricity of initial orbit[-]	l_b	Length of body section	[m]
$E_{2'}$	Eccentric anomaly[deg]	L_{cc}	Length of the conical combustion chamber	[m]
e_2	Eccentricity of final orbit[-]	L_c	Crewed launch rate per year per vehicle \dots [1	/year]
e_d	Eccentricity of the de-orbit trajectory [-]	L_c	Length of boat tail	[m]
E_{req}	Energy required [Wh]	L_c	$Length\ of\ the\ cylindrical\ combustion\ chamber.$	[m]
F	Solar Constant[W/m]	l_f	Fractional length	[%]
$F_{\mathcal{S}}$	Solar radiation force[N]	l_n	Length of nose section of MEV	[m]
f_4	Cost reduction factor [-]	LTR	Total length of the MEV	[m]
•	re Dynamic pressure force[N]	M	Magnetic moment	. [Nm]
F_{rec}	Reaction force	M	Mass	[kg]
F_{SHL}	Horizontal component of the tension force, left [N]	M	Molar mass[§	ʒ/mol]
F_{SHR}	Horizontal component of the tension force, right[N]	M	Moment	. [Nm]
F_{SVL}	Vertical component of the tension force, left[N]	M	Number of signal levels	[-]
F_{SVR}	Vertical component of the tension force, right[N]	m_0	Mass of orbiting object	[kg]
	Tension force in the fabric	m_{dry}	Dry mass of the MEV	[kg]
		$M_{e2'}$	Mean anomaly	. [rad]
F_{top}	Force carried on form upper panels[N]	$m_{prop,a}$	Propellant used for ascent	[kg]
$F_{\mathcal{X}}$	Forces in x	$m_{prop,a}$	Propellant used for decent	[kg]
$F_{\mathcal{Y}}$	Forces in y	M_{rec}	Reaction moment	. [Nm]
g	Gravitational acceleration [m/s ²]	N	Noise	[dB]
g ₀	Gravitational acceleration on the surface of Earth $[m/s^2]$	n	Number of layers of insulation	
G_r	Receiver gain[dBW]	N_{v}	Number of vehicles produced	
G_t	Transmitter gain [dBW]	Na	Number of crew members on board	
G_{max}	$Maximum \ G\text{-}force \ experienced} \ \dots \ \ [m/s^2]$	O/F	Mixture ratio oxygen over fuel	
h	Angular momentum [kg rad/s]	P	Orbital period	
h	Height	p	Pressure differential	
H_0	Topographic datum line height [m]	P_r	Power received	
-	Altitude at maximum heat flux [m]	P_t	Transmission power	
Hent	Entry altitude[m]		Power for communication	
h_e	Altitude of EI	P_{crit}	Buckling force	
	Altitude of maximum G-force experienced [m]	p_{c}	Combustion chamber pressure	
h_i	Altitude of initial circular orbit	p_e	Ambient pressure	
$H_{\mathcal{S}}$	Density scale height [m]	q	Dynamic pressure	
I I	Area moment of inertia [m ⁴]	q	Reflectance factor	
i	Inclination [deg]	Q_{ins}	Heat flow through insulator	
		Q_{in}	Heat flow in to ship	
I_{circ}	Area moment of inertia circle	Q_{out}	Heat flow out of ship	
I_{rec}	Area moment of inertia rectangle [m ⁴]	R	Gas constant [J/	(kg K)]
I_{sp}	Specific impulse[s]	R	Orbital radius	
J_2	Second order zonal harmonic	r	Radius circle	
J_{sun}	Incoming radiation[W]	r	Radius ratio	
k	Boltzmann constant $[m^2 kg/(s^2 K)]$	r	Radius	
k	Stiffness	R^*	Nozzle throat radius	
L	Beam length[m]	R_e	Reynolds number	
L	Time	R_{α}	Contraction radius	[m]

CONTENTS vi

R_c	$Combustion\ chamber\ radius\ [m]$	T_c	$Combustion \ chamber \ temperature \ [K]$
r_{eq}	Equatorial radius of Mars [km]	t_{c}	$Combustion\ chamber\ wall\ thickness\\ [m]$
R_{MCF}	Mars-centred inertial reference frame	T_h	Temperature due to entry[K]
R_{MCI}	Mars-centred fixed reference frame	T_r	Thrust of the MEV
R_n	Radius of the nose[m]	T_{sp}	Torque due to solar radiation [Nm]
SNR	System to noise ratio[dB]	и	Velocity at Earth max Q
T	Mission duration [days]	V	Velocity MEV at Mars max $Q \dots [m/s]$
T	Normal operative thrust[kN]	V_1	Impulsive burn at Earth [km/s]
t	Skin thickness [m]	V_2	Impulsive burn at Mars [km/s]
t	Time	$V_{\psi_{qmax}}$	Velocity at maximum heat flux[m/s]
T_a	Aerodynamic Torque [Nm]	V_{c3}	Circular velocity[km/s]
T_g	Torque due to gravity[Nm]	$V_{\mathcal{C}}$	$Chamber \ volume \ \ [m^3]$
T_m	Magnetic torque[Nm]	V_{ent}	Atmospheric interface velocity [m/s]
$T_{\mathcal{S}}$	Noise Temp [K]	$V_{g_{max}}$	Velocity at maximum acceleration [m/s]
$t_{2'}$	Time of manoeuvre	V_{ins}	Insertion velocity [km/s]
T_2	Time of flight	x	$Distance\ between\ chosen\ axis\ system\ and\ centroid[m]$
Tana	Average temperature[K]	ν	Distance from neutral axis [m]

Executive Overview

Project Cardinal, also known as the Mars 2030 mission, aims to provide a reusable system for manned return missions to Mars. The project goal is to perform a first launch by 2030, where a crew of 10 astronauts will stay on Mars for a minimum of one month before returning to Earth. This is summarised in the Mission Need Statement.

Mission Need Statement: To provide a realistic means of transporting people and payload to and from Mars in order to allow for future settling and further space exploration.

The purpose of the Final Report is to provide a preliminary design of the Mars Excursion Vehicle (MEV), which provides transport between Low Mars Orbit (LMO) and the Martian surface, and outline the future phases of the project. This has been carried out as explained before.

Functional Analysis

Functional Flow Diagrams (FFDs) have been generated for the specific function of the MEV, which includes docking, landing, and launch from the Mars surface. A specific sub-FFD shows the procedure for firing the propulsion system. A Functional Breakdown Structure (FBS) was generated for more specific functions of the MEV, including those that are time independent.

Market Analysis

A Strengths, Weaknesses, Opportunities and Threats (SWOT) analysis was done. Stakeholders have been analysed, and categorised by management strategy. Finally, required investment has been estimated, as well as expected returns on investment. The total project initiation cost of 9.6 billion USD can be met by governmental investment of multiple space agencies, private investment and crowdfunding. The returns can be estimated to be 17.2 billion USD in addition to significant increase in employment and a 10 billion USD return on space tourism. A major part of the returns consist of scientific data and prestige.

Cost Breakdown

There are multiple costs associated with Project Cardinal such as unit production, maintenance, ground operations and refurbishment costs. The cost analysis was only performed for the MEV since there is a commercially available launch vehicle that can be used for the project. The overall mission costs were estimated to be 25,000 USD per kilogram of payload for a return trip with a cost of 12,500 USD for a one way trip to Mars. The total vehicle cost was calculated to be 67.66 million USD. The operational cost is 6.405 million USD which includes maintenance, testing, verification and refurbishment. The total mission cost for the MEV is the sum of the above presented costs divided by the number of estimated flights and the payload capacity. This gives total cost per flight per kilogram of payload of 182.53 USD.

Technical Risk Assessment

Technical risks were assessed using risk maps and risk mitigation strategies. These risks were categorised and split into technical, schedule and cost risks. Each risk was numbered with an assigned probability of occurrence and severity of impact coefficients with a scale of 1 to 5. The risk magnitude was estimated to be the product of these coefficients. The riskiest event found is related to the MEV reusability requirement where there is a risk that the MEV deteriorates too quickly to complete 100 launches/landings. This risk was mitigated by doing research on material fatigue and implementing innovative reusability solutions and techniques.

Sustainable Development Strategy

Design choices influenced by sustainability are propellant-type, the vehicle reusability, the choice for a Nuclear Thermal Rocket (NTR) for the Interplanetary Transfer Vehicle (ITV) and the standardisation of parts. Furthermore, a lean

manufacturing methodology is adopted and recyclable materials are chosen. Contamination is minimised using cleanrooms, Vapor Hydrogen Peroxide (VHP) for sterilisation and a strict separation between the crew and the Mars environment.

Propulsion

The propulsion section looked at the design of the main engines, the sizing of the propellant tanks, and the design of the reaction control system (RCS) thrusters.

The MEV will have eight main 50 kN engines, which will use liquid oxygen oxidiser and liquid methane propellant. These engines will have a chamber pressure of 70 bar, and an expansion ration of 276. This provides a specific impulse, I_{sp} of 340 s and a maximum mass flow per engine of 14.98 kg/s. In order to allow for the engine to be throttlable, it will use a pintle injector, and as the propellant choice is non hypergolic, a spark torch igniter will be used. The eight engines will only be throttled at 60% during launch, meaning that even if two engines fail, the remainder will only have to throttle to 80% to compensate. These remaining six will still have sufficient thrust vectoring for control, even if two adjacent engines fail, as a launch abort to orbit was deemed the safest option. The walls of the chamber and the bell nozzle will be made from Niobium C-103, meaning the mass of one entire engine including including pumps and valves is 104.8 kg.

For the RCS thruster, the propellant is required to be easily storeable, due to the length of time for which the MEV spends in standby in LMO. As only non-toxic propellants can be used, as to reduce complexity in the system, gaseous oxygen-gaseous methane will be used. Each thruster will operate at a chamber pressure of 8 bar, provide 400 N of thrust, and have a total mass of 1.9 kg. There will be 28 of these on the MEV, in order to provide not only sufficient control but also redundancy for safety.

The propellant tanks are sized to house the propellant needed for ascent and descent, the pressure the propellant is held under and the loads induced due to acceleration. This leads to an oxidiser tank with a height of 2.73 m, a radius of 2.3 m and a skin thickness of 4.78 mm. Adding a 0.5 mm aluminium liner leads to a dry mass of 487 kg. The fuel tank has a height of 2.19 m, a radius of 2.3 m and a thickness of 4.78 mm. With the 0.5 mm aluminium liner, the dry mass adds up to 417 kg.

Structures

The total mass of the structure of the MEV is 1,674 kg, divided as follows: 581 kg for the skin, 81 kg for (vertical) stiffeners, 308 kg for the floors between the levels and 705 kg for the beams supporting the floor. This was found by dividing the MEV into five levels, each with its own dimensions and structural elements, which were subject to change by an evolutionary solver. This solver was taken to minimise the structural mass while insuring the MEV can successfully resist the loads induced by the four critical load cases: Earth take-off with positive acceleration, Earth take-off with negative acceleration, Mars re-entry and Mars take-off.

The air brake was designed using the same evolutionary solver and designed to be able to resit the load case of Mars reentry which is the critical load case. Note that the air brake consists of 12 panels, conforming to the MEV hull that deploy out to 60 degrees from vertical. Between these (heat shielded) panels a heat shielded fabric is present to increase the surface are of the air brake. The total air brake mass is 1,100 kg of which 469 kg are panels and their heat shielding and 631 kg is the fabric placed between the panels.

Aerodynamics, Astrodynamics & Control

This report mainly focuses on the descent and ascent trajectories. However, some insight is also given for the transfer to Mars. The manned missions will be performed with a Hohmann transfer with a total transfer ΔV of 5.7-5.9 km/s and all cargo mission will be performed with a gravity assist via Venus with a total transfer ΔV 9.0-11.5 km/s. This value excludes the launch from Earth. It is expected that the fist cargo mission will take place in 2028 with the first manned mission in 2030. Once the the ITV arrives at Mars it will capture at 200 km altitude orbit with 25.2 degrees inclination. The MEV will land at approximately -2 degrees south latitude and 354 degrees east longitude. The landing region was decided based the Opportunity rover mission. Locations closer to the equator maintain higher temperatures and the terrain is relatively flat at an elevation of -2 km. The landing trajectory has been split into two phases. The first one represents a ΔV de-orbit burn of 239.6 m/s with an Entry Interface (EI) at 150 km. The time of flight to EI is 6.9 minutes with entry velocity of 3.045 km/s and flight path angle of -4 degrees. The second phase looks into the trajectory from 150 km to the surface and takes into account aerodynamic disturbances. The descent trajectory is accomplished by deploying the air brakes in order to slow the vehicle as much as possible before the atmosphere becomes significant, in order to reduce the maximum g-forces on the passengers; the passengers will experience a maximum deceleration of 2.8 g, which is safe for manned missions. Once the MEV hits 8.7 km, the

burn begins and burns until the MEV is just above the ground, and then lands at a speed of about 1.8 m/s. The MEV burns about 13 tonnes of fuel, and lands 1,148.319 km away from the entry point and lands at an angle of 89.8 degrees, where 90 degrees is considered a perfect landing. The descent time from 150 km to -2 km is 8 minutes and 40 seconds.

During ascent, the thrust vector needs to be actively controlled in order to increase the velocity in both the parallel and tangential direction with respect to the surface in order to reach orbit. The SimScape environment in MATLAB is used to model the MEV during ascent. Inputs for the simulation are thrust and gimbal angle. The outputs are accelerations, velocities and altitude with respect to the surface. With a dry mass of 9,040 kg and a fuel mass of 38,400 kg, the MEV is able to reach an altitude of 250 km after 600 s using a 350 s, 60% throttle burn.

After the MEV reaches 200 km altitude, an insertion burn of 1.45 km/s is initiated for 100 s in order to circularise the orbit. Rendezvous is not performed immediately due to the fact that the rotation of the planet and the velocity of the ITV make the timing very difficult. Consequently, the MEV is sent into an elliptic orbit with a semi-major axis of 4,490 km in the same plane of the initial circular orbit. Then the MEV will perform a rendezvous manoeuvre with the ITV taking only into account the position and velocity of the two vehicles. The total ΔV required to perform the manoeuvre is 346.2 m/s and the time of flight is 76.11 minutes.

Life Support

The life support system consists of two oxygen and two nitrogen tanks, which are spherical. The dimensions are calculated with the consumption of oxygen, the losses due to the airlocks, the pressure in the tanks and the accelerations working on the tanks. For the oxygen tank, the radius is 0.304 m, the height is 0.608 m, the skin thickness is 4 mm and the wet mass is 74.8 kg. For the nitrogen tank, the radius is 0.425 m, the height is 0.85 m, the skin thickness is 9.5 mm and the wet mass is 251 kg.

Communications

The MEV will be able to communicate back to Earth via either the ITV or another relay satellite around Mars using its high gain X-band antenna. The antenna weighs 20 kg and has a diameter of 0.45 m. Using the worst case scenario, a signal-to-noise ratio of 10 dB is experienced between MEV and ITV. The antenna will send communication signals of 50 W transmission power, that is amplified by an amplifier with efficiency 0.55, meaning the power required for the subsystem including all other equipment is 116.9 W. Because of redundancy, two high gain antennas are installed. They will be deployed out of the ITV via deployable booms. This whole subsystem weighing 58.2 kg will be able to send 2.66 Mbps video and MP3 0.16 Mbps of audio.

Power

There are two distinct power phases when looking at the MEV: Standby mode and crewed phase. During the standby mode the system requires 341 W of power, that will be produced by two deployable solar panels both consisting of three panels adding to a total area of 8.72 m². The configuration was chosen for less complexity when retracting, its packing factor to ease storage in the MEV, being shielded when entering Mars atmosphere and interference when installing a docking port. The panels will produce 740 W of power, recharging the batteries that power the MEV during eclipse. For the second phase of the mission, the MEV will dock to the ITV and also to its power supply. It will fully recharge its batteries that are capable of storing 200 kWh, that will provide power of 2,484 for three days to the 10 settlers that will land on Mars. The energy storage is achieved by using 32 Lithium-ion modules similar to the Tesla Model S P100D battery modules. While on Mars, the MEV will have to be hooked up to the power supply of the habitat. The mass of the batteries (1,250 kg) and solar panels (43 kg) combined add to a total mass of 1,293 kg.

Thermal

For the thermal subsystem, the radiator has been sized, as well as a general overview of the coolant loop layout. The external radiator has been sized to 10.7 m^2 , and will have a white exterior. The spacecraft itself shall have a white exterior as well, and will be covered in multi-layer insulation. The number of layers varies along the ship: two for the crew/cargo section, 11 for the methane tank and 36 for the oxygen. These numbers result from an optimisation for the total mass of the thermal system, which is found to be 537 kg.

Embarkment and Disembarkment

Embarkment and disembarkment happens via a motorised crane on an extending arm, which is a low mass, low power way to transport all cargo and personnel between the ground and the airlock. The total energy budget for the crane is about 280 Wh.

Overall Subsystem Design Considerations

For the iteration phase, a set pattern is followed. The ascent and descent propellant masses are established, after which the propellant tank mass is computed. After this, the new structural mass is computed, to give a new dry mass, which is then plugged in into the ascent and descent to give new propellant masses. As well as iteration, safety factors also need to be taken into account, such as a safety factor of 2 for the tensile strength of pressurised vessels.

RAMS Analysis

For the reliability, only rough estimates can be made. The MEV is compared to the Space Shuttle, leading to a reliability of 0.985%. However, as one of the Space Shuttle failures was not actually a failure of the Space Shuttle itself (but of one of the solid rocket boosters), this failure is discarded and an estimate of a reliability of 0.9926% is estimated. When doing a long term analysis, assuming a maintainability efficiency of 80%, a reliability of 0.9579% is found after 10 years.

The uptime of the MEV is ensured by using multiple MEVs such that the crew can immediately be transferred to and from the Mars surface. Also, the MEV is recharged by the ITV in both power and propellant, increasing downtime (however deemed insignificant) but decreasing the initial investment.

For maintainability, corrective maintenance (in case of (sub)system failure) is separated into four categories, all requiring a different path of action depending on the severity of the failure and the accessibility on Mars. The preventive maintenance (planned maintenance) is divided into two groups: parts that need frequent maintenance, such as the heat shields, and parts that do not need frequent maintenance, such as the power system.

For the safety, 15 safety critical functions are found which, when failing, would catastrophically influence the full system. Examples are reactions between propellants during supply transfer or engine failure. For all safety critical functions, redundancy is implemented to decrease the impact of these failures.

Compliance Matrix

In the compliance matrix, the requirements are stated with whether the requirement is met and an explanation. Many of the requirements are directed towards the ITV, which means it is at this stage not possible to evaluate whether the requirement is met. For some requirements related to the MEV, it is also not yet clear whether the requirement is met, such as **TEC-04.1: The system shall transport the cargo without damage**, as tests would need to be performed to ensure this requirement is met.

For the project, two killer requirements were identified for this project which is as follows. As can be seen only **GEN-01** was met, while **REG-07** still needs more analysis, before it can fully determined whether or not the killer requirements kill the project.

- ✓ GEN-01: The system shall not rely on in-situ propellant production during the initial set-up period, 2030-2035.
- * **REG-07:** The system shall comply with NASA Human Rating Certification[1].

Post-DSE Activities

The post-DSE phase is split into eight different phases: the detailed design, the initial investment, the operational logistics, the prototype building, testing, certification, start-up phase production and the start-up phase itself. These are then divided into a flow diagram and a breakdown structure. From the flow diagram, a Gantt Chart is made, with the detailed design starting in July and the start-up phase starting in 2028. A production plan for the prototype production is made, including the manufacturing methods for the components of each subsystem and the assembly plan.

Conclusions and Recommendations

The design as proposed in this report is seen as the most optimal configuration for a mission of this scope. The proposal as done by SpaceX is not feasible without using ISRU. However even assuming ISRU is possible, the preliminary design indicates that there are better ways of going to Mars. Specifically, with the future development of specific technologies such as ISRU would allow for higher performance or less complex designs. For the design as presented by Project Cardinal, further research is recommended for the aerobraking solution, gravity assist trajectories, and the operational life cycle.

Introduction

Project Objectives

The first technical proposal for a Mars settlement programme was written by Werner von Braun in early 1947¹. Shortly after, multiple American companies such as Aeronutronic Ford and General Dynamics presented theoretical human missions to Mars including a Venus fly-by. Additionally, in 1956 multiple mission proposals from Soviet companies entered the space competition for human trips to the red planet. One such proposal was The Mars Expeditionary Complex, or "MEK" that would take a crew from three to six to Mars and back with a total mission duration of 630 days. Similar space exploration initiatives were suggested by NASA in the 1990s. However, all of them lacked the in-depth studies and resources to actually initiate the missions and send human beings to Mars.

One of the first long-term visions for manned missions was represented by the European Space Agency (ESA) Aurora Programme. It was initiated in 2001 with a proposal for robotic exploration and aims to send people to Mars in 2033. However, multiple objections from ESA partners delayed the schedule and ESA was able to send the first ExoMars orbiter no earlier than 2016. In 2016 SpaceX presented their plans for a future Mars exploration mission. To achieve these plans SpaceX is currently designing the new interplanetary vehicles called the Big Falcon Rocket (BFR) which is expected to be capable of landing on Mars no later than 2022. However, these plans have drastically changed due to limited resources. The expected performance was decreased and due to financial constraints it became a challenge to keep the original vehicle design. More and more parties are becoming concerned with the feasibility of the entire mission and if the proposed schedule and development phases can be actually met.

The aim of Project Cardinal is to develop a new Mars settlement programme which is safe, realistic, time-bound and affordable. The project will specifically focus on the design of a Mars lander named the Mars Excursion Vehicle (MEV) and its performance characteristics. By doing this, more insight is gained in the feasibility of the Mars settlement programmes presented by SpaceX and other companies where each aspect can be critically investigated.

Mission Need Statement of Project Cardinal: To provide a realistic means of transporting people and payload to and from Mars in order to allow for future settlement and further space exploration.

Project Objective Statement of Project Cardinal: To design a preliminary mission profile and a Mars Excursion Vehicle for continuous manned exploration and future settlement of Mars, with a capability to transport a payload of 5,000 kg to the Martian surface, and a first mission launch scheduled before 2030.

https://web.archive.org/web/20100116233913/http://astronautix.com/craft/vonn1952.htm(Last accessed 19-06-2018)

Project Overview

This chapter aims to provide an overview of the project so far. It begins by summarising all of the work performed in the previous phases, including a summary of the key trade-offs made. After this a functional analysis of the MEV will be provided, along with the operations and logistics involved in a single mission. Finally, an overview of the current market will be provided.

3.1. Project Description

The goal of this project was set as creating a means of transporting people to and from Mars to allow for exploration and settlement. This Design Synthesis Exercise focused on the preliminary design stage of this project. This phase was split into a number of phases, the planning, midterm and final phase.

3.1.1. Project Plan

The planning phase focused on defining the mission, and how the preliminary design phase would be carried out. The project team was organised using an organogram where roles and responsibilities were allocated. These responsibilities were divided into organisational roles, such as the project manager and the system engineer who were responsible for ensuring an overview of the project was maintained, and more technical roles, including chiefs of every subsystem. A SWOT (Strengths, Weaknesses, Opportunities and Threats) analysis was also conducted to identify the strengths and weaknesses within the team, and approaches to manage these weakness were addressed, such as talking to professors for the lack of knowledge. To organise how the project was carried out a number of Project Management and Systems Engineering (PMSE) Tools were used. A work breakdown structure and work flow diagram were used to plan what packages the work would be tackled in, as well as how they inter-related and what sort of dependencies existed within work packages. A Gantt Chart was similarly used to visualise the order these tasks would be performed in and how resources should be distributed. Finally, a risk assessment and sustainable development strategy were developed. The former to allow for project development risks to be preemptively mitigated, and the latter was to ensure that the project is completed in a sustainable manner.

3.1.2. Baseline Phase

The purpose of the Baseline phase was to further define the project as well as establish the requirements to be imposed for the rest of the project. A market analysis was conducted in order to estimate the market opportunities present. These were seen to be space tourism, with a market size of 100 billion USD and a minimum price of 3,000-4,000 USD per kg, launch services, with a market of 8.88 billion USD to 27.18 billion USD, space mining, with a market of 330 billion USD, and space debris removal, with a market of 3 billion USD. A further discussion of this is presented in subsection 3.6.4 In order to assist in the requirement generation a functional mission planning was conducted. This entailed a number of functional flow diagrams stating what each mission element and system must be capable of doing. A functional breakdown structure was also made. The most updated version of these diagrams may be found in section 3.4. Next the requirements on the system were generated. This was done by using a requirement discovery tree, and then expanded upon in the the final requirement list. This list has been further updated and reviewed a number of times. The final version is displayed in section 6.4. Finally, design option trees were generated for the different mission profiles. These looked at all the possibilities for leaving Earth, performing the interplanetary transfer, and landing on Mars, and how combinations of these different possibilities formed a full mission profile.

3.1.3. Midterm Phase

The Midterm phase endeavoured to finalise the system and subsystem choices. This was done by first conducting two subsequent trade-offs on the system level design. The first trade-off considered the 12 mission profiles that remained after those that were deemed infeasible, primarily based on their TRL, were dismissed. These options

were assessed under criterion that were translated from the mission requirements. Table 3.2 displays this trade off. The best four options were taken from this trade-off for a more in-depth analysis to be conducted on each before choosing the optimal mission profile. The mission profile of SpaceX's BFR concept did not emerge from the trade-off as one of the best options but it was included in the in-depth assessment as it is the only manned Mars mission currently being worked on, and was kept as a control mission profile. To allow for a basis with which to assess these options, an analysis of the astrodynamic trajectories available for Mars missions was conducted. Four possible trajectories were identified, being a Hohmann transfer, Fast trajectory, Low-thrust transfer and gravity assist via Venus. A Hohmann transfer was chosen for human mission due to one-way travel time of 260-270 days and ΔV of 5.7-5.9 km/s. Gravity assist via Venus was chosen for cargo mission with a travel time of 310-380 days and ΔV of 9.0-11.5 km/s. Equipped with this knowledge a final system trade off was conducted. The criteria in this trade off were evaluated in a more quantitative manner than the first trade off. Table 3.1 shows this trade off.

The optimal outcome of the trade-off was the use of a conventional rocket to an Earth Excursion Vehicle (EEV) to an Earth orbit, where the passengers and cargo are transferred to a larger Interplanetary Transfer Vehicle (ITV). The EEV returns to Earth, and propellant variants of the vehicle are used to resupply the ITV. Once the ITV is filled and stocked, it accelerated on a transfer orbit to Mars. It then decelerates into a Martian orbit, where it docks with a Mars Excursion Vehicle (MEV). The passengers are then transferred to the MEV, while the MEV is refuelled by the ITV. The MEV carries the passengers and cargo to the Martian surface, before returning them after the duration of a month to the ITV. The ITV is used once more to return the passengers to Earth orbit where they will be ferried back to the surface with the EEV. Figure 3.1 illustrates this system. This system level architecture was found to be the best option with the requirements chosen, in particular with the requirement that the system does not rely on in-situ resource utilisation (ISRU) for propellant production.

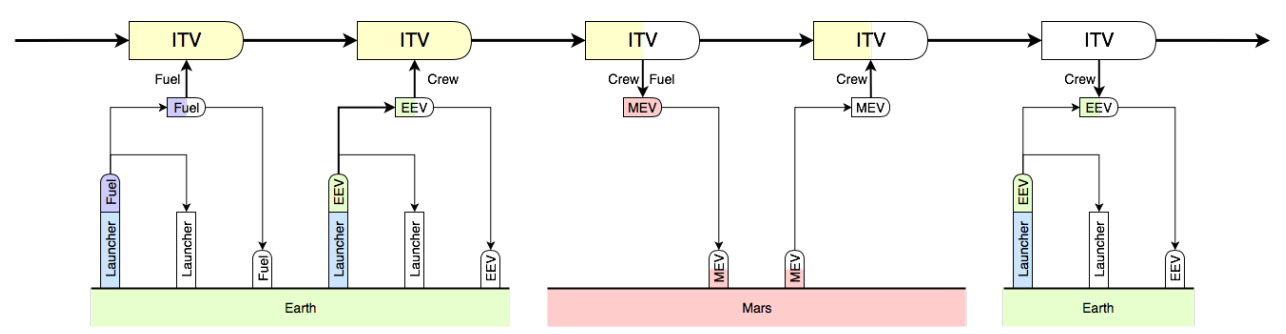


Figure 3.1: A schematic representation of the mission profile of one return trip. The level of colour in each vehicles represents the fuel level.

With a system selected, the subsystems to be employed in the chosen vehicles were tackled. This process was begun by employing an N2 chart to identify the interfaces between all subsystems. The first subsystem to be defined was the landing method for the MEV. Retropropulsive landings on the main engines were chosen from the trade off presented in Table 3.3. The next subsystem to be chosen was propulsion, with this subsystem being assessed for the launcher vehicle, the EEV and MEV, and the ITV. At this stage the EEV and MEV vehicle are considered to be the same, with minor adjustments to allow for the different operating conditions. This commonality reduces the complexity of developing the project, with the cross compatibility also allowing for greater ease of maintenance in the operational phase. Feasible propellant combinations for the launcher were analysed based in a quantitative manner and traded off, with LOX-LH₂ emerging as the winner. However, during subsequent sizing of the launcher it was realised that the proposed design was very close to the falcon heavy, so it was decided upon to use it as the launcher for the mission, even though the propellant choice is different. The propulsion system of the ITV was assessed in a more analytical manner, with chemical engines and Nuclear Thermal Engines (NTR) being pitched against each other. NTR engines were chosen for the ITV based on their drastically higher I_{sp} . The propulsion system for the MEV and EEV was assessed in a similar manner to the launcher, with a quantitative assessment of propellants choices. Only propellant combinations that would be cross compatible with the NTR engines were considered. Thus the same fuel the ITV would have to bring to Mars for the MEV, is the fuel it would use in its own engines, reducing complexity and increasing compatibility again. The propellants traded off were also selected for their compatibility with ISRU on Mars, as while it will not be used during the start up phase, it would be very beneficial in later mission phases when the TRL is sufficient. Thus LOX-LH₂ and LOX-LCH₄ were both assessed in Table 3.4, from which liquid methane was chosen as the preferred fuel. Next the power system was sized based on the power requirements of different subsystems as well the area of the radiators necessary for cooling of the systems. Table 3.7 and Table 3.5 show the trade-off for the power sources of the ITV and MEV respectively. Solar cells and batteries are the best choice for both.

Thereafter the communications system is sized, the preliminary configuration for each craft decided and radiation shielding for the vehicles from space sources as well as the NTR decided upon. The ADCS system was then assessed and the methods of control moment gyros and thrusters chosen. The decision was made to focus the in-depth design on the MEV, as a pre-existing launcher had already been chosen and the in-depth design of the ITV would focus more on the habitats and less on the aerodynamics and structural capabilities. As such, the preliminary design of the ITV described in section 3.3 is as far in depth as it will be designed.

Finally the Midterm phase involved some PMSE methods to ensure the smooth completion of the project. This involved a discussion on how contingency management would be implemented on technical resource budgets throughout the implementation of the project. Margins were applied to all characteristics of the vehicles, depending on the type of system, to allow for growth in other areas while maintaining a coherent design. The technical risk assessment conducted previously was reviewed and improved with the greater resolution now known of the system. With the configuration defined, the logistics of preparing and operating such a system were analysed and mapped, to be used as a resource during the further development of the project. A discussion on how sustainability is considered during different parts of the project so far is presented, explaining how the different trade-offs have considered sustainability as a criterion of assessment. The verification and validation (V&V) employed in the sizing of different systems is detailed, describing the different cases used to validate them and explain how they were assessed for verification.

3.1.4. Final Phase

The final phase of the design is the focus of this report. As mentioned in the previous section, the focus will be on the MEV. The report focuses on finalising the in-depth design of the sub systems, as well as the integration of these subsystems into the full system. Following on from this finalised conceptual design, the plans to ensure the continuation of the project in an efficient and accurate manner are laid out. This project development plan will cover everything from the full detailed design and the sourcing of funding right up to beginning of the first manned mission phase. Full plans for the production of the MEV, as well a full discussion on its maintenance and the risks involved with its use will also be provided.

3.2. Trade-Off Summary for MEV Subsystems

During every phase of the design, trade-offs have been performed to come to certain design solutions. During the midterm phase two major trade-offs were performed in order to reduce the twelve proposed mission profiles first to five, and in the end choose, with the help of a more quantitative analysis, the final design.

The twelve preliminary mission profiles were traded-off using criteria based on key mission requirements, namely the 2030 deadline, the ability to perform the mission without IRSU, how much degradation the equipment on Mars experiences, the ability of the design to meet the requirement of a crew of 10, the operational risk involved, how reusable the design is, how easy it is to maintain the design, and how sustainable it is. This trade-off is shown in Table 3.1 where also the weights and given scores are seen for the 12 options. As discussed in subsection 3.1.3, the four highest scoring designs and the design similar to SpaceX's proposal were selected.

System Design	Mass (2)	Reliability (3)	Reusability (3)	Cost (2)	Sustainability (1)	Score
Air launched, Earth Station,	9.8	6.5	4.8	3.2	10.0	6.37
Mars Orbiter/Lander						
Rocket, Earth Station,	9.8	8.6	9.4	5.3	8.4	8.43
Mars Orbiter/Lander	9.0	0.0	9.4	3.3	0.4	0.43
Rocket, Earth Orbiting Ship,	10.0	8.6	10.0	5.3	9.0	8.67
Mars Orbiting Ship	10.0	0.0	10.0	3.3	9.0	0.07
Rocket, Earth Orbiting ship,	9.8	8.6	9.4	5.3	8.4	8.43
Mars Orbiter/Lander	9.0	0.0	9.4	3.3	0.4	0.43
Big Falcon Rocket	0.0	10.0	6.1	10.0	4.7	N.A.
Big Falcon Spaceship	0.0	10.0	0.1	10.0	4.7	IN.A.
0						

Table 3.2: Consolidated trade-off on five design options.

These five design options that were subjected to a more quantitative analysis looking at mass, reliability, reusability, cost, and sustainability. This trade-off is shown in Table 3.2. For these criteria, a score 10 is used to indicate the best option, while a 5 would indicate an option which is twice as bad relative to the best option. As can be seen in in this table, and as was discussed in subsection 3.1.3, the optimal solution is to use a rocket to launch from Earth and

Table 3.1: Preliminary trade-off for the remaining design solutions.

	Score	2.353	2.471	2.118	2.294	2.412	2.059	2.412	2.647	2.294	2.000	2.235	1.882
Sustainability	(1)	က	က	က	2	2	2	2	2	2	1	1	1
Maintainability	(1)	2	2	2	2	2	2	1	1	1	8	က	က
Reusability	(3)	E C	က	2	3	3	2	က	3	2	2	2	1
Operational	KdSK (3)	1	1	2	1	1	2	2	2	9	2	က	က
Payload	(3)	က	m	က	က	33	33	8	3	33	2	1	2
Equipment	Degradation on Mars (2)	8	ю	1	က	က	1	က	3	1	8	က	1
In-Situ	Fropellant (2)	ဇ	е	2	8	3	2	3	3	2	2	2	1
2030	Deadline (2)	1	2	2	1	2	2	1	3	3	1	33	3
		1. Air Launched Rocket Earth Docking Station Mars Orbiting Shin	2. Air Launched Rocket Earth Docking Station Mars Orbiter + Lander	3. Air Launched Rocket Earth Docking Station Directly to Mars Surface	4. Rocket Earth Docking Station Mars Orbiting Ship	5. Rocket Earth Docking Station Mars Orbiter + Lander	6. Rocket Earth Docking Station Directly to Mars Surface	7. Rocket Earth Orbiting Ship Mars Orbiting Ship	8. Rocket Earth Orbiting Ship Mars Orbiter + Lander	9. Rocket Earth Orbiting Ship Directly to Mars Surface	10. Rocket Refuel Only Mars Orbiting Ship	11. Rocket Refuel Only Mars Orbiter + Lander	12. Rocket Refuel Only Directly to Mars Surface

dock with a interplanetary ship in LEO. After this the ITV will perform the transfer to Mars, where it will meet a ship already orbiting the planet, which will be used to perform the Mars launch and landing.

During the preliminary subsystem design, more trade-offs were performed. Most of these trade-off focused on the design of the MEV, though one or two briefly touched upon the ITV. First the method of landing the MEV on Mars was traded-off. The result was a powered landing with the main engine was the best solution, as it scored highest for all criteria as shown in Table 3.3.

				-			
Criterion	Criterion Scaling		Scaling Mass Budget Reusability		Landing	Technology	Score
(weight)	Required (1)	Usage (2)	(2)	(2)	Accuracy (3)	Readiness (3)	Score
Main Engine	3	3	3	3	3	3	3.0
Skycrane	1	1	1	1	2	3	1.7
Wings	2	0	3	2	2	2	1.8
(Auto)rotor	2	1	3	0	1	2	1.5

Table 3.3: MEV Mars landing trade-off.

The propellant used for the main engine of the MEV (and also the EEV) is traded-off in Table 3.4, where NTR compatibility is focused on the I_{sp} of the fuel. LOX/LCH₄ the clear winner over LOX/LH₂, mostly due to the high scores for volumetric energy density, operational temperature extreme and ISRU compatibility. This decision also means that liquid methane will be used as a fuel for the NTR on the ITV, to reduce complexity and add redundancy in the system. As the combination of LOX/LCH₄ is not hypergolic, an external ignition is required. Discussion led to the only viable option being a spark torch, but a more in-depth analysis will be provided in subsection 5.1.2. Based on this propellant choice, a preliminary mass estimate of 42 tonnes, and a thrust to weight ratio of 2, the estimated thrust needed on Mars is 318 kN. For redundancy, the engines will be designed for a total of 400 kN, which is eight 50 kN. Eight engines were taken as it provides sufficient redundancy for thrust and thrust vectoring

NTR Volumetric Graviometric Operational ISRU Cost per Compatibility Compatibility **Criterion:** Energy Energy **Temperature** Score I_{sp} (3) kg (1) (2) Density (2) Density (1) Extreme (3) (2) LOX + Methane 6.7 8.1 8.3 10 4.3 10 10 8.6 $LOX + LH_2$ 10 10 10 4.3 10 1.8 5 6.7

Table 3.4: Propellant trade-off for the Excursion Vehicles.

The possibilities for powering the MEV during the standby phase in orbit are traded off in Table 3.5. It can be seen that the use of solar panels and batteries resulted in far more favourable masses than the use of a Radioisotope Thermoelectric Generator (RTG). For the landing and launch phases, it was decided upon to only use batteries to power the MEV, as panels would not survive the loads during those phases. For standby, a total surface area of $8.7 \, \mathrm{m}^2$ is required.

 Power Generation Mass [kg]
 Power Storage Mass [kg]
 Total Mass of Power Subsystem [kg]

 RTG
 127
 0
 127

 Solar + Batteries
 43
 4.9
 48

Table 3.5: Mass comparison of MEV required standby (orbiting) power.

Finally, as shown in Table 3.6, a trade-off was performed to determine the best material to be used for radiation shielding. Kevlar scored significantly higher than the other options, however, a combination of both Kevlar and aluminium would most likely be used, to make sure there is sufficient structural integrity. However, it should be noted that this trade-off does not account for the option of placing water tanks in the walls to provide additional shielding. Also, as most of the time the crew will be inside the MEV will be within the Mars atmosphere, which will significantly reduce the dosage, it might not even be necessary to have additional shielding. As such the shielding will again be analysed in more detail in subsection 5.4.2

Criterion	Thickness (1)	Strength to Mass ratio (2)	Score
Polyethelyne	7.00	0.49	2.66
Aluminium	5.83	3.25	4.11
Liquid Hydrogen	10.00	0.00	3.33
Kevlar	7.00	10.00	9.00

Table 3.6: Radiation shielding trade-off.

A trade-off was also performed in order to determine the best means of performing the communications. The network contains five segments; the Deep Space Network (DSN), the ITV, the MEV, the relay satellites, and the Mars ground station. However, only the the communication between the DSN and the ITV (as this is essential for control, telemetry and mental health), and between the ITV and the MEV (which is essential for docking), were looked at. For this, the ITV is equipped with a 150 W Ka-band system and a 100 W X-bandsystem, while the MEV is equipped with one 50 W X-band system. A more in-depth link budget linked to this can be found in subsection 4.1.4.

Finally, the options for the Attitude Determination and Control System (ADCS) were discussed. For the MEV, zero momentum (thrusters, wheels, Control Moment Gyros (CMG)), Sun sensors, Inertial Measurement Units (IMU), star sensors, and horizon sensors will be used. This provides an attitude control accuracy of \pm 0.001° to \pm 1° and an attitude determination accuracy of \pm 0.003° to \pm 0.01°.

3.3. Preliminary Design of Mission Vehicles

As mentioned in subsection 3.1.3, only the MEV will be designed in depth in this report. However, some preliminary sizing was performed for the interplanetary transfer vehicle and the Earth excursion vehicle, and research performed into the capabilities of the commercial launcher chosen, as is discussed below.

3.3.1. Interplanetary Transfer Vehicle

The ITV will be used to bring a crew of 10 from a LEO of 400 km to a LMO of 200 km. In addition to crewed missions, it will also be used to transport cargo to Mars, as well as docked MEVs. The latter will be at the ends of the habitat modules, as is as shown in Figure 3.2. Crew transfers will be taken via a Hohmann Transfer while cargo will be taken using a gravity assist via Venus. Each transfer, the ITV will transfer additional propellant for use on the MEV. It has a maximum payload capacity of 150 tonnes, which includes approximately 50 tonnes of MEV propellant. While the ITV will be manufactured on Earth, it will be launched in modules and rendezvoused in orbit.

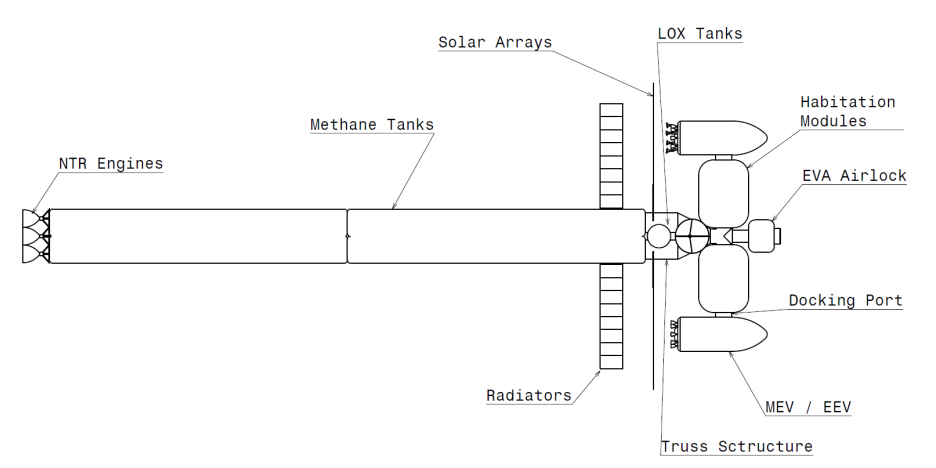


Figure 3.2: ITV with two docked MEVs.

Based on the MEV propellant choice of LOX/LCH₄, the ITV will use liquid methane as a fuel to reduce redundancy. While methane can be used in both a chemical engine and a NTR, it was decided upon to use the latter. This was as NTRs have much higher I_{sp} values and can be possibly used as power sources, even if their thrust to weight ratio is sub-par, due to the additional mass needed for radiation shielding. For a Hohmann return trip to and from Mars, the ITV will require 11.8 km/s of ΔV . The NTR will be operated at a temperature of 2,800 K, with an I_{sp} of 606 s, and a burn time of 1 hour. These are the expected values of values of a thermonuclear rocket engine using methane and water, as discussed in Zubrin [2]. A thrust of 910 kN is required for this ITV. As such three 350 kN engines will be used,

each with a mass of 7,135.7 kg.

The propellant tanks on the ITV, will serve as a form of radiation shielding and a means of transferring loads from the engine to the main structure, in addition to being a propellant storage. A preliminary sizing was done on these tanks. Based on the knowledge the tanks must fit within the fairing of the Falcon Heavy, it was found the 28 cylindrical tanks of 4.1 m diameter by 6.5 m in height were needed. These will be made from carbon fibre, designed as a pressure vessel with a safety factor of 2.

Similar to the MEV power trade-off, a trade-off was performed on the operational power required for the ITV, as is shown in Table 3.7. This power requirement was primarily based on the power required for a habitat with a crew of 10, which came down to 27.28 kW. For this a surface area 704 m² is required.

	•	• •	•
	Power Generation Mass [kg]	Power Storage Mass [kg]	Total Mass of Power Subsystem [kg]
RTG	10,259	0	10,259
Solar + Batteries	3,473	393	3,866

Table 3.7: Mass comparison of ITV required operational power.

For the habitats, it was chosen to use two Bigelow B330s docked together, as one is sufficient for six astronauts to work and live in on a long-term basis 1 . These inflatable habitats are based on the BEAM habitat currently installed on the ISS, and weighs 20,000 kg and inflates to a size of 330 m 3 1 . The primary structure of the Bigelow habitat is aluminium and Kevlar, including significant radiation and micrometeorite shielding, and several life support elements are included in the 20,000 kg launch mass. Additional radiation shielding was also considered for the ITV, an was based upon the same trade-off performed in Table 3.6.

Based on all the dimensions determined above, a preliminary drawing of the ITV was made, as is shown in Figure 3.3.

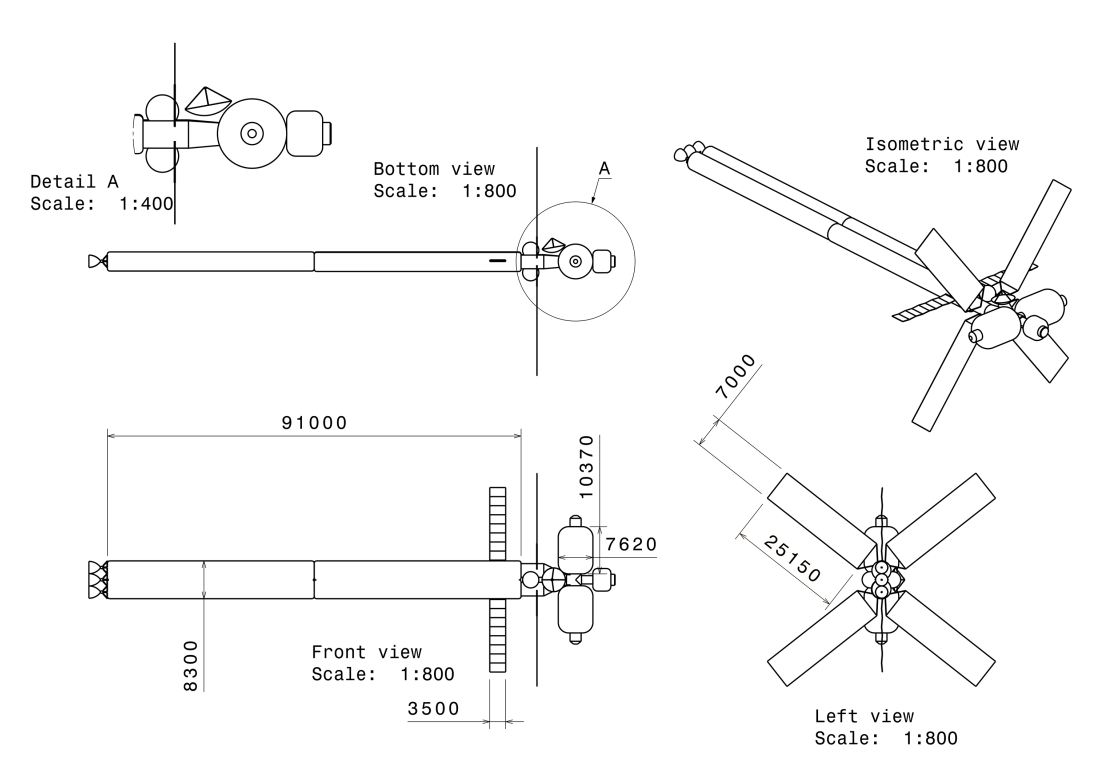


Figure 3.3: Preliminary design of the ITV.

Finally, a preliminary mass budget for the ITV was made, as is shown in Table 3.8. Here the dry mass does not include the payload, but everything was sized with the assumption of needing approximately 1,079 tonnes of liquid methane to transport a payload of 150 tonnes.

 $^{{}^{1} \}texttt{https://web.archive.org/web/20121023123821/http://www.bigelowaerospace.com/ba330.php} (Last accessed 25-05-2018) \\$

3.4. Functional Analysis

		-	
Component	Mass [kg]	Amount	Total mass [kg]
Propellant tanks	1,285.71	28	36,000
Engine mass	7,135.7	3	21,407
Habitat (structure)	15,000	2	30,000
Habitat (consumable)	35,000	2	70,000
Habitat (life support)	20,000	2	40,000
Micrometeorite shielding	-	-	22,000
Radiation shielding	10,000	2	20,000
Nuclear shielding	2,504	3	7,512
Total Dry Mass			246,919

Table 3.8: Mass budget ITV.

3.3.2. Earth Excursion Vehicle

As was mentioned in subsection 3.1.3, it is assumed that the EEV will be very similar to the MEV. There will be three versions of this vehicle available; one for transporting cargo, one for crew, and one for refuelling the ITV. It will dock with the ITV in a similar manner to the MEV, as shown in Figure 3.2, and will be launched on top of a Falcon Heavy as shown in Figure 3.4. Similar to the MEV, its shape is based on the dimensions and shape of the fairing of the Falcon Heavy, which additional drag calculations showed to be sufficient for Project Cardinal's purposes. Note that the crewed EEV variant is expected to be cheaper to operate due to part commonality with other EEV and MEV than other manned ascent vehicles currently available.

As the EEV is so similar to the MEV, all of the trade-offs made in section 3.2 are still applicable. Both vehicles will use the same propellant for redundancy, and the EEV will also perform a powered landing, with the use if additional air brakes. The only trade-off which is not applicable is the need for solar panels, as the EEV will not be spending long periods in orbit like the MEV, so can simply perform its mission to the ITV with battery power.

3.3.3. Launcher

As opposed to designing a new launcher, it was opted for to use a commercially available launcher, as one with the specifications required already exists. This will also save drastically on development costs, and will increase the likelihood of the 2030 deadline being met. It will however increase the launch costs, but this was deemed to be less important than the time it was being traded for. For this, SpaceX's Falcon Heavy will be used. The fully reusable version of this will be used, as oppose to the expendable version, in order to meet the launcher reusability requirements. The payload capacity of this version is substantially less, being capable of launching only 23,000 kg to LEO². It is know that the fully expendable version has a launch cost of 1,411 USD/kg to LEO³, and while the exact cost per kg is not yet known for the reusable version, it is assumed to be within this ballpark.

The propellant of this launcher supercooled LOX with chilled RP-1, which is the main way in which this launcher differs from one which would have been designed as a part of Project Cardinal. As during the Midterm Report, a trade-off showed LOX/LH_2 to be the optimal propellant choice[3].



Figure 3.4: MEV launched from a Falcon Heavy.

3.4. Functional Analysis

For the more detailed design of the MEV, a functional analysis is performed first. Since this report is focused on the design of the MEV, this functional analysis only presents the functions of the MEV, rather than the entirety of the system as presented in the Baseline Report. This section looks at the FFD and the FBS. The two differ in the sense that the flow diagram only represents functions that occur chronologically, while the breakdown also includes continuous activities.

²https://www.teslarati.com/how-spacex-falcon-heavy-costs-undercuts-competition/(Last accessed 25-06-2018)

³http://www.spacex.com/about/capabilities(Last accessed 01-07-2018)

3.4. Functional Analysis

3.4.1. Functional Flow Diagram

The MEV has to perform a set of functions, which have been summarised in the top level Functional Flow Diagram in Figure 3.5. The flow starts with the MEV rendezvousing and docking with the ITV. When it undocks, it has an option is to either going to the Mars surface and back, or entering standby in LMO to await the next ITV.

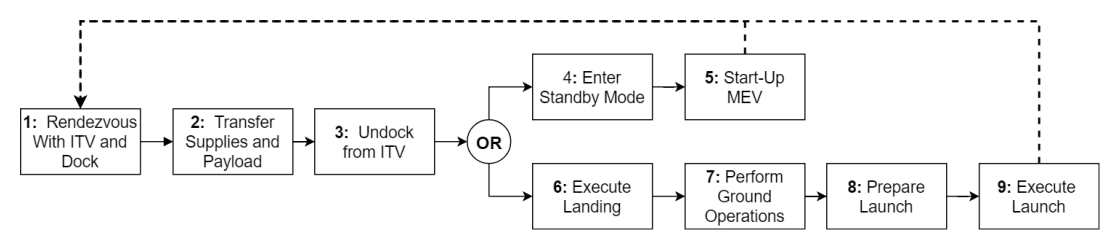


Figure 3.5: Top level Functional Flow Diagram.

The top level functions are numbered with a single number. The sub level Functional Flow Diagrams are Depicted below and contain functions with 2.x., another sub level denoted with a 2.x.x. identifier. Go (G) and No Go (G) functions have been defined with a Letter. All red boxes imply the propulsion system is being fired, and the functions are given in Figure 3.9.

The first phase of the missions is given in Figure 3.6 which looks at all of the function involved in the MEV rendezvousing and docking with the ITV, transferring cargo and then unlocking again.

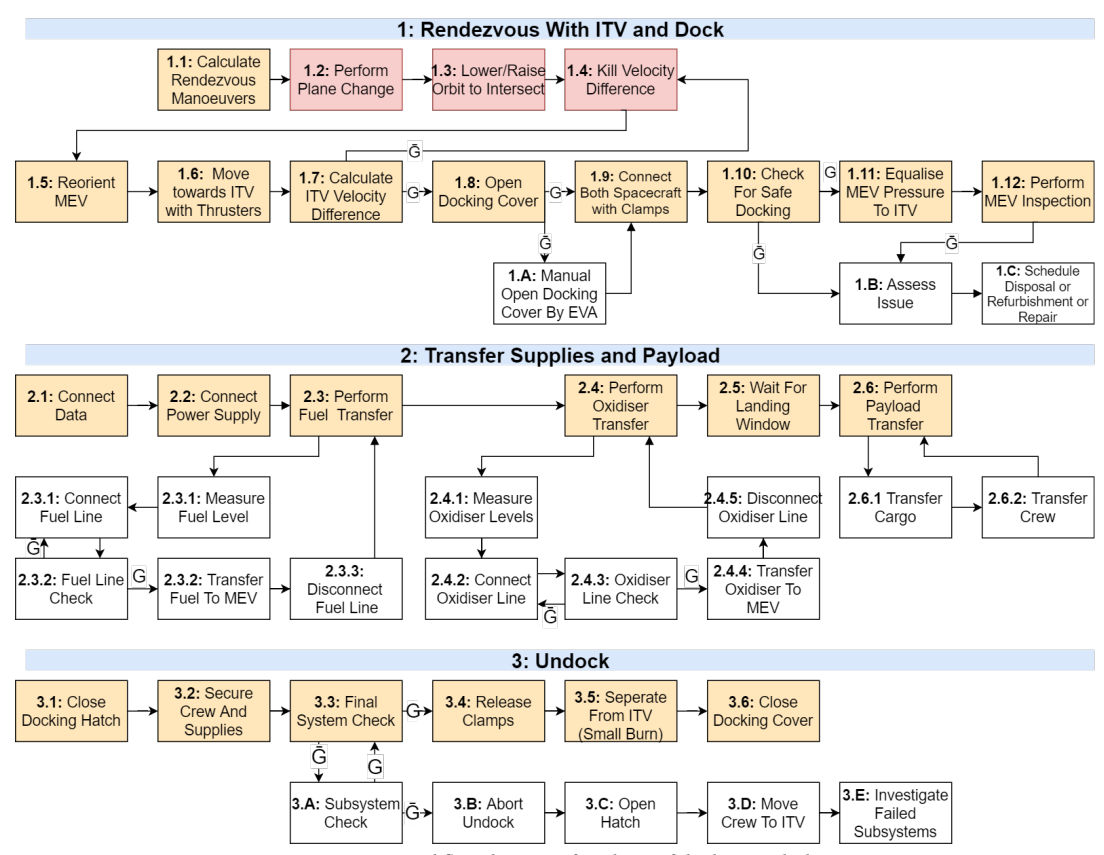


Figure 3.6: Functional flow diagrams for phase of docking with the ITV.

The second phase of the missions is given in Figure 3.7 which looks at the landing of the MEV on Mars, the operations it must perform before being put into standby on the surface, and finally the launch back up to LMO.

3.4. Functional Analysis

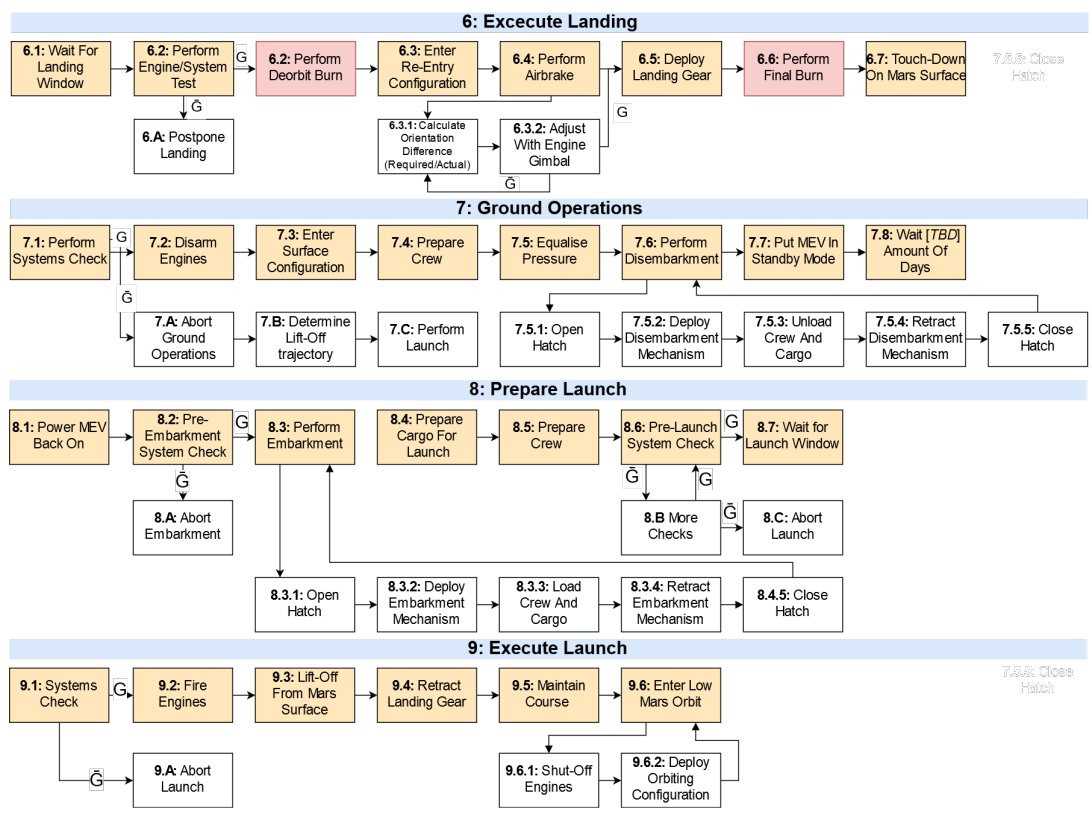


Figure 3.7: Functional Flow Diagrams for phase of Mars landing.

The third phase of the missions is given in Figure 3.8 which looks at the period where the MEV remains on standby in LMO between missions.

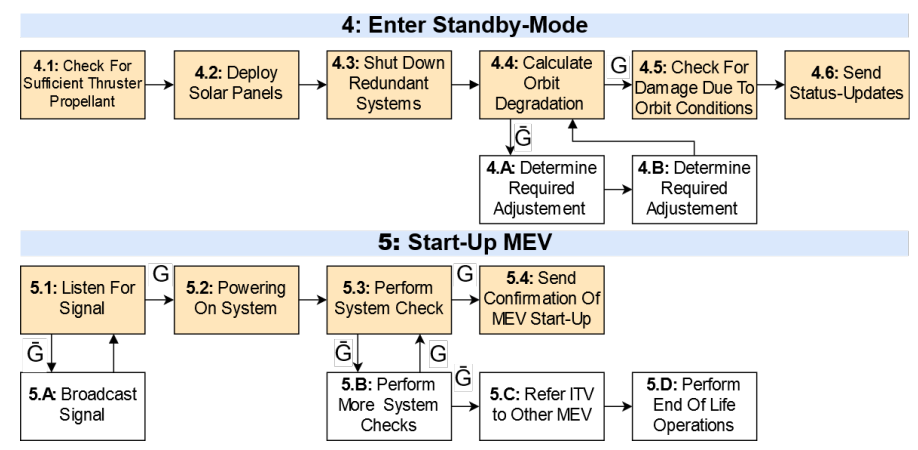


Figure 3.8: Functional Flow Diagrams for phase of Mars landing.

Finally, the flow diagram of the process followed every time the propulsion system is ignited is given in Figure 3.9. As mentioned before, it represents the procedures followed every time there is a red box in Figures Figure 3.6 to Figure 3.8.

3.4.2. Functional Breakdown Structure

In addition to the functional flow diagram, a functional breakdown structure is included in Figure 3.10. This looks at all the functions that the MEV must be able to perform, even those which are continually ongoing and therefore not accounted for in the previous subsection.

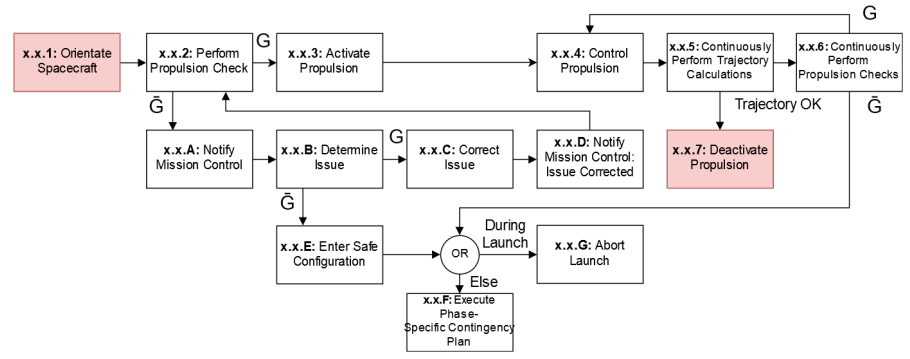


Figure 3.9: Functional Flow Diagram for all phases where the propulsion system is used.

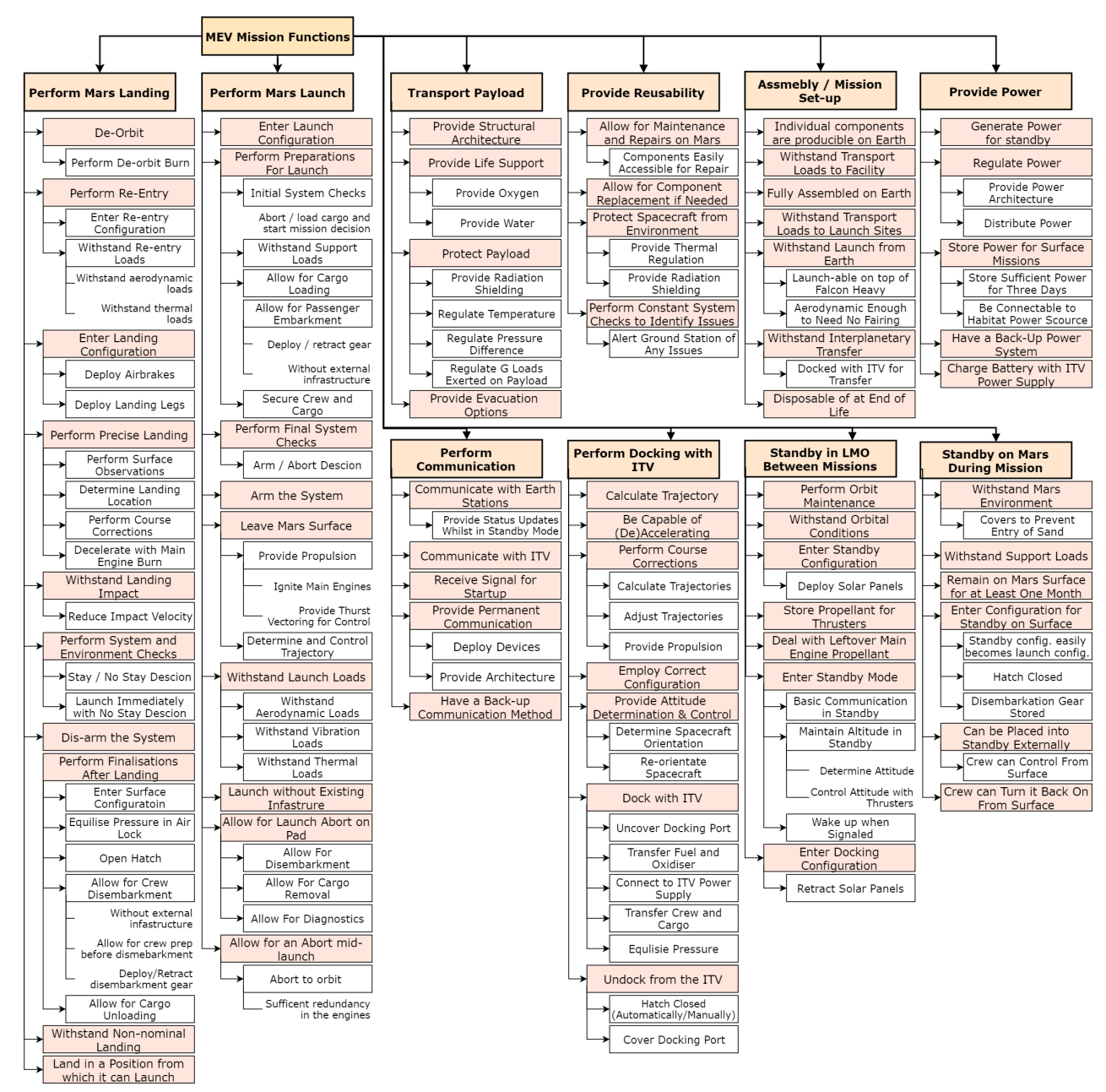


Figure 3.10: MEV Functional Breakdown Structure.

3.5. Operations and Logistics

In the Midterm Report [3], a detailed overview of the different operations of the overall mission was presented. This section aims to extend these operations by placing the overall objectives for the project on a timeline and by going deeper into the operations associated with the MEV.

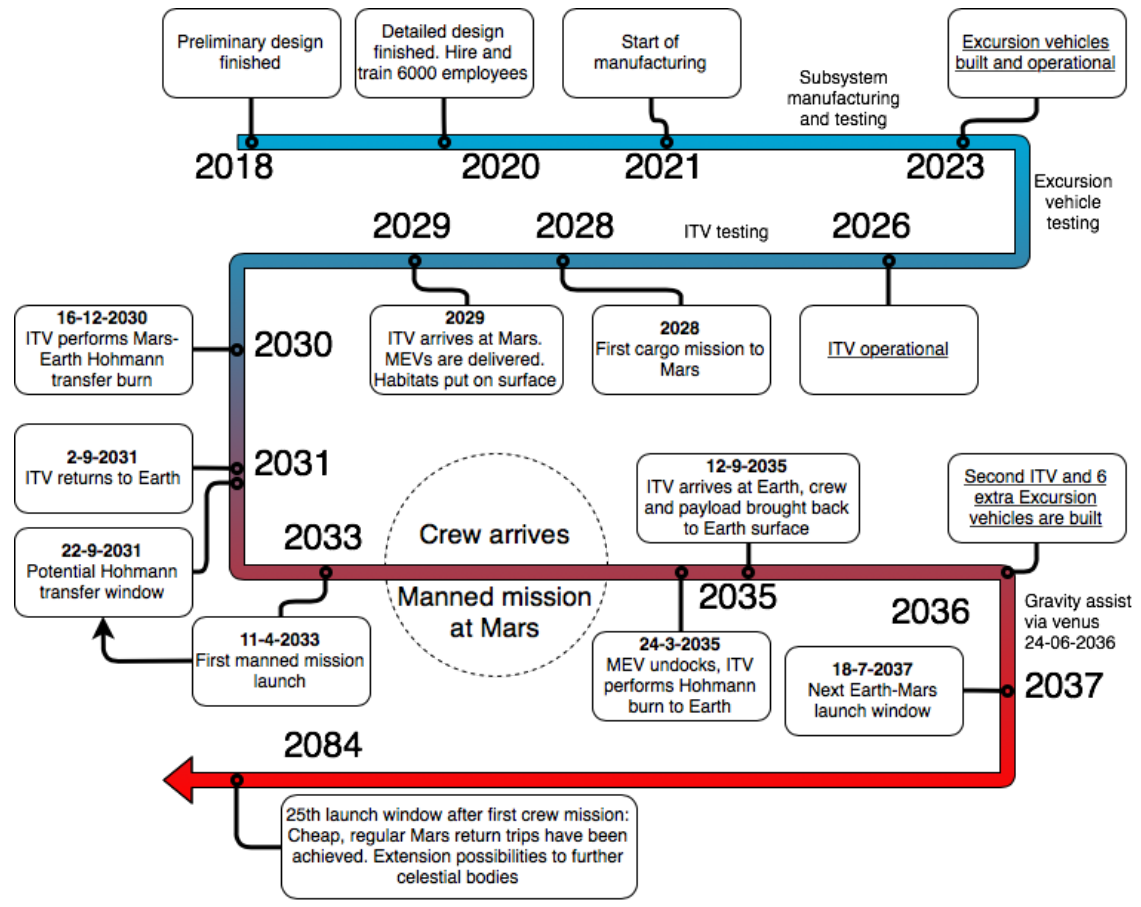


Figure 3.11: Timeline on critical operations including MEV specific operations.

Figure 3.11 shows the critical operations associated to Project Cardinal. The design phase ends in 2020 with a full detailed design of each vehicle. Manufacturing can start in 2021 and the operational phase is expected to start with the first cargo mission in 2028. It can be assumed that, after the first crewed Mars mission, every Earth-Mars transfer window will be used. After the DSE has ended on July 5th, 2018, the preliminary design is considered to be finished. In order to keep this pace, efforts should be made to finish a detailed design within the time frame of two years, meaning that by 2021, manufacturing can start. During the cost determination of the ITV, a cost of 24,000 Manyears was found for the production of one ITV, from which a manufacturing time can be easily determined. In order to make sure the requirements set by the client are met, around 6,000 Full-Time Equivalent employees are required. Although significantly fewer Manyears are required for the Excursion Vehicle, as is determined in section 4.2, the Excursion Vehicles will be considered more mission critical, meaning more manufacturing effort goes into their manufacturing and testing. By 2026, the ITV will be operational after which the cargo will be sent to Mars. Due to limited launch opportunities for a gravity assist before 2030 the first cargo mission will be sent by a Hohmann transfer in 2028. The first manned mission is scheduled for 2033 while the first transfer via Venus will be performed in 2036. Given the motion of the planets and maintenance required, there is a 20 days window between the ITV arriving at Earth and the next Hohmann transfer. Although efforts can be made to reach this, it is assumed that this is not feasible, meaning that the next Hohmann transfer window will be used. During every Hohmann transfer window after the first manned mission, either one or multiple ITVs will be sent to Mars.

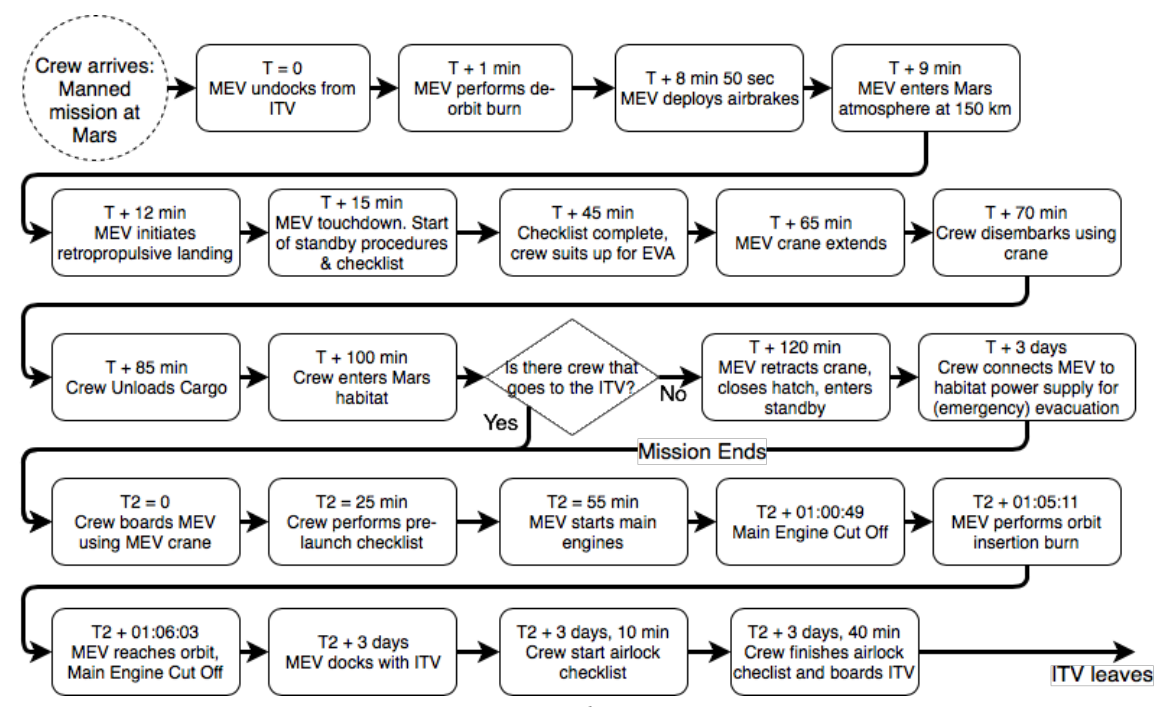


Figure 3.12: Critical MEV operations.

The MEV aspects mission specifics are given in Figure 3.12. Depending on the timing of the mission, it might be required for some or all members of the crew to the ITV just after the MEV has landed, meaning the MEV will take off again soon after touchdown. If this is not the case, the full crew shall enter the habitat, and the MEV will be connected to the habitat power supply until the next launch.

3.6. Market Analysis

Now that Project Cardinal is reaching the detailed design phase, the commercial value and initial investments of the project need to be reassessed. First of all, a market SWOT (Strengths, Weaknesses, Opportunities and Threats) analysis is created in subsection 3.6.1. Next, a stakeholder analysis is done in subsection 3.6.2. In subsection 3.6.3, the initial investment is broken down, as well as some opportunities to gather this investment. In subsection 3.6.4, the direct returns from project Cardinal are established. Finally, in subsection 3.6.5, secondary opportunities for returns of investment are shortly addressed.

3.6.1. SWOT

The following section discusses the SWOT analysis based on the findings for the market opportunities that were explained in the Baseline Report [4]. Adjustments to Table 3.9 since the baseline are indicated in orange. The general approach for the SWOT was explained in the baseline report under the market analysis. Weaknesses are the only aspects that can be controlled and transferred to opportunities and consequently to strengths. This is possible since weaknesses are harmful but internal and are dependent on the project and the market analysis approach.

High price is the main weakness capable of preventing further development. Currently space travel is an expensive experience for which very few have the ability to pay, which significantly decreases the potential of the market. However, this can be turned into an opportunity by improving the quality of the service whilst maintaining the same price, which retains a small amount of valuable customers who are willing to go more than more than once. By doing so, even with a small customer base and high ticket price, the potential companies that enter the market can maintain high profit margin. There is also uncertainty regarding technical risks related to development and reliability of the vehicle that goes into space, potential technical failures, cost increases, schedule delays, and customer dissatisfaction. Some of the risks considered can be mitigated by simply transferring them to other parties, whose abilities to handle them are better. This can be immediately transformed into an opportunity since it provides more design freedom and flexibility on the choices made at any stage of the development process.

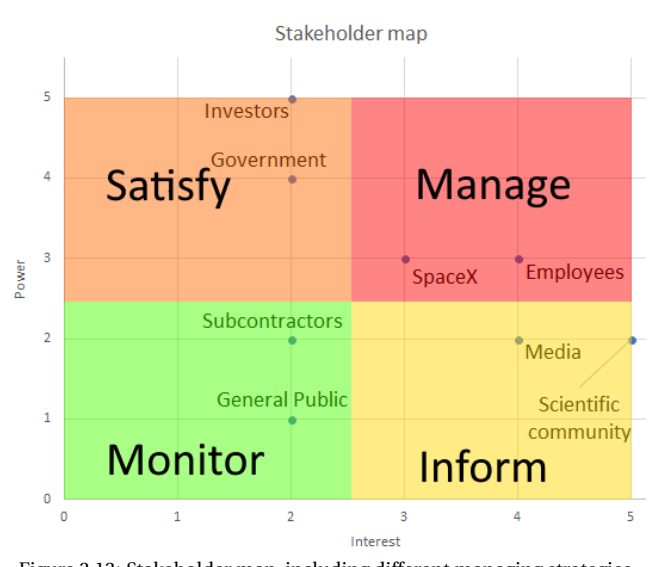
Table 3.9: Market SWOT analysis.

	Helpful	Harmful
	Strengths:	Weaknesses:
	•Lack of competition (market is relatively unexplored	•High price (might discourage most potential customers);
	with very few companies involved in it);	•Inaccessibility (might not be suitable for people
Internal	 Market size (potential is huge with high profit 	without training to withstand loads);
mternai	margins possible);	•Small customer base (very few people actually able to
	•Job opportunities (talented workforce required	afford it which increases the value of a single customer);
	for prestigious positions);	•Uncertainty (multiple/complex risks associated
	 Available Resources (funding, technology, talent); 	with the idea);
	Opportunities:	Threats:
	•Innovative (new and futuristic look into the space	•Human rating certification procedures (safely transport
	related services);	humans both during launch and in space);
	 Adventurous (possibility of involving various 	•Sustainability and Emissions regulations (none
External	exciting activities for the bravest customers);	compliance with the contamination and waste
	 Educational (multiple-level learning and 	reduction requirements);
	instructional activities and projects);	•Lack of fit for purpose technology available (requires
	 Public participation (public is involved and 	different levels of infrastructure and technological
	market size and popularity increases);	developments that are applicable for the given project);

3.6.2. Stakeholder Analysis

Besides having a sustainable product, a sustainable project plan should also be achieved in order to succeed as a project. This means that a proper analysis and management of stakeholders are needed to ensure the continuation of the project. Beyond the scope of the DSE, there are several stakeholders including governmental instances, private investors, scientists, and the general public. In order to ensure the continuation of the project, the needs of the stakeholders should be satisfied. Different management strategies are applied to different stakeholders, based on their interest in, and the power they have over, the project, as is shown in Figure 3.13.

There are four different strategies for managing stakeholders; satisfying, informing, managing, and monitoring them. The most important stakeholders for the first stages of the project are considered to be those that have a lot of power over the project. These were found to be the investors in the project, governmental instances, and the launch provider SpaceX. In order to ensure proper continuation of the project, these stakeholder needs must be achieved. The investors and governments can be satisfied by introducing the returns, as will be explained below in subsection 3.6.4. However, contact with the launch provider SpaceX should be monitored closely in order to ensure that enough launches can take place for the mission. At this stage, there is no vehicle besides the SpaceX Falcon Heavy capable of performing this mission, meaning that a good relation with the company should be maintained. This can be done by ensuring that the vehicles will be prop-



can be done by ensuring that the vehicles will be propFigure 3.13: Stakeholder map, including different managing strategies.
erly prepared before flight, as well as communicating and if necessary adjusting all requirements for launch. Less critical stakeholders should either be informed about the progress of the project or be monitored, but these are not considered for this market analysis.

3.6.3. Initial Investment

It is assumed that the mission is initiated from the perspective of a private company, meaning an initial investment is necessary to make Project Cardinal a reality. From section 4.2 it was found that the optimal solution required a total cost of \$7.6 billion. This is considered to be solely for production of one ITV and six excursion vehicles: four MEVs and two EEVs.

After production, approximately \$2 billion is required for operations, which include not only the operations for the crewed mission, but also recovery and refurbishment. The propellant cost is ignored at this stage, given that it is

less than one percent of the total costs. While a total cost of \$9.6 billion may seem to be a significant amount, it is only a fraction of the ISS costs, which were estimated to be more than \$30 billion [5], and is close to the cost of the Global Positioning System (\$10 billion [6]). There are three possible ways of acquiring this initial investment: Crowdfunding, Private investors and Governmental investment.

Crowdfunding

With the rise of Kickstarter, crowdfunding has reached an all time high with a total revenue of \$34.4 billion⁴. Even higher numbers can be found when looking into blockchain development where amounts up to \$4 billion have been raised for single projects⁵. However, crowdfunding is not a sustainable means of income since it can only be acquired once. Also, due to the high investment costs of this project, a crowdfunding campaign is highly unlikely to finance the entire mission. Nonetheless, a crowdfunding campaign can help raise global awareness while providing a small amount of finical assistance.

Governmental Investment

Space agencies such as ESA have a significant amount of possibilities for startups. However, this is mainly focused on smaller ideas which revolve around Earth monitoring and data handling. Nonetheless, as a government instance, ESA has a lot of resources which can be used for the development of the mission, for instance, helping to improve international relations. As ESA is a governmental organisation, direct monetary profit is not important, but the total annual budget of 5.8 billion USD⁶, is less than the initial investment required for Project Cardinal. Therefore, multiple organisations such as JAXA, NASA and Indian Space Research Organisation (ISRO), should also be contacted for collaboration to finance it. The mission may potentially improve international relations, but this could delay the mission to a significant extent. It is therefore considered as unfeasible use governmental investment if the requirements on the schedule are to be adhered to.

Private Investors

A more flexible option would be using a loan from private investors to fund the initial phase of the project, ensuring the investor gets a predefined return. While this return does not have to be monetary, it is very likely that the interest on the investment would be the preferred choice. This means that a monetary flow is needed, which will be discussed in subsection 3.6.4 and subsection 3.6.5. The advantages of this approach is the flexibility after the initial investment. For a private company, like SpaceX, more design freedom is given than when working with a governmental instance. Furthermore, gathering resources from multiple different sources is easier than acquiring money from one single governmental entity, making private investors the best option for funding the initial investment.

3.6.4. Mission Returns

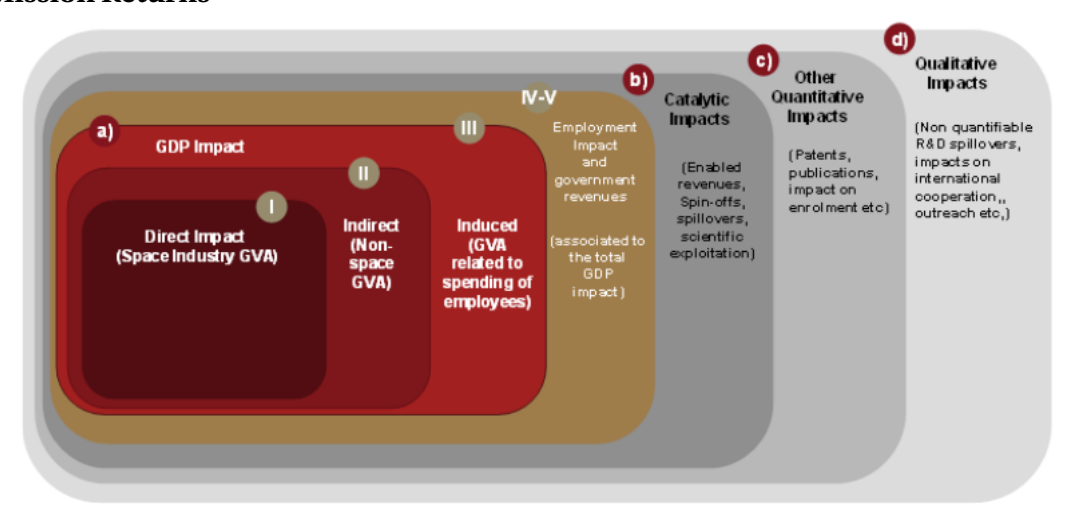


Figure 3.14: Direct impacts of the ISS to the economy [7].

⁴http://crowdexpert.com/crowdfunding-industry-statistics/(Lastaccessed 05-06-2018)

⁵https://www.cnbc.com/2018/05/31/a-blockchain-start-up-just-raised-4-billion-without-a-live-product.html(Last accessed 05-06-2018)

 $^{^6}$ http://www.esa.int/spaceinimages/Images/2016/01/ESA_budget_2016_by_domain(Last accessed 05-06-2018)

Figure 3.14 shows that a space mission such as the ISS, not only has a direct impact on the economy (employment in the space industry), but also induces a cascade of other benefits. This cascade is divided into four phases, consisting of direct impact (as described above), indirect impact (people being employed outside of the space industry), induced impact (employees spending money in stores), and employment impact and government revenues (employees paying taxes). These are the only impacts considered for this project.

Research shows that these first phase impacts vary within the space industry. Each dollar invested by ESA in the ISS has a return of 1.8 USD, so over the period 1995-2016 a 9.36 billion USD investment returned 17.08 billion USD, as well as a 8.19 billion USD governmental revenue. In addition, for every 100 people employed within the space industry (direct impact), another 90 people were employed outside of the space industry (indirect impact) [7].

3.6.5. Other Return Opportunities

If the investor requires more than these mission returns, there are some alternative solutions within the market to attain profits. It will be possible for the ITV to take satellites to Mars, ensuring that they are protected during the transfer. This is part of the launch service market which, according to the findings from the Baseline Report [4], are currently worth over \$5.5 billion per year. Rover missions like Curiosity have a total cost of up to 2.5 billion USD⁷. Providing such transfer services can definitely increase the profits generated from the project. Space tourism is also considered, as the ITV could be used for space tourism between the transfer windows. A NASA/Shuttle Training Aircraft (STA) study shows that the expected annual turnover for flights to LEO is 10-20 billion USD per year by 2025. A TU Berlin study suggests a 9 billion USD annual turnover and on average 100,000 space tourists per year globally with a ticket price of under 100,000 USD [8]. Finally, scientific patents created during research could also increase revenues, especially for new solar cell technology, dust resistance structures, or ISRU technologies. These could be commercialised back on Earth which also helps in the creation of revenues.

3.6.6. Entering the Market

Given that a financer for the mission can be acquired, the right moment to enter the market should be established. Despite the fact that the market for manned interplanetary travel and space tourism can be considered non existent at this point, estimations suggest that by 2025 the market size will be over 1.5 billion USD⁸. This number could grow further if the proper infrastructure is laid down. During the mission phase, the ITV could bring scientific payloads to Mars orbit or surface, which could also be used as proofs of concepts in the first transfers in 2025, which is shown to be the first launch opportunity in section 3.5. Given that the crewed missions starts at 2030, the first ITVs will be decommissioned after 10 return trips, which will be around 2055. Decommissioned ITVs will be refurbished in LEO after which it could be used as housing for space tourists.

Finally, it should be noted that given the need statement of the mission, the creation of revenues is considered to be of less importance. As stated by Wilson [9]: "We're drowning in information and starving for knowledge". Project Cardinal is driven to explore and find new worlds. There is more knowledge to be found, which one cannot express in money.

https://www.space.com/10762-nasa-mars-rover-overbudget.html(Last accessed 04-06-2018)

⁸http://www.abnewswire.com/pressreleases/space-tourism-2018-global-market-expected-to-reach-usd-158063-\million-with-cagr-of-1623-by-forecasts-2025_190989.html(Last accessed 26-04-2018)

Project Management

A project with out proper management and planning is likely to face issues such as going over budget or encountering risks which had not been planned for. As such, this chapter first provides the budgets for the ΔV , mass, and power, and the link budget. Then a breakdown of all the costs is provided, followed by the risks involved the project and how they can be mitigated. Finally the V&V of the design, as well as the approach to developing it in a sustainable manner will be provided.

4.1. Resource Budgets

The budgets of each subsystem have to be defined in order to proceed to a more detailed design; the ΔV budget, mass budget, the power budget and link budget. These are all preliminary values and are subject to change, and are expected to change. A pointing accuracy budget for ADCS sensors could not be determined at this time due to the wide variety of available sensors. The chosen star and Sun sensors are mentioned in section 4.2 and the expected accuracy is approximately 1 arc second. The main attitude control system hardware will be the reaction control system which was sized in section 5.1. Please note that each of the values presented is a target budget for with it is designed for. The actual result of each analysis is given a precise calculation in subsequent chapters in the report.

4.1.1. ΔV Budget

The ΔV budget for the MEV can be seen in Table 4.1 along with the specific impulse, I_{sp} . The ΔV is split into powered and aerobraking, though the mission will consider only aerobraking, as the propellant mass would increase fourfold, and thus be infeasible without it. A 5% margin is added on to the ΔV budget along with a 10% margin the on the I_{sp} budget [10]. The I_{sp} was also considered as the margin included influences the mass required later on. The actual ΔV for landing will likely fall somewhere between the aerobraking and powered landing values. Generally it is expected that the magnitude of the ΔV for landing will be closer to the aerobraking value.

Table 4.1: ΔV budget and I_{sp} for the MEV mission profile.

	Units	Aerobraking	Powered	Margin (%)	Aerobraking	Powered
ΔV landing	[km/s]	0.123	4.1	5	.129	4.305
ΔV launch	[km/s]	4.1	4.1	5	4.305	4.305
I_{sp}	[s] _	366	366	10	333	333

4.1.2. Mass Budget

The mass budget was developed by presenting the mass estimations given in the Midterm Report [3] and applying a margin depending on the predicted readiness level of the subsystem [10], and then applying a 20% system margin to the entire dry mass, as based on [10]. The entire mass budget for the MEV is illustrated in Table 4.2. The estimated dry mass increased to 9,351 kg and initially it was 7,793 kg, as stated in the Midterm Report [3], though due to additional changes, and the presence of margins, the dry mass was changed. This

Table 4.2: Mass budget of the MEV; the values with asterisks * are not expected, the actual value will be much closer to the bold values.

Descriptions	Input [kg]	Margin [%]	Mass [kg]
Structure	3,300	10	3,630
ADCS	356	10	391
Power	1,718	5	1,804
Propulsion	1,060	10	1,166
Communication	20	50	30
Tank sizing	701	10	771
Dry Mass	7,793	20	9,351
Payload	5,000	0	5,000
Propellant	43,300 to 194,288*	5	45,465 to 204,002*
Total Mass	56,093 to 207,081*	-	59,816 to 218,353*

4.1. Resource Budgets 23

change does not affect any subsystem significantly aside from the tank sizing, which has been altered. The thrust to weight ratio is still high enough with the change, with a thrust of 400 kN [3] and with the gravitational acceleration of Mars being $3.711 \, \text{m/s}^{21}$, the launch thrust to weight ratio is 1.79. Additionally, some values used for the cost analysis are not presented in the above table, in section 4.2; the dry mass without the main engine is $8.834 \, \text{kg}$. The propellant mass has a large deviation due to the ΔV budget; the full powered landing is actually not likely to occur, as drag would help reduce the ΔV greatly even if the MEV were to not use large air brakes. Generally the propellant mass should be closer to the minimal value, likely around 50 to 70 tonnes. With the estimates made, the total mass is expected to be around 60 to 80 tonnes. It must be noted that the high margin on the communication is due to the relatively low mass estimation: it is expected that low mass components are more likely to increase over the course of the design than high mass components.

4.1.3. Power Budget

The power budget is a combination of power used, power available and power gained. The losses are presented in Table 4.3 and the Power available, and the net power is presented in Table 4.4. All values were taken from the Midterm Report [3].

Table 4.3: Peak Power needed throughout crewed mission.

Table 4.4: Power availab	le throughout t	the mission, and	d the net power.
--------------------------	-----------------	------------------	------------------

Subsystem	Power Required [W]
Thermal	14
Communication	167
Propulsion	0
DHS	146
Life support	1,936
Mechanics	15
GNC	0
Harness	207
Total Power Required	2982

Value	Units					
Power Available						
740	- W					
417.3	kWh					
3	Days					
3,224	W					
Net						
242	$\bar{\mathbf{w}}$					
	vailable 740 417.3 3 3,224 et					

Note that the total losses value includes a 20% margin in order to account for unexpected hardware/connection losses and thus the positive net power balance becomes 242W.

4.1.4. Link Budget

The link budget for the ITV and the MEV are presented in Table 4.5; the values are determined from the Midterm Report [3]. The ITV is included as it is sometimes used as a relay for the MEV. A data rate of 2.66 Mbps (Table 5.44) is provided to the passengers on the MEV, and is included in the link budget; this rate allows for basic video chat, which is deemed a necessity for the psychological health of the crew [3]. A data rate of 4.82 Mbps is provided to the passengers on the ITV.

4.1.5. Margins

Margins are generally introduced to cope with critical uncertainty. Prof. Dr. Shufan Wu [10] represents a way to select proper margins for each subsystem. As explained the margin for the mass budged is dependent on the readiness level of each subsystem. 5% margin is added if the subsystem is well known and does not require additional analysis on mass estimation. 10% mass margin at subsystem level must be considered if the related technology is not well known and already space proven and 20% is required when the technology for the subsystem is under development or is new on the market. Additionally, since this is a new proposal for a mission to Mars a margin of 20% is applied on the entire system mass budget due to uncertainties and possible changes in requirements.

Once the mass budget includes all margins, the ΔV budget can be estimated based on energy equations and later used to compute the possible performance characteristics of the system. The ΔV values that are required do not change with the chosen system. That is why it was assumed that each change in the target ΔV will be a result of the change in the mass budget. Thus, only 5% margin was added to this computation which includes gravity and atmospheric losses.

As explained, 20% margin was added on power [10] due to power losses and the margin for link budget was already presented to be 10 dB in the Midterm report. This value was chosen as design margin typical for reliable data transmission.

 $^{^{\}rm 1} {\tt https://en.wikipedia.org/wiki/Mars} \ (Last \ accessed \ 04-06-2018)$

4.2. Cost Breakdown 24

		Uplink		Downlink	_
Parameter	Units	DSN->ITV	ITV/relay->MEV	ITV->DSN	MEV->ITV/relay
Transmitted Power	W	400,000	150	100	50
Transmitted Power	dBW	56.02	21.76	20	16.99
Frequency [11]	Hz	3.25E+10	8.45E+09	3.25E+10	8.45E+09
Wavelength	m	9.23E-03	3.55E-02	9.23E-03	3.55E-02
Diameter (Receiver Antenna)	m	4.25	0.45	70	1.74
Diameter (Transmitter Antenna)	m	70	1.74	4.25	0.45
Receiver Antenna Efficiency	-	0.5	0.5	0.7	0.5
Transmitter Antenna Efficiency	-	0.7	0.5	0.5	0.5
Gain (Transmitter Antenna)	dBi	85.99	40.74	60.20	28.99
Gain (Receiver Antenna)	dBi	60.20	28.99	85.99	40.74
Noise Temperature [12]	K	763	763	424	424
Max Distance	m	3.98E+11	5.03E+06	3.98E+11	5.03E+06
Loss (propagation loss)	dB	-294.68	-185.00	-294.68	-185.00
Bandwidth	Hz	2.41E+06	4.23E+09	2.41E+06	1.33E+06
Design Margin	dB	10	10	10	10
Signal Power Received	dBW	-102.47	-103.51	-138.49	-108.28
Noise Power Received	dBW	-135.95	-103.52	-138.51	-141.09
C/N	dB	33.4858	0.0042	0.0168	32.8043

4.1.6. Payload

The MEV is designed to carry a payload of 5,000 kg. Of this 1,000 kg is reserved for the 10 crew members located on level 3. Each crew member will have an individual chair to help endure launch and landing accelerations. 4,000 kg is dedicated to carrying payload such as consumables, personal items, maintenance materials, scientific equipment, rovers etc.

The cargo MEV is a modified version of the crewed MEV. It is designed to autonomously deliver cargo to a designated landing site. Its first task will be to deliver the habitat, power supply, consumables and assorted equipment to the Mars surface prior to the arrival of the crew to Mars. The cargo MEV will have a significantly expanded payload capacity since it does not need to carry any payload back to Mars orbit, furthermore several systems, such as life support can be eliminated to increase payload capacity. Note that the cargo MEVs will have as much commonality with its crewed brethren to keep production cost down and facilitate maintenance.

4.2. Cost Breakdown

There is a large variety of costs associated with a programme like Project Cardinal. In this section, these different aspects will be broken down. Subsection 4.2.1 talks about the unit production cost of every subsystem, then in subsection 4.2.2 the cost from maintenance, ground operations, and refurbishment will be elaborated upon. Finally in subsection 4.2.3, the total mission costs will be given.

4.2.1. Overall mission costs

The current preliminary calculations will only involve the cost analysis of the Mars Excursion Vehicle since the team found that a commercially available launch vehicle suits the mission needs. As in the Midterm Report [3], Koelle [13] will be used for cost estimations, historical data and formulas in this section unless stated otherwise. All cost formulas are given in Manyears. One Manyear was equivalent to 208,700 USD in the year 2000. Using historical data², the inflation between 2000 and 2018 was found to be 49%. This results in the current price of a Manyear, equal to 311,000 USD. The reader should note that this Manyear covers all expenses for the section that is analysed, not just employment costs.

In the midterm report, the overall mission costs were traded off for the five different mission profiles in Table 3.2. The overall mission costs depend on a variety of items, where the most prominent is the cost for the ITV and its refurbishment. In the midterm report, the overall mission cost was found to be just below 25,000 USD per kg, which accounts for all Earth launches and for the refurbishment of all the vehicles, including the ITV. Since this can be considered as the cost per kg for a roundway trip, the cost per kg for a ticket from Earth surface to Mars surface is

²https://tradingeconomics.com/united-states/inflation-cpi (Last accessed 21-06-2018)

4.2. Cost Breakdown 25

considered to be half, resulting in 12,500 USD per kg.

Structural Cost

The MEV can be considered to be a winged orbital rocket vehicle due to its re-entry and flyback capabilities. It is assumed that the formula that can be used for the production of the winged orbital vehicle only makes use of the structural mass, as given in subsection 4.1.2. Equation 4.1 gives the unit production cost of a single MEV, given the structural mass of 5,250 kg.

$$C_{unit} = 0.3758 \cdot N_v \cdot (m_{dry})^{0.65} \cdot f_4 \tag{4.1}$$

Where C_{unit} is the unit production cost based on the number of vehicles produced, N_{v} is the number of vehicles, m_{dry} is the structural mass of the MEV without the main engines as seen from subsection 4.1.2 and f_{4} is the cost reduction factor which is a function of the number of units produced, the production batch per part, the learning factor of the personnel and production modifications. Usually the cost reduction factor is in the range of 0.8 to 1. However, due to the complexity of the mission and the different levels of technology readiness, a cost reduction factor of 0.98 is chosen. The total production cost of the MEV structure therefore becomes 29.99 million USD. Note that Equation 4.1 is independent of material used, as most costs are in Manhours. For the propellant tanks, a cost estimation is made where the material used is taken into account.

Engine Cost

The engines, including their certification and tests, are considered as a vital part of the mission. The costs for the engine production can be estimated using Equation 4.2

$$C_{\text{eng}} = 3.0 \cdot m_{dry}^{0.535} \cdot f_4 \tag{4.2}$$

 f_4 is considered to be 0.85, given that experience with and information on rocket engines is readily available. With a total engine dry mass of 909.7 kg, the total engine costs are estimated to be 30.36 million USD for eight engines.

ADCS Cost

In order to facilitate the search for cost for the ADCS, off the shelve components have been researched. The SSOC-D60-2 axis digital Sun sensor, costing 12,200 EUR, granting around 14,400 USD, is considered. Next, the NST-1 Nano star tracker is considered, costing 80,000 EUR or 93,500 USD, using exchange rates of 1.17 USD per EUR³. Finally, the MAI-SES IR Horizon sensor is used, costing 15,000 USD⁴. Given that 12 sun sensors, eight star trackers and one horizon sensor are used, the total cost become 970,000 USD. It should be noted that these numbers are expected to be significantly lower, since in-house production or bulk order discount is not considered for this cost estimation.

In addition, there will be 28 RCS thrusters, which is a total dry mass of 53.2 kg. The cost of these can be found using Equation 4.3 below, in which f_4 is equal to 0.80. This results in a cost of 3.96 million USD, meaning the entire ADCS system costs 4.93 million USD.

$$C_{\text{RCS}} = 1.9 \cdot m_{dry}^{0.535} \cdot f_4 \tag{4.3}$$

Tank Cost

Since the propellant and environment tank will be made from carbon fibre, an estimation can be made by estimating the amount of Manhours, as well as raw material mass. Meredith et al. [14] gives an estimation of the labour costs for carbon fibre manufacturing which is equal to 75 USD per Manhour, including the consumables used. The material cost is found to be around 8.50 USD per kg. This means that the material cost for the propellant tank is equal to 284,000 USD. Manhours are the largest cost. Using the equation given in Equation 4.1 gives an estimation of the amount of Manyears required for the tank. One Manyear is assumed to be equal to 2,000 Manhours. Using the same dry mass of the tanks, equal to 1,632 kg, and a learning factor of 0.8 for the composite structure, 72,000 Manhours are required for the tank. Using 75 USD per Manhour, the salaries will be around 5.4 million USD. This gives a total price of 5.69 million USD for the tank.

 $^{^3 \}texttt{https://www.xe.com/currencyconverter/convert/?Amount=1\&From=EUR\&To=USD (Last accessed 22-06-2018)}$

 $^{^4 \}texttt{https://www.cubesatshop.com/product-category/attitude-actuators/(Last accessed 22-06-2018)}$

4.2. Cost Breakdown 26

Propellant Cost

Since it is given that methane and LOX will be used, the price estimate per launch for the propellant can be estimated. The price of LOX is found to be 0.15 USD. The price for methane is found to be 1.35 USD⁵. Given an O/F ratio of 3.4 and a total fuel mass of 51,350 kg, the fuel cost can be found as follows

$$\left(\frac{51350}{1+3.4}\right) \cdot 1.35 + \left(\frac{51350}{1+1/3.4}\right) \cdot 0.15 = 21,707USD \tag{4.4}$$

It should be noted that these costs are diminished if ISRU is used. In that case, the power budget will increase in return for fuel creation. These costs are only the raw fuel cost, and do not include refuelling operations.

Total Vehicle Cost

Given all the structural cost, including manufacturing and management, the total MEV production cost can be found. Adding all of the calculated cost, the total cost for manufacturing is given in Equation 4.5. It should be noted that some margin should be added to this to this value, as the power and communication subsystems were not directly accounted for in this value.

$$C_{\text{MEV}} = \sum \text{investment} = 70.99 \text{million USD}$$
 (4.5)

4.2.2. Operational Cost

The next step is to calculate the operations costs which include the cost of the mission itself and the refurbishment costs. As explained, the phase where the ITV is used is no longer part of cost calculation for the entire mission which initially included the ITV and the launch from Earth.

Operations and Maintenance

Since the ITV mission phase is not included anymore, the mission cost for the MEV can be given by Equation 4.6.

$$C_{ma} = 75 \cdot T^{0.5} \cdot Na^{0.5} \cdot L_c^{-0.8} \cdot f_4 \tag{4.6}$$

Where C_{ma} is the crewed vehicle mission cost, T is the mission duration of MEV in orbit which is approximately three days, Na is the number of crew members on board which is 10, L_c is the crewed launch rate per year per vehicle and f_4 is a learning cost reduction factor of 0.9. Note that each MEV will be launched once per year based on the available launch windows. However, the three days are included in the 600 days of the total mission. Therefore, T is considered to be 600, where only $1/200^{th}$ of the costs are considered. This number includes not only the in-orbit activities such as docking but also the cost of the crew, the ground support and its training. The total cost for the three days of operations of the MEV are equal to \$8.13 million.

Next, the assessment of the refurbishment costs is given by the optimised cost model which is a function of the unit production cost, the launch rate and the refurbishment cost factor given as a percentage of unit production cost.

$$C_{ref} = 0.015 \cdot L \cdot C_{unit} \tag{4.7}$$

One can estimate the factor of vehicle fabrication cost to be approximately 0.15 based on the number of flights per vehicle which is estimated to be 100 for the MEV. The maintenance cost is estimated to be 106.48 million USD.

Testing and Verification

For any space mission, testing is required to validate the design, either via the use of static tests or test flights. However, despite the fact that space agencies like NASA record lots of data, no data is published outside of the programme in order to facilitate test design and estimate testing cost. This is confirmed by [15], which states there currently is not an organised process for the systematic improvement of testing based upon test experience. However, the methods provided by Koelle [13] do include a wide variety of cost within the different sets of historical data. It is therefore assumed that the costs for testing and verification are included within the previously determined cost for unit production.

⁵http://www.thespacereview.com/article/2893/1(Last accessed 05-06-2018)

Refurbishment

Since the MEV is a reusable vehicle, it can be stated that it has to be taken out of service after a predefined amount of flights to undergo detailed inspection and potential exchange of parts before they wear out. These are considered to be off-line activities, not much unlike the 'Major Overhaul' of aircraft. Refurbishment is considered to be only for off-line activities. Everything that needs to be done between two consecutive flights of the MEV is considered to be part of maintenance, as calculated in subsection 4.2.2. This includes eventual refurbishment of air brakes and small repairs.

An estimate for the maintenance cost can be made by once more looking at historical data. The maintenance cost per flight for reusable orbital vehicles can be found to be 0.25% of the new vehicle cost. This cost is found to be equal to 70.99 million USD, meaning that the added cost per flight or refurbishment are assumed to be

$$C_{\text{maintain}} = 0.0025 \cdot 70,990,000USD = 177,469USD$$
 (4.8)

4.2.3. Total Cost

The total cost of the mission is then estimated to be the sum of the production cost and the sum of the mission operation cost including production per flight of the MEV. This is then divided by the payload capacity in order to calculate the cost per kilogram of payload.

$$C_{total} = \frac{C_{unit} + C_{ref} + C_{ma}}{\text{Number of Flights \cdot Payload capacity}} + \frac{C_{\text{maintain}}}{\text{Payload capacity}}$$
(4.9)

The total cost per flight per kilogram of payload then becomes 406.69 USD per kg of payload from Mars orbit to Mars surface, given the payload capacity of 5000 kg and the number of flights of 100. However, these costs can be further decreased, given that these are solely the first unit costs. The biggest cost factor is that of the unit, and the cost given the learning curves of the individual items per unit number are given in Figure 4.1. As can be seen, as much as 1.47 million USD per MEV can be saved, significantly decreasing the cost of the MEV with over 11%.



Figure 4.1: Cost savings with respect to the first produced unit due to learning curve (f_4) effects.

In addition, the launch cost per kg from Earth to LEO was also found. This will be approximately 1411 USD per kg for the Falcon Heavy, as is discussed in subsection 3.3.3.

So to conclude, although the ticket price, or cost per kg to the surface of Mars is currently above the required 10,000 USD per kg, the cost saved given the learning curve of solely the MEV shows that this requirement can be met over the course of the programme.

4.3. Technical Risk Assessment

The Technical Risk Assessment presented in the Midterm Report is reassessed for its applicability at this stage of the project where more is now known about the system design and potential new risks that may occur. Tables 4.6, 4.7, and 4.8 present the technical, schedule, and cost risks respectively. For each of these risk, the probability of

occurrence and the severity of the impact are given on a scale of 1 to 5. A number of risks have been eliminated and new ones identified, which are highlighted in orange.

Table 4.6: Technical risks, probabilities and impacts.

Number	Risk Description	Prob.	Impact	Risk
1	Cannot meet safety factors: The system can only be designed without taking safety	2	4	8
	factors in account;			
2	Theory is too complicated: Required mathematics cannot be understood by Bachelor students;	1	2	2
3	Tools needed are not available: Design of the system requires software or hardware	3	3	9
	which cannot be obtained or does not exist;			
4	ΔV insufficient: The stages of the journey combined require an unobtainable large amount of ΔV ;	1	5	5
5	Cannot meet regulations: The system can not be certified by authorities due to non-compliance with regulations;	1	5	5
6	Cannot be reusable: System can only be designed as an expendable vehicle;	2	4	8
7	Cannot meet reliability: Design can only be completed with a reliability lower than 99.6%;	2	4	8
8	Cannot meet MEV reusability requirement: MEV design deteriorates too quickly to complete 100 launches/landings;	5	4	20
9	Cannot meet payload requirement: Design only allows too small a payload to complete the journey;	2	5	10
10	Cannot be manufactured: System design requires manufacturing processes which do not exist:	1	5	5
11	Cannot meet spaceship reusability requirement: Spaceship design deteriorates too quickly to complete 10 Earth-Mars return flights;	3	4	12
12	Faces opposition from nuclear regulations and the public perception surrounding nuclear power.	3	4	12
13	Cannot meet mass budget.	2	4	8
14	Cannot meet power budget.	2	4	8
15	Cannot meet link budget.	2	3	6
16	Trade-off is not valid. Important aspects not considered.	2	3	6
17	Incorrect Verification & Validation. Design has mistakes and irregularities.	1	3	3

Table 4.7: Schedule risks, probabilities and impacts.

Number	Risk Description	Prob.	Impact	Risk
18	Design cannot be finalised in 11 weeks: Design requires more time to be completed;	2	3	6
19	Deadline not met: Specific milestones and deliverables are not completed on time;	2	5	10
20	One subsystem design over schedule: Delay of a single subsystem causes delays in the rest of the project;	3	4	12
21	Cannot be ready by 2030: First journey of the craft cannot be launched in or before 2030;	2	3	6
22	The launcher contractor does not meet the required launch schedule.	2	5	10
23	Launcher is discontinued.	2	5	10

Table 4.8: Cost risks, probabilities and impacts.

Number	Risk Description	Prob.	Impact	Risk
24	Cannot meet launch budget;	1	4	4
25	Cannot meet overhaul cost limit;	2	3	6
26	Cannot meet cost per kg to Mars limit.	1	5	5

Risks 13 to 15 have been added as with further defined resource budgets there is now a possibility to over run these budgets. The impact of each of these risks vary as going over budget on some of them these has much more impact than others. The risk of the trade off not being valid is added as further analysis of the previous Trade Offs has shown that they have the possibility of not being accurate exists. Incorrect V&V has been included as with a greater emphasis on this practise there is also a chance it may be done incorrectly. Finally the risk that the launcher is discontinued as it is not definite the Falcon Heavy may remain in service.

4.3.1. Risk Map

The risk discussed above are placed in Table 4.9. Risk in the orange and red zones must be mitigated, as is discussed in subsection 4.3.2.

Probability						
5				8		
4						
3			3	11, 12, 20		
2			15, 16, 18, 21, 25	1, 6, 7, 13, 14	9, 19, 22, 23	
1		2	17	24	4, 5, 10, 26	
	1	2	3	4	5	Impact

Table 4.9: Risk map: shows which risks need to be assessed.

4.3.2. Risk Mitigation

In this section each of the risks discussed above, that are in the red or orange risk areas of Table 4.9, are addressed. These risks can be mitigated using different methods, as shown in the risk map in Figure 4.2. Avoid means to change plans to circumvent the problem. Reduce means to reduce the impact or likelihood of the event. Transfer means to outsource risk, by sharing the risk with a third party or an insurance contract. Accept means to take the chance of the negative impact or budget the cost, while continuing to monitor the risk and reassess it throughout the project.

The following risks are to be avoided due to their combination of high probability of occurrence and the severity of their impact, meaning they are highly undesirable to occur.

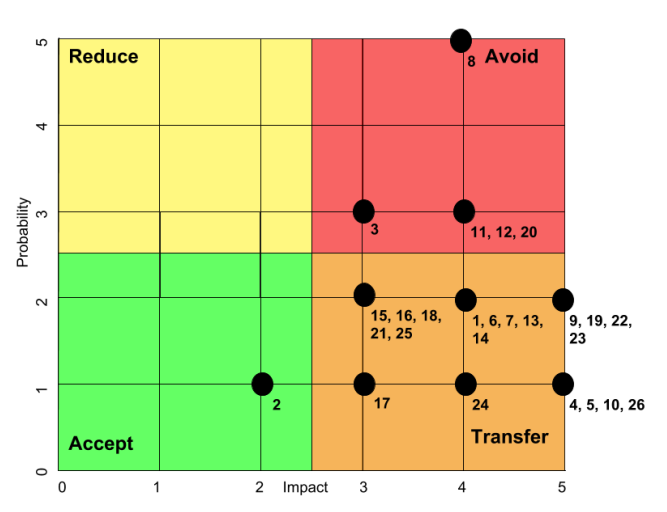


Figure 4.2: Risk chart: a representation of how the risks should be handled.

8: MEV cannot meet the reusability requirement of

100 flights. Avoided by doing research in materials and reusability techniques. One could also use more technologies that have a high technology readiness. More testing and unmanned flights can also be used to avoid this risk.

- 11: Spaceship cannot meet the reusability requirement of 10 Earth-Mars flights Avoided by reducing the reusability requirement or by performing more research in materials and reusability. Adjusting the mission profile would also tackle this risk.
- 12: The nuclear systems face obstacles from regulatory or perception issues One way to avoid this risk could be to invest some project funds in a public education campaign, demonstrating the relative safety of Nuclear Thermal Engines, illustrating the major misconceptions surrounding nuclear power, and teaching the public how the engine works to generate interest and abate concern. This would mean that the probability of this risk would be avoided.
- **20:** A single subsystem design is over schedule This risk is avoided through allocating more time and resources towards subsystems estimated to go over schedule; by incorporating margins for critical paths, make designs independent of each other. This means delays do not cause the subsequent delay of other subsystems.

Similarly, the following risks should all be transferred because while their probability of occurrence is relatively low, the impacts are severe enough that the project would benefit from them being someone else's responsibility.

- **9: The system cannot meet the payload requirement** Transferred by using a commercial launch provider and contractually enforcing them to provide a certain payload to to LEO per unit of time.
- **19: Deadline is not met** This risk is transferred. Internal deadlines can be ensured by incentivising meeting deadlines or completing work before deadlines or by negotiating an extension with the Tutors, or whomever is leading the project post DSE. Overall this is a risk that will have to be monitored, and likely the scheduling reassessed if it turns out to be a reoccurring event.
- **22:** Launch contractor does not meet schedule This risk is transferred. Contractual incentives may be used to motivated the launcher contractor to meet their deadlines. These included bonuses or guaranteed continuation of contracts in the event that they meet their deadlines or are ahead of schedule. This both reduces the probability of

this risk occurring and as well as reducing the (financial) impact. Hence the risk is transferred.

23: Launcher being discontinued This risk is transferred. The MEV, EEV, and ITV modules may be designed to be compatible with future launchers. The contractor may be requested to maintain the same interface geometry and payload capacity on a future launcher. Additionally contractual obligations may be put in place to incentivise the continuation of the Falcon heavy.

 Probability

 5
 4
 3
 3, 20
 4
 4
 4
 4
 4
 4
 5
 1, 6, 7, 8, 11, 13, 14
 4, 5, 10, 26
 1
 2
 17
 22, 23, 24
 4, 5, 10, 26
 1
 1
 1
 1
 1
 1
 1
 1
 1
 1
 1
 1
 1
 1
 1
 1
 1
 1
 1
 2
 1
 1
 1
 1
 1
 1
 1
 1
 1
 1
 1
 1
 1
 1
 1
 1
 1
 1
 1
 1
 1
 1
 1
 1
 1
 1
 1
 1
 1
 1
 1
 1
 1
 1
 1
 1
 1
 1
 1
 1
 1
 1
 1
 1
 1
 1
 1
 1
 1
 1
 1
 1
 1
 1
 1
 1
 1
 1
 1
 1
 1
 1
 1

Table 4.10: Risk map: with mitigation applied.

Table 4.10 shows the risk map, indicating the probability and severity of each risk, after the mitigation strategies have been applied. As can be seen, there are still risks that are currently not yet discussed. Although less critical than the discussed risks, the mitigation strategy which they fall under still applies in case the risk occurs. It should be noted that especially the risks that have a high probability will be monitored throughout the project.

4.4. Verification and Validation Procedures

Technical verification and validation (V&V) consists of verifying and validating the calculations performed during the design process. Verification involves checking that calculations were performed correctly, with the use of unit tests and system tests. A unit test is a test where a specific component of a model is tested, providing an input to that model, and comparing the output with a known or calculated output. A system test is a test which tests the inputs and outputs of the entire model, usually by comparing the results to that of a similar model, or sometimes by results calculated by hand. The assumptions used for verification can be simplified.

The System Engineer is responsible for ensuring all verification steps are performed. For each test case, the inputs are given, as well as the expected (verification) output and the actual output, and the percent error. In general if the error is greater than 5% a good explanation is given for why the discrepancy is acceptable.

Validation is performed by comparing results with other models, real life development and/or other analysis performed on the subject. In general, this will prove difficult for the MEV, as similar vehicles do not yet exist. Instead, as part of verification, any results can be compared with existing vehicles with different purposes, such as the ISS, or with mission concepts for a similar Mars lander, such as ESA's proposal.

Finally, it is specified how the system will be verified during and after development. This is in one of four ways⁶:

- **Inspection:** the design can be inspected to show compliance with requirements using human senses (e.g. if you want to check that something shall be 27 cm long);
- · Analysis: a mathematical analysis can show that the product complies with the requirement;
- **Demonstration** indicates compliance through manipulation of the system as it is intended to be use (e.g. when the button is pressed the correct thing happens);
- **Test** show that the system performs correctly by a comprehensive test with predefined variables and inputs (preferably in the field).

4.4.1. Implemented V&V Techniques

The techniques described above are implemented in the report when there are calculation methods are involved. the specific V&V (if applicable) is described in the designated sections. In Table 4.11, all the different techniques applied in the project are applied.

 $^{^6} http://www.modernanalyst.com/Careers/InterviewQuestions/tabid/128/ID/1168/What-are-the-four-fundamental-methods-of-requirement-verification.aspx(Last accessed 05-06-2018)$

	Unit tests	Analytical Models	Literature Examples
Structures	Singularity tests (zero-stress in-	Use of analytical methods by Hi-	Comparison with examples by
	put), sensitivity tests	bbeler and Yap [16]	Hibbeler and Yap [16]
Ascent	Signal scoping, singularity tests	Using party rendezvous software, simplified trajectory (vertical launch and circularisation)	-
Descent	Individual forces	Approximate equations for descent trajectories	-
Thermal	Temperature distribution tests	Use of the Midterm preliminary sizing sheet Midterm report initial calculations	Comparison with ESA's proposal and ISS values
Pressure tanks	Confirmation of mass and volume reference using CATIA	-	Comparison with examples by Hibbeler and Yap [16]
Engine	Area calculations	Delft Aerospace Rocket Engineering (DARE) cryogenic engine sizing sheet	Comparison to LE-5 engine

Table 4.11: A summary of all the V&V techniques applied.

4.4.2. Final Design Qualification

The final design, when completed, will require extensive qualification in order to confirm it meets the requirements. For specific requirements, verification procedures have already been determined, i.e. test, analysis, etc.

For the subsystems and eventually the full system, there must be additional proof that the combination of components meets the design. The procedures use the following philosophy: testing is in all cases preferred, considering that this is a high risk and manned mission. Analysis will be used only where testing is infeasible. It must be noted that unmanned missions will take place before manned missions, meaning that this 'start-up phase' may act as the final stage of validation for manned transfer. The list below focuses on the testing of the MEV, but is in general also applicable to the other vehicles.

- The structural component of the MEV requires full testing, similar to procedures currently utilised on commercial aircraft. Destructive testing may even be considered in case this is economically feasible.
- The propulsive system will be tested extensively. For the engines, this includes cold flow tests, static firing tests, as well as firing tests to validate more specific functions, such as vectoring and re-ignition. Vacuum function requires analysis, although it may be opted to provide the engine as testbed for other missions.
- The trajectory, including re-entry, must be analysed. Interplanetary transfer, rendezvous/docking and Mars reentry is currently well understood, so special attention should be put towards ascent trajectories from Mars. However, all ADCS components can be easily tested both in test facilities as well as potentially in orbit. Especially if readily available components are used, testing costs can be lowered significantly.
- Although full validation of the full thermal system may prove difficult, individual components and subsystems, like the coolant loops, can be tested on Earth. The system may require analysis for the performance over the full temperature range.
- The life support system is rudimentary and very similar to existing architecture. Depending on the actual hardware selected, testing of the components may already be done, which means only integration testing is necessary.
- The communication system's components can be tested, although confirmation of their performance over large distance requires an analytic approach. Transmission gains can be artificially reduced to emulate space losses. It must be noted that crew and operations must take into account the 30 minute communication delay, which is important for planning and training.
- The power system can be tested intensively for high power draw, this includes the solar panel at artificially lowered solar intensities. Performance losses due to degradation must be analysed, however.
- The mechanical systems for embarkment and docking can be tested on Earth. This includes components as well as the full systems. Test dockings may take place in Earth orbit as well.

4.5. Sustainable Development Strategy

On a mission of this scale, it is important to consider sustainability, as a small reduction in resource use can have a large impact over many missions. As is shown on Figure 4.3, sustainability must be considered for both mission and production phases, and for both, the energy, the emissions, the reusability and the contamination levels must be analysed. First, the sustainability of design choices made will be analysed in subsection 4.5.1, after which several production and operational phases shall be looked at in depth, including transportation of components and the manufacturing of materials.

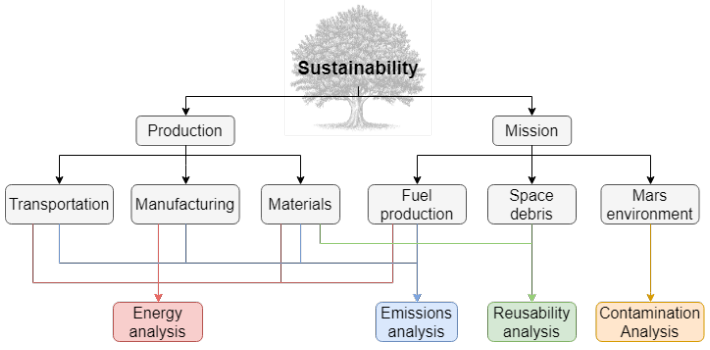


Figure 4.3: Branches of the sustainability tree.

4.5.1. Sustainable Design Choices

Throughout the design of the MEV and other mission vehicles, a number of design choices were consciously made in order to ensure the sustainability of Project Cardinal.

The fuel selected for use on both the ITV and MEV is liquid methane. Due to its high density, relatively small fuel tanks are required, which reduces the structural mass. This mass reduction means a higher fraction of the mass can be dedicated to useful payload. Methane is also chosen for its compatibility with in-situ resource utilisation (ISRU) on Mars, as methane can be produced on the Mars surface, from the carbon dioxide in the atmosphere, using the Sabatier process [17]. However this requires hydrogen, power, and some chemical infrastructure to be available, hence, ISRU will only be used in later phase. However, making fuel on Mars means that the ITV does not need to bring the fuel for the MEV or for the return journey, as it can be refuelled in Mars orbit by (modified) MEVs. This will improve the sustainability of the project, as it reduces the mass to be launched from Earth, which greatly reduces emission output. It was found in the Midterm Report that employing ISRU would reduce the mass of the system by about half [3]. It may also be possible to make oxidiser for the MEVs on Mars, through the electrolysis of water. However, electrolysis has high power requirements, so at this stage is not being considered.

The ITV uses a NTR this allows for a much higher I_{sp} than conventional chemical engines [2]. This higher I_{sp} more than halves the mass of the overall system [3]. This is as the mass reduction from the needing less fuel and no oxidiser, which reduces the tank mass, is significantly larger than the mass increase from the additional shielding for the radiation. This makes the system more sustainable since fewer resources are required to construct the ITV, which also reduces the launch mass, reducing CO_2 emission. However, the use of NTR involves launching nuclear material. If there were to be a failure during launch, and nuclear waste thrown out into the atmosphere, the consequences to the environment and human life could be far more detrimental than the emissions being reduced.

Every vehicle designed as a part of Project Cardinal is designed to be reusable. This was done to reduce costs, as well as to increase sustainability, as it will decrease both the amount to be manufactured, as well as the mass to be launched, with both reduce emissions and waste. This will be achieved through the selection of materials which can withstand the hostile environments, as well as well planned maintenance, as is discussed in subsection 6.3.3. This philosophy is also reflected in the choice of launch vehicle, for which the fully reusable version of SpaceX's Falcon Heavy, further increasing sustainability. However, this reusable vehicle has a smaller payload than the expendable one, meaning more Earth launches must be performed, which will increase emissions. As such, further analysis should be performed to ensure the consequences do not out weigh the benefits.

Another aspect is that the standardisation of parts and the use of similar or identical vehicles for multiple purposes. For instance the EEV and MEV are expected to be virtually identical, this will increase production efficiency and hence save resources. Furthermore the same ITV is designed to carry people on the Mars-Earth route and cargo on

both the Earth-Venus-Mars and the Earth-Mars route [3], which will reduce the amount of vehicles to be manufactured.

4.5.2. Transportation

Transportation of parts on Earth, is a major use of resources and contributor to greenhouse gas emissions. Even electric vehicles in the United States contribute to emissions and resource depletion, as 64.2% of electric power comes from non-renewable resources, though it should be noted this number varies wildly between regions⁷. Using the lean manufacturing methodology, all parts of the spacecraft can be produced in the same factory to minimise the amount of transportation. However, the need for transportation of the spacecraft to the launchpad and from the launch site will always remain.

4.5.3. Manufacturing of Materials

On both the MEV and the ITV, the main materials used are aluminium, carbon fibre and Kevlar. While these materials have structural advantages, their manufacturing can be resource heavy and produce a lot of emissions.

Aluminium

Aluminium is often used in aerospace applications because of its excellent mechanical properties and low weight. Unfortunately the primary production process is energy intensive. However, the impacts of this can be mitigated through the of renewable energy such as hydro-electric, as is already prevalent in the industry⁸. Furthermore aluminium is 100% recyclable without loss of properties⁹, meaning vehicles can be deconstructed at their end of life, and used for other purposes. The sustainability can also be improved through the use of recycled aluminium, as recycling aluminium only requires 5% of the energy needed to smelt primary aluminium¹⁰.

Carbon Fibre

Current practices for producing carbon fibre is a very wasteful process (30% waste ¹¹, and the technology to recycle it without heavily degrading the mechanical properties is still under development, meaning it is not the most sustainable material selection. However, demonstrations for a recycling technique have been performed, which is expected to flourish as a technology in the near future ¹². Currently carbon fibre is made from fossil resources, there are efforts to develop biomass-based carbon fibre ¹³. This ties into the importance of the reusability of the vehicles mentioned in subsection 4.5.1, in order to reduce the amount of carbon fibre which has to be produced.

Kevlar

Kevlar is a synthetic, aramid fibre, composed of poly-para-phenyleneterephthalamide. It is made from a chemical reaction between para-phenylene diamine and terephthaloyl chloride. Para-phenylene diamine is higly toxic when orally ingested, is not carcinogetic and exposure to the skin can lead to chronic dermatitis¹⁴. When working with para-phenylene diamine proper skin protection must be used. Terephthaloyl chloride is an acid chloride which, at room temperature, is a corrosive cristalline. It is incompatible with alcohols, oxidisers, water and strong bases, and causes severe burns and eye irritation¹⁵. When working with terephthaloyl chloride, special skin protection must we worn and special attention should be given to storage. This indicates the importance of reusable vehicles in order to reduce the amount which has to be produced. Fortunately, Kevlar is 100% recyclable, as the Kevlar fibres can be chopped up or pulped and spun into new Kevlar fibres¹⁶. As such, the use of recycled Kevlar within the project will improve sustainability.

General Manufacturing

In order to increase the sustainability during the manufacturing process, some general measures should be taken. First, waste can be reduced by adopting a lean manufacturing philosophy such as 5S, 6σ or just-in-time. These

⁷https://www.eia.gov/(Last accessed 05-06-2018)

⁸ https://www.aluminiumleader.com/production/how_aluminium_is_produced/(Last accessed 05-06-2018)

 $^{^9 \}texttt{http://www.aluminum.org/industries/production/recycling} (Last accessed \, 05-06-2018)$

¹⁰ https://www.hulamin.com/about/aluminium-todays-world(Last accessed on 05-06-2018)

¹¹http://zoltek.com/products/recycled-fiber/(Last accessed 02-07-2018)

 $^{^{12} \}mathtt{https://www.compositesworld.com/columns/recycled-carbon-fiber-its-time-has-come-(Last accessed 05-06-2018)}$

¹³ https://www.energy.gov/eere/articles/energy-department-announces-11-million-advance-renewable-carbon-fiber-production(Last accessed 05-06-2018)

 $^{^{14} \}texttt{https://www.epa.gov/sites/production/files/2016-09/documents/p-phenylenediamine.pdf} (Last accessed 05-06-2018)$

¹⁵https://www.alfa.com/en/catalog/A11224/(Last accessed 05-06-2018)

 $^{^{16} \}mathtt{https://kevlarchemistry.neocities.org/about 3.html} (Last accessed \ 05-06-2018)$

methods aim to increase the efficiency of the production process by reducing waste, therefore increasing the sustainability. As mentioned above, another method to make the process more sustainable, is the use of renewable energy sources, such as hydro-electric energy, making the project more sustainable than when using conventional energy sources such as fossil fuels.

4.5.4. Fuel Production

The Mars Excursion Vehicle uses LOX/LCH $_4$ as propellant. These propellants require both energy and natural resources to be produced on Earth. LOX will be produced by the energy intensive process of cryogenic distillation with a net electrical energy of roughly 16,560 MJ/tonne of LOX produced [18]. The required amount of LOX on the MEV is 35.98 tonnes, thus needing about 595,897 MJ of energy. Natural gas produces about 0.051 kg CO_2/MJ thus filling up an MEV with LOX will cost 3,039 kg of carbon dioxide (CO_2) [19]. Therefore it is recommended to reduce the structural mass of the MEV as much as possible, which in turn will reduce the propellant required.

4.5.5. Contamination Prevention

One of the key issues to be considered when becoming an interplanetary species, is the avoidance of cross-contamin ation between planets. Procedures for forward contamination prevention are well established. Construction of sensitive parts must be performed in cleanrooms: NASA requires International Organisation for Standardisation (ISO) Class 5 or better, meaning Project Cardinal requires paid utilisation or construction of certified cleanrooms. Completed systems are historically sterilised using dry heat microbial reduction (DHMR), akin to a large dry heat oven, as this is currently the only method fully approved by NASA¹⁷.

In addition to this method being potentially damaging to components, performing DHMR on the full MEV design would require construction of a much larger oven. As such, other methods are currently being researched. Vapor Hydrogen Peroxide (VHP) is certified by NASA, but procedures have not been published [20]. This will likely be finalised during the development process. VHP is expected to be more convenient for a system the size of the MEV, however, the hydrogen peroxide may affect surface materials, so this must be considered during construction.

The pre-launch handling of the MEV is therefore suggested as follows: components are constructed in cleanrooms, and the full MEV will be sterilised preferably by VHP. Any other material which may come in contact with the Martian environment, such as spacesuits and habitat materials, will also be sterilised. It is advised that human crews are separated from the Martian environment at all times. The crew will always be within wither a pressurised vehicle, habitat, or spacesuit. However, during the transfer between any two, issues with contamination could still arise. However, ESA's proposal spacesuits [11] suggest the suits have a hatch on the back and are connected to the outside of the ship. Astronauts can enter and exit the suit through the hatch, without need for an air lock. This prevents contamination, by improving the separation between the Mars environment and the controlled crew environment.

This form of separation will be applied to surface samples as well, with it being advised to keep them separate from both crew and other cargo. In fact, samples should remain in quarantine even when back on Earth, as well as during on-Earth research. This is the main prevention method against back contamination. While NASA is currently planning the construction of a Mars sample return facility for these exact purposes, it may also be useful to determine the actual hazard levels of the sample while in space, e.g. while on the ITV.

4.5.6. Space Debris

In Earth orbit space debris is already a concern¹⁸ posing risks to vehicles and satellites alike. Project Cardinal is not expected to produce space debris during nominal operations since the EEV, ITV and MEV are reusable and will be properly decommissioned once they reach their end of life. The MEV will probably be decommissioned at Mars. The EEV can be decomissioned on the Earth surface. The ITV can be decommissioned in orbit around Earth. The chosen launcher, SpaceX's Falcon Heavy, has a reusable first stage¹⁹ and fairings²⁰. The second stage does not produce space debris either²¹. Therefore, in terms of waste left in the space, the project can be deemed to be sustainable.

 $^{^{17} \}verb|https://mars.nasa.gov/mer/technology/is_planetary_protection.html| (Last accessed 05-06-2018)$

¹⁸ http://www.esa.int/Our_Activities/Operations/Space_Debris/FAQ_Frequently_asked_questions(Last accessed 05-06-2018)

¹⁹https://www.theverge.com/2018/5/9/17254384/spacex-falcon-9-block-5-upgrade-rocket-reusability-savings (Last accessed 05-06-2018)

²⁰https://spaceflightnow.com/2018/06/01/new-photos-illustrate-progress-in-spacexs-fairing-recovery-attempts/(Last accessed 05-06-2018)

²¹https://space.stackexchange.com/questions/7814/what-happens-to-the-falcon-9-second-stage-after-payload-separation(Last accessed 05-06-2018)

Subsystem Design

In this chapter a preliminary design of the subsystems of the MEV is done. Trade-offs are done, programs are explained and verification is performed. Alongside this, a sensitivity analysis of the tools is done.

This chapter details the design of the subsystems that the MEV consists of. Many of the subsystems design necessitate the use of sizing tools created by the Project Cardinal team, these tools are described in this section too. In section 5.1, the design of the main engines, the sizing of the main propellant tanks and pressurant tanks and the sizing of the RCS system is described. section 5.2 describes the orbits used during the detailed design of the MEV, as well as the atmospheric trajectories and landing locations. The outputs of this system such as propellant necessary for ascent and descent are used integrally in the structures and propulsion sections. In section 5.3, the sizing of all structural elements of the MEV is discussed. This involves an outline of the tool created and the load cases involved in sizing the skin and floor thicknesses. This section also discusses the sizing of the air brakes and the landing legs.

In section 5.4, an overview is given of the necessary hardware for the life support system. This entails the sizing of the oxygen and nitrogen tanks that allow for the entire crew to survive for three days. Then, section 5.5 elaborates on the communication system integrated into the MEV. It consists of two X-band antennas to provide for a signal-to-noise ratio of 10 dB. In section 5.6, the batteries and solar panel size, location and design is discussed. In section 5.7 the tool developed to size the thermal system is elaborated upon. In section 5.10 the main hardware, communication-, mechanical- and power hardware diagram are given. It also lists the communication flow diagram, data handling block diagram and the electrical block diagram. In subsection 4.1.6 the payload of the MEV is specified. Finally, section 5.12 explains how safety factors and margins were used during the design process, and explains how iterations were performed and shows the conclusion of these iterations.

5.1. Propulsion

This section contains an overview of the propulsion system. First the injector and igniter type will be chosen, after which full sizing of the engine chamber and nozzle will be provided. Then the propellant tanks will be fully sized, after which a discussion on cooling and a trade-off for the RCS thruster propellant will be held. Finally, the storage of the propellant and the launch abort system will be discussed. Any values taken from literature that are used in the propulsion section are clearly cited, though all values for chemical properties of the combustion process are taken from the program Rocket Propulsion Analysis¹.

5.1.1. Injector

A qualitative trade-off was performed for the injector with five criteria, where a grade of 0 means it is unacceptable, a grade of 1 means it is not favourable, but possible. A grade of 2 means it is definitely possible, but not the best option, and a grade of 3 means it is entirely suitable:

- **Use in LOX/Hydrocarbon:** this is important as an injector not compatible with LOX/Hydrocarbon cannot be used, however modifications to existing injectors could be made at the cost of time, money and complexity, therefore it is given a weight of 2.
- **Throttlability:** is the ability to throttle, which is essential to perform a power landing, and is therefore given a weight of 3.
- **Combustion stability:** is related to the disturbances introduced during the injection, as these can cause vibrations which can then magnify these disturbances. As it is not the most important factor, it has been given a weight of 1.
- Mixing properties: affect the efficiency of the engine, as it determines how well the fuel and oxidiser mix before combustion. It has therefore been given a weight of 2.

¹http://propulsion-analysis.com(Last accessed 15-06-2018)

• **Inherent cooling:** affects the complete cooling system, as the external cooling system does not have to be as extensive when inherent cooling is present. It has been given a weight of 1.

Type of injector			Use in LOX/ Hydrocarbon (2)	Throttlability (3)	Combustion Stability (1)	Mixing (2)	Inherent Cooling (1)	Total
	Like	Doublet	3	1	2	3	1	2.0
Impinging jet	LIKE	Triplet	3	1	2	1	1	1.6
injector	Unlike	Doublet	3	1	2	2	2	1.9
	Ullike	Triplet	3	1	3	3	2	2.2
Coaxial injector	Shear		0	1	3	3	3	1.7
Coaxiai injector	Swirl		2	1	2	3	3	2.0
Pintle Injector			2	3	2	2	3	2.4

Table 5.1: Injector Trade-off.

All information on the injectors is based on Huzel and Huang [21], unless stated otherwise.

Use in LOX/Hydrocarbon

A coaxial shear injector has not been used in LOX/hydrocarbon engines before, therefore it has been given a grade of 0. The impinging jet injectors are generally used with LOX/hydrocarbon engines, therefore they have been given a weight of 3. A coaxial swirl injector and pintle injector have been used in the past, however not as frequently as the impinging jet injector, therefore it has been given a grade of 2.

Throttlability

Upon a literature analysis it was found that most injector types are not easily throttlable, they tend to lose efficiency and mixing characteristics, except for a pintle injector which can retain its efficiency. Therefore the pintle injector has been given a grade of 3, while the others have a grade of 1.

Combustion stability

The coaxial swirl injector, the impinging jet injectors (except for the unlike triplet) and the pintle injector induce small disturbances into the engine structure, however these are not very severe, therefore they have been given a grade of 2. The unlike triplet impinging jet injector and the coaxial shear injector induce negligible disturbances, and have therefore been given a grade of 3.

Mixing

The like doublet and unlike triplet impinging jet injector and the coaxial injectors produce the smallest droplets, therefore increasing the mixing properties and have been given a grade of 3. The unlike doublet impinging jet injector and the pintle injector have a slightly lower performance, and have therefore been given a grade of 2. The like triplet impinging jet injector does not have good mixing properties, therefore it has been given a grade of 1.

Inherent cooling

The like impinging jet injectors do not have inherent cooling, and have therefore been given a grade of 1. The unlike impinging jet injector have some inherent cooling, and have therefore been given a grade of 2. the coaxial injectors and the pintle injector all adopt some sort of inherent cooling, and have therefore been awarded a grade of 3.

For each injector, the grade for each criterion is multiplied by the weight of each criterion and is then added up to get a total score. As can be seen from Table 5.1 above, the pintle injector is the highest ranked option.

Sensitivity Analysis

When changing the weights, the winning option shifts between the triplet unlike impinging jet injector and the pintle injector. However, as the throttlability of the impinging injector is very poor, this is not seen as a fully feasible option. Also, the pintle injector does not score poor on any criterion, while all other injectors have at least one grade of 1 assigned. This implies that the pintle injector is indeed the best option.

5.1.2. Igniter

There are two main ignition categories: either using a hypergolic propellant or using an external ignition system. As LOX/LCH₄ is not hypergolic, an external ignition system must be used. This could either be a chemical or an electrical igniter. A chemical igniter uses a separate hypergolic propellant to ignite the main propellant, however, as it can run out during the mission it is not seen as the optimal solution. An electrical ignition uses either a resistant

wire to produce enough heat to induce combustion, or a spark torch or a laser to ignite the propellant². Laser ignition is a technique which is currently under research, but has an insufficient technology readiness level to be considered and option. Similarly, a resistant wire has proven to be successful, but has never been used on such a large scale before. This leaves a spark torch as the only viable option for the MEV.

5.1.3. Chamber and Nozzle Sizing

The MEV will have eight identical main engines, each of which will have a thrust of 50 kN, as mentioned in section 3.2. In order to size the engine's chamber and nozzle, a number of inputs were determined based upon existing engines. A chamber pressure of 70 bar was chosen based upon other LOX/LCH₄ engines, in particular those which are upper stage engines, such as the RD-183 which had a chamber pressure of 73.8 bar³. The atmospheric pressure at the surface on Mars is approximately 0.006 bar⁴. However, the exit pressure taken was 0.015 bar based on the p_e the LE-5 was sized for⁵, as sizing for perfect expansion to vacuum pressure would output an infinitely large nozzle.

The ratio of these pressures and the coefficient of specific heats, γ , gave an expansion ratio, ϵ , of 276.0 as shown in Equation 5.1 [22].

$$\epsilon = \frac{A_e}{A^*} = \frac{\Gamma(\gamma)}{\sqrt{\frac{2\gamma}{\gamma - 1} \left(\frac{p_e}{p_c}\right)^{\frac{2}{\gamma}} \left[1 - \left(\frac{p_e}{p_c}\right)^{\frac{\gamma - 1}{\gamma}}\right]}}$$
(5.1)

$$\Gamma(\gamma) = \sqrt{\gamma \cdot \left(\frac{1+\gamma}{2}\right)^{\frac{1+\gamma}{1-\gamma}}}$$
 (5.2)

In order to size the chamber and nozzle, a number of assumptions were made. This included the fact that the chamber will be maintained at constant pressure throughout the burn, which implies a constant mass flow. The thrust will change slightly through out the

Table 5.2: Inputs for nozzle and combustion chamber sizing.

Inputs	Symbol	Value	Unit
Chamber Pressure	p_c	70.00	[bar]
Exit Pressure	p_e	0.015	[bar]
Mixture Ratio	O/F	3.40	[-]
Chamber Temperature	$T_{\mathcal{C}}$	3,551.00	[K]
Molar Mass	M	21.67	[g/mol]
Ratio of Specific Heats	γ	1.17	[-]
Normal Operative Thrust	T	50.00	[kN]
Characteristic Length	L^*	1.01	[m]
Contraction Angle	$\boldsymbol{\beta}$	30	[deg]
Conical Expansion Angle	α	15.00	[deg]
Total Engine Efficiency	η_{en}	0.92	[-]
Contraction Ratio	ϵ_c	7	[-]
Fractional Length	l_f	80	[%]
Wall Angle Exit	$ec{ heta_e}$	7.0	[deg]
Wall Angle	θ_p	32.5	[deg]

burn, as the ambient pressure decreases from Mars sea level to the vacuum of space. However, as the increase in thrust between these two altitudes is less than 2.5%, the engine was sized assuming a constant thrust, and that thrust is the thrust at Mars sea-level.

The specific impulse of the engine, accounting for the efficiency, is found to be 340 s, which will be used for all calculations throughout the remainder of the report. As constant thrust, T, is assumed, the maximum mass flow can be found using Equation 5.3. Therefore, eight engine at 60% throttle have a total mass flow of 71.91 kg/s.

$$\dot{m} = \frac{T}{g_0 \cdot I_{sp}} \tag{5.3}$$

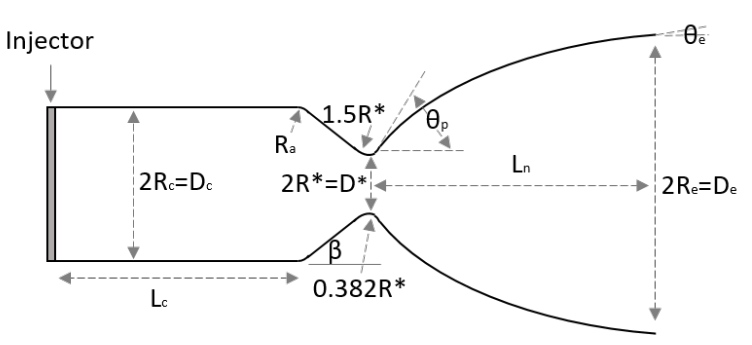


Figure 5.1: Chamber and nozzle geometry.

²https://blogs.nasa.gov/J2X/tag/ignition/(Last accessed 22-05-2018)

³http://www.astronautix.com/r/rd-183.html(Last accessed 14-06-2018)

⁴https://nssdc.gsfc.nasa.gov/planetary/factsheet/marsfact.html(Last accessed 14-06-2018)

⁵http://www.astronautix.com/l/le-5.html(Last accessed 14-06-2018)

Chamber Sizing

The throat area, A^* , is determined using Equation 5.4 which gives a throat diameter, D^* , of 70.3 mm. From this, a chamber diameter, D_c , of 186.0 mm, and an exit diameter, D_e , of 1,168.1 mm are found, based on the contraction and expansion ratios respectively. The contraction ratio is taken to be 7, given that for stability it must be larger than 3 [23] and that when using a pintle injector, a larger contraction ratio should be taken [24]. All of this geometry is depicted in Figure 5.1. Here the contraction radius is taken as $R_a = 0.2 \cdot D_c$, as typically $R_a < 0.5 \cdot D_c$ [23].

$$A^* = \frac{\dot{m} \cdot \sqrt{R \cdot T_c}}{p_c \cdot \Gamma(\gamma)} \tag{5.4}$$

The chamber volume, V_c , is calculated based on the characteristic length, L^* , as shown in Equation 5.5. There are varying definitions of the chamber volume. Huzel and Huang [21] and Sutton [25] define it as all of the volume between the end of the injector and the nozzle throat, while others define it as only the volume of the cylindrical section [23]. A L^* of 1,016 mm was taken, based on a LOX/Liquid Natural Gas engine with a similar injector [26], which was deemed sufficiently close to this LOX/LCH₄ engine. By replicating the calculations for this engine, based on the numbers provided [26], it was found that the L^* was for an engine where the V_c was defined as the volume of only the cylindrical part. From this, the length of the cylindrical part of the combustion chamber, L_c , was found to be 145.1 mm using Equation 5.6.

In addition the length of the conical part of the engine was found using Equation 5.7, where the contraction angle, β , is taken as 30° based on typical values for other engines [23]. The length of this section was found to be 100.2 mm, meaning the entire length between the end of the injector and the nozzle throat section is 245.3 mm.

$$V_c = L^* \cdot A^*$$
 (5.5) $L_c = \frac{V_c}{A_c}$ (5.6) $L_{cc} = \frac{R_c - R^*}{\tan(\beta)}$ (5.7)

Nozzle Sizing

It is decided upon to use a bell nozzle, due to its improved efficiency over a conical one. In general, due to the possibility to achieve shorter nozzle length, which allows for a lighter mass, this design can be seen to be more sustainable. This is not only as there is a lighter launch mass, which results in less emissions, as was discussed in subsection 4.5.1, but a lighter mass means a smaller cost, as was discussed in subsection 4.2.1. It is sized based on the RAO parabolic approximation, which is based on the length of a 15° conical nozzle [21]. While this method is a good approximation, the actual RAO parabola is much more complex and an improved approximation [23], but was deemed too extensive for this report. The fractional length is taken to be 80% as this typically lies in the range of 75-85% for bell nozzles⁶. From this the wall angles are determined to be $\theta_n = 32.5^\circ$ and $\theta_e = 7^\circ$ [21].

The length of the bell nozzle is found by multiplying l_f by the length of a 15 ° conical nozzle as is shown in Equation 5.8 [21]. Here, $\alpha = 15^{\circ}$, and $R_u = 0.382 \cdot R^*$ as defined by Huzel and Huang [21], and as is depicted in the Figure 5.1 above.

$$L_n = l_f \cdot \frac{R^* \cdot (\sqrt{\epsilon} - 1) + R_u \cdot (\sec(\alpha) - 1)}{\tan(\alpha)}$$
(5.8)

Then the coordinates (x_p, y_p) , which denote the beginning of the parabolic bell curve, and (x_e, y_e) which denote the exit, are found using Equations 5.9 to 5.12 [21].

$$x_p = R_u \cdot \sin(\theta_p)$$
 (5.9) $y_p = R^* + R_u \cdot (1 - \cos(\theta_p))$

$$x_e = L_n (5.11) y_e = R_e = \sqrt{\epsilon} \cdot R^* (5.12)$$

The equation of the parabola is determined from the known points and the wall angles [23].

⁶https://engineering.purdue.edu/AAECourses/aae439/2008/aae439_class_lecture/lecture_notes/chap4_71_95.pdf(Last accessed 14-06-2018)

Engine Size and Preliminary Mass Estimate

The final engine chamber and nozzle dimensions output by the program are shown in Figure 5.2. The total length of the entire engine is found to be 1.90 m.

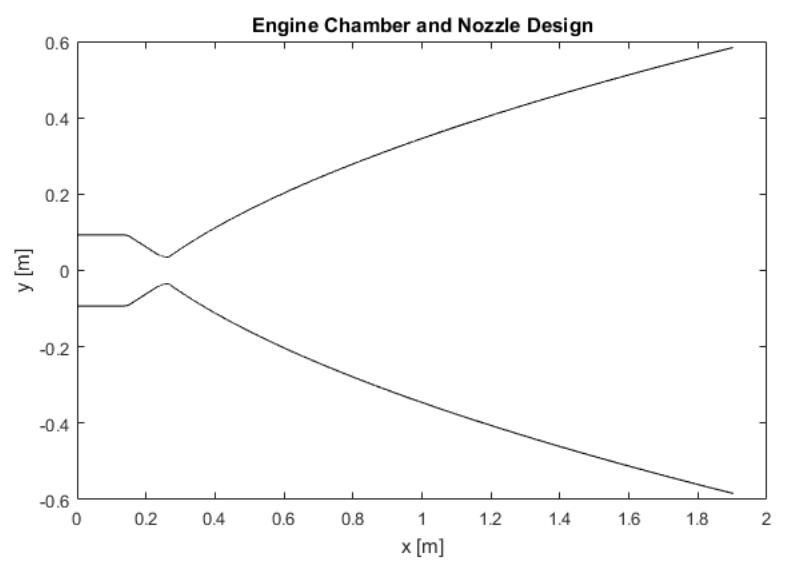


Figure 5.2: Engine chamber and nozzle sizing.

The required thickness of the combustion chamber is calculated using Equation 5.13. It is assumed that the chamber will be made out of Niobium C-103, which has a strength of 650 MPa⁷. This alloy was included as it is commonly used for rocket engines, including the main engine of the Apollo Lunar Modules [27]. This results in a thickness of 2.0 mm, which is accounting for a safety factor of 2. This thickness calculation does not account for the deterioration of the material strength due to the high temperatures, as it is assumed that the engine chamber will be cooled whilst it is being fired, as is discussed in subsection 5.1.5.

$$t_c = \frac{P_c \cdot R_c \cdot 2}{\sigma} \tag{5.13}$$

Due to the preliminary nature of this design, it is assumed that the chamber and nozzle are both made from the same material with the same thickness, and that the density of the Niobium C-103 is $8,870 \text{ kg/m}^3$, the wall mass is 66.8 kg. In order to determine the mass of the total engine, including the pumps and feed system, statistical relations are used. It is known that for a sea level booster, the wall mass is approximately 38.5% of the total engine mass [21]. By resizing the engine for sea level, the mass of everything except the wall mass was determined to be 38.0 kg. Assuming that as the ambient pressure is decreased only the mass of the wall structure is increased, and that the mass of the feed system remains constant, the total mass per engine can be found to be 104.8 kg. This is a total of 838.3 kg for all eight engines.

Sensitivity Analysis

In order to examine the stability of the propulsion design a brief sensitivity analysis was conducted where the requires thrust of the system is increased by 10% to 55 kN. This results in a 16% increase in the mass of the main propulsion system. This indicates that if the thrust continued to increase the propulsion system mass would diverge but the effects on the mass of the overall system could still be beneficial, if the reduction in propellant required is significant. This could be combated by decreasing the chamber pressure to circa 40 bar which would maintain the propulsion systems mass at the same level, but would drop the I_{sp} to 334 s. As such, during the detailed design phase a closer look at the benefits and disadvantages to the overall system mass of increasing the thrust by 10%.

A brief sensitivity was also performed on other key input parameters. The chamber pressure was first increased by 10%, which resulted in a 3.4% increase in engine mass, and a 0.3% increase in I_{sp} , while a 10% decrease in the cham-

⁷http://www.matweb.com/search/datasheet.aspx?matguid=2baabd47407946f183d091c199bf7914&ckck=1(Last accessed 10-06

ber pressure resulted in 1.8% decrease in mass, and an 0.3% reduction in I_{sp} . As such the system can be concluded to be fairly insensitive to a change in pressure.

Verification

In order to ensure there were no mistakes in the code, the data from the LE-5 engine, which is an upper stage LOX/LH₂ engine, is used as inputs. These known input values are shown in Table 5.3, with the rest of the inputs being assumed to be the same as for MEV. Using these values, a D_c of 248.1 mm is found, while the actual value is only 3% less [23]. It is also found that the total length is 2,605.8 mm which is 4.7% larger than than the actual value⁸, but this is still deemed acceptable as the exact fractional length of the bell nozzle is not known. Therefore it can be concluded that there were no major errors in the code.

Table 5.3: LE-5 reference data [23].

However, this method of verifying the code was not sufficiently accurate. Whilst reworking the equations by hand, it was found that the wrong temperature had been taken for calculating the throat area. This meant the diameter of the throat was 1.5 mm too small, but given this was only a difference of less than 2%, it was within the margin of error of the verification model. Based on the hand calculations and verification data, the code was deemed to be sufficiently accurate.

Table old III o folololice data [20].							
Inputs	Symbol	Value	Unit				
Chamber Pressure	p_c	36.80	[bar]				
Expansion Ratio	ϵ	140	[-]				
Mixture Ratio	O/F	5.50	[-]				
Chamber Temperature	T_c	3,304.00	[K]				
Molar Mass	M	11.80	[g/mol]				
Ratio of specific heats	γ	1.21	[-]				
Normal Operative Thrust	T	103.00	[kN]				
Characteristic Length	L^*	0.84	[m]				
Total Efficiency	η_{en}	0.95	[-]				
Contraction Ratio	ϵ_c	3.11	[-]				

5.1.4. Propellant Tank Sizing

In order to size the propellant tanks, a number of input values have to be established, which are given in Table 5.4.

*			· ·
Parameter	Symbol	Unit	Value
Propellant used descent	$m_{prop,d}$	kg	11,500
Propellant used ascent	$m_{prop,a}$	kg	24,000
Mixture Ratio	O/F	-	3.4
Oxidiser density	ρ_{Ox}	kg/m ³	1,141
Fuel density	$ ho_F$	kg/m ³	442.5

Table 5.4: Set inputs for the propellant tank sizing.

The propellant tanks are sized following the flow diagram as given in Figure 5.3.

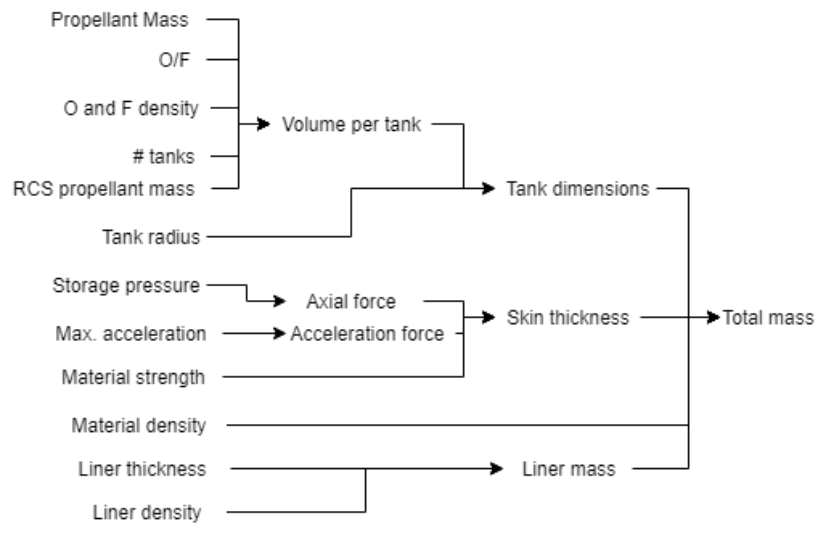


Figure 5.3: Flow diagram of the propellant tank sizing.

First, the required volume per tank is determined from the propellant mass (which is obtained from aerodynamics),

⁸http://www.astronautix.com/l/le-5.html(Last accessed 15-06-2018)

the oxygen-over-fuel ratio, the density of the oxygen and the fuel and the number of tanks, which can be varied. A 7% ullage is added [28]. Then an assumption is made that the tanks consist of a cylinder with two ellipsoid bulkheads at both ends, and with a tank radius almost spanning the full radius of the MEV, a tank height is found.

The thickness of the walls of the tanks is determined by the forces and pressures working in and on the tank. First the force on the bulkheads is determined (caused by the pressure on the bulkheads and carried by the skin of the tank), after which the added force due to the acceleration is added by multiplying the maximum acceleration (at Mars landing) with the propellant mass. This force is distributed over the area of the skin to get a stress, and with the ultimate stress of the material used for the tanks, the minimum thickness can be found. With the hoop stress, another thickness is calculated, and the most critical (higher) one is chosen as thickness of the propellant tank. Note that a safety factor of 2 is added to the ultimate strength of the material. For simplicity it is assumed the whole tank has equal thickness.

As Carbon Fibre Reinforced Polymer (CFRP) is not air tight, an aluminium liner is added. With the tank dimensions and the liner thickness, the liner mass is found. Together with the density of the CFRP, the total mass of the tank can now be found

Table 5.5 gives the variable inputs for the flow diagram. As material for the tank, T800/DGEAC CFRP is chosen, as it is a very high strength CFRP which is applicable for cryogenic temperatures. During launch from Earth, the tanks will not be filled with propellant. However, to prevent buckling, they will be pressurised.

	*			O
	Parameter	Symbol	Unit	Value
Material	Chosen Material	-	-	T800/DGEAC
	Aluminium density	$ ho_{Al}$	kg/m ³	2,700
	Aluminium thickness	t_{Al}	mm	0.5
Fuel	Number of tanks	$\bar{N}_{F,t}$		1
	Tank radius	$r_{F,t}$	m	2.3
	Storage pressure	$p_{F,t}$	Pa	2,400,000
	Ultimate strength	$\sigma_{F,ult}$	Pa	2,310,000,000
	Tank density	$\rho_{F,t}$	kg/m ³	1,570
Oxidiser _	Number of tanks	$\overline{N}_{Ox,t}$		1
	Tank radius	$r_{Ox,t}$	m	2.3
	Storage pressure	$p_{Ox,t}$	Pa	2,400,000
	Ultimate tensile strength	$\sigma_{Ox,ult}$	Pa	2,310,000,000
	Tank density	$\rho_{Ox,t}$	kg/m ³	1,570

Table 5.5: Variable inputs for the propellant tank sizing.

When considering all the above variables and calculations, a tank geometry and mass can be computed. The results are given in Table 5.6.

	Parameter	Unit	Value
Fuel	Radius	m	2.3
	Height	m	2.19
	CFRP skin thickness	m	0.00478
	Total mass (dry)	kg	417
Oxidiser	Radius	m	2.3
	Height	m	2.73
	CFRP skin thickness	m	0.00478
	Total mass (dry)	kg	487

Table 5.6: Propellant tank dimensions.

In order for the fuel to get to the engines, a fuel line is passed through the oxidiser tank.

Propellant Tank Pressurisation

As the tanks need to pressurised also when propellant is used, a separate tank with helium needs to be on board. Helium was chosen as it is commonly used for pressurisation. Assuming two spherical helium tanks (which eliminates the hoop stress) and using the same method as above and a safety factor of 2 a radius of 0.72 m and a thickness of 1.3 mm is found. Note that in this case, the helium tanks will be launched from Earth while filled, therefore the launch acceleration is taken as equal to a launch from Earth. This gives a total dry mass of 43.6 kg and a dry mass of 130 kg.

The helium will be strictly separated from the LOX and LCH₄ to avoid mixing. This will be done by placing either a piston or a bladder will be placed between the two to also maintain the pressure.

Verification

The program made to establish the dimensions, thickness and mass of the propellant tanks is verified using two different methods.

First, the computed dimensions of the tank are verified by constructing a similar shaped hollow tank in CATIA and checking whether the volume needed for the propellant and the volume enclosed by the tank are equal. For the oxidiser tank, a volume error of 0.02% is found, while for the fuel tank, a volume error of 0.27% if found.

For the thickness of the tank, a few simple examples of cylindrical and spherical tanks are plugged in to the program, and the results are compared. As the equations used in the examples are equal to the equations used in the program, no error was found.

Then, for the mass of the tanks, the thickness and the material are applied in CATIA, and the mass computed by CATIA is compared to the mass calculated by the program. For the oxidiser tank, a mass error of 0.02% is found and for the fuel tank, a mass error of 0.07% is found. These results are deemed sufficiently accurate to assume the program is correct.

Sensitivity Analysis

It is observed that, when changing the total propellant mass with 10%, the tank mass increases with 5.64%. This implies stability of the propellant tank mass, meaning that it is easily scalable and will not increase the total dry mass to an unreasonable amount. This behaviour is also observed during the iteration phase. When increasing the storage pressure in both tanks with 10%, the dry mass of the tanks increases with 5.14%.

5.1.5. Cooling

As the combustion temperature of LOX/LCH₄ is approximately 3,551 K, and the hot gasses of combustion have such a high heat transfer to surrounding structures, a means of cooling is necessary in order to prevent the material comprising the combustion chamber from failing. A number of options exist to allow for the cooling of thrust chamber walls; **regenerative cooling** - routing one of the propellants around the chamber to carry the heat away, **dump cooling** - similar to regenerative cooling where an amount of one of the propellants is used to cool the chamber before being dumped overboard, **film cooling** - where an amount of one of the propellants is injected into the chamber from small holes strategically placed along the chamber, this region of uncombusted propellant keeps the hot gasses away from the wall and is often used in combination with other methods of cooling, **transpiration cooling** - a propellants in gaseous or liquid form introduced to the chamber through a porous wall, a form of film cooling, **ablative cooling** - regions of the chamber are made from a sacrificial material that melts and vaporises, carrying the heat away as it is expelled, and **radiation cooling** - where heat is radiated away from the outer surface of the walls, most applicable to nozzles for use in space.

The injector that has been chosen, the pintle injector, possesses favourable inherent cooling characteristics, as illustrated in Figure 5.4[29]. As the fuel is injected through the coaxial annulus, the outer regions of the chamber are fuel rich zones and thus have a lower temperature than the inner regions. This alone will not be enough to cool the chamber. Calculations of the heat transfer along the chamber are considered outside of the scope of the preliminary design, though it can be said with certainty from analysing the current state of the rocket engine field, that regenerative cooling will be necessary, with perhaps additional film cooling in critical regions such as the throat.

5.1.6. RCS Thrusters

The Reaction Control System (RCS) is a system of thrusters providing attitude control. In this subsection, a trade-off will be performed to determine the propellant, and them a preliminary sizing of the thrusters will be done. Five trade-off criteria are used, since this is a wieghted trade-off each of these criteria is also given a weight:

- *I*_{sp}, given a weight of 3 as it is one of the most important factors in thrusters,
- **Toxicity**, as safety of both the ground- and aircrew is important, however with extra measures a toxic propellant could still be used, given a weight of 1,
- **Compatibility** with the system, as, preferably, one would take use the same fuel as for the main engine to reduce complexity in the system and to induce extra redundancy, given a weight of 3,
- **Operational Temperature**, as cryogenic propellants require an extensive cooling system, adding to the complexity of the system, given a weight of 2,

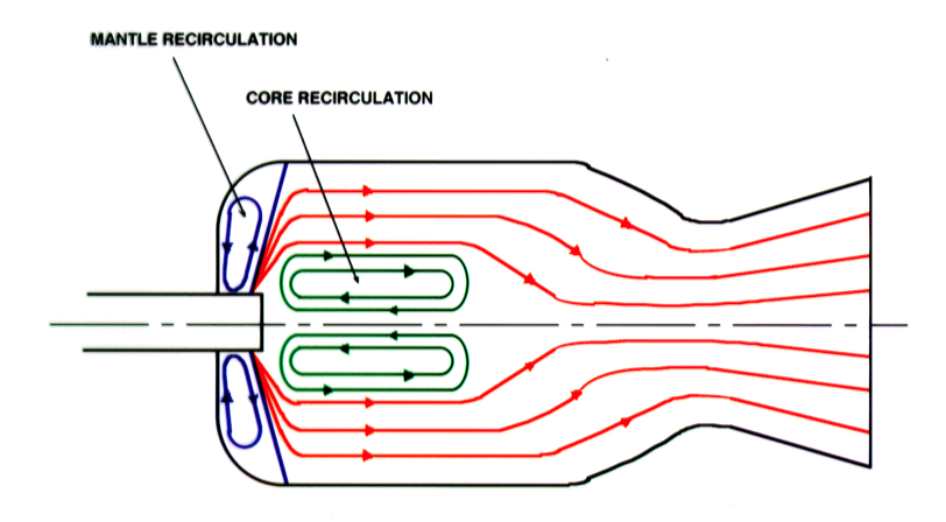


Figure 5.4: Cooling recirculation of a pintle injector.

• **Startup Behaviour**, as it is not desirable to have to wait before the thrusters can be utilised, especially at critical moments, given a weight of 2.

Hydrazine (MMH/NTO) is included in the trade-off since it is the most common RCS propellant, and it would be interesting to compare its performance to other propellants.

	I_{sp} (3)	Toxicity (1)	Compatibility (3)	Operational Temperature (2)	Startup Behaviour (2)	Total
MMH/NTO	2	0	1	2	3	1.73
RP-1/H ₂ O ₂	2	2	1	2	3	1.91
AF-M315E	2	3	1	3	1	1.82
H ₂ O ₂	1	2	1	2	1	1.27
GOX/GCH ₄	3	3	3	3	2	2.82
LOX/LCH₄	3	3	3	1	2	2.45

Table 5.7: Trade-off of different propellants for the RCS thrusters.

Specific Impulse

The I_{sp} for MMH/NTO is found to be 228 s at sea level⁹, for RP-1/H₂O₂ an I_{sp} of 273 s is found¹⁰. For AF-M315E (a hydroxylammonium nitrate based monopropellant) an I_{sp} of 235 is found [30], an I_{sp} of 164 s is found for H₂O₂ monopropellant¹¹ and 324 s is found for LOX/LCH₄ (which is calculated in subsection 5.1.3) and for GOX/GCH₄ an I_{sp} slightly higher than that of LOX/LCH₄ is assumed, as gaseous fuels tend to have a slightly higher I_{sp} than their liquid version.

Toxicity

Hydrazine is considered incredibly toxic and hazardous, and is even banned from this project. Therefore it has been given the unacceptable grade of 0. Hydrogen peroxide based propellants are corrosive and toxic in high concentrations, however they are way much safer than hydrazine based propellants, therefore these are given a grade of 2. AF-M315E and CH_4 are considered green, non-hazardous propellants, therefore they have been given a grade of 3.

Compatibility

The most compatible propellants are GOX/GCH₄ and LOX/LCH₄, as the main engine already uses this propellant, these are therefore given a grade of 3. All other propellants require separate propellant tanks and are therefore given a grade of 1.

⁹http://www.astronautix.com/n/n2o4mmh.html(Last accessed 12-06-2018)

 $^{^{10} \}mathtt{http://www.astronautix.com/h/h2o2kerosene.html} (Last accessed 12-06-2018)$

¹¹ http://www.esa.int/About_Us/Business_with_ESA/Small_and_Medium_Sized_Enterprises/SME_Achievements/Green_ Hydrogen_Peroxide_H202_monopropellant_with_advanced_catalytic_beds(Last accessed 12-06-2018)

Operational Temperature

 LOX/LCH_4 needs to be cryogenically stored, and is therefore given a grade of 1. MMH/NTO, RP-1/H₂O₂ and H₂O₂ monopropellant all have one component that needs cooling, and are therefore given a grade of 2. AF-M315E and GOX/GCH₄ can be kept at room temperature and are thus given a grade of 3.

Startup Behaviour

AF-M135E and H_2O_2 monopropellant both need catalyst beds that need preheating before they can operate, therefore these are given a grade of 1. GOX/GCH_4 and LOX/LCH_4 work with normal ignition, therefore still need some ignition structure and some delay is introduced, and are therefore graded a 2. MMH/NTO and $RP-1/H_2O_2$ are hypergolic, which means a combustion delay is minimal, and are therefore given a grade of 3.

Multiplying the weight of each criterion with the grade assigned and adding all grades for a certain propellant gives the total score. From the total score, a clear winner can be found: GOX/GCH_4 . Its main advantages are high I_{sp} and compatibility with the main engine.

Sensitivity Analysis

When changing the weights of the different criteria, GOX/GCH₄ still scores the highest. It can be seen from the score that its only weaker spot is the startup behaviour, however it more than makes up for this with compatibility and toxicity.

Preliminary Thruster Design

The thruster design was based on sizing and configuration of the RCS thrusters on the ESA Automated Transfer Vehicle (ATV) for ISS missions. The ATV has 28 thrusters¹², which are placed in a configuration with four forwards clusters of two thrusters, and four aft clusters of five thrusters¹². As this configuration provides sufficient redundancy and control, it will also be adopted for the MEV.

The ATV thrusters do not use GOX/GCH_4 as was selected for the MEV thrusters, but instead use MMH/MON-3¹² which is a hydrazine based propellant. As such, while these thrusters can be used as a preliminary basis for the MEV, new thrusters must still be designed. Each thruster will have chamber pressure of 8 bar based on the propellant selection, and a thrust of 400 N. This thrust was based on the fact that the ATV has a wet mass of approximately half of the MEV [31] and thrusters with 200 N of thrust¹². An L^* of 1.25 m was used, as the typical range of L^* for gaseous oxygen - hydrocarbons lies between 1.25 m and 2.5 m [23]. Using the program written to size the main engine, a rough sizing of the RCS thrusters was also performed as is shown in Figure 5.5. It has an overall length of 362.9 mm, a throat diameter of 19.4 mm, a chamber diameter of 51.3 mm and an exit diameter of 133.3 mm. The RCS thruster will have impinging injector, which is the same injector type as used in the ATV thruster¹², and the propellant will be ignited with a spark plug, based on the discussion in subsection 5.1.2.

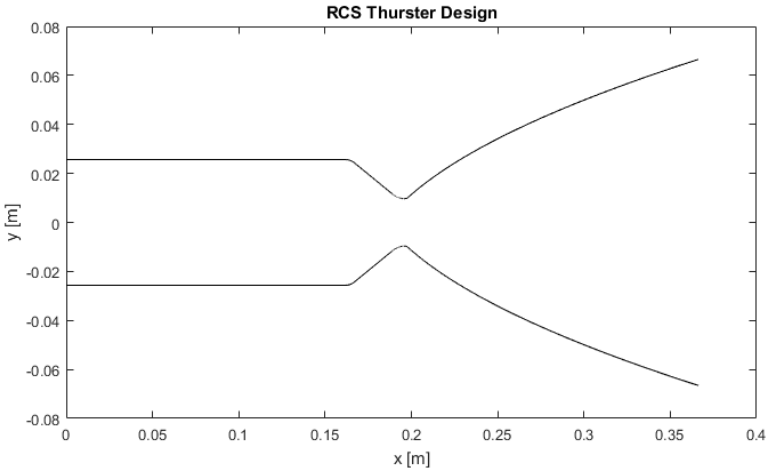


Figure 5.5: Preliminary thruster sizing.

¹² http://www.space-propulsion.com/spacecraft-propulsion/bipropellant-thrusters/200n-bipropellant-thrusters. html(Last accessed 14-06-2018)

Once the thruster had been sized, the required thickness of a chamber made from Niobium C-103 was determined. This thickness was found to be 0.047 mm which infeasibly thin, therefore the thruster was sized with the same material thickness as the main engine, 2 mm. Again it was assumed that the chamber and nozzle were made from the same material and had the same thickness. As such a mass of 1.336 kg was found for the total wall mass of each section, but this does not account for all the other mass of the engines, such as the valves. As such the mass of the ATV thrusters will be used, meaning each of the MEV's RCS thrusters will weight 1.9 kg 12 , which means the total of the 28 thrusters is 53.2 kg. A propellant mass estimation was not considered extensively at this phase of the project as a correct estimation would require a detailed analysis of the moments of inertia of the entire craft as well as the manoeuvres required during an entire mission profile. For now the propellant mass is taken as the same as the upper stage of the Ariane launcher of 450 kg[32].

5.1.7. Propellant Storage

Whilst the MEV is in standby in orbit between missions, it will use GOX/GCH_4 for the RCS thrusters as was discussed in subsection 5.1.6. This will be stored in the same fuel tanks as was used for the LOX/LCH₄ for the main engines. As such, the fuel tanks shall contain a bleed valve so as to lower the pressure in the tanks. However, the tanks will still be kept at a sufficient pressure for the thrusters to be used.

On the Mars surface, radiators will be required as the both the fuel and the oxidiser are cryogenic. As the period for which the MEV remains on the Mars surface, the largest issues with storing the propellant will be supplying the power for it. As such, this will be discussed in more detail in section 5.7.

5.1.8. Launch Abort System

A decision was made for the launch abort mode to be an abort to orbit, as opposed to an abort in which the MEV would return to the Mars surface. This was based on the lack of infrastructure and supplies on Mars possibly making returning to the surface more dangerous for the crew than them being placed in orbit, where they can be rendezvoused with the ITV. This abort mode is deemed safe for human flight, and was one of the four Space Shuttle abort modes, even being used on one of the missions¹³. The use of a separate launch abort capsule was deemed to add too much mass and complexity into the system for an abort to orbit, so instead sufficient redundancy was added to the main engines. The eight main engines are only throttled at 60% during nominal flight, meaning that even if two engines failed, the remaining six engines would only have to be throttled to 80% in order to maintain the thrust-to-weight ratio. In the case that two engines positioned next to each other both fail, the remaining six will have the ability to thrust vector sufficiently that MEV is still controllable.

5.2. Astrodynamics, Aerodynamics & Control

The following chapter will describe the astrodynamic and aerodynamic characteristics of both the landing and ascending trajectories of the MEV. Moreover, a section on control will be added for the ascent that discusses the thrust vectoring system.

5.2.1. Transfer Trajectory and Specifications

The transfer trajectories were already discussed in the Midterm Report [3]. However, for consistency purposes the required ΔV s and time of flight will be summarised for both the Hohmann transfer and the gravity assist transfer.

The production of the first MEV vehicle is expected to start around 2021 while for the first ITV it is 2026. The first launch to Mars via Hohmann transfer can be expected in 2028 while the first gravity assist launch happens no earlier than 2034. These dates are based on the possible launch windows from Earth to Mars. Table 5.8 and Table 5.9 present the near future possibilities for launching. In order to meet the ΔV requirements each transfer should be performed within these dates. There is a possibility to launch multiple times in a given year and this is determined by the excess velocity at launch.

 $^{^{13} \}mathtt{https://www.nasa.gov/mission_pages/shuttle/shuttlemissions/archives/sts-51F.html} (Last accessed \ 14-06-2018) the substitution of the s$

Table 5.8: Hohmann transfer launch opportunities dates.

				•	
Leave	from E	arth	Arriv	ve at Ma	ars
Month	Day	Year	Month	Day	Year
8	7	2022	4	22	2023
9	26	2024	6	11	2025
11	15	2026	7	30	2027
1	3	2029	9	19	2029
2	22	2031	11	7	2031
4	11	2033	12	26	2033
5	30	2035	2	15	2036
7	18	2037	4	4	2038
9	7	2039	5	22	2040
10	26	2041	7	11	2042
12	15	2043	8	30	2044
2	3	2046	10	18	2046

Table 5.9: Notable Earth-Venus launch windows.

V_{∞} , launch	C3	∆V _{EVburn}
[km/s]	$[km^2/s^2]$	[km/s]
4.50	20.25	4.07
5.50	30.25	4.49
4.75	22.56	4.17
5.50	30.25	4.49
5.75	33.06	4.60
5.00	25.00	4.27
	[km/s] 4.50 5.50 4.75 5.50 5.75	[km/s] [km²/s²] 4.50 20.25 5.50 30.25 4.75 22.56 5.50 30.25 5.75 33.06

As the Hohmann transfer analysis did not change from the Midterm Report [3], this report will present only transfer times and velocity increments for this transfer. However, additional research and analyses are performed for the gravity assist trajectory and it was found that the required ΔV for a gravity assist transfer will increase. The preliminary design for the ITV was performed for a Hohmann transfer. The result of sizing for gravity assist will result in bigger fuel tanks for the Interplanetary Transport Vehicle. The total mass of the vehicle is expected to increase between 30 and 35%. This is worst case scenario and the value will decrease if the launches are optimised and the cargo mass is decreased. For this report, the ITV will be sized for a Hohmann transfer for consistency purposes. The MEV design will not change and is not affected by the increase of transfer ΔV .

The timeline of the critical operations presented in section 3.5 suggests that the first gravity assist launch opportunity is in 2036. This is because the current plan for operational activities does not allow to use this type of transfer earlier. However, as can be seen in Table 5.9, another possibility is to send cargo to Mars in 2034 which can be achieved with lower launch excess velocity and thus save ΔV . Such transfer is plotted in Figure 5.6 which was generated using and open source software provided by David Eagle¹⁴. The software is a general mission analysis tool for single gravity assist trajectories where the gravity disturbances of all planets in the Solar system are taken into account. The simulation uses the gravity field of Venus to change the direction of the velocity vector with the help of a single slingshot at a specified flyby altitude.

¹⁴ https://nl.mathworks.com/matlabcentral/fileexchange/39462-gravity-assist-trajectory-design-and-analysis? s_tid-prof_contriblnk(Last accessed 24-06-2018)

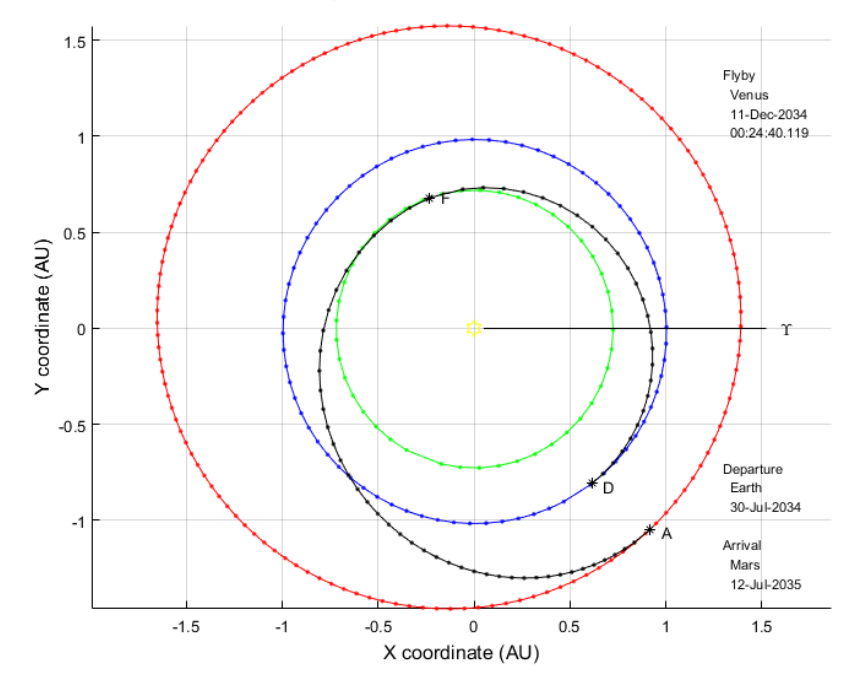


Figure 5.6: Patched-conic gravity assist trajectory.

The green circle (inner) represents the orbital trajectory of Venus, the blue circle (middle) represents the orbital trajectory of Earth, the red circle (outer) is the trajectory of Mars and the black one (the spiral) is the transfer trajectory. The coordinates are given in astronomical units.

The software uses a non-linear optimiser to find possible launch windows and targets trajectories for minimum total energy. The main physics behind the software is the so-called Lambert's problem which is concerned with the determination of an orbit that passes between two positions within a specified time-of-flight. Since this report is dedicated to landing and ascending trajectories more about this problem will be presented in subsection 5.2.6 and subsection 5.2.5 where the rendezvous manoeuvre uses the same type of orbital two boundary value problem.

The software provides the heliocentric orbital elements and state vectors of each leg of the transfer trajectory in the Earth mean ecliptic and equinox of J2000 coordinate system. The position of each planet in the Solar system was modelled with the help of a JPL DE 421 ephemeris file which defines the location of each planet provided by NASA¹⁵. The user interacts with the tool by defining a launch window and selecting appropriate dates for launch, flyby and arrival as well as search range in days for each date. The software finds minimum energy trajectory and constructs it for the desired launch window. Please note that the launch window is slightly different from the one presented in Table 5.9. This is because the launch window presented in the table minimises the launch excess velocity while the launch window defined by the software minimised the total energy required for the mission including the flyby. However, the difference between the two launch dates is only one month which will not affect the production plan for the MEV. This, however, explains why gravity assist is chosen for multiple cargo transfers. By a slight change in the excess velocity a list of launch dates can be obtained which are all in the desired yearly launch window. Such possibility is shown in Table 5.10 where it can be seen that multiple launches can be achieved in a single year [3]. C3 represents the energy at launch which is the square of the excess velocity [3]. This shows that multiple launches are possible by slightly increasing or decreasing the launch energy.

 $^{^{15} \}mathtt{https://ssd.jpl.nasa.gov/?planet_eph_export} (Last \, accessed \, 24-06-2018)$

Launch date	$V_{\infty,launch}$	C3
[dd/mm/yyyy]	[km/s]	$[km^2/s^2]$
22/11/2021	4.50	20.25
03/12/2021	5.10	26.01
04/12/2021	5.20	27.04
08/12/2021	5.50	30.25
14/12/2021	6.00	36.00

An interesting part about the gravity assist trajectory is the flyby around Venus. Different approach altitudes around Venus and a slight trajectory correction manoeuvre may change the path after the slingshot which is extremely useful when Mars is a bit behind or ahead of the planned arrival time. Since the trajectory presented above applies for a launch window in 2034 a flyby approach was constructed using the same software. The velocity and state vectors were propagated with a time step of five days. Figure 5.7 presents the exact flyby trajectory for the chosen coordinate system and launch boundaries. The closest approach is achieved at 6,572 km altitude. Note that the black body axis defines the tangent of the orbital trajectory of Venus around the Sun and the yellow body axis points towards the Sun. The coordinates are given in Venus Radius (VR).

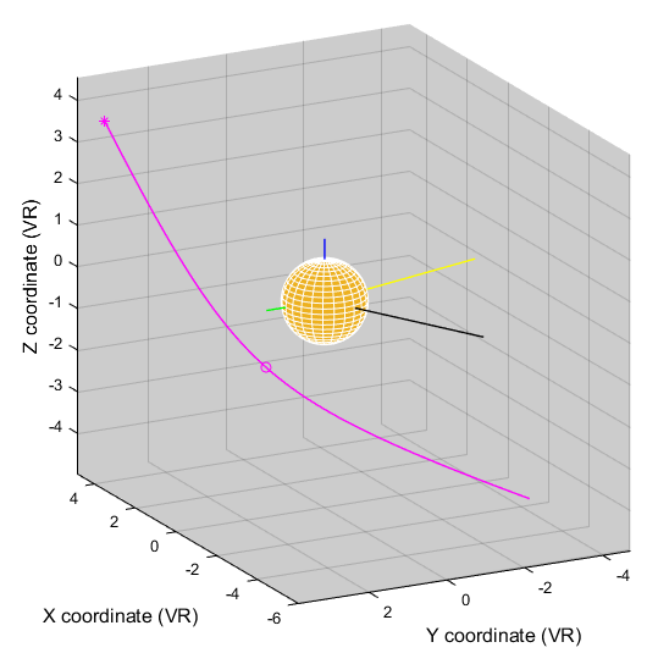


Figure 5.7: Venus flyby trajectory.

Table 5.11 represents the final outputs of the software for the chosen launch window. By running multiple launch windows in the tool a range of time of flight of 310-380 days was achieved for optimal total energy. This is a one way TOF. As explained earlier, the heliocentric total ΔV increased to 9.306 km/s including launch and arrival burns. This is because the initial calculation for transfer ΔV was not optimised for the desired launch window and neglected the burn required to a insert the ITV into initial hyperbola conditions. This issue is now taken into account and the model is precisely calculating the entire transfer trajectory including the launch from LEO. The entire mission summary for launch window in 2034 can be seen in Table 5.11.

Table 5.11: Gravity assist mission summary.			
Launch conditions		_	
Departure calendar time	[-]	30-07-2034	
Launch ΔV	[km/s]	3.739	
Launch energy	$[\mathrm{km}^2/\mathrm{s}^2]$	13.98	
Asymptote right ascension	[deg]	223	
Asymptote declination	[deg]	32	
Patched-conic flyby conditions			
Flyby calendar date	[-]	11-12-2034	
Launch-to-flyby time	[days]	133	
$V\infty_{in}$	[km/s]	6.081	
$V\infty_{out}$	[km/s]	6.081	
Flyby altitude	[km]	6572.4	
Maximum turn angle	[deg]	72.6	
Heliocentric ΔV	[km/s]	4.99	
Arrival conditions			
Arrival calendar date	[-]	12-07-2035	
Flyby to arrival time	[days]	213	
Arrival ΔV	[km/s]	5.566	
Mission summary			
Total ΔV	[km/s]	9.306	
Total energy	$[\mathrm{km}^2/\mathrm{s}^2]$	44.9	
Total mission duration	[days]	346	

Table 5.11: Gravity assist mission summary.

The new ΔV does not affect the sizing and design of the MEV. However, it affects the fuel tank design and total launch mass of the ITV. When further detailed design of the ITV is performed it is recommended to reassess the sizing procedures and calculate the new vehicle masses based on the new ΔV .

Table 5.12 summarises the time of flight and the updated velocity increment required for each of the two trajectories. Note that, the Δ V for inclination changes is included in the total value per manoeuvre.

		Hohmann transfer	Gravity Assist via Venus
From Earth to LEO	$\Delta V [\text{km/s}]$	9.3-10	9.3-10
	TOF [days]	2-3	2-3
From LEO to LMO	$\Delta V [\text{km/s}]$	5.7-5.9	9.0-11.5
	TOF [days]	270-260	380-310
From LMO to Mars	$\Delta V [\text{km/s}]$	3.8-4.2	3.8-4.2
	TOF [days]	1-2	1-2

Table 5.12: Trajectory comparison for each transfer.

Initially the difference between the orbital planes of Earth and Mars was assumed to be negligible. For this report, a detailed inclination change ΔV will be quantified in order to make the final model more precise. The orbital plane of Earth was considered to be the initial reference plane. Mars orbits the Sun in a different orbital plane which is 1.7 degrees from the chosen reference plane. Additionally, both Earth and Mars are tilted with respect to their axes by 23.5 and 25.2 degrees respectively. In order to perform each interplanetary transfer efficiently it is required that the trajectory between the parking orbits stays in the same plane. This is represented in Figure 5.8.

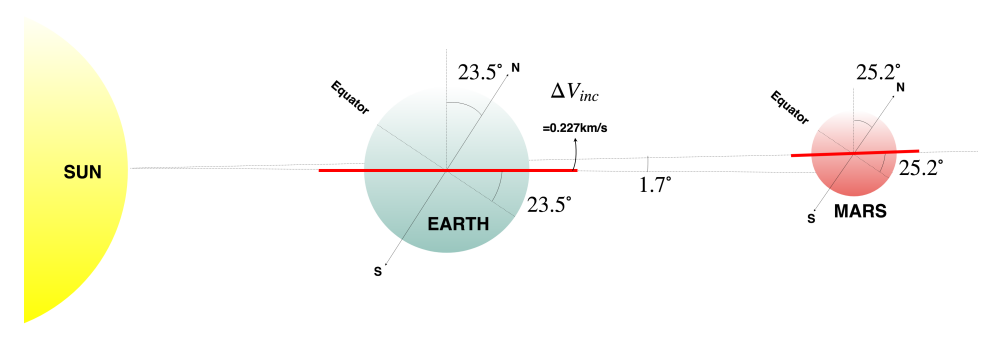


Figure 5.8: Representation of the orbit inclination change.

The ITV will be directly inserted into a circular parking orbit with 28 degrees inclination and immediately changed to 23.5 by a single dog-leg manoeuvre. Next, the plane inclination change of 1.7 degrees will be performed by a small burn which makes the vehicle to directly orbit the Earth in same transfer plane. This eliminates any additional ΔV burns for orbit corrections right before the initiation of the transfer manoeuvre. In this case the ΔV_{inc} = 0.227 km/s. This manoeuvre will be mainly performed for the Hohmann transfer since each gravity assist orbital plane is dependent on the exact launch window.

Most US launching sites that are currently in operation have a lower bound on inclination due to their latitude coordinates. For example, launches from Cape Canaveral can enter orbits between 28 and 57 degrees without a dog-leg manoeuvre¹⁶. This means that possible launching sites that can easily reach an orbit inclination of 23.5 should be located closer to the equator. Another restriction on the choice of launching sites is that some launch trajectories pass over largely populated regions.

One solution is implementing a dog-leg manoeuvre from Cape Canaveral and decrease the parking orbit inclination to 23.5. This method uses a simple cosine rule that keeps the original velocity as small as possible and is given by Equation 5.14.

$$\Delta V_{inc2}^2 = V_1^2 + V_2^2 - 2V_1 V_2 \cos(i)$$
 (5.14)

The ΔV required to go from 28 degrees from Cape Canaveral to 23.5 is 0.602 km/s with $V_1 = V_2 = V_0 = 7.67$ km/s being the circular velocity at 400 km altitude and i is 4.5 degrees. By performing this manoeuvre the two impulsive ΔV burns can be summed to give the total velocity change required to enter the plane of the transfer orbit:

$$\Delta V_{tot} = \Delta V_{inc} + \Delta V_{inc2} = 0.834 \text{ km/s}$$
(5.15)

Another possibility is to launch directly into orbit. One such launching site that makes this possible is SHAR Centre, Sriharikota in India which is located at 13 degrees latitude to the north. However, India lacks the infrastructure resources to maintain a Mars interplanetary program and transporting readily built vehicles to India is costly. That is why each vehicle for Project Cardinal will be launched from Cape Canaveral since it is one of the most developed launching sites and is close to the Kennedy Space Center which can manage multiple complex launches.

5.2.2. Landing Region Determination

The first step before actually performing the descent is to analyse the surface of Mars and choose proper landing site. However, there are several factors that affect the choice for a landing spot on the surface.

With the current orbit altitude and inclination it is possible to go as high as 38 degree latitude to the north or south on Mars without any additional inclination changes. Usually locations near the equator are preferred since temperatures there remain moderate compared to other locations on the planet. Mars cannot maintain high temperatures throughout the year due to the thin atmosphere which mainly consists of carbon dioxide. Mars is known to be tilted 25.2 degrees from its axis which creates seasons and along with the greater distance from the Sun this creates temperature differences ranging from minus 125 degrees Celsius during winter months at the north pole to 20 degrees Celsius during the summer months at the equator 17. Thus, it is better to choose a location in which the temperatures are relatively high in order to prevent the hardware from freezing.

The next factor is the condition of the terrain. Mars surface is covered with impact craters and due to the lack of environmental forces these remain unchanged. This introduces various elevation changes. Low elevation are ideal for landing since the atmosphere in these areas is slightly thicker and will definitely help when aerobraking during the descent. Various obstacles such as rocks are also something that may introduce difficulties during landing. Figure 5.9 presents the some of the potential regions which are suitable for human landing¹⁸. It should be noted that most of these zones are closer to the equator and at low elevation.

 $^{^{16} \}mathtt{http://www.astronautix.com/c/capecanaveral.html} (Last\ accessed\ 15-06-2018)$

¹⁷ https://www.space.com/16907-what-is-the-temperature-of-mars.html(Last accessed 12-06-2018)

¹⁸ https://www.theatlantic.com/science/archive/2017/04/mars-landing-site/521715/(Last accessed 13-06-2018)

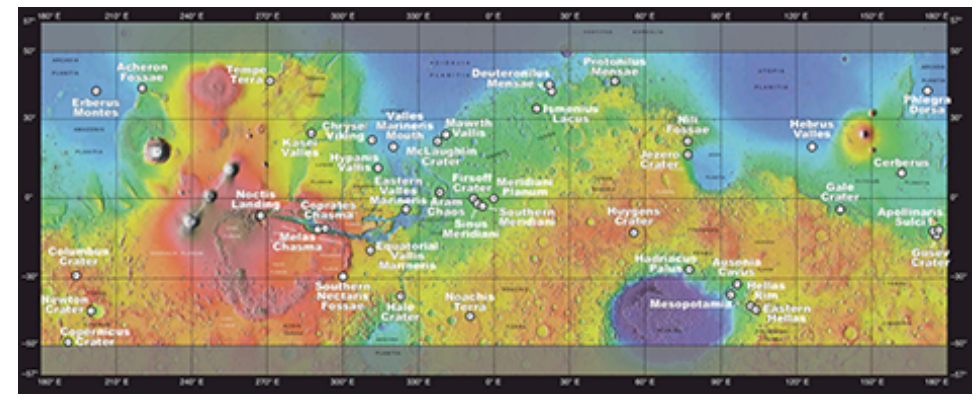


Figure 5.9: Potential exploration zones for human missions.

Looking into past missions it can be seen that rovers and landers landed close to the equator in order to maintain constant level of power supply and charge their batteries during daytime. Figure 5.10 shows the exact location of the landing sites of some notable past missions. Green and yellow areas represent zero elevation while blue areas represent negative elevation reaching -5 km. Red areas on the other hand represent higher elevation of approximately 3 km¹⁹. One very interesting location is the landing site of the Opportunity Rover. It landed at 1.94 degrees latitude to the south and 354 degrees longitude to the east. The landing location was at minus 2 km elevation and the terrain is relatively flat without any large obstacles or craters²⁰.

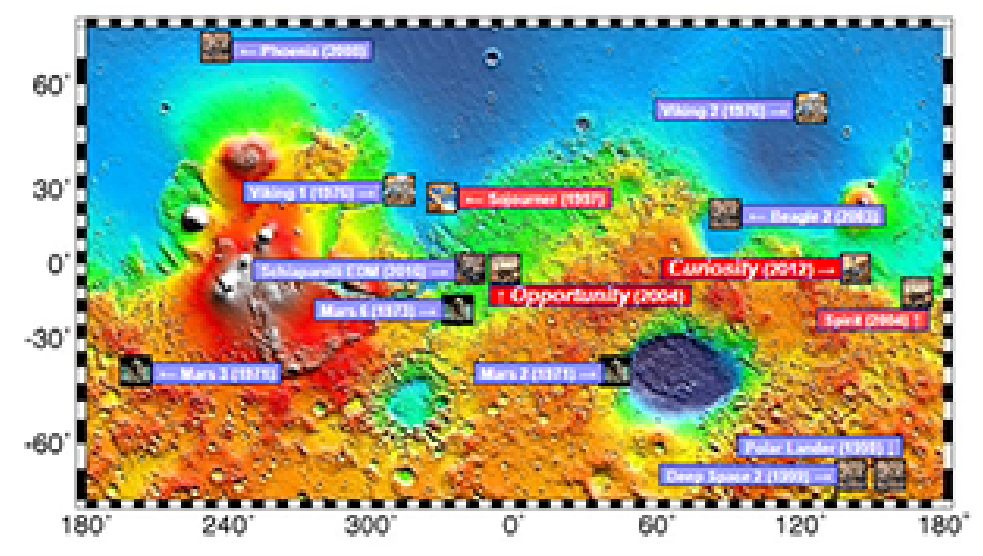


Figure 5.10: Notable locations of past Mars missions.

Due to the capabilities of the chosen orbit (25.2 degrees inclination) the maximum reachable latitude is 38 degrees from the equator given that the landing is performed in the same orbital plane and no additional impulsive burns are performed to change the inclination of the landing trajectory. This means that going more to the north or south of the equator is also a possibility. However, a human mission to Mars is something never done before and the best possible option for landing site is close to the equator. This decision is made based on the findings presented above. That is why the chosen landing region is 2 degrees south latitude and 354 east longitude. The area is very well researched and is currently the most suitable place for a human mission.

¹⁹https://www.nasa.gov/sites/default/files/atoms/files/grunsfeld-151027-mars-human-landing-site-workshop-final-jmg_tagged.pdf(Last accessed 13-06-2018)

²⁰ https://nssdc.gsfc.nasa.gov/nmc/spacecraftDisplay.do?id=2003-032A(Last accessed 20-06-2018)

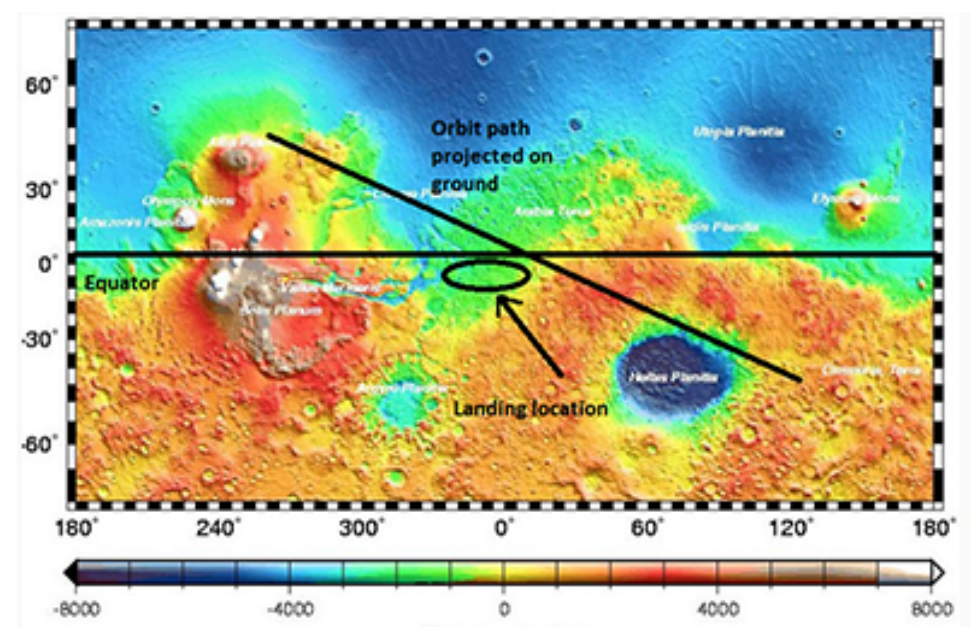


Figure 5.11: Chosen landing location on the surface of Mars.

In subsection 5.2.5, the actual landing trajectory and how the MEV de-orbits and enters the atmosphere is discussed. However, a very important question is the when to initiate the de-orbit burn in order to exactly land at the chosen location given that the rotation of Mars cannot be neglected. The equatorial velocity of Mars is 860 km/h with a day length of 24 hours and 39 minutes. The orbital period of the MEV is 1 hours and 48 minutes which means that for one full orbit a point at the equator (which will be the chosen landing location) will travel approximately 1548 km. Additionally, the same point at the equator will cross the orbit exactly 2 times every day and as can be seen in subsection 5.2.5 the time from de-orbiting to actually landing on the surface is 15 minutes. Thus, based on the equatorial velocity the location change is 215 km in 15 minutes. This means that the burn should be initiated such that chosen landing location is 215 km behind the point where it crosses the orbit. The exact true anomaly and entry parameters will be presented in the subsequent sections.

Last but not least, the MEV needs to land with a certain landing accuracy. A special landing trajectory software was written for this purpose that can be further investigated in subsection 5.2.5. It uses the entry interface (EI) parameters and calculates possible trajectories based on variation in propellant masses. It was estimated that the range of possible landing regions is within 19.41 and 19.43 degrees from a chosen reference which is the MEV position at EI; this was determined through an iterative process via a sensitivity analysis using the model generated in subsection 5.2.5. The landing accuracy can be visually represented in Figure 5.12 where the green and red dotted lines represent the lower and upper bound of landing locations given as a degree from the chosen reference. The landing accuracy is taken as the difference between the horizontal distances travelled taken as a percentage of total circumference. The corresponding distances for 19.41 and 19.43 are 1,147.75 km and 1,148.93 km respectively which gives a landing accuracy of ± 600 m. Entry conditions are defined in subsequent sections. The variation of the gravitational field of Mars is in the range of 3.69-3.74 m/ s^2 . For the lower bound the maximum achievable landing acceleration is 27 m/ s^2 while for the upper bound it is 27.9 m/ s^2 . This difference results in minor changes in the g-force applied and that is why the gravity field is considered constant for the landing trajectory. Please note, that this does not apply for the ascent. The ascent trajectory (including the insertion burn) required more time and thus the influence of gravitational changes and rotation is higher. More on that can be found in subsection 5.2.6.

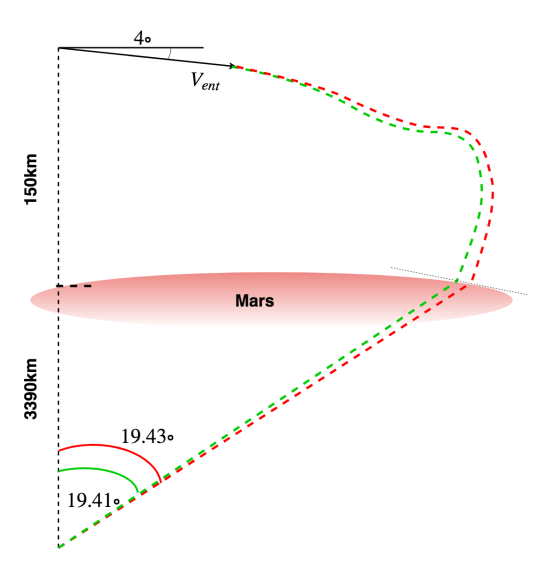


Figure 5.12: Variation in possible landing trajectories.

5.2.3. Aerodynamic Characteristics

While the Martian atmosphere has very little drag, determining the drag coefficient is important for the ascent and descent trajectories. The drag was estimated by assuming the MEV is the shape of a conventional rocket, and using drag estimations to determine the body drag, and the base drag; the fin drag and interference drag were ignored as the MEV does not use fins for stability [33].

The body drag is found using Equation 5.16 [33].

$$C_{D(fb)} = \left[1 + \frac{60}{(LTR/d_b)^3} + 0.0025 \frac{l_b}{d_b}\right] \left[2.7 \frac{l_n}{d_b} 4 \frac{l_b}{d_b} + 2 \left(1 - \frac{d_d}{d_b} \frac{l_c}{d_b}\right)\right] C_{f(fb)}$$
(5.16)

The coefficient of viscous friction is found using Equation 5.17 and the characteristic length of the body. The Reynolds number is found using Equation 5.18 where the dynamic viscosity, μ_v , is equal to 1.422e-5 kg/m-s [33].

$$C_{f(fb)} = \frac{1.328}{\sqrt{Re}}$$
 (5.17) $Re = \frac{\rho V l_b}{\mu_v}$

The base drag is found using Equation 5.19 [33].

$$C_{D(f)} = 0.029 \frac{\left(\frac{d_d}{d_b}\right)^3}{\sqrt{C_{D(fb)}}}$$
 (5.19)

The total drag is the superposition of the body drag and base drag. The total drag coefficient is found to be 0.4. Based on the configuration of the MEV, the estimated L/D ratio is 0.5 to 0.6, thus the lift coefficient is 0.2. As mentioned in Equation 5.2.5, the drag coefficient for descent (with air brakes deployed) is 1.4, while the lift coefficient is assumed to remain 0.2 [11].

The centre of pressure was found to be 6.5 me from the floor[3]; in order for a stable landing trajectory, the centre of gravity has to be lower than the centre of pressure. The centre of gravity was found to be 5 m from the floor, and as such the MEV is stable for descent. For ascent the stability is fixed by thrust vectoring.

5.2.4. Orbital Decay

As the orbital altitude is 200 km above the Martian surface, there is still a slight atmosphere and thus the MEV and ITV will experience altitude losses. Gravity losses and tidal effects are considered negligible as the orbiting bodies are relatively small. The Aerodynamic properties of the MEV have to be defined first: the Effective Area, A_e , and the Drag coefficient, C_d are the two quantities needed [34]. The effective area is defined as the area of the cross-section, which is found to be 21 m². The drag coefficient is found to be 1.4 as a high estimate [34]. The change in altitude

due to drag is found by finding the change in orbital period due to drag, found in Equation 5.20; The orbital period, P, used for the iteration, can be found in Equation 5.21 [34].

$$\frac{dP}{dt} = -3R\pi\rho_{atm} \frac{A_e C_d}{m_o}$$
 (5.20)

The Martian atmosphere was modelled in order to determine the atmospheric density at certain altitudes [35]. By iterating the value for 30 days and two years, the total altitude drop for each case can be determined in order to best assess if a short time period is better or worse than a shorter time period. After 30 days, the total altitude drop is 366 m, and 4,864 m, or 4.86 km, after two years. The MEV fully deorbits after 52 months of orbiting without burns. Of course there will be station keeping propellant to keep the MEV in orbit. The full orbital decay without any burns is presented in Figure 5.13.

Validation

The orbital decay of the International Space Station was determined by following the same process and determining if the expected orbital decay in one month is close to the actual orbital decay. The ISS has effective area of 1,641 m^2 , a mass of 420 tonnes, and a drag coefficient of 2^{21} . The orbital altitude of the ISS varies

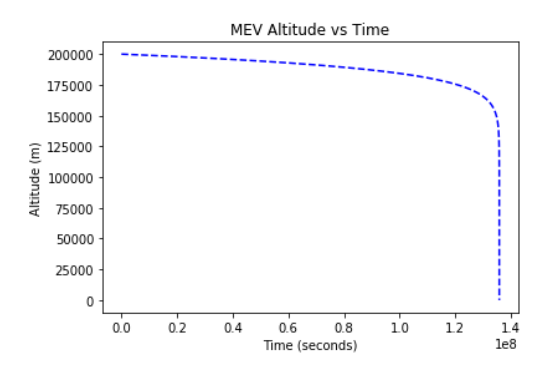


Figure 5.13: Orbital decay of the MEV without any station keeping.

greatly due to solar flux and other factors such as the effective area changing due to solar panel deployment²²²³.

The altitude change of the ISS in one month is anywhere from 0.5 km to 4.5 km, thus if the estimated altitude drop within one month falls within this range, then the method and program can be considered validated. Using the Earth's atmospheric density [35], the altitude change in one month is estimated to be 3 km, and thus falls within the expected range. The upper expected value, 4.5 km, is 1.5 times higher than the estimate, and thus a margin of 50% is applied to the orbital decay of Mars.

5.2.5. Landing Trajectory

After performing the transfer the ITV enters the circular parking orbit at 200 km and disconnects the MEV so it can land on the surface. For such purpose a proper de-orbiting trajectory needs to be constructed. The trajectory is split into two main components. The first one looks into the phase from 200 km to 150 km altitude and takes into account only astrodynamic characteristics. However, the atmosphere starts affecting the landing trajectory at an altitude from 150 km and that is why the second phase includes aerodynamic characteristics and atmospheric disturbances as well. The component of the trajectory is constructed with the help of a MATLAB software that computes the optimal impulsive manoeuvre required to de-orbit the MEV. The program was written by David Eagle (a retired aerospace professional with professional interests in aerospace trajectory optimisation)²⁴, and then modified by the team of Project Cardinal to fit the desired mission objectives subsection 5.2.1.

The code uses a simple guess shooting method in which the spacecraft equations of motion are numerically integrated when subjected to Mars' J_2 coefficient. The algorithm uses an initial guess from the analytical solution relative to a spherical non-rotating Mars and two-body Keplerian motion. Then a Sparse Nonlinear OPTimizer (SNOPT) is used to find the most optimal solution for the trajectory that is described by a system of dynamic variables. The program iterates an initial guess for the de-orbit ΔV by using Equation 5.22.

$$\Delta V = V_{c3} \left(1 - \sqrt{\frac{2(r-1)}{\left(\frac{r}{\cos \gamma_e}\right)^2 - 1}} \right) \tag{5.22}$$

²¹https://spaceflight.nasa.gov/realdata/sightings/SSapplications/Post/JavaSSOP/orbit/ISS/SVPOST.html(Last accessed 05-06-2018)

²²http://wsn.spaceflight.esa.int/docs/EUG2LGPr3/EUG2LGPr3-7-ISS.pdf)(Last accessed 05-06-2018)

²³https://www.heavens-above.com/IssHeight.aspx(Last accessed 05-06-2018)

²⁴https://nl.mathworks.com/matlabcentral/fileexchange/38907-a-matlab-script-for-optimal-single-impulse-de-orbit-from-earth-orbits Copyright ©2012, David Eagle (Last accessed 12-06-2018)

Where V_{c3} is the local circular velocity of the initial orbit which for the 200 km altitude is 3.45 km/s. γ_e is the flight path angle at enrry interface which is calculated to be 4 degrees and r is the radius ratio given by:

$$r = \frac{h_i + r_{eq}}{h_e + r_{eq}} \tag{5.23}$$

Where h_i is the altitude of initial circular orbit of 200 km, h_e is altitude of EI which is 150 km and r_{eq} is the equatorial radius of Mars of 3,390 km.

The same is done with the time-of-flight between perigee of the de-orbit trajectory and the entry true anomaly which is given by Equation 5.24:

$$t(\theta_e) = \frac{\tau}{2\pi} \left[2 \arctan \sqrt{\frac{1 - e_d}{1 + e_d}} \tan \left(\frac{\theta_e}{2}\right) - \frac{e_d \sqrt{1 - e_d^2} \sin \theta_e}{1 + e_d \cos \theta_e} \right]$$
 (5.24)

Where τ is the Keplerian orbital period of the orbit trajectory which is 108 minutes, e_d is the eccentricity of the de-orbit trajectory right after the de-orbit manoeuvre of 0.133 and θ_e is the entry true anomaly of of 205 degrees measured counterclockwise from the positive horizontal axis.

After the impulse burn is initiated the reference frame is changed from Mars-centred inertial to Mars-centred fixed with the use of the transformation matrix given by Equation 5.26.

$$\mathbf{R}_{MCF} = [\mathbf{T}]\mathbf{R}_{MCI} \tag{5.25}$$

$$\mathbf{T} = \begin{vmatrix} \cos(\theta) & \sin(\theta) & 0 \\ -\sin(\theta) & \cos(\theta) & 0 \\ 0 & 0 & 1 \end{vmatrix}$$
 (5.26)

Where θ is the apparent sidereal time at the moment of interest measured from Airy-0 which is defined as the prime meridian on Mars.

The program reads a file with input from the user where each parameter defines the initial conditions. Then it iterates the initial values for ΔV and $t(\theta_e)$ and propagates the trajectory based on the inputs for the orbital Keplerian elements. These parameters can be seen in Table 5.13.

Table 5.13: Input parameters for the optimal single impulse de-orbit trajectory.

Parameter	Value	Units
Initial orbit semi-major axis	3,590.0	km
Initial orbit eccentricity	0.0	_
Orbital inclination	25.2	deg
Argument of perigee	0.0	deg
Right ascension of ascending node	0.0	deg
Initial guess for true anomaly	145	deg
Upper bound for true anomaly	150	deg
Lower bound for true anomaly	140	deg
Target geodetic altitude	150	km
Entry flight path angle	-4.0	deg

These values are chosen such that the trajectory is optimised in terms of ΔV and entry velocity. The reason for the small flight path angle is that the entry velocity magnitude increases with it and thus the MEV requires higher braking force when reaching the surface of Mars. The manoeuvre is performed in the same orbital plane as the initial orbit in order to save ΔV for inclination changes. By doing so, the transfer time increases and a proper range for true anomaly needs to be given in order to land at the desired location at approximately 0 degrees latitude as presented in subsection 5.2.2. An initial position true anomaly of 145 degrees was chosen in order to enter the atmosphere with velocity of approximately 3045 m/s and geodetic declination of 7.7 degrees from the equator to the north.

Two and three dimensional visualisation of the single impulse de-orbit manoeuvre can be seen on Figure 5.14 and Figure 5.15. Note that the coordinates are given as a function of Mars Equatorial Radius (MR).

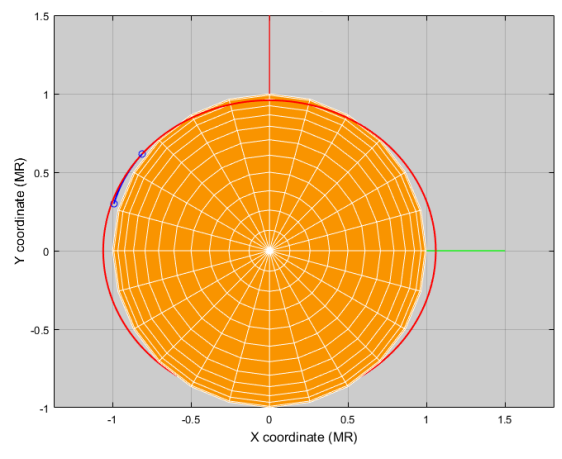


Figure 5.14: Two dimensional de-orbit impulse manoeuvre.

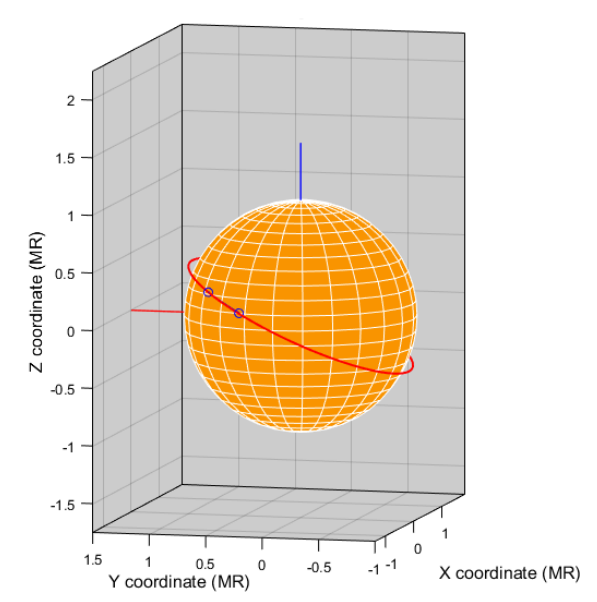
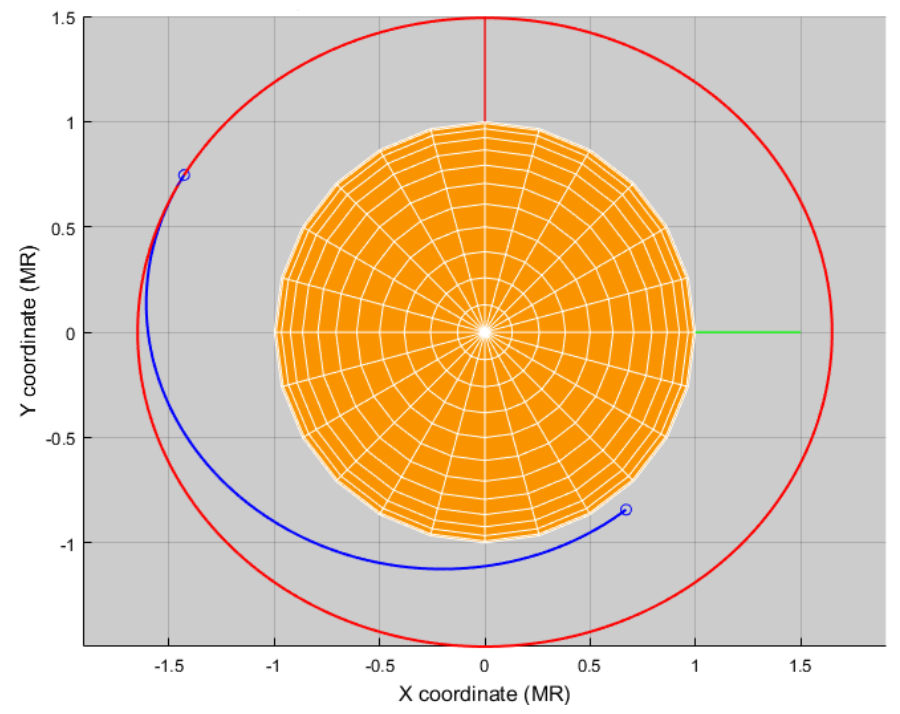


Figure 5.15: Three dimensional de-orbit impulse manoeuvre.

For better visual purposes a not-to-scale representation was generated given by Figure 5.16 which shows the initial position of the MEV in orbit and the transfer trajectory in blue. The optimised iterative solution includes the rotation of the planet and uses SNOPT to optimise the user's initial guess for the true anomaly on the initial orbit at the time of the impulsive manoeuvre. The initial coordinates with respect to the Mars Centred Inertial reference frame (MCF) are given by the relative flight path coordinates - the geodetic declination, the geographic longitude and flight azimuth. These are computed from the user's initial input parameters.



 $Figure \ 5.16: \ Not \ to \ scale \ de-orbit \ impulse \ manoeuvre \ for \ visual \ purposes.$

The final results of the de-orbit trajectory are presented in Table 5.14 and Table 5.15. Multiple possibilities are present for de-orbit trajectory. The orbit inclination and true anomaly can be varied in order to land at the same spot but in most cases this is achievable at the expense of more ΔV or time of flight. The solution presented in this report is optimised for minimum ΔV . With this simulation this value is 239.6 m/s.

Table 5.14: Conditions of transfer orbit at EI.

Parameter	Value	Units
Semi-major axis	3170	km
Eccentricity	0.133	_
Inclination	25.2	deg
Argument of perigee	316	deg
Right ascension of ascending node	0.0094	deg
True anomaly	205	deg
Argument of latitude	161	deg
Period	90.3	min
Velocity in X	-0.833	km/s
Velocity in Y	-2.86	km/s
Velocity in Z	-1.34	km/s
Velocity scalar magnitude	3.24	km/s

Table 5.15: Relative coordinates at EI.

Parameter	Value	Units
East longitude	69.9	deg
Geocentric declination	7.7	deg
Flight path angle	-4.0	deg
Relative azimuth	115.9	deg
Velocity magnitude (w.r.t. rotating Mars)	3.045	km/s
Total Δ V	239.6	m/s
Geodetic altitude	150	km
Flight time from manoeuvre to EI	6.91	min

The second phase of the descent involves the trajectory component from an altitude of 150 km to the surface of Mars at landing elevation of 2 km below the topographic datum of Mars. Since the reference frame is already MCF, the landing trajectory including the aerodynamic disturbances will be generated with respect to the same reference frame and a non-rotating Mars. In fact, there is a slight difference between the landing velocities of the MEV if Mars is rotating and if Mars is considered fixed. The magnitude of the entry velocity before the powered burn with respect to a rotating planet is 900 m/s with horizontal and vertical components 800 m/s and 400 m/s respectively. This results in total acceleration of 24.5 m/s² which is 2.5 g.

The magnitude of velocity of the vehicle right before the powered burn with respect to a non-rotating planet is 800 m/s with horizontal and vertical components of 700 m/s and 400 m/s respectively. The total acceleration that the MEV experiences is 27.5 m/s^2 which is 2.8 g. As can be seen the difference is minor and does not affect the final design of the vehicle and that is why the assumption for non-rotating planet is considered valid for the second part of the trajectory where aerodynamic forces are involved in the calculation.

The landing trajectory uses the entry parameters given in the first phase. The angle of entry was varied throughout the process in order to reduce the maximum acceleration. From the initial conditions set, a physics model was created in order to determine the optimal descent trajectory. It was based on basic flight dynamics principles mentioned later on. The model was created in Python using the atmospheric calculator determined earlier in the subsection 5.2.4. The curvature of Mars was not ignored as the horizontal displacement was significant. Thus, accounting for the shift in gravitational force and drag was essential. The vehicle was assumed to be aerodynamically stable, with the engines pointed towards the velocity vector.

The variables that were considered were the flight path angle, the interface velocity, the entrance altitude, the air brake surface area, the resultant force

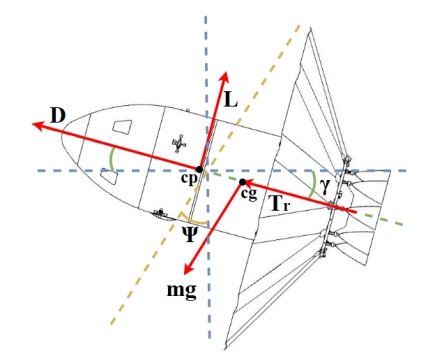


Figure 5.17: Forces on the MEV during descent.

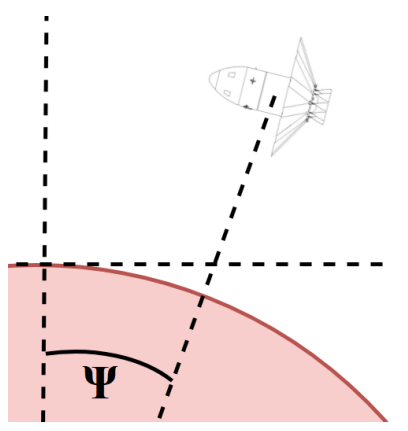


Figure 5.18: Angle Ψ in relation to the MEV during descent.

coefficients and the propellant mass. The flight path angle was set as low as possible at 150 km, which is the point at which the Martian atmosphere becomes significant for drag [35]. This value was chosen in order to minimise the maximum g-forces. Other systems enter at an angle of 28.5 degrees [36] and at a higher velocity. The experienced deceleration is up to 10 g, which is too high for a human mission.

The general method used a two-dimensional X-Y coordinate system, illustrated in Figure 5.17 in order to simplify the problem. The curvature of Mars was taken into account for both the altitude and gravitational forces. The equations of motion are presented in Equation 5.27 and Equation 5.28. The flight path angle, γ , follows the trajectory of the MEV, and the angle Ψ , which is the angle change of Mars in relation to the initial conditions. An illustration for Ψ is

given in Figure 5.18. The thrust is only relevant when the burn occurs and otherwise it is zero.

$$F_x = D\cos(\gamma) - L\sin(\gamma) - Mg\sin(\Psi) + T_r\cos(\gamma) \quad (5.27) \qquad F_y = D\sin(\gamma) + L\cos(\gamma) - Mg\cos(\Psi) + T_r\sin(\gamma) \quad (5.28)$$

The drag always opposes the velocity vector. However, the lift in the X direction actually pulls the MEV forward, albeit only slightly, and thus it follows the sign of the velocity vector. The thrust is always assumed to oppose the flight path.

Air brakes

There was a serious design choice between more propellant or larger air brakes, as an increase in air brake size would increase the propellant mass for the MEV, and an increase in landing propellant mass would affect the carrying capability of the ITV. A compromise between the two was chosen, based on keeping the propellant mass down, while maintaining the mass budget as close to the lowest value. Additionally, the air brakes are limited by the geometry of the MEV.

The highest drag coefficient at a stable configuration for an aeroshell-style air brake is 1.4 at an angle of 60 degrees from the vertical axis of the MEV [11]. At this configuration, the lift coefficient is very low, at around 0.2 [11]. The 60 degree configuration reduces the effective area by 14%, but the drag coefficient increases by 40%, and thus the total drag increase is greater than a 90 degree. This is the so-called flat configuration [11]. Based on the constraints on the size of the MEV, mainly the available wall space, the largest air brakes possible is 243 m² with an effective area of 213 m². The air brake shape and design is presented in more detail in section 5.3. In general there are 12 panels, which fold out from the skin, with a strong, heat resistant fabric that fills the gap between them. This is further explained in the heat shielding section. The amount of panels is selected in order to keep as much area within the panel sections while allowing for the support of the fabric. Moreover, the landing legs are considered for the spacing as well.

60°

Figure 5.19: Illustration of the air brakes, units are in mm and degrees.

Heat shielding

The maximum heat flux can be determined by Equation 5.29, where k is 1.9027e-4 kg^{1/2} for Mars [37]. The radius of curvature, R_n , of the MEV while the air brakes are deployed is 7.1 m, and the maximum heat flux, ψ_q , is found

to be 5 W/cm^2 . If the actual radius were used for R_n then the value would be 8.225 m, though the radius of curvature, 7.1 m, is the worst case scenario and thus will be used. The hot wall correction can be ignored at hypersonic speeds, but in general would reduce the heat load [37].

$$\psi_q = k \left(\frac{\rho}{R_n}\right)^{1/2} V^3 \tag{5.29}$$

Non-ablative heat shielding would have to be used, as ablative heat shielding loses mass over time and thus affects the reusability of the MEV. The heat shielding material on the Space shuttle, LI-900, has a thermal conductivity of 0.126 Wm⁻¹K⁻¹, and only 0.6% of the heat is transferred into the MEV. The rest is reflected [38]. The maximum temperature on the MEV can be found using Equation 5.30. ϵ is the emissivity of LI-900, which is 0.85, and σ is the Stefan–Boltzmann constant: 5.67e-8 Wm⁻²K⁻¹. The maximum temperature was found to be 1,025 K, which is well below the maximum reusable temperature of 1,533 K [38].

$$T_h = \left(\frac{\psi_q}{\epsilon\sigma}\right)^{.25} \tag{5.30}$$

The thickness of the heat shielding is found by taking the thermal conductivity, κ , the maximum temperature and the maximum heat flux on the structure. The material thickness required was found to be 3 mm. With a material density of 144.3 kg/m³, and a surface area of 130 m², the total mass is found to be 66 kg [38].

$$t_s = \frac{T_h \kappa}{\psi_q} \tag{5.31}$$

Similarly, the fabric sections of the air brakes have to be designed as well. The fabric has to withstand the same heat flux and temperature, but also be structurally sound and flexible. A two layer Nextel fabric was used as the Thermal Protection System (TPS)²⁵ with a double layer of pyrgogel 3350 as the insulator and a double layer of Kapton as the laminated gas barrier [39]. This configuration was chosen as it can handle over 25 W/cm² for extended periods of time and is strong enough for use as an air brake [39]. Other possible configurations are available though the material characteristics are worse compared to the aforementioned design[39]. A great benefit of using preexisting heat shielding designs is the fact that the materials are widely used and manufactured. This would reduce the cost of the air brakes and the heat shield considerably.

Powered landing

The propellant mass is heavily dependent on the mass of the structure and the amount of air braking possible. Based on the upper limit of the air braking size, the minimum propellant needed is 12,900 kg. This is a preliminary value and could be optimised further. The propulsion characteristics are provided in section 5.1. A constant thrust was assumed as first burn occurs at 8.7 km, and thus the pressure can be assumed constant. The thrust vector is assumed to be against the velocity vector, and the MEV is assumed to be aerodynamically stable with the engines facing towards the flow [11].

The landing velocity is less than 1.8 m/s at an angle of 0.2 degrees off the vertical. As the engines also thrust to deorbit the MEV, any anomalies in the engine thrust can be detected early on. In case of non-nominal thrust, a choice can be made to start the burn at a higher altitude, increasing the thrust-over-weight ratio. This results in a higher propellant usage. However, either a second MEV can be sent down to Mars orbit to retrieve the people, or payload can be left on Mars surface.

Final results

The final results and values are presented in Table 5.16. As can be seen, the landing is well within the requirements. The descent trajectory is illustrated in a few graphs, which illustrate the forces, velocities and the angle change.

The acceleration as a function of altitude is given in Figure 5.20. As can be seen, the acceleration forces experienced are low enough for a manned mission with inexperienced pilots. The thrust can be seen at the short spike after the drag induced curve.

The angle change is given in Figure 5.21. The angle change at the landing, Φ , is also the angle difference between the flight path angle, γ , and the angle change of the Mars with respect to the entry position, Ψ. The Velocity as a function of altitude is given in Figure 5.22, illustrating the areas where the drag becomes significant and where the thrust begins.

As mentioned in the powered landing section, the MEV lands at a

Table 5.16: Final results of descent trajectory of the MEV.

Description	Value	Unit
\mathbf{q}_{max}	6,083	Pa
\mathbf{A}_{e}	213	m^2
γ_{ent}	-4	deg
V_{ent}	3,045	m/s
\mathbf{M}_{p}	12,900	kg
$\psi_{q_{max}}$	5	W/cm ²
Ψ	19.42	deg
Φ_{land}	89.8	deg
\mathbf{v}_{land}	1.8	m/s

velocity of 1.8 m/s which is below the required 2 m/s. The landing angle, Φ, is 89.8 degrees, or 0.2 degrees off the vertical, thus the MEV lands almost perfectly straight. The angle change, used to determine the circumferential distance from the initial position, is 19.41996 degrees, which is a distance change of 1148.319 km.

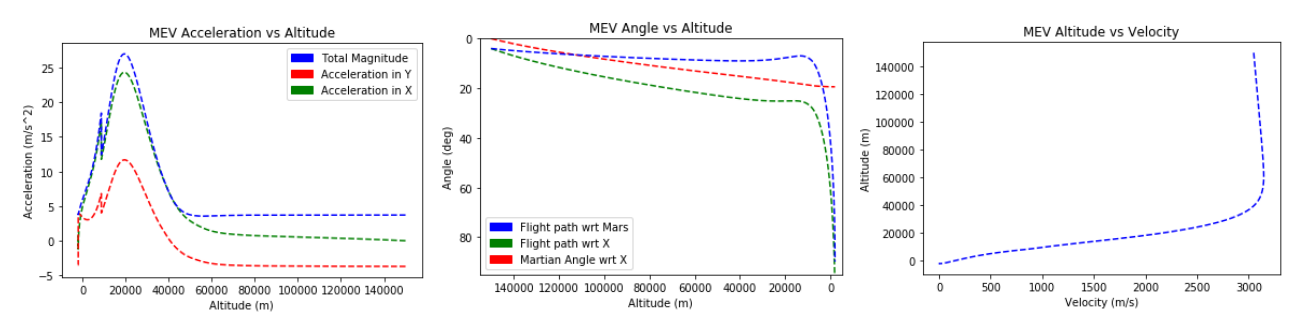


Figure 5.20: Acceleration vs Altitude curve for the MEV descent; the acceleration magnitude is shown, in actuality the sign is negative.

Figure 5.21: Angle vs altitude curve: red is Ψ , green is γ and blue is Φ .

Figure 5.22: Altitude vs velocity curve for the MEV descent.

rud(Last accessed 21-06-2018)

Verification

Verifying the de-orbit software was done by setting the variables and the environment to a model that is already known. This model is a de-orbit manoeuvre proposed by David Eagle²⁶ who calculated de-orbit parameters for a circular orbit at 500 km altitude around Earth.

The tool developed for the second phase of the landing was used to estimate certain values and trajectories for other Mars missions, though the specifics on them is incomplete, and thus a full analysis is not possible. The main variables analysed were the dynamic pressures, the g force load and comparing landing trajectories. Most missions landing on mars have an entrance angle above 20 degrees, much higher than the 4 degrees used for the MEV, though this is due to a greater flight path angle results in much higher g-forces [36].

The maximum acceleration estimated was 27.5 m/s^2 ; an estimation for the g-forces experienced is found in Equation 5.32 and Equation 5.33 [40]. The atmospheric interface velocity, V_{ent} , is 3,045 m/s; the maximum magnitude of acceleration is estimated to be 14 m/s^2 , which is lower than the 27.5 m/s^2 modelled, though this is based on a vehicle with minimal drag [41], if the MEV were to have a low drag coefficient, the maximum deceleration would be around 11 m/s^2 [41]. The rest of the equations do take into account the Ballistic coefficient, β , and thus the drag of the MEV.

$$G_{max} = \frac{V_{ent}^2 \sin(\gamma_{ent})}{53.31 H_s} = 14 \text{ m/s}^2$$
 (5.32)
$$H_s = \frac{H_{ent} - H_0}{\ln\left(\frac{\rho_0}{\rho_{ent}}\right)} = 8,555.5 \text{ m}$$
 (5.33)

Additionally, the altitude of g_{max} can be found using Equation 5.34, where C is found using Equation 5.35 and β is the ballistic coefficient, found using Equation 5.36 [41]. The altitude at the maximum acceleration is estimated to be 17,557 m, while the model calculates it to be 19,427 m.

$$H_{gmax} = H_s \ln(-2C)$$
 (5.34) $C = \frac{\rho_0 H_s}{2\beta \sin(\gamma_{ent})} = -3.9$ (5.35) $\beta = \frac{M}{C_d A} = 220 \text{ kg/m}^2$ (5.36)

The heat flux was found to be 5 W/cm², occurring at a height of 28,662 m. The maximum heat flux can be estimated using Equation 5.37[41] and the height it occurs at is found using Equation 5.38 [41]. The estimated heat flux was found to be 3 W/cm², which may look like close to a 50% deviation, however as the heat flux can range up to 150 to 200 W/cm² for high entry angles, the value is rather close in comparison.

$$\psi_{q_{max}} = 0.3502k\sqrt{\frac{-\beta\sin\gamma_{ent}}{H_sR_n}}V_{ent}^3 = 3 \text{ W/cm}^2 \quad (5.37)$$

$$H_{\psi_{q_{max}}} = H_sln(-6C) = 26,955 \text{ m} \quad (5.38)$$

The velocity at maximum acceleration is calculated to be 2,105 m/s, and the Velocity at maximum heat flux is calculated to be 2744 m/s. The estimated values for V_{gmax} and $V_{\psi_q max}$ are given in Equation 5.39 and Equation 5.40 [41]. As can be seen, the estimated values are very close to the modelled values.

$$V_{g_{max}} = 0.6065 V_{ent} = 2,035 \text{ m/s}$$
 (5.39) $V_{\psi_{q_{max}}} = 0.8465 V_{ent} = 2,578 \text{ m/s}$ (5.40)

In general the estimated values are slightly lower than the modelled values, though this is due to the estimated values not taking drag and lift fully into account as only the equations using the ballistic coefficient, β , account for drag and even then they do not take into account the variations in mass due to thrust, and the addition of a lift. In general the magnitude is close enough to consider it verified.

The velocity at a certain altitude compared to other reference missions to Mars can be found in Figure 5.23[36]. This illustrates that the end trajectory does match other missions. The key difference between the Cardinal mission and other reference missions is the entrance velocity, as the MEV enters at a very low entry angle and thus results in a low atmospheric interface velocity. If the MEV were to enter at a higher entry angle similar to those of Viking and Phoenix, then the interface velocity would be around 5 km/s, thus right within the region of those missions. The Landing is slightly different, as most reference missions deploy their air brakes, or extend them further, towards the end of the descent, around 10 to 20 km, which would slow the descent considerably compared to the initial velocity; the MEV has a consistent air brake area and as such their is less of a flat line before the drop.

²⁶https://nl.mathworks.com/matlabcentral/fileexchange/38907-a-matlab-script-for-optimal-single-impulse-de-orbit-from-earth-orl Copyright ©2012, David Eagle (Last accessed 12-06-2018)

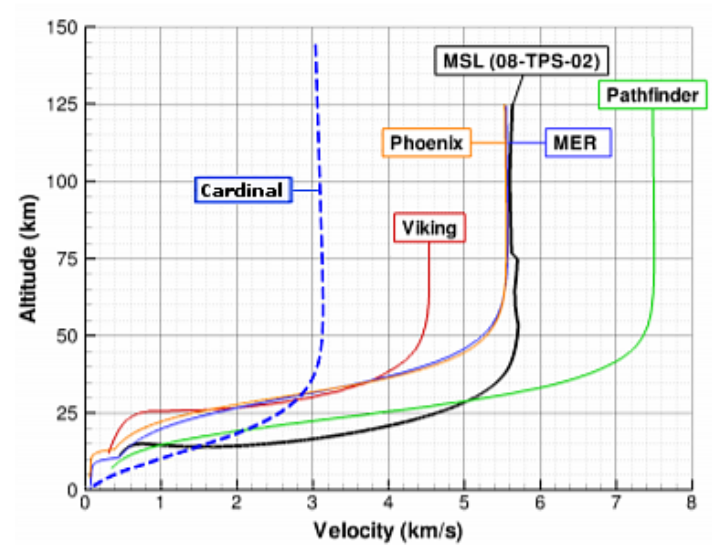


Figure 5.23: Altitude vs velocity curve for the MEV descent, designated as Cardinal, compared to reference Martian descent trajectories [36].

Further work on the Landing trajectory can be done in order to increase the accuracy. Adding a 3rd dimension while considering more accurate, varying the force of gravity with respect to the altitude and position of the MEV and including the use of more precise control characteristics, such as control moments, would be ideal, however for a preliminary analysis of the landing trajectory the deviations between the values modelled and the values estimated are small.

Sensitivity analysis

Determining the stability of the methods used is important, in order to guarantee the design decisions are valid. The key variables for the descent trajectory are the entry values, such as the flight path angle, the interface velocity and the altitude, and the MEV specific values, such as the thrust to weight ratio, the air brake effective area and resultant force coefficients, and the propellant mass.

The entry values are not viable for alterations, as maintaining a low g-force is imperative for the safety of the passengers, though in general the entry values do not vary much for a 10% increase in entry angle. The most important values are the MEV specific values, especially the dry mass; the dry mass is the most influential value for the landing trajectory, as the landing trajectory relies on it in addition to the launch mass, which relies on the dry mass. The effects are exponential and thus a 10% increase in dry mass, while maintaining the same values, can lead to the MEV not being able to land. The main reason for this is a result of the thrust to weight ratio dropping.

The best way to counteract any change in total mass is to increase the thrust by the same amount, in other words, maintain the thrust to weight ratio; the ΔV increase would be almost negated. A 10% increase in dry mass and a 15% increase in thrust results in the same necessary descent propellant mass. The worst way to counteract any changes in total mass in increasing propellant mass, since this may lead to a runaway increase in required propellant mass. The middle of the road approach would be to increase the air brake size, though this would not be very effective since the increased structural mass would negate most of the gains. In general the model is stable, and all instabilities can be quantified.

5.2.6. Ascending Trajectory and Rendezvous

During ascent, the thrust vector needs to be actively controlled in order to increase the velocity in both the parallel and tangential direction with respect to the surface. Additionally the MEV is not stable in ascent due to centre of pressure being higher than the centre of gravity, and thrust vectoring is necessary as a result. In order to increase the understanding of such a system, a simulation of the system was created in the SimScape environment.

The system consists of a variety of 'blocks', which all have a separate function. By connecting the blocks, a physics simulation of the system is generated, including a graphical overview. An overview of the system can be found in Figure 5.24.

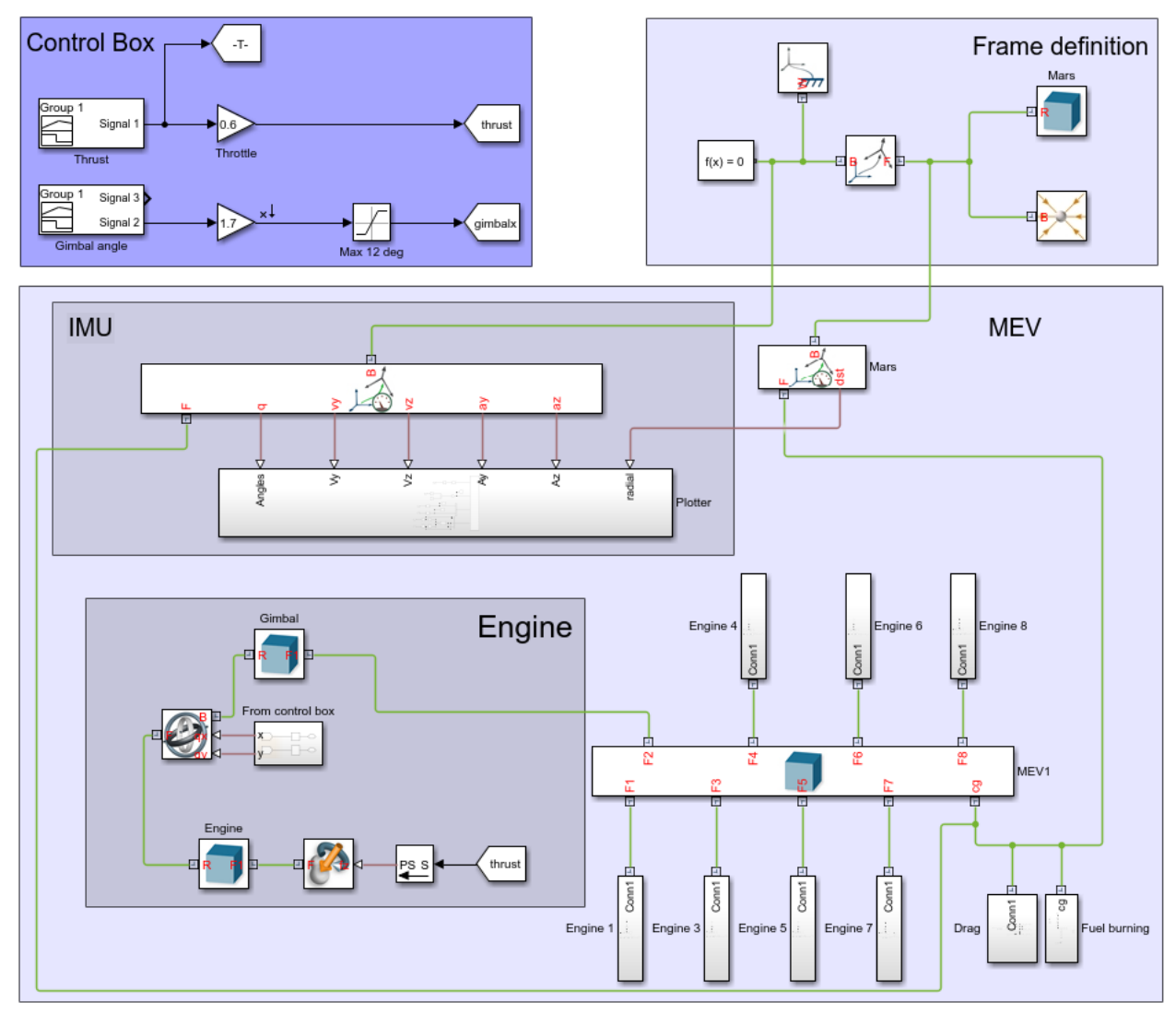


Figure 5.24: Overview of the ascent control diagram created in the MatLab SimScape environment.

There are five different subsystems that are considered for this analysis. These are the 'Frame definition', 'Control box', 'IMU', 'Engine' and 'MEV'.

Frame definition defines the location of the world frame. This can either be the surface or the centre of Mars, depending on the method of simulation that is chosen. To generate a complete model, Mars is assumed to be spherical, having a mass of $6.39e27 \, \mathrm{kg}^{27}$. Given this mass, a gravity field is generated using the gravity field block on the bottom right. Finally, the model is connected to the solver block, which solves the system for the given input. In order to do this, a set of differential equations is generated by the software, which is solved using ODE15s within MATLAB²⁸.

Control box gives the signals required for active control. These are the thrust level and the gimbal angle. Due to time constraints, the system is currently modelled as an open loop, meaning that a predefined signal needs to be used. For the thrust, a fuel mass of 38,400 kg (based on a 4.2~km/s required ΔV is used with a mass flow of 71.91 kg/s section 5.1. The gimbal signal is an impulsive signal to introduce an increasing angular velocity which is halted by an impulse in the opposite direction after the right angle is reached. A saturation is added for later implementation of the project, where the loop can be closed. In this case, the program should take into account that the maximum gimbal angle is assumed to be 12 degrees [21]. These signals are fed into the engine and the gimbal joint respectively. At around 600 s, an apogee of about 250 km is reached, after which the insertion burn is initiated. The gain for thrust is the throttle of the engine. The thrust signal (before throttle) is shown in Figure 5.25. The reader should note that a 5% increase in thrust is applied for the insertion burn to account for increased efficiency in vacuum.

 $^{^{\}overline{27}} https://nssdc.gsfc.nasa.gov/planetary/factsheet/marsfact.html (Last accessed 13-06-2018)$

²⁸https://nl.mathworks.com/help/matlab/ref/ode15s.html(Last accessed 13-06-2018)

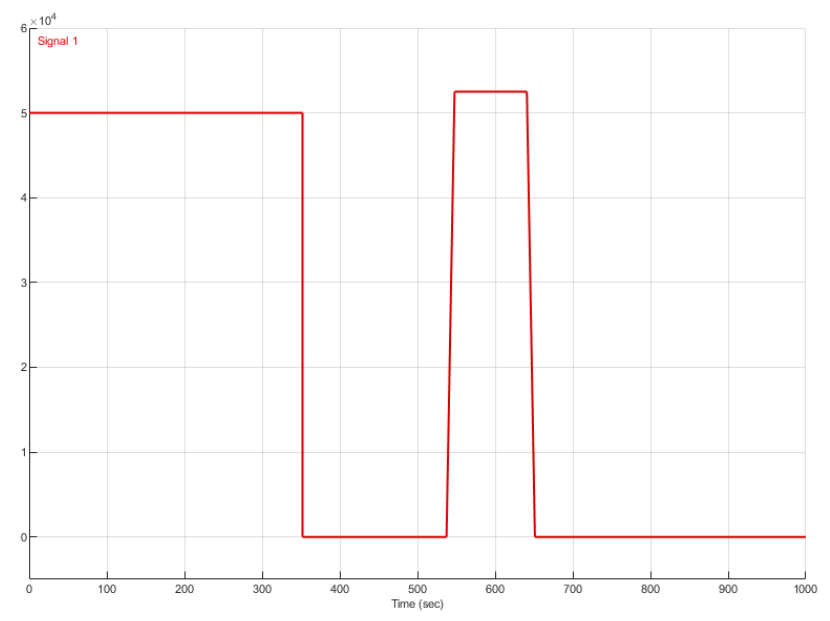


Figure 5.25: Unitless signal provided for the engines.

The IMU is placed in the centre of gravity of the MEV and calculates the accelerations, velocities and altitude of the MEV with respect to the world frame. In the program, this is a modelled as an ideal transform sensor which looks at the differences between the reference frame of both the 'Base' and 'Follower'. The result is projected in a frame of choice, which is here chosen to be the centre of Mars. All following plots result from the IMU.

The engine is part of the MEV, and includes the gimbal joint. As can be seen in the block diagram, the input signal is transferred into the gimbal joint as a position. This position can be given in degrees or radians. For this program, degrees are used. All engines are attached at the corresponding sections underneath the MEV, given by the different frame names (F1-F9). Currently, only an input around the x direction is given. However, the program does allow for full 3D movement without any modifications if the signal for gimbal in y is given. The thrust aligned with the axial direction of the engine is given by the thrust signal. The thrust vector is placed inside the nozzle. A small, massless area is added in the CATIA generated engine STEP file to ease the placement of the thrust vector.

MEV is the block that represents the MEV. A CATIA-generated STEP file is used to get the shape of the model in the diagram. Next, the reference frames for the engines are defined. Although SimScape provides the opportunity to calculate moment of inertias, masses and cg locations based on the geometry, it is chosen to manually enter the values since this is considered to be more accurate. Only three impulsive 10 degree manoeuvres are needed to get to the right orientation. Finally, since fuel is burned, changing the weight and location of the cg, another block is introduced which accounts for this. A signal similar in time to the thrust signal is given as an input for this change in weight. However, the signal has an amplitude which is equal to the mass flow. This is integrated over time and subtracted from the total fuel mass to generate the actual mass that is still in the tanks.

As stated earlier, the system is currently uncontrolled, meaning that it is an open loop system. However, estimations can be made for a trajectory to 200 km, using few manual iterations. Changes that can be made are the burn-time, gimbal angle signal and the gains. Using this method, the following results have been acquired. An initial burn of 350 s, followed by an insertion burn of 100 s is used. As stated, during the insertion burn the thrust is assumed to be 5% higher, due to the increased efficiency of the engine in vacuum. For the gimbal, only a few impulses are used to orient the MEV to roughly 45 degrees in the first stage, and tangential to the velocity vector at apogee. In Figure 5.27, the surface altitude and total acceleration are given over time. The two sharp changes in the acceleration represent the orbit insertion manoeuvre. The estimated surface velocity can be seen in Figure 5.26. This value is estimated,

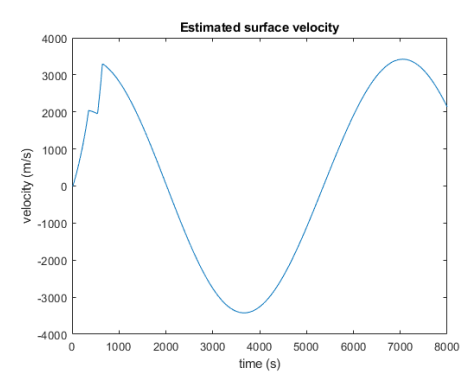


Figure 5.26: Estimated surface velocity.

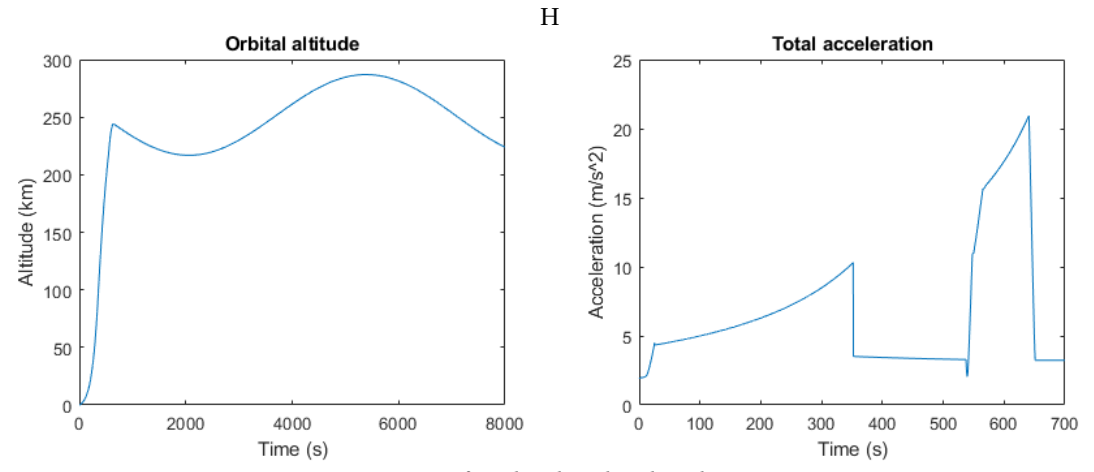


Figure 5.27: Surface altitude and total acceleration.

since surface rotation is not included in this measurement.

As explained, the vehicle is launched with an angle of 45 degrees from the vertical axis and reaches altitude with a velocity vector that is aligned with the direction of the orbital velocity. However, this component has a magnitude which is lower than the required circular velocity to enter a parking orbit. This means that an additional insertion burn needs to be performed. Figure 5.28 represents the insertion burn. Please note that the horizontal component V_y at altitude of 200 is aligned with V_{c3} , but for visual purposes it is not represented in the graph in this way. Prior to reaching orbit, the vertical component of the velocity has a magnitude, but since the MEV coasts before reaching orbit its total velocity direction is aligned with the velocity of the orbit and thus making $V_z = 0$ m/s. The ΔV required to reach orbit is 2263 m/s excluding the insertion burn, with $V_y = 2,000$ m/s, $V_{c3} = 3,450$ m/s, $V_z = 0$ m/s and $\Delta V_{ins} = 1450$.

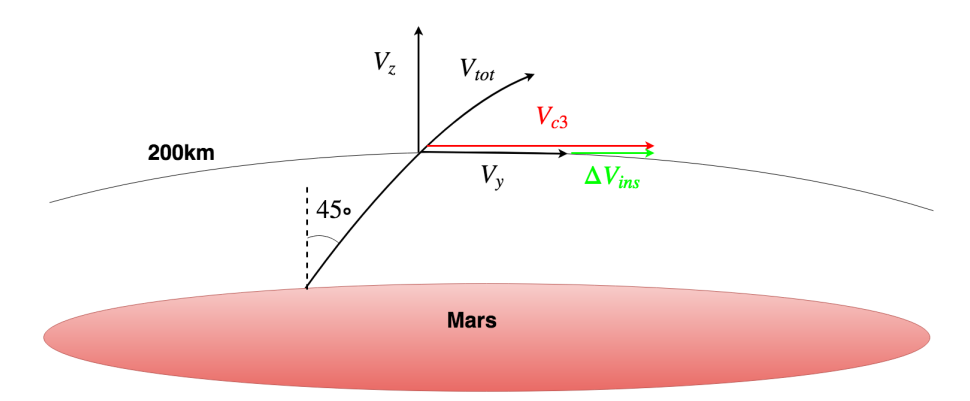


Figure 5.28: Representation of orbit insertion burn.

Since this assumes an impulsive manoeuvre, whereas the actual manoeuvre is around 100 s, the velocity in z direction is not 0 at all times. However, the burn is timed such that it occurs around apoapsis, meaning 50 s before until 50 s after apoapsis. The fact that a constant orientation, namely parallel to the surface, is held means that the model is not optimised. It is recommended that this is investigated in the detailed design.

As can be seen, an ascent is made to 250 km, where the insertion burn is performed. This raises the apoapis of the orbit to just under 300 km, where the periapsis is now just above 200 km, meaning the orbit is slightly elliptic. However, the remaining fuel, which is around 400 m/s or 1800 kg, will be used for docking to the ITV. The maximum accelerations are well below the limits of what humans can handle, with only 20 m/s^2 or approximately 2 g.

It is recommended to further iterate this model, including effects such as Mars rotation on the velocity of the space-craft and closed loop control, in order to further optimise the fuel required for ascent.

Sensitivity analysis

During working with the tool, it was found that the limits of launch mass are close to being reached. During an iterative process, a 10% increase in dry mass resulted in an 18% increase in fuel required for take-off after a few system-wide iterations. Furthermore, when the dry mass is increased with another 10%, the fuel required for only take-off increases with roughly 4.2%. Since this extra mass influences the mass required for landing and the fuel tank structures, it is expected that this snowballs to a point where landing will be close to unfeasible.

Rendezvous

Once the MEV is into orbit, it needs to perform a rendezvous manoeuvre with the ITV. There are two factors that limit the direct docking of the MEV with the ITV right after the launch. These are the rotation of Mars around its own axis and the orbital velocity of the ITV around the planet. In order to simplify the manoeuvre, the MEV will be first send into an elliptical orbit with a perigee coinciding with the perigee of the circular orbit of the ITV. The rendezvous will be performed at this point and thus the rotation of the planet can be neglected since both vehicles will be in orbit with a certain velocity with respect to Mars.

A special chase manoeuvre code was used for this purpose that uses the Lambert's problem for optimised solution. Simply presented, the Lambert's problem describes an orbit that is constructed with the use of two position vectors and a time of flight. An open source software developed by Bogdan Danciu²⁹ solves the rendezvous problem based on user's input.

The code starts the timing iteration by calculating the angular momentum of the initial and the final orbit given by Equation 5.41 and Equation 5.42. By calculating the angular momentum the position and velocity state vectors \vec{r} and \vec{v} can be constructed.

$$h_1 = \sqrt{\frac{a_1 \mu}{1 - e_1^2}}$$
 (5.41)
$$h_2 = \sqrt{\frac{a_2 \mu}{1 - e_2^2}}$$

Where a is the input semi-major axis and e is the eccentricity defined by the user. The state vectors are given by:

$$\vec{\mathbf{r}} = \frac{h^2}{\mu} \left(\frac{1}{1 + e \cos \theta} \right) (\cos \theta \begin{bmatrix} 1 \\ 0 \\ 0 \end{bmatrix} + \sin \theta \begin{bmatrix} 0 \\ 1 \\ 0 \end{bmatrix}) \qquad (5.43) \qquad \vec{\mathbf{v}} = \frac{\mu}{h} (-\sin \theta \begin{bmatrix} 1 \\ 0 \\ 0 \end{bmatrix} + (e + \cos \theta) \begin{bmatrix} 0 \\ 1 \\ 0 \end{bmatrix}) \qquad (5.44)$$

Where h is the angular momentum calculated above and used for both the initial and final position and velocity vectors. μ is the gravitational parameter of Mars and θ is the true anomaly based on the user input.

After the position and velocity vectors are defined the code estimated the eccentric anomaly at initial position with Equation 5.45. The time passed since perigee at that point is given by Equation 5.46 and the time at rendezvous point is computed with Equation 5.47.

$$E_2 = 2 \tan^{-1} \left(\sqrt{\frac{1 - e_2}{1 + e_2}} \tan \left(\frac{\theta_2}{2} \right) \right)$$
 (5.45)

$$t_2 = \frac{T_2}{2\pi} (E_2 - e_2 \sin E_2)$$
 (5.46)
$$t_{2'} = t_2 + \Delta t$$
 (5.47)

After the time interval Δt , the MEV will be at the rendezvous position 2'. The corresponding mean anomaly at this position is given by Equation 5.48 and the new eccentric anomaly is calculated by Equation 5.49

$$M_{e2'} = 2\pi \frac{t_{2'}}{T_2}$$
 (5.48)
$$E_{2'} - e_2 \sin E_{2'} = M_{e2'}$$

Finally, the true anomaly at rendezvous is given by Equation 5.50 where each parameter in the equation is calculated with the above presented steps.

²⁹ https://nl.mathworks.com/matlabcentral/fileexchange/66212-chase-maneuvers-using-lambert-s-problem(Last accessed 15-06-2018)

$$\theta_{2'} = 2 \tan^{-1} \left(\sqrt{\frac{1 + e_2}{1 - e_2}} \tan \frac{E_{2'}}{2} \right)$$
 (5.50)

By following this algorithm the user can obtain various scenarios for rendezvous based on the desired timing and the altitude of transfer orbit. As explained, the intercept trajectory is defined by the Lambert's problem which yields the values for the velocity vectors given by Equation 5.51 and Equation 5.52.

$$\Delta \vec{v}_1 = \vec{v}_{1-2} - \vec{v}_1 \tag{5.51}$$

$$\Delta \vec{v}_2 = \vec{v}_2 - \vec{v}_{2-2} \tag{5.52}$$

Where $\Delta \vec{v}_1$ is the initial impulse burn \vec{v}_{1-2} is the velocity vector at the beginning of the chase manoeuvre, \vec{v}_1 is the velocity of the vehicle at the initial orbit, $\Delta \vec{v}_2$ is the final impulse burn, \vec{v}_2 is the velocity of the vehicle at the final orbit and \vec{v}_{2-2} is the velocity vector at the end of the chase manoeuvre.

The final output is velocity increment (given as a sum of the above presented velocity increments) required to perform the manoeuvre with the desired time of flight and true anomaly. The parameters that describe the initial and final orbits and are given by Table 5.18. This is one of the possible solutions that is within the ΔV requirement. Multiple other solutions are possible by varying the semi-major axes of the orbits and the desired position given as a function of true anomaly.

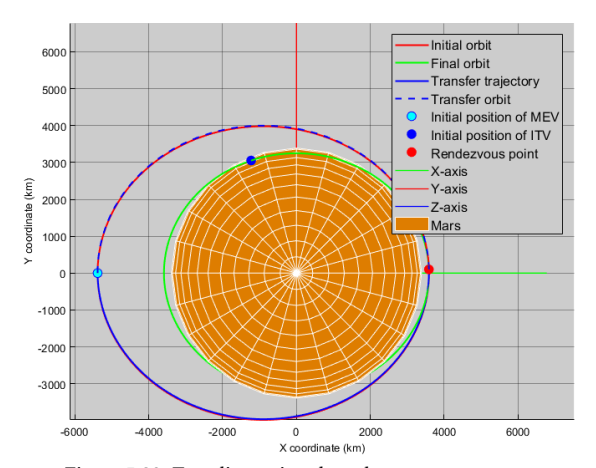
Table 5.17: User inputs for elliptic transfer orbit.

Initial Orbit Parameters							
Parameter	Value	Units					
Semi-major axis	4,490.0	km					
Eccentricity	0.2	_					
Inclination	25.2	deg					
Right ascension of ascending node	0.0	deg					
Argument of perigee	0.0	deg					
True anomaly	180.0	deg					

Table 5.18: User inputs for rendezvous.

Final Orbit Parameters						
Parameter	Value	Units				
Semi-major axis	3,590.0	km				
Eccentricity	0.0	_				
Inclination	25.2	deg				
Right ascension of ascending node	0.0	deg				
Argument of perigee	0.0	deg				
True anomaly	110.0	deg				
Orbital direction	Posigrade					
Target transfer time	4,567.0	s				

Figure 5.29 and Figure 5.30 represent a two and three dimensional plot of the chase manoeuvre with rendezvous points. Note that the transfer trajectory coincides with the initial orbit. This is one solution optimised for ΔV where the transfer trajectory coincides with the elliptical orbit. If a faster or slower trajectory is taken, that affects the initial impulsive burn which drastically increases the velocity increment needed for the MEV to precisely dock with the ITV. The transfer is initiated with a pre-defined position of the ITV and the true anomaly of the MEV is such that both vehicles can dock with each other at a point which lies on the initial circular orbit. Please note that the rendezvous manoeuvre is performed counterclockwise when looking into the figures.



 $Figure \ 5.29: Two \ dimensional \ rendezvous \ manoeuvre.$

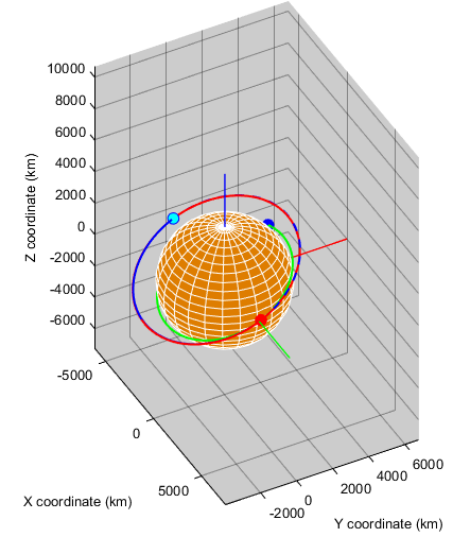


Figure 5.30: Three dimensional rendezvous manoeuvre.

The final output parameters for one of the possible solutions are presented in Table 5.19 and Table 5.20. This is a summary of the velocity vector decomposed in all three axes and a total ΔV magnitude required.

Table 5.19: Orbital elements of transfer orbit.

Orbital elements of transfer orbit after the final impulse						
Semi-major axis	4,488.7	km				
Eccentricity	0.2	_				
Inclination	25.2	deg				
Argument of perigee	358.0	deg				
Right ascension of ascending node	0.0	deg				
True anomaly	307.0	deg				
Period	9,130	S				

Table 5.20: ΔV vectors and magnitude.

Initial Delta-V vector and magnitude							
X component of Delta-V	14.55	m/s					
Y component of Delta-V	0.51	m/s					
Z component of Delta-V	0.24	m/s					
Delta-V magnitude	14.56	m/s					
Final Delta-V vector and magnitude							
X component of Delta-V	-23.7	m/s					
Y component of Delta-V	-299.2	m/s					
Z component of Delta-V	-140	m/s					
Delta V magnitude	331.6	m/s					
Transfer time	4,567	_ s					

Verification

Validation of a rocket launch from Mars can, at this point in time, be considered impossible, given that no rockets have ever been launched from Mars surface. However, efforts can be made in order to manually verify the code that has been generated. In order to ease the manual calculations, avoiding any mistakes, some assumptions need to be made. The MEV is assumed to be a point mass, with one resultant force acting on it in a varying gravity field of 3.711 m/s^2 at the surface and 3.32 m/s^2 at 200 km altitude. The fuel flow is constant, so the average mass between start and end of the burn is chosen. This constant mass results in a constant acceleration, for which basic dynamic formulas can be applied. The calculations are checked on three different, mission critical aspects: altitude, time and accelerations. After applying the basic dynamic equations, the following results are acquired Table 5.21.

Table 5.21: Verification of thrust and mass.

Parameter	Units	Manual	Program	Error [%]
Apoapsis	m	15,137.67	15,046.8	0.6
Time to apoapsis	S	118.7	118.23	0.4
Acceleration	m/s^2	5.102	5.13	0.5

The MATLAB environment uses a precise model that includes all variations in gravity field and gravity distribution, rotation of the planet and the changing atmosphere. That is why the errors are less than 1%. Given these low errors, which can be considered to be rounding errors, the model can be considered verified for the vertical launch case.

In the second scenario, the thrusters are turned to 90 degrees for 1 s at 75% throttle, creating a pure torque around the centre of gravity of the MEV. It should be noted that the gimbal limit has to be removed in order to check for this situation. In the system, the angular acceleration around the cg is measured. Using the measured angular acceleration and known inertia, the torque around one axis can be easily computed. This torque should be equal to the moment generated by the thrust of the engines. During the verification process, it was found that the inertia of the model was too high, since the inertia of the wet mass was implemented in both the fuel burning and the MEV block. This problem was resolved, yielding the results from Table 5.22.

 ${\it Table 5.22: Verification of gimbal values.}$

Parameter	Calculated	Found	Error [%]
Torque [Nm]	1,560,000	1,533,000	1.7%

Which can be considered significantly small, given the fact that the centre of gravity of the entire model might have a slight offset with respect to what is used as input due to the connection of the blocks.

Verifying the code written for docking is not considered necessary since it is a proven working software developed by third parties and partially modified by Project Cardinal. These modifications are mainly related to changes in the celestial body specific variables. For example, the environment was changed and many constants were re-written to be suitable for Mars rather than Earth. The algorithm and the interface did not change since the program was flexible and was able to compute various rendezvous scenarios under changing conditions.

5.2.7. Return Trip

The above presented transfers consider the one-way trip to Mars. However, additional options for a return transfer should be discussed. The arrival time after a Hohmann transfer to Mars does not allow for a direct efficient return to Earth. This means that either a combination of orbits need to be used or one of the single way trips needs to be high energy. In order to perform each return trip efficiently each transfer trajectory should be optimised for ΔV and TOF. Since there will be fewer return trips (only crewed missions and less cargo missions) the return trajectories can be constructed such that each launch window can be used.

One option is to extend the mission time on Mars in order to wait for the next efficient Hohmann transfer window back to Earth. This is considered as a realistic option since the time spent on Mars is assumed to be less risky than time spent in space. Given the synodic period of Mars and Earth, this will mean a Mars-based mission time of roughly 1.5 years before the next most efficient launch window. This means that there will at least one vehicle that will be brought back to Earth for each Hohmann window. The ΔV will in the same range as the Earth-Mars trip with 5.7-5.9 km/s. Alternative options are proposed such as using ballistic trajectory optimisation and captures at Earth in order to minimise the second burn. Precise return trajectory analysis is proposed in the post-DSE activities.

5.3. Structures

The purpose of the structural subsystem is outlined in three different keypoints shown below:

- Withstand the loads during the spacecraft operation;
- Protect the subsystems;
- · Support the attachment of subsystems and unloading of cargo

Furthermore this section will also detail the overall structural and air brake design, materials, safety factors and lifetime, as well as the landing legs.

5.3.1. Primary Load Cases

A preliminary layout of the lander with major load forces is sketched in Figure 5.32. The spacecraft is divided into five segments, as shown in Figure 5.31. As shown in the free body diagrams, five load cases are considered; **Load A:** compression from the base of MEV, **Load B:** tension from base of MEV, **Load C:** compression from aerobraking, **Load D:** aerodynamic compression from launch loads, and **Load E:** tension due to internal pressure.

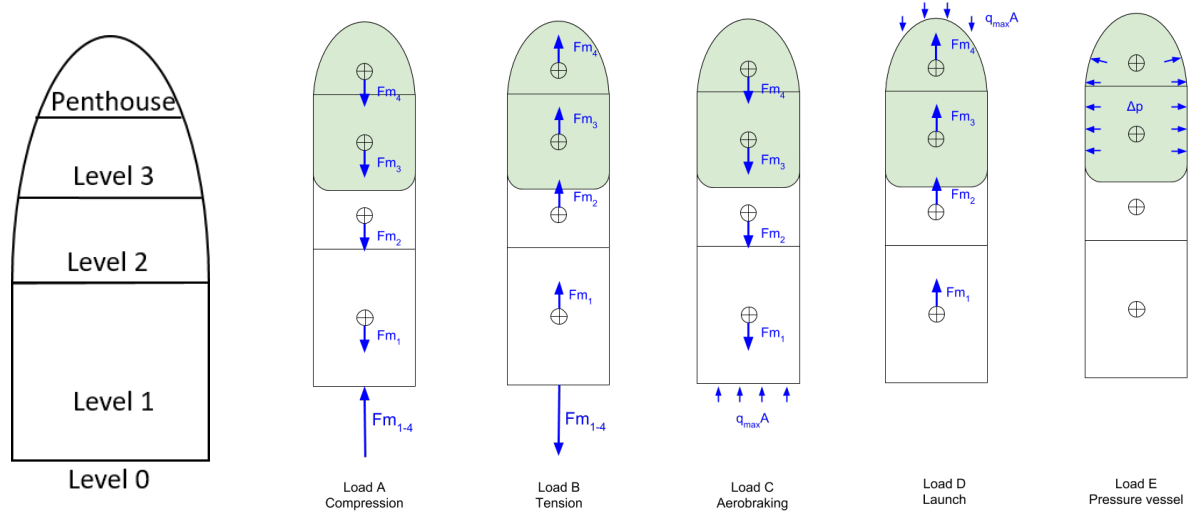


Figure 5.31: MEV sections.

Figure 5.32: All structural load forces on the MEV.

Four scenarios are considered in which critical combinations of these loads may occur, as are listed below.

1. **Launch from Earth, compression:** During launch, the launch vehicle applies a large force at the base of the MEV, causing accelerations. Dynamic pressure is also applied to the structure (Loads A, D and E). This is the maximum compressive force the vehicle needs to resist. Note, he MEV is launched without propellant.

2. **Launch from Earth, tension:** During launch from Earth, the launcher may also cause vibrations which exert a tension on the bottom of the lander (Loads B and E). This is the largest tension load the MEV needs to resist, and again considers the case the when the MEV is launched unfuelled.

- 3. **Landing on Mars:** During landing, the engines are fired to deaccelerate the vehicle, which exerts a compression force. Furthermore, pressure and aerodynamic loads are also present (Loads A, C and E). This is the largest compressive load the lander needs to take whilst fuelled.
- 4. **Launch from Mars:** Launch accelerations, aerodynamic, and pressure loads are applied to the structure (Loads A, D and E).

For each case, the accelerations caused by the Falcon 9 launcher (similar to the falcon heavy) are shown in Table 5.23. This table also accounts for whether or not the pressure differential, fuel mass and payload mass are included in each of the acceleration calculations.

Table 5.23: The accelerations of the Falcon 9 in each load case [42], including an indication of the parameters accounted for.

Load Case:	1	2	3	4
Longitudinal acceleration [m/s ²]	58.9	-19.6	27.5	20
Pressure differential	✓	✓	✓	✓
Payload mass	✓	✓	✓	✓
Fuel mass	×	×	✓	1

The Earth launch accelerations listed in subsection 5.3.1 were taken from the launch acceleration of the Falcon 9 [42] and the Mars decent and ascent accelerations are respectively taken from subsection 5.2.5 and subsection 5.2.6

5.3.2. Safety Factors

NASA Technical Standards [43] prescribe safety factors specific to load bearing members, pressure vessels, metallic and non-metallic member. These are given in Table 5.24. These factors consider both prototype (separate test part) and protoflight (test the part that flies) cases, although for structures all parts can be tested as a prototype.

Table 5.24: NASA standard factors of safety [43].

		Factor of Safety		
	Structure type	Yield	Ultimate	
Metallics	Flight structure	1.00	1.40	
Composites	Flight structure		1.40	
	Discontinuities, cut-outs	-	2.00	
Habitat	Pressure vessel	1.65	2.00	
	Doors, hatches	1.65	2.00	

5.3.3. Material Selection

Only two material types are currently used or considered for manned re-entry vehicles: aluminium alloys and CFRP. These are the only materials currently used for manned reentry capsules. These materials were traded off for the MEV primary structure. It was assumed for simplicity that the pressure and compression structures are combined into one isotropic structure, and the two options were traded off based on mass and structural life.

Mass

The structure should be made as light as possible while still meeting all loading requirements. Material properties relating to mass are shown in Table 5.25. A 28% increase in specific strength is already seen in the specific strength of carbon fibre compared to the alloy, which already indicates a significant weight savings.

Table 5.25: Properties of Aluminium-Lithium alloy and carbon fibre multiply considered for primary structure.

Material	Density [g/cm ³]	Stiffness [GPa]	Toughness $[MPa\sqrt{m}]$	Tensile strength [MPa]	Specific Stiffness $\left[\frac{GPa}{g/cm^3}\right]$	$ \begin{aligned} & \textbf{Specific} \\ & \textbf{Toughness} \\ & \left[\frac{\textbf{MPa}\sqrt{\textbf{m}}}{\textbf{g}/\textbf{cm}^3} \right] \end{aligned} $	Specific Strength $\left[\frac{\text{MPa}}{\text{g/cm}^3}\right]$
Al-Li alloy ³⁰	2.7	76.5	36	476	28	13	176
CFRP ³¹	1.58	60.1	87.6	356	38	55	225

³⁰ https://www.constellium.com/sites/default/files/markets/airware_2050_t84_plate.pdf(Lastaccessed 07-06-2018)

³¹ https://www.scribd.com/document/76975806/Carbon-Fiber-Quasi-Isotropic-Laminate(Last accessed 11-06-2018)

Fatigue life

For the materials trade-off, fatigue is assumed to be the major factor affecting the durability of the spacecraft. The stress-cycle life relations are shown in Figure 5.33. The straight slanted line shows how the cycle life of a composite element increases exponentially with decreasing stress amplitude. For the aluminium alloy, a fatigue limit at about fatigue limit (55%) and no degradation to the material below the limit.

Materials that corrode are expected to have a much shorter fatigue life, and due to the lack of oxygen on Mars. The leftmost line in Calle et al. [44] illustrates an Al-Li sample which has been scratched and left to corrode, decreasing both the cycle life and removes or greatly decreases the fatigue limit.

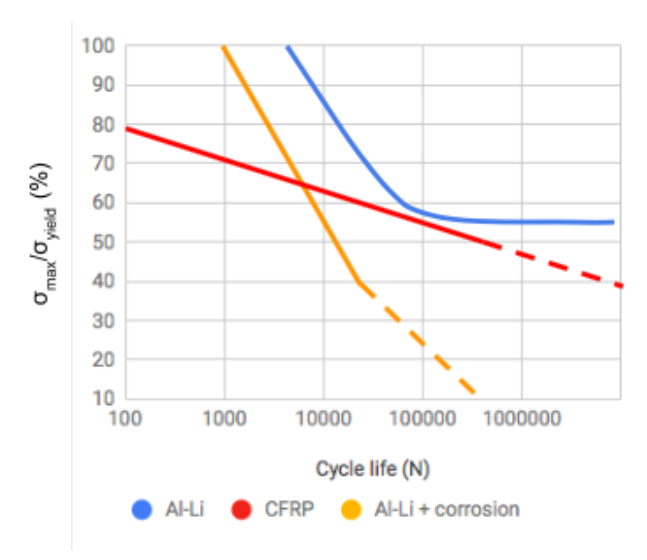


Figure 5.33: Stress vs. fatigue of three samples: Aluminium–Copper–Lithium alloy 2050, the same alloy including the effect of corrosion, and a worst-case scenario for carbon fibre reinforced polymer³².

Result

Table 5.26 shows the final trade-off between materials. For this trade-off, a preliminary version of the model described in the next section was used to estimate the total primary structure mass. Carbon fibre reinforced polymer was chosen for the primary structure, due to two reasons: 1) significant mass reduction of 35% and 2) similar or better fatigue and durability properties.

Table F 2C.	Matariala	trada off for	the nuin	owy otwarotane
1able 5.26:	Materiais	trade-on for	the prim	ary structure.

Material	Mass (kg)	Durability issues	Fatigue life at 60% of yield (N. launches) ^{33 34}
Al-Li alloy	1,616	Outgassing, gamma radiation, corrosion	$10^4 - 10^5$
CFRP	1,055	Outgassing, gamma radiation, UV radiation	10^{5}

5.3.4. Structural Design

In this section the sizing of various structural members will be explained. This will be done by first explaining the overall approach, then by elaborating on how the various loads were found and ending with a discussion of how the stresses were calculated. The formulas and general approach for this section are taken from Hibbeler and Yap [16] unless mentioned otherwise. All the calculations that follow were performed in Microsoft Excel.

Global Structural Approach

The MEV is divided into five levels as explained in subsection 5.3.1. Every level of the MEV is modelled as a beam in either tension or compression. Additionally there are five floors. Each of these consists of a number of I-beams which are sized to take the forces caused by the mass of the appropriate propellant and/or payload and/or subsystems and/or structure.

 $^{^{32}} https://www.constellium.com/sites/default/files/markets/airware_2050_t84_plate(Last accessed 21-06-2018)$

³³https://www.sciencedirect.com/science/article/pii/S0142112305001015(Last accessed 21-06-2018)

³⁴ https://hal.archives-ouvertes.fr/hal-01264391/document(Last accessed 21-06-2018)

Assumptions made:

- All materials are assumed to be isotropic;
- All forces are assumed to be axially applied to the MEV, in other words, no sideways-forces are considered;
- Introduction of loads is not considered;
- Thermal loads are neglected;
- Every level is assumed to be clamped at both ends when considering buckling loads, because this most accurately represents the attachment between the levels that is expected to be present in real life.
- Load introduction between levels is not considered, loads are introduced on the centre of gravity of each level;
- Every level is assumed to be a cylinder, except when calculating the mass, in which case it is a assumed to be a conical frustum (cone intersected by a plane);
- Shear stress in the floor beams is assumed to be continuous;
- Floor beam cross-sectional area tapers linearly from the centre of the floor to the outer skin;
- Floor beams are modelled by assuming the relevant force is applied a the centre of the MEV (end of the beam) and evenly divided between the floor beams;
- All forces are applied to the geometric centre of each section;
- Floor space over and between the floor beams is assumed to be 2 mm tick. In reality this would probably be two sheets of structural material with a honeycomb between them.

General Formulas for Structural Design

Equation 5.53 and Equation 5.54 are used to find the area moment of inertias of rectangles (I_{rec}) and circles (I_{circ}) respectively. Here b is the width of the rectangle and h is its height, and r is the radius of the circle in question.

$$I_{rec} = \frac{1}{12} \cdot b \cdot h^3$$
 (5.53) $I_{circ} = \frac{1}{4} \cdot \pi \cdot r^4$

Travelling through the atmosphere at high speeds causes an aerodynamic force to be applied. This is modelled by finding the maximum dynamic pressure applied to the vehicle (also called max Q). For the Mars descent and ascent this pressure was found in section 5.2. For Earth ascent the maximum dynamic pressure was found using Equation 5.55³⁵. Here u is the airspeed and ρ is the density of the air at max-Q taken from the falcon heavy launch³⁶. Equation 5.56 is used to find the stress (σ_{ax}) caused in a beam by the application of either a compressive or tension force (F) where A is the area of the beam perpendicular to the applied force.

$$q = \frac{\rho u^2}{2} \tag{5.55}$$

$$\sigma_{ax} = \frac{F}{A}$$

Equation 5.57 and Equation 5.58 were used to find the hoop, σ_1 , and axial, σ_2 , stress caused in the skin of a cylinder by the presence of a pressure differential (p). Here, r is the radius of the cylinder and t ut's thickness. The two stresses are tangential to each other, and the MEV is pressurised to 101,300 Pa (Earth sea level pressure)

$$\sigma_1 = \frac{pr}{t} \tag{5.58}$$

Equation 5.59 can be used to find the buckling force of a beam, P_{crit} . It should be noted that a beam cannot buckle under tension forces. Here, E is the Young's modulus (stiffness) of the material, I is the moment of inertia and E is the length of the beam in question. In Equation 5.60 E is the moment in the beam at the relevant point and E is the distance between the neutral axis and the point in the beam where the stress is to be calculated.

$$P_{crit} = \frac{\pi^2 EI}{(0.5L)^2}$$
 (5.59)
$$\sigma_{bending} = \frac{My}{I}$$

Equation 5.61 was used to find the maximum stress in a structural element caused by the application of two tension and/or compressive stresses and a shear stress. Where σ_x and σ_y are the stress in the x and y planes respectively, while τ_{xy} is the shear stress. Note that σ_x and σ_y are derived from the equations listed above such as Equation 5.60 or Equation 5.57 and others. Equation 5.62 was used to determine the height of the centroid above the chosen axis system, c. This is found from c, the distance of the centroid of a given element from the chosen axis system, and c, the area of this element.

 $[\]overline{^{35}} http://www.aerospaceweb.org/question/aerodynamics/q0025.shtml (Last accessed 13-06-2018)$

³⁶https://www.youtube.com/watch?v=wbSwFU6tY1c(Last accessed 14-06-2018)

$$\sigma = \frac{\sigma_x + \sigma y}{2} + \sqrt{\left(\frac{\sigma_x - \sigma y}{2}\right)^2 + \tau_{xy}^2}$$
 (5.61)
$$c = \frac{\sum xA}{\sum A}$$

5.3.5. Level and Floor Structural Sizing

All structural calculation described here are performed in Microsoft Excel and based on the equations mentioned in subsection 5.3.4. This spreadsheet has 10 sections. Before the function of and interactions between the systems is explained it is valuable to elaborate on the overall functioning of the spreadsheet. The structure of the MEV is defined by 35 procedural parameters. These are skin thickness, number of stiffeners, number of radial beams, beam width, height, web and flange thickness. The first two parameters listed here define the outer hull of the MEV. The other five are used to size the floor of each level of the MEV. Using the applied loads and these parameters one can find out if the MEV fails structurally for a given load case. Repeat this across all load cases and one knows if the MEV successfully resists the loads or not. One can then also find the structural mass of the MEV for these 35 procedural parameters. At this point the built-in evolutionary solver of Excel is used to vary the 35 procedural parameters, finding a combination that minimises the weight while still resisting all loads successfully. The interactions between these sections is also shown in Figure 5.34.

- **Section 1: UI** or user interface gives a clear summary of the results of the calculations performed. It does not perform any calculations.
- **Section 2: Material properties**, this section list the material properties used in later calculations. It list the modulus of elasticity, density, tensile yield strength and compressive yield strength.
- Section 3: Load cases, are listed in a table similar to Table 5.23 this is then referred to in calculations to apply the correct masses and loads for each of the load cases.
- Section 4: Subsystem masses, list the masses included in each level. It is divided into: structural masses (floor, hull, stiffeners, etc.), subsystems masses (ADCS, thermal, etc.), payload, and propellant masses. Table 5.30 gives an overview of the location of the various subsystems in the MEV.
- Section 5: Procedural elements table and stress checker, in order to perform the requires iterations the geometrical properties of the procedural elements are varied. These procedural elements are for the level: the skin thickness and amount of stiffeners (assumed to be ten by ten mm squares). For the floor: the number of floor beams and their height, width and flange and web thicknesses. Each of these procedural parameters has to be constrained for mathematical reasons (to allow the solver to function) and practical reasons (to prevent unrealistic or unmanufacturable structures). Note that no thickness less than 1 mm is permitted to ensure manufacturability, however this criteria is not binding, e.g. decreasing this to 0.2 mm would not influence the outcome. This section also checks if allowable stresses are not exceed and that the structure does not exceed its buckling load.
- Section 6: Structural parameters of the level, in this section the area moment of inertia and area of the level's cross-section is calculated for both the top and the bottom. The top and bottom can vary based on the MEV radius at the specific level. In addition the mass of these structural elements is also calculated.
- Section 7: Structural parameters of the floor, similar to section 6, here the cross-sectional areas and area moment of inertias of the floor beams are sized as well as their masses.
- **Section 8: Applied forces and pressure stresses**, this section has eight distinct sub-sections, each of which calculates a load, and one of which calculates a stress directly.
 - Max q force Earth launch, calculates the force applied by the dynamic pressure using the frontal area of the relevant level (not counting area occluded by upper level) and Equation 5.55. The velocity and altitude at max Q were based on the falcon heavy launch³⁷ and atmospheric density for that altitude³⁸.
 - Max q force Mars decent, calculated similarly to max q at Earth except using the dynamic pressure given in Equation 5.2.5. Note that this force is coming from "under" the MEV unlike the other two max q forces.
 - Max q force Mars take-off, calculated similarly to max q at Earth except using the dynamic pressure given in section 5.2.
 - Pressure vessel using Equation 5.58 and Equation 5.57 the hoop and axial stress is calculated. Note that these two stresses are only taken into account if they increase the stress. For instance during axial compressive loading of the MEV under external forces the axial pressure stress will actually relieve part of the first stress (or vice versa, depending on magnitude). However this is risky since it would mean that a loss of pressure might lead to structural failure.

³⁷https://www.youtube.com/watch?v=wbSwFU6tY1c(Last accessed 21-16-2018)

³⁸http://www.wolframalpha.com/input/?i=density+of+air+at+11.1+km(Last accessed 21-16-2018

Acceleration compression force Earth, this force is calculated by taking the acceleration compression
force induced by upper levels as relevant and adding to it the force produced by the acceleration of the
mass of the level in question for the load case (presence of propellant, etc.) in question.

- Acceleration tension force Earth, similar to the acceleration compression force Earth, but with a different acceleration.
- Mars acceleration deceleration force, similar to the acceleration compression force Earth, but with a different acceleration.
- Mars acceleration launch force, similar to the acceleration compression force Earth, but with a different acceleration

This is repeated for every level and every load case. Note that the forces upper levels are also taken into account. For instance the force developed by the Max Q force Earth of level 3 passes onto to level 2, and then to level 1, etc.

• Section 9: Level maximum stress and buckling calculations

- Axial stress, calculated for the top and bottom, based on Equation 5.56.
- Stress combination finds the stress caused by the combined loading cased by axial stress and hoop stress, using Equation 5.61. If relevant (e.g. if it leads to a higher overall stress) the axial stress due to pressure is also taken into account.
- Buckling calculated using Equation 5.59 the force for which the structure buckles is calculated. Clearly
 the applied force should always be less then this buckling force. Note that this subsection is not considered when dealing with tension loads, since structures cannot buckle in tension.
- Acceptable Stress this section applies the safety factors as listed in Table 5.24), namely 2 for the outer hull and floor, by multiplying the stresses and buckling loads with the safety factor before subtracting them from respectively the allowable stress and applied force. The result found then has to be positive, otherwise the structure fails. These are summarised in section 1.

This is repeated for every level and load case.

• Section 10: Floor maximum stress calculations'

- Force applied, this force is calculated based on accelerations applied to the mass the floor has to hold (payload, propellant, subsystems and the mass of the floor and its beams). Note that this force is assumed to apply in the centre of the floor and to be equally distributed between the available floor beams.
- Shear stress, is calculated using Equation 5.56 as applied to the relevant force and beam area. This assumes that the shear stress is constant across the cross-sectional area of the beam.
- **Bending stress**, is found using Equation 5.60 filling in worst case values for M and y, namely the largest moment achieved in the beam (M), and the largest distance from the neutral axis (y).
- **Stress combination** finds the stress caused by the combined loading cased by bending stress and shear stress, using Equation 5.61.

This is repeated for every level and load case. Since the dominant stress for this type of load case is bending the beams are assumed to taper linearly from their design width at the hull to no width at the exact centre of the MEV. In the detailed design phase a more thorough analysis of the ideal taper is expected to be made. Note that buckling as a failure mode is not considered for the floor beams.

It should be noted that sections 4 and 5 were repeated for every level and floor, and that sections 6, 7 and 8 were repeated for every load case and every level and floor.

Solver

The Excel solver was used to perform the iteration that can be seen in Figure 5.34. The evolutionary solver is used³⁹. The solver tries to minimise the structural mass, by changing the procedural structural parameters, while subject to constraints. The first set of constraints is to ensure that the structure can withstand all loads effectively. Practically this means that only solutions for which the structure does not fail are considered viable. The second set of constraints, as found in Table 5.27 are present to ensure manufacturability and to ensure that the elements fit in the MEV design (for instance, the floor beams are limited to a height and width of 20 cm to prevent them taking up too much volume, though this is increased to 1 m for level 1 to account for the extra vertical volume available there. Note that the evolutionary solver does not converge to the "perfect" solution, merely to a "good" solution for which it satisfies its constraints. Given more time and computational resources and/or a different starting point and/or starting seed it is possible to find a better solution. However, this is not expected to decrease the mass significantly.

³⁹https://www.solver.com/excel-solver-algorithms-and-methods-used(Last accessed 21-06-2018)

Table 5.27: Constraints on the procedural parameters.

	Skin [mm]	Number of stiffeners	Number of radial floor beams	Beam height [mm]	Beam width [mm]	Web width [mm]	Beam flange width [mm]
Min value Penthouse	1	0	4	1	1	1	1
Min value level 3	1	0	4	1	1	1	1
Min value level 2	1	0	4	1	1	1	1
Min value level 1	1	0	4	1	1	1	1
Min value level 0	1	0	4	1	1	1	1
Max value Penthouse		500	20		200	100	$ \overline{100}$
Max value level 3	10	500	20	200	200	100	100
Max value level 2	10	500	20	200	200	100	100
Max value level 1	10	500	20	1,000	1,000	100	100
Max value level 0	10	500	20	200	200	100	100

Section 1: UI									
Material properties	Section 2: Material properties						Material properties	Material properties	Material properties
		Section 3: Load cases	List of masses to include						
Masses of relevant subsystems			Section 4: Sub systems masses				Masses of relevant subsystems		
Procedural elements sizes and masses				Section 5: Procedural elements tabel and stress checker	Procedural elements sizes	Procedural elements sizes			
					Section 6: Structural parameters of the level		Structural parameters of the level	Structural parameters of the level	
						Section 7: Structural parameters of the floor	Structural parameters of the floor		Structural parameters of the floor
							Section 8: Applied forces and pressure stresses		
Achieved stress levels				Achieved stress levels				Section 9: Level maximum stress and buckling calculations	
Achieved stress levels				Achieved stress levels					Section 10: Floor maximum stress calculations

Figure 5.34: N2 chart of the spreadsheet.

Using the constraint, solver and approach explained above the final answer was found. The number and size of all the elements are shown in Table 5.28, the masses are listed in Table 5.29.

Table 5.28: Table li	sting the number o	f and size of	procedural	structural elements.

Procedural element	Penthouse	Level 3	Level 2	Level 1	Level 0
Skin [mm]	3.5	2.1	2	1.1	1.3
Numbers of stiffeners	154	27	21	19	75
Number of radial beams	6	4	16	4	16
Beam height [mm]	187.3	199.4	188.4	215.7	157.4
Beam width [mm]	66.7	198.9	188	624.5	152.6
Flange width [mm]	13.2	16.2	14.4	11.7	9.1
Beam top/bottom width [mm]	5.9	15.2	16.4	12.3	14.3

Table 5.29: Table listing the masses of various procedural structural elements.

Mass		Penthouse	Level 3	Level 2	Level 1	Level 0	Total
Skin	[kg]	52	177	126	184	41	581
Stiffeners	[kg]	24	15	8	20	14	81
Floor	[kg]	40	67	67	67	67	308
Floor beams	[kg]	29	72	276	145	182	705
Total	[kg]	145	331	478	416	305	1,674

In Table 5.30 the mass and location of the subsystems is listed. This is used in the structural design to determine the loads induced by the masses of the subsystems. Note that propellant masses are also listed.

Table 5.30: Table listing the masses and locations of various subsystems of the MEV.

Item	Mass [kg]	Location in MEV
Air Brake	1,100	Level 0
Landing Legs	1,500	Level 0
Propulsion	909.7	Level 0
Propellant tank	$-99\overline{4.4}$	Level 1
Environmental tanks	632.5	Level 1
Propellant decent	12,900	Level 1
Propellant ascent	38,450	Level 1
Propellant for RCS	539	Level 1
Airlock	385	Level 2
Thermal	590.7	Level 2
Power	1,300	Level 2
Payload (cargo)	4,000	Level 2
ĀDCS	450	Level 3
Communications	60	Level 3
Payload (passengers)	1,000	Level 3
Structures	1,674	[-]
Total	65,947.3	[-]

Verification

The spreadsheet was verified in various ways. It was checked by another member of the team in terms of logic, applied theory and implementation in the spreadsheet. One of the verification tests was to set the acceleration, max q and pressure differential to zero. The solver then converged to the minimum permitted values for each procedural structural element. Overriding the constraint by setting all procedural values to 0 or 0.0000001 (to prevent division by 0 problems) lead to an effectively non-existent structure which was still able to resist the now non-existent loads. When loads were applied to this virtually non-existent structure it failed as expected. The beam buckling unit was test comparing to a problem from Hibbeler and Yap [16] with a know solution. Both values were identical. The Moment Of Inertia (MOI) of the cylinder was similarity verified, again with identical results. The MOI of the floor beams was verified using a known problem and solution from [45], here a difference of 0.00643 % was registered. The calculation of applied forces was verified by hand calculation. The stress caused by the pressure differential was verified by comparison with an example from Hibbeler and Yap [16] and found to be identical. The overall interaction between various section was checked by using some of Excel's built in verification features such as tracing formula dependants and precedents, etc.

Validation

A comparable problem is the design of ISS modules. These need to resist launch loads and hold atmospheric pressure. As listed in Table 5.28 the skin thickness varies between 3.5 and 2 mm for the pressurised part of the MEV this is in line with expectations given that the hull thickness of the international space station is 2.5 mm⁴⁰. A notable difference is the use of aluminium on the ISS compared to carbon fibre on the MEV. Notable uncertainties are the safety factors applied to the ISS design, as well as precise dimensions.

Sensitivity Analysis

A sensitivity analysis was performed by increasing the safety factor by varying amount and then running the solver from the same starting values, with the same solver parameters. The results are listed in Table 5.31. Note that increasing the safety factors is practically identical to doubling all the applied forces on the structure. Taking note of some inherent variation in solver solutions, one can conclude that the sensitivity analysis shows it is a robust design. This means that the structure of the MEV does not have a disproportional effect on the mass of the MEV as whole when other masses change.

Safety factor [-]	Change safety factor [%]	Structural mass [kg]	Change structural mass [%]
1	-50	1,120	-34
2	0	1,695	0
2.2	10	1,723	2
3	50	2,466	45

Table 5.31: Table listing structural mass for various safety factors, and the percentual change.

Table 5.32 list the changes in structural mass for various changes in the applied loads. Baseline is the load case for which the MEV is designed as described above. The most significant conclusion that can be draw from this would seem to be the sensitivity to increases in payload mass. However for this case floor beam and width parameter were reaching their maximum allowed values for level 3 and 2, as listed in Table 5.27. This means that a lighter structure can be designed if the constraint are lifted (and in light of the mass penalty imposed by them, this seems probable). Another conclusion is the relative lack of sensitivity to max Q.

•		
Load case	Structural mass [kg]	Change structural mass [%]
Baseline	1,674	0
Double internal air pressure	2,355	41
No internal air pressure	1,562	-7
Double max Q pressure	1,753	5
No max Q pressure	1,482	-11
Double payload mass	8,787	425
No payload mass	1,253	-25

Table 5.32: Table listing structural mass for various load case variations, and the percentual change.

5.3.6. Air Brake

In this subsection the structural sizing of the air brake is performed. In subsection 5.2.5 it was determined that use of an air brake would be essential to reduce the required propellant mass during landing. The formulas and general approach for this section are taken from [16] unless mentioned otherwise. After some consideration it was decided to use a series of 12 aluminium panels on the outside of the MEV, as explained in Equation 5.2.5. Each of these covers 30 degrees of the hull of the MEV when fully retracted. Each of these panels is 6.5 meters tall, covering 109 m². Note that these panels conform to the curve of the MEV hull. When deployed they extend out to 60 degrees from vertical. However more surface area is needed to slow the MEV. This is provided by placing fabric between the panels. Both the panels and the fabric are heat shielded.

However the presence of angled panels and fabric between them leads to a rather complex load case. In order to solve this problem the same "big picture" approach is taken as for the overall structural design of the MEV. Namely 11 procedural variables changed by a solver subject to constraint to ensure manufacturability and ensure the structure can successfully resist all loads. One of the procedural parameter is the angle made by the fabric with respect to the panels when under maximum load. The other 10 procedural variables are the height of the stiffening stiffeners (with

⁴⁰https://www.youtube.com/watch?v=jqE68lwPS9o(Last accessed 22-06-2018)

a width equal to one-fourth of their height) placed at the tip of the curved panel. As one may deduce from this each panel is divided into 10 part along its length. Each sub-panel is hence 0.65 m long. However only one load case is considered. Namely the case of maximum dynamic pressure applied to the air brake. Since the loads during landing are minimal compared to this dynamic pressure load and applied along the same axis, albeit in opposite direction. Furthermore the air brake is to be stored during accent to minimise drag, which is much less taxing load case then the one described above. One should also note that this air brake sizing is considered to be conservative since it is designed without the presence of an actuation system which is expected to massively reduce the load applied to the structure by providing bending relive somewhere along the span of the air brake, since the actuation system is anticipated to be a hydraulically actuated extending strut connecting a point on the MEV hull a point on the air brake. A safety factor of 1.4 is applied to the loads as per Table 5.24.

Assumptions made:

- All materials are assumed to be isotropic;
- The only external force applied to the air brake is caused by the dynamic pressure;
- Introduction of air brake loads into the MEV is not considered;
- Thermal loads are neglected;
- The fabric and air brake are assumed to not deform under loading;
- Load introduction is not considered between fabric and panel;
- Every panel is assumed to be a flat plate, except for MOI, cross-sectional area, distance from neutral axis and neutral axis determination;
- Nextel is assumed to be the sole load carrying material in the fabric part of the air brake.
- The forces introduced by the fabric and dynamic pressure are assumed to act at the end of each panel.

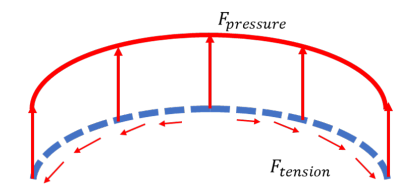
Fabric

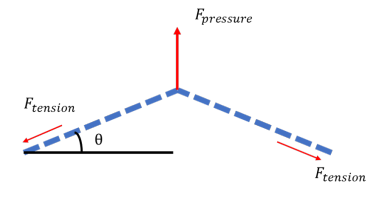
The fabric consists of multiple layers as explained in subsection 5.2.5, with varying properties, as summarised in Table 5.33. Note that the assumption is made that only the Nextel resists loads and that the other two layers are attached to the Nextel. Note that calculation are performed to verify that the Nextel does not fail for the given load case.

Table 5.33: Table summarising the properties and total mass of the various layers of the fabric portion of the heat shield.

Properties	Pyrogel 3350 [46]	KAPTON [47]	Nextel 720 [39]
Thickness [m]	0.003	0.001	0.00106
Density [kg/m ³]	170	1420	3,400
Total mass [kg]	58	161	413
Youngs modulus (modulus of elasticity) [Pa]	[-]	[-]	2.5E+11
Tensile strength [Pa]	[-]	[-]	1,940,000,000

As can be seen in Figure 5.35 the assumption is made that the aerodynamic force on the fabric is a point load, not a distributed load. The larger the angle θ becomes the lower the tensile loads applied to the fabric (and hence indecently the lower the tensile forces applied to the aluminium panels). Hence this angle θ is made a procedural variable and found to be 7.22 degrees by the solver.





(a) Reality: distributed pressure load leading to a continuous varying angle, force and deformation.

(b) Model: point force equal to distributed load leading to continuous angle, tension force and deformation.

 $Figure\ 5.35: Figure\ clarifying\ the\ difference\ between\ reality\ and\ the\ load\ case\ the\ fabric\ is\ assumed\ to\ be\ under.$

Panel design

For each sub panel a number of calculation are performed to find check whether or not is can successfully resist the applied loads. The solver is then instructed to reduce the stiffener size to minimise the mass, while simultaneously ensuring that the stress never reach unacceptable levels.

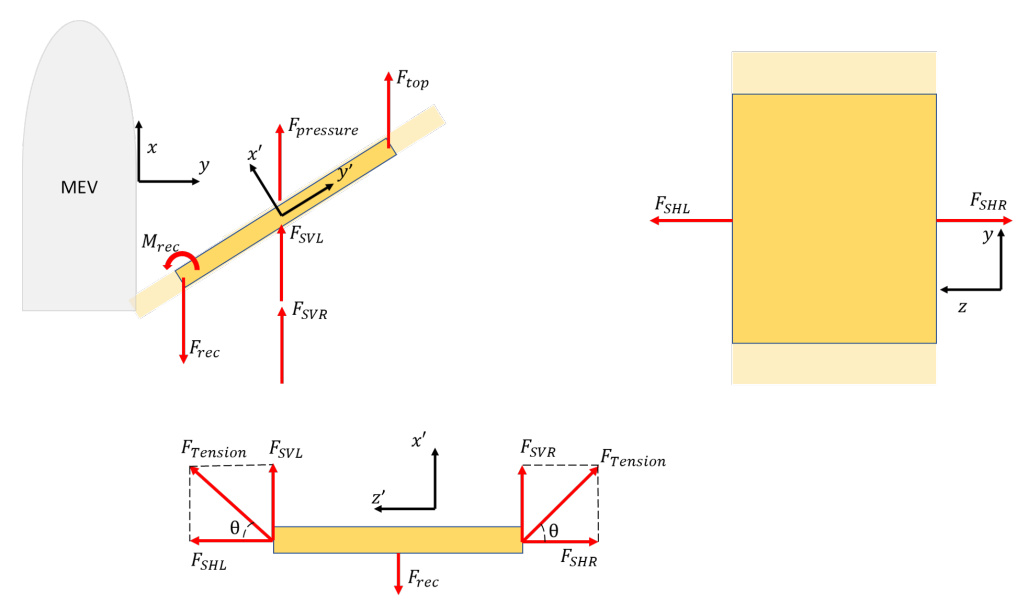


Figure 5.36: Free body diagram of a single sub-panel of the air brake.

• Calculation of geometrical properties, the geometrical properties of the curved plate are found from an identical model in CATIA. The MOI of the aluminium panels was found in CATIA and then multiplied with 37 [48] to simulate the use of a honey comb structure to increase bending resistance. Which is (by far) the largest source of stress in the structure. Except for the centroid, MOI and maximum distance from the neutral axis calculation the panels are assumed to be flat. Note that the panel thickness was set to 1 mm for every sub panel. Using Equation 5.62 and Equation 5.53 the MOI and centroid of the cross-section of every sub panel is found. The cross-sectional area is also found.

· Calculation of forces

- Based on Figure 5.36 and Figure 5.35 the forces induced in the plate by the fabric is found and decomposed into F_{SVR} , F_{SHR} , F_{SVL} and F_{SHL} . This calculation used the dynamic pressure during landing (found in subsection 5.2.5) and the procedural angle of the fabric with respect to the plate.
- F_{top} is the sum of forces along x carried on from sub section further from the MEV than the on in question
- The other applied force is $F_{pressure}$, is also calculated based on the dynamic pressure.
- **Finding the total stress**, based on the forces and geometric properties four stresses can be found, which must then be combined to find the maximum stress in the structure.
 - Tensile stress along y' is found by finding the components of F_{SVL} , F_{SVR} , F_{top} and $F_{pressure}$ along the y' axis and dividing this by the perpendicular area.
 - Bending stress is caused by the components of F_{SVL} , F_{SVR} and $F_{pressure}$ along the x' axis and multiplying these with the appropriate moment arm to find the total moment applied to this sub section. Then as per Equation 5.60 using the moment of inertia and maximum distance from the neutral axis the maximum bending stress can be found.
 - based on the components of F_{SVL} , F_{SVR} , F_{top} and $F_{pressure}$ along the x' axis the shear stress can be found.
 - Using F_{SHL} and F_{SHR} the stress developed in the x'-z' plane can be found.
 - The maximum stress is found by using Equation 5.61 to find the maximum stress occurring in the x'-z' plane caused by the bending and shear stress. Subsequently the Pythagorean theorem is then used to find the maximum stress in the structure, regardless of the angle under which it occurs. Subsequently, three stresses are then combined by using the Pythagorean theorem to find the maximum stress that occurs in the structure.

Air brake parameters

Table 5.34: Table listing the stiffener height and sub section mass for the 10 subsections of each of the 12 air brakes. Note that subsection 1 is closest to the MEV, while 10 is the furthest away.

Panel number [-]	Stiffener height [m]	Sub section mass [kg]
1	0.065	6.573
2	0.058	5.741
3	0.049	4.941
4	0.039	4.174
5	0.027	3.457
6	0.001	2.839
7	0.002	2.841
8	0.001	2.838
9	0.001	2.838
10	0.001	2.838

The total mass of one air brake panel is 39 kg, and the mass of 12 panels is 469 kg. Adding the total mass of the fabric between theses panel leads to a total air brake mass of 1100 kg.

Verification

The calculations performed above were verified in several ways. The code was checked by another member of the team, both in execution and overall logic. Unit test were also performed, e.g. checking that the code behave as expected, checking for singularities. Unit testing of the centroid, area and MOI was performed using CATIA to check a cross section, including stiffeners. The answer was identical to the numerical solution. Unit verification of the beam bending was performed using hand calculation and by comparison to example exercises, however these were not inclined as the air brake is, the results were identical. System testing included: setting dynamic pressure to zero, which as expected lead to no stress in the air brake. Changing the inclination angle of the air brake also influenced the results as expect, e.g. a larger angle lead to larger bending stresses and less axial tension and vice versa. The combination of the various stresses was verified by manual calculations in a series of unit tests. Furthermore built in verification features of Excel were used such as tracing formula precedents and dependants.

Sensitivity analysis

Table 5.35 list tabulates the change in the mass of the air brake for changing dynamic pressure. The air brake appears to be very stable. This is partly due to the fact that the mass of the fabric between the plates is not varied for the cases listed below, and neither is the mass of the heat shield applied to the aluminium.

Table 5.35: Table listing air brake mass for various safety factors, and the percentual change.

Dynamic pressure [Pa]	Change dynamic pressure [%]	Mass air brake [kg]	Change mass air brake [%]
3,050	-50	982	-11
6,100	0	1,100	0
7,320	20	1,159	5
12,200	100	1,411	28

5.3.7. Structural Life

Durability is the ability of a structure to withstand wear. On a mission between Mars orbit and Mars surface, wear may be caused by several things such as fatigue, UV radiation, gamma radiation out-gassing or corrosion. Because the spacecraft must be reused 100 times, the structural life and thus the durability must be analysed.



Figure 5.37: Stress loads over time, with the peaks representing a landing and a launch. Positive loads are tension and negative are compression.

Among all the causes, fatigue was found the dominating cause of wear. In order to find the dominating fatigue loads, the repetitive tension and compression loads from pressure and launch/landing are calculated and shown in Figure Figure 5.37. The maximum stress amplitude is found to be 172 MPa. Combined with a fatigue analysis factor of 1.15 this results in 198 MPa, or 56% of the ultimate load of the carbon fibre.

To calculate the fatigue life from the stress, charts are consulted relating the load amplitude and cycle life of the material. These trends are illustrated in Figure 5.33. The analysis shows a durability of tens of thousands of cycles. Even including the cycle safety factor of 4.0 as dictated in NASA guidelines, the fatigue life is clearly greater than the required 100 trips, or 200 cycles.

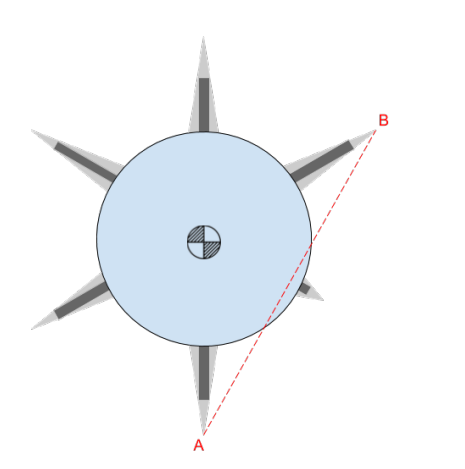
Regarding environmental effects, composite interactions are complex and little data is available for composites in the space environment However, in general the properties of most thermoset reinforced polymers are not significantly effected by radiation and vacuum environment [49] and corrosion is also not expected to be a concern with carbon fibre composites.

Other factors to look into include surface finish, anodising, temperature, size effect, plating, and spraying. The thermal expansion loads of carbon fibre are a topic for further investigation

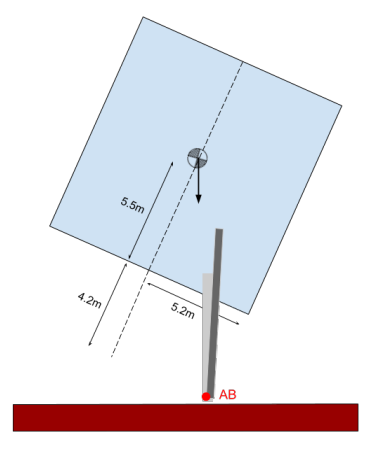
5.3.8. Landing Gear Design

The landing gear is designed for the following driving requirements:

- Provide 1.0 meter clearance between the ground and the engine at all times;
- Static stability on the ground if tipped at 15° to horizontal with failure of one landing leg on that side;
- Absorb the impact of a 3 m/s landing, incurring no more than an acceleration of 24.0 m/s² on the ship.



(a) In case one leg fails to deploy, the lander tips most easily over line A-B.



(b) A cross section parallel to line A-B.

Figure 5.38: The tipping condition is when the cg is over line A-B.

⁴⁰https://www.nap.edu/read/11424/chapter/3#5 (Last accessed 21-06-2018)

Number of legs

To ensure the spacecraft can still stand following the failure of one landing leg, at least five landing legs are required. An additional leg is added, so six in total, in order to fit symmetrically with the air brake configuration.

Leg configuration

Shown in Figure 5.38, the design condition for the leg size and spread angle is when the legs are fully extended except for one, which fails to deploy (b). In this case, the weight of the the lander is supported by the two nearest legs, and at 20° the c.g. is directly between these two legs. A 2.0 m clearance is used, as the legs compress about 1.0 m during landing. The resulting leg dimensions for the required stability are given in Table 5.36

Table 5.36: Landing gear leg size results.

Dimension	Value	Units
Deployed span	9.3	m
Length from hinge	4.1	m
Splay angle	30	deg

Impact

The critical condition for the stiffness and damping coefficients of the landing gear is the maximum expected impact. Two large assumptions are made in order to design the landing gear suspension, 1) that the struts are vertical to the ground and 2) the struts act as a classical spring-damper systems. The first assumption is made because the leg angle of 17° is considered to be small. The second assumption assumes that . In reality the suspension would be made from a piston of compressed gas, which

$$\ddot{x} = g - \frac{k}{m}x - \frac{c}{m}\dot{x} \tag{5.63}$$

$$x(0) = 0 (5.64)$$

$$\dot{x}(0) = v_{max} \tag{5.65}$$

The first constraint on the spring-damper tuning is the deceleration of the lander must not be higher than 24.0 m/s^2 . The second is that the maximum displacement must be minimised as much as possible. After several iterations are made with a Python script until the spring-damper values are achieved. This shows that the required deceleration is possible in even the worst landing condition, still allowing 1.0m of margin between the engine and Mars surface.

Table 5.37: Landing gear dynamics results.

Dimension	Value	Units
Spring constant	400,000	kg/s ²
Damping constant	450,000	kg/s
Decompressed ground clearance	1.4	
Final ground clearance	1.0	m
Deceleration force	1,127	kN
Deceleration	24.0	m/s^2

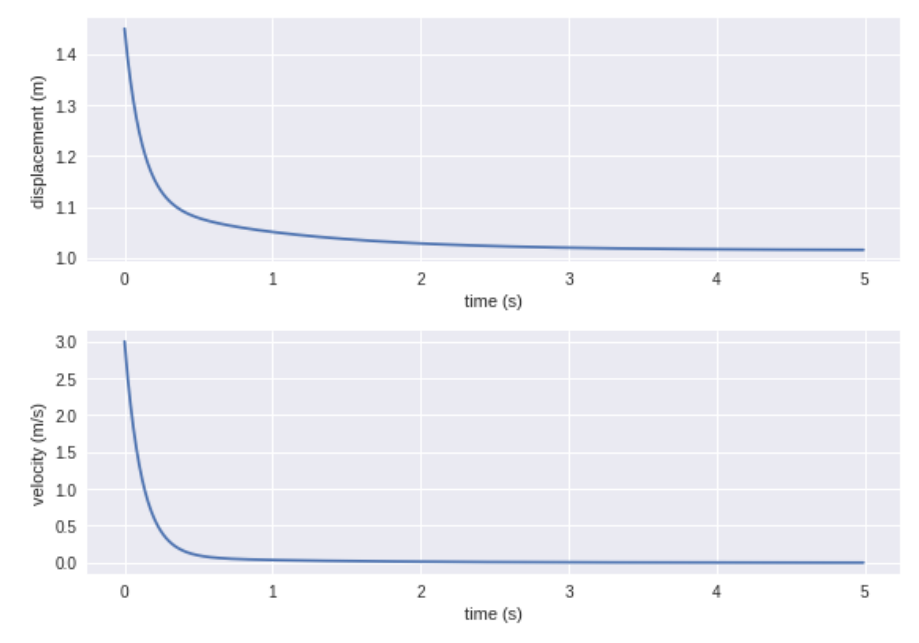


Figure 5.39: Tuned spring-damper system results for mass of the lander and maximum landing velocity.

Verification

The landing gear dynamics were verified by using two different programs to solve equations Equation 5.63-Equation 5.65. These equations and boundary conditions were solved using both Python and Mathematica and the results were compared with no errors.

Validation

The validation approach for the landing legs was to use the same approach used in the landing gear sizing above, but using measured data from the Falcon 9. Two major differences are that the Falcon 9 only has four landing legs, and non are redundant. Dimensions were checked with actual images of the rocket to be accurate.

Table 5.38: Validation of landing leg sizing.

Parameter	Value
C.G. height	20-30%
Ground clearance	2 m
Tipping angle	10-20%
Height	70 m
Diameter	3.7 m
Predicted Leg angle	50-76°
Measured Angle	63°
Error	0°

Sensitivity analysis

The effect of the total landing mass to the required landing gear mass was analysed. As the landing gear is expected already to be relatively lightweight, the sensitivity is not significant.

Table 5.39: Effect of landing mass on landing gear mass.

Change in	Affects
landing mass	landing gear mass
-10%	-5%
+10%	+5%

The effect of the landing speed to the minimum ground clearance during landing was analysed. This is significant, however there is already a large margin applied for the emergency landing speed, which may not be necessary.

5.4. Life Support

Effect of landin		

Change in	Affects
landing speed	minimum clearance
-10%	1m
+10%	+.1m

5.4. Life Support

The MEV's Life Support System (LSS) will not be designed to allow a comfortable multiple day stay, but rather for 3 days of contingency. The nominal crew occupation time, and therefore the LSS running time, should remain within the order of hours. The expected level of comfort should be equal to that of the Soyuz capsules.

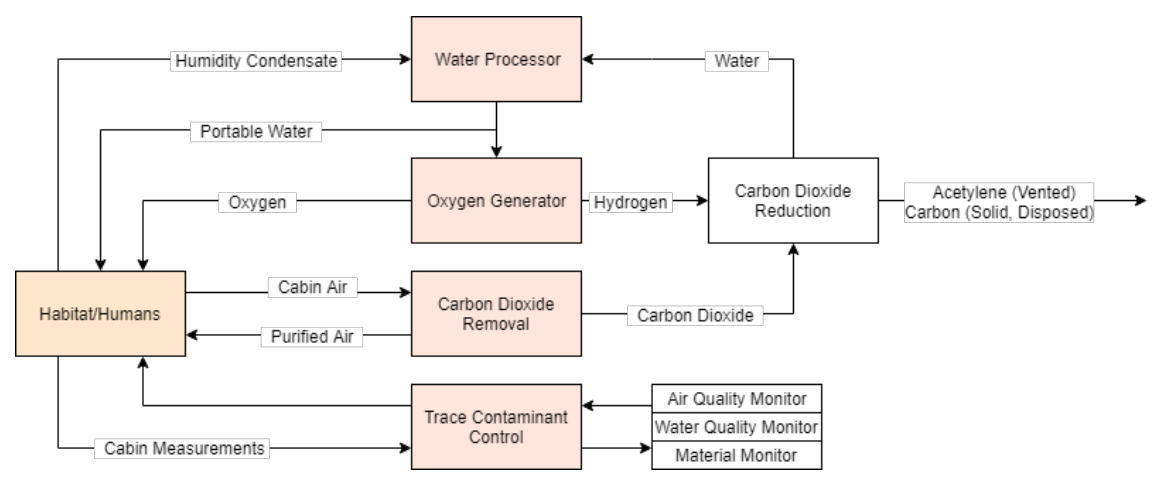


Figure 5.40: Life support of the MEV.

5.4.1. Oxygen and Nitrogen Tanks

Table 5.41: Inputs for the life support system tank sizing.

Parameter	Unit	Value
O ₂ volume	_	21%
N ₂ volume	_	78%
MEV runtime	days	3
Breathing volume per day	m^3	0.011^{41}
Number of people	_	10
O ₂ consumed	_	25%
N ₂ consumed	_	0%
MEV volume (inhabited)	m^3	93.24
O ₂ density at 1 bar	kg/m ³	1.429
N ₂ density at 1 bar	kg/m ³	1.2504
Airlock volume large	m^3	49
Airlock usage large	_	2
Airlock volume small	m^3	2.87
Airlock usage small	_	10
O ₂ storage pressure	Pa	2e7
N ₂ storage pressure	Pa	3.4e7
Number of O ₂ tanks	_	2
Number of N ₂ tanks	_	2
O ₂ tank tensile strength	Pa	1.54e9
N ₂ tank tensile strength	Pa	1.54e9
O ₂ tank density	kg/m ³	1.57e3
N ₂ tank density	kg/m ³	1.57e3

 $^{^{41} \}verb|https://health.howstuffworks.com/human-body/systems/respiratory/question 98.htm| (Last accessed 29-06-2018) | Compared to the compared for the compar$

5.4. Life Support 84

For the life support system, two different tanks are used: nitrogen and oxygen. The properties of these tanks are obtained in a similar way as in subsection 5.1.4, however the method to obtain the volume per tank differs. This is given in the following flow chart.

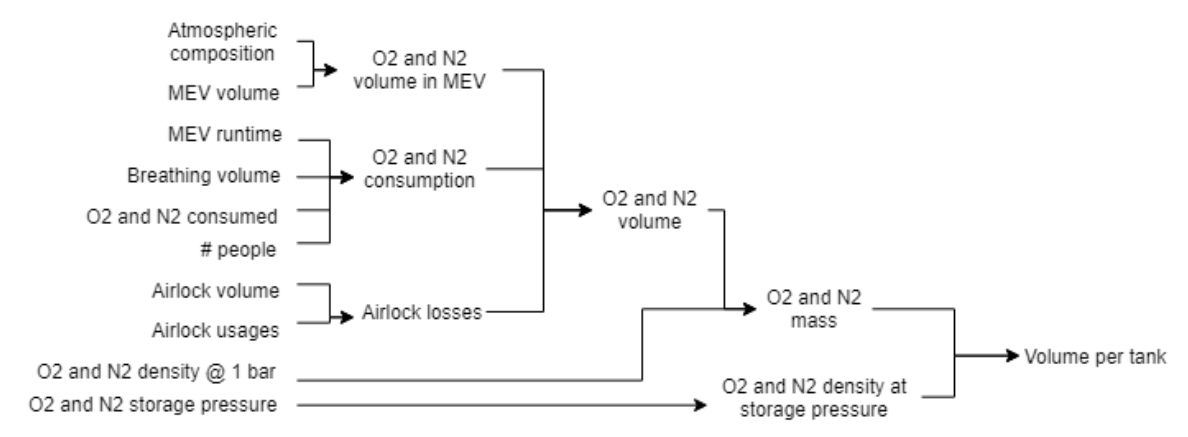


Figure 5.41: Flow diagram of the life support tank sizing.

First, the inhabited MEV volume and the atmospheric composition are used to get the separate volumes of O_2 and N_2 in the MEV. To this, the O_2 and O_2 consumed by humans during the time in the MEV is computed. Note that humans do not consume nitrogen, and they only consume 25% of the oxygen breathed in⁴². This total volume is doubled, to account for a breach and to be able to completely refill the MEV with air. Then the air lost by using the airlocks is added to the total volume. From this volume, the mass of the O_2 and O_3 is found, after which this is pressurised and a volume per tank can be found. The pressure under which the two substances are kept, are common pressures for these substances. From here onward, the same approach as in subsection 5.1.4 is used. Note that the tank geometry assumed is spherical (which eliminates the hoop stress) and the maximum acceleration occurs at Earth launch. For the environmental tanks, a safety factor of 2 is applied.

The results of the calculations can be found in Table 5.42.

	Parameter	Unit	Value
Oxygen	Radius	m	0.304
	Height	m	0.608
	CFRP skin thickness	m	0.0059
	Total mass (dry)	kg	8.8
	Total mass (wet)	kg	74.8
Nitrogen	Radius	m	-0.425
	Height	m	0.85
	CFRP skin thickness	m	0.0143
	Total mass (dry)	kg	36.9
	Total mass (wet)	kg	251

Table 5.42: Dimensions of the life support tanks.

Consumables

The MEV will carry sufficient food and water for the 10 man crew for at least three days. The mass of this is included in the payload. For the ITV, rations similar to the ISS will be taken on board to ensure volume efficient, nutritious meals.

Verification

For the verification of the life support tanks, the same method is used as in subsection 5.1.4. For the oxygen tank, a volume error of 0% and a mass error of 0.97% is found, while for the nitrogen tank a volume error of 0.37% and a mass error of 0.13% is found. This is deemed sufficiently accurate.

 $^{^{42} \}texttt{https://health.howstuffworks.com/human-body/systems/respiratory/question 98.htm} (Last accessed 29-06-2018)$

5.5. Communications 85

Sensitivity analysis

When increasing both the pressure of the oxygen tank and the pressure of the nitrogen tank with 10%, the total (wet) mass of the tanks increases with 1.2%.

5.4.2. Radiation Protection

The radiation environment on Mars surface and in Mars orbit is 22 millirad per day⁴³. The hull of the crewed section consists of 2 mm of CFRP, where the resin is polyethylene or equivalent. The shielding efficiency of such a panel is 0.55 [50], which means that the resulting radiation throughput is 12.1 millirad per day or 0.0121 rem per day.

The recommended yearly dose for astronauts is 0.5 rem. This means that even with worst case excursion time of three days in the MEV does not add to the receive radiation significantly, even without additional radiation shielding. It must be noted that a nominal orbital occupancy time of the MEV is in the order of three hours. This also excludes the shielding behaviour of the insulation or any electronics components lining the inside of the crew segments. Radiation is not expected to be an issue with respect to electronics, since the radiation received inside the MEV is such that that radiation hardened electronics can be expected to function correctly for decades. Radiation endured during transit is also not expected present any problems[51].

It must be noted that during transfer from Earth to Mars, the MEVs are not inhabited.

Additional shielding can be considered for the crew compartment and pressure suits, although it is not strictly necessary at this point. It was found in the Midterm Report that Kevlar has the highest specific shielding performance [3]. Therefore, in order to reduce the radiation dose further, an internal Kevlar lining can be added to the crew compartment.

5.5. Communications

The preliminary link budget shown in subsection 4.1.4 is used to perform further calculations on the communication subsystem. In Table 5.43 the determined values for the subsystem have been listed. They have been sized by using the equations for the received power and the system noise, given combined as the System to Noise Ratio (SNR) in Equation 5.66. It was chosen to use a value of 10 dB for the SNR in order to ensure for enough losses such as rain, system losses or other external losses [52]. This value will serve as a safety factor for the communication subsystem.

$$SNR = \frac{P_r}{N} = \frac{P_r G_t G_r}{(4\pi d/\lambda)^2 k T_s B}$$
 (5.66)
$$\eta_{amp} = \frac{P_t}{P_{comm}}$$

The architecture is shown in Figure 5.42 and the different elements are described in the following subsections.

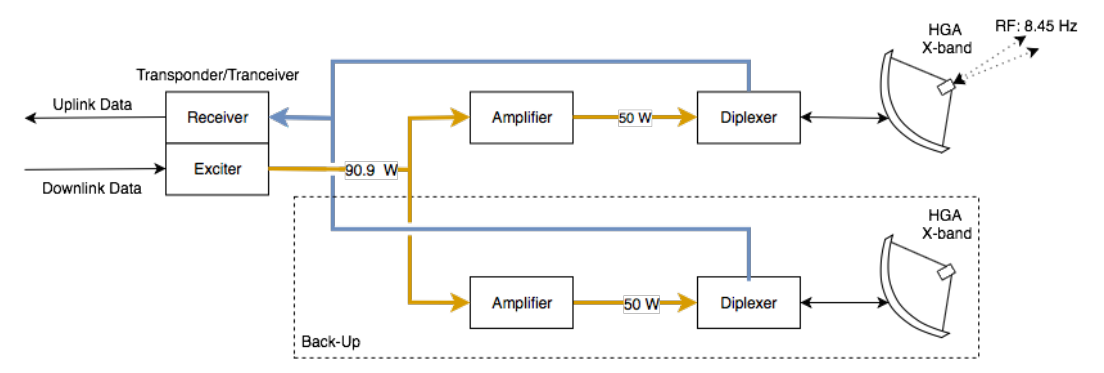


Figure 5.42: Schematic representation of the communications subsystem architecture.

Antenna

Two X-band antennas of 20 kg are chosen, with a RF transmission power P_t of 50 W. The Watts in the table are not doubled since they will only be operating separately. The choice for the X-band frequency of 8.45 GHz was chosen to be compatible with the existing orbiters (MRO, MAVEN, Mars Odyssey) which also operate at X-band frequencies. This way, when the ITV leaves back to Earth or is on the opposite side of Mars, the architecture is still sufficient

 $^{^{43} \}mathtt{https://phys.org/news/2016-11-bad-mars.html} (Last \ accessed \ 21-06-2018)$

5.5. Communications 86

to provide communication with the ITV or Earth. A parabolic antenna was considered in order to achieve high antenna gain. Since they have to withstand re-entry heat, they will have to be deployed in and out of the MEV. This deployment is shown in Figure 5.43. By adding a communication device on both sides of the MEV and having them be able to rotate 180 degrees, covering all possible directions.

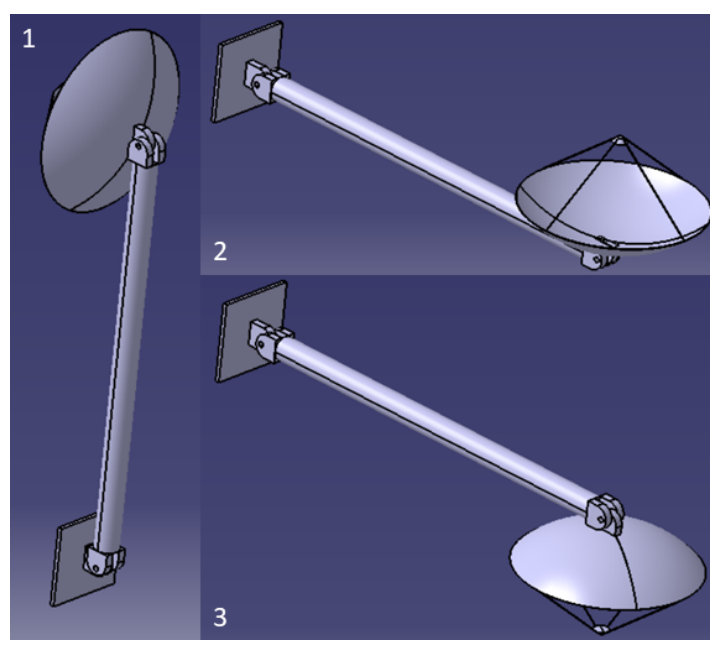


Figure 5.43: Deployment of X-band High Gain Antenna.

Amplifier

Before the system can be send to the ITV, it will have to be amplified. This will be done by a Travelling wave tube amplifier (TWTA) since the transmitter power of the spacecraft exceeding 15 W (otherwise an solid-state power amplifier would be sufficient [12]). The efficiency for the amplifier sates the relationship as shown in Equation 5.67. TWTAs have a typical efficiency of 55% for X-band communication, thus leading to an input power required P_{comm} of 90.9 W. The mass for such an amplifier system is approximately 2.5 kg, which is added twice because of the double instalment redundancy [12].

Other components

For all the other components, including the transceiver/transponder, diplexer and general cabling, an approximated mass and power estimate was produced. Using the Deep Space TT&C system data table [12] it was found that two diplexers (couples the receiver and transmitter signals onto a single RF cable) of 1.2 kg, a 6 kg transponder/transceiver using 26 W and about 6 kg of cables. The total mass and power budget has been summarised in Table 5.43

		,	O
Parameter	Symbol	Value	Unit
Parabolic dish diameter	d_{dish}	0.45	m
Antenna Efficiency	η_{comm}	0.5	_
Amplifier Efficiency	η_{amp}	0.55	_
Transmission power	P_t	50	W
Communication power	P_{comm}	116.9	W
Mass of communication system	m_{comm}	58.2	kg
Data bit rate	R_b	2.66	Mbit/s

Table 5.43: Communication antenna/subsystem sizing.

The bit rate for the data transfer was estimated using the requirements for the people on board of the ITV/MEV. They will have to stay in contact with their families and have to send videos and audio fragments back home. The values have been listed in Table 5.44. The video transmission values have been defined from the requirements of 1080p

video for the ITV and 720p for the MEV⁴⁴. The audio bit rates have been defined by MP3 standards which are 160 (CD quality) and 320 (best MP3 bit rate) kbps⁴⁵.

	Video transmission [Mbps]	Audio [Mbps]	Total bitrate [Mbps]
ITV <-> DSN	4.5	0.32	4.82
MEV < -> ITV	2.5	0.16	2.66

$$C = 2B \cdot \log_2(M) \tag{5.68}$$

From this the bandwidth in Hz can be determined by using Equation 5.68 where C is the bit rate in bps and B is the bandwidth in Hz. The M is the number of signal levels, 2 for binary signals. They are shown in Table 4.5. The frequency, antenna efficiencies, noise temperature, maximum distance and design margin are other inputs for the table, after which the transmitted power and antenna diameter are iterated until the SNR for each budget is greater than zero.

5.6. Power

It was chosen to have the MEV perform ground operations using batteries, and having solar panels recharge the spacecraft when waiting in orbit for a new ITV to require Mars descent. The power cycle that the MEV encounters is shown in Figure 5.44. Blue indicates power produced by solar panels, orange indicates power produced by battery storage. When at Mars orbit, solar panels power the spacecraft at daylight and recharge the batteries that are used to power the spacecraft during eclipse (only three cycles shown). When docked to the ITV, people and cargo board the MEV and power consumption increases, which is supplied by the ITV charging up the batteries for ground operation. After performing Mars descent and ascent it docks to the ITV again, after which it goes back to normal power mode (which is the same for the Mars orbit before). This cycle repeats every ITV encounter.

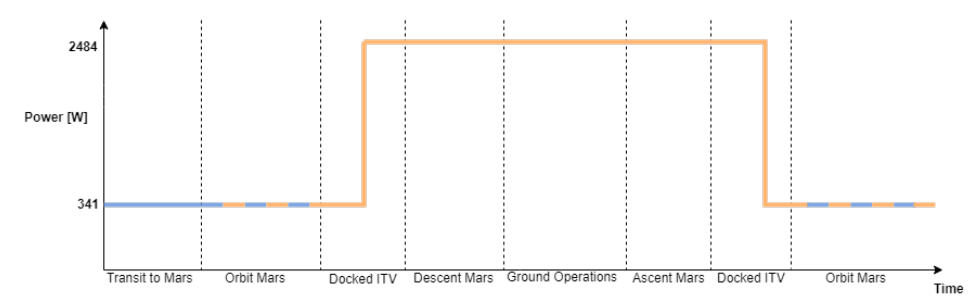


Figure 5.44: Power diagram of MEV divided into solar (blue) and battery power (orange).

The battery storage cycles are shown in Figure 5.45. Using the same reasoning as above, the energy levels in the batteries can be shown. During orbit phase, the batteries get recharged by the solar panels, and when on the ground, it runs of the charged battery, charged by the ITV during docking. It is seen the batteries are not depleted more than 20% because of the chosen depth of discharge.

 $^{^{44} \}mathtt{https://support.google.com/youtube/answer/2853702?hl=en(Last\ accessed\ 31-05-2018)}$

⁴⁵ https://computer.howstuffworks.com/mp32.htm(Last accessed 31-05-2018)

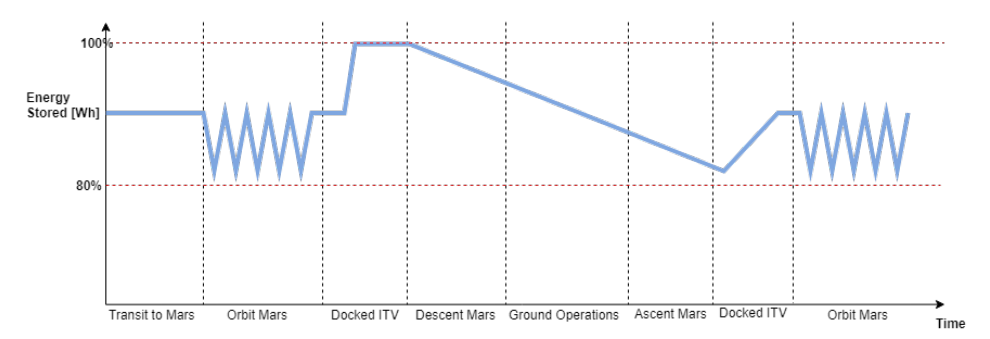


Figure 5.45: Battery power of the battery during different mission phases.

5.6.1. Solar Panels

Sizing the Solar panels was first done by thinking of different options to orient them with respect to the MEV. As seen in Figure 5.46, eight options are displayed that can possibly be applied on the MEV. Noteworthy is that option 2 is based on the SpaceX design, option 3 is based on the Orion spacecraft, option 4 is based on the Cygnus cargo module by Orbital ATK and option 5 is inspired by the Hubble Telescope. A trade-off needs to be performed, with the following criteria in mind:

- 1. Packing factor when stored in MEV;
- 2. Interference with docking ports of the ITV and MEV;
- 3. Complexity deploying/retracting;
- 4. Compatibility with Landing on Mars.

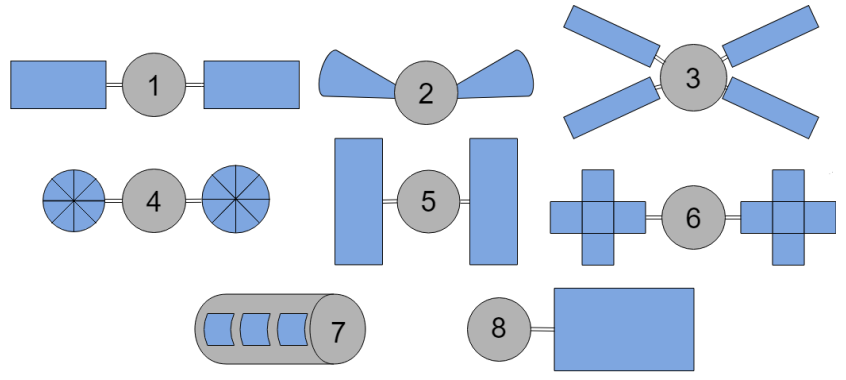


Figure 5.46: Different options for solar panel configurations.

Option 7 is eliminated because the solar panels may not be able to survive reentry at Mars, since they can not be stowed away. In addition, this option would require reorientation of the entire spacecraft in order to point the panels towards the Sun, with is clearly less efficient than a self-pointing solar array. Option 2 is also discarded since the way of deploying panels SpaceX-style requires unfeasible packing in the spacecraft. With the information that is currently available, this option appears to also require reorientation of the full spacecraft.

All the other options will score sufficient on interference with docking ports of the ITV and MEV since they can be retracted and let the MEV run on batteries and ITV power when docked. Thus, this criteria is not further analysed. Retracting solar panels has not been applied to many spacecraft (ISS is able to retract, but has a too complex system for the MEV). Thus, an easy folding method is required. This eliminates options 2 and 6 since they require multiple intricate motors to be able to retract the panels. Option 8 causes issues with its asymmetric configuration, potentially adding complexity to attitude control with the array deployed. Leaving with options 1, 3 and 5 it was chosen to proceed with option 1 since it is most easily stored in the diameter of the spacecraft (eliminating option 5), and leaves enough space for docking interfaces and other appendages (eliminating option 3). The dimensions and characteristics of the solar panels are listed in Table 5.45.

The size of the solar panels is identical to the sizing done in the Midterm Report [3], which will be summarised here. One important difference is the reduction of the time the MEV has to be able to support a crew on Mars without an external power supply from seven to three days. The required power was taken from Table 4.4.

$$P = 2\pi \sqrt{\frac{a^3}{\mu}} \tag{5.69}$$

Using Equation 5.69 and the orbital altitude around Mars subsection 5.2.4 and the relevant standard gravitational parameters $(4.2828*10^{13} \text{ km}^3/\text{s}^2)$ [12] the orbital periods for the MEV around Mars is 109 min. Using the radius of Mars (3390 km⁴⁶) and assuming the MEV orbit is co-planar with the Mars-Sun plane the percentage of the orbit spend in eclipse can be calculated. Subsequently, using the orbital period the eclipse and day time can be found.

$$P_{sa} = \frac{\left(\frac{P_e T_e}{X_e} + \frac{P_d T_d}{X_d}\right)}{T_d} \tag{5.70}$$

Equation 5.70 [12] uses the power requirements P, time T and path efficiency from panel through battery to individual load, X, for in daylight d and while eclipsed e. The path efficiency during day being assumed to be 0.85, and 0.65 during the night [12], while the requirements are the same during the day and night. Note that at this point there is no differentiation between day and eclipse power consumption. The result of this are summarised in Table 5.45

Symbol **Parameter** Value Unit Power produced P_{solar} 0.74 kW Area of solar panel 8.72 m^2 A_{solar} Solar panel efficiency 0.29 [53] η_{solar} Mass solar panel m_{solar} kg

Table 5.45: Solar Panel sizing data.

For the deployment of the solar panel, it is important that the deployment mechanism is also able to retract the array. In Table 5.46 the options are listed that are suited for both deploying and retracting. [54]. Regular electric motors often use only two spools while the stepper motor uses multiple coils. Because the latter can only operate in given steps, an electric motor was chosen to deploy/rotate the solar panels to ensure continuous precision instead of step wise precision. Note that the solar panel will be positioned in such a way that (with the help of the electrical motors) they are perpendicular to the Sun light. This means that the panels will be positioned on either side of the MEV.

Deployment Mechanism Advantages Disadvantage Electric Motor High precision, Position lock, No release Additional energy and circuits, Larger volume, mechanism, Large torques available requires gears, Harder to mount at panel Mechanical Guidance Precise guidance, Predictable, Includes artic-Many components, One panel only, Lubricaulation mechanism tion, Cold welding, Only rigid solar cells Stepper Motor High precision, Position lock, No release Additional energy and circuits mechanism, Large torques available

Table 5.46: Solar Panel deployment system.

The total area of the solar panel A_{solar} is divided up in six panels, three on each side of the MEV with an area A_{panel} of 1.5 m². These three panels will be hinged and folded up as shown in Figure 5.47. The adaptor is also hinged so the whole package is small enough to fit in the MEV shielding. These shields are needed to withstand re-entry and launch environment, plus the sand contamination on Mars itself.

 $^{^{46} \}mathtt{https://solarsystem.nasa.gov/planets/mars/in-depth/(Last accessed 02-07-2017)}$

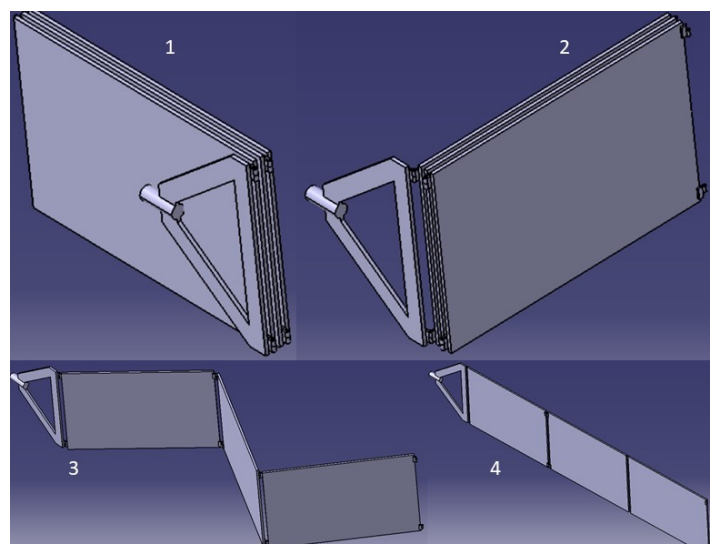


Figure 5.47: CATIA representation of folding mechanism of a 3 panel solar array with adaptor.

5.6.2. Batteries

The main load case for the battery is the interval between undocking, Mars operations and docking again. The MEV has been designed to be able to support three days of autonomous flight with no rechargeable power source. This value was based on landing times and transfer windows in section 5.2. This value came down to three days between undocking and docking again. In order to provide the 2,484 W of power for three days, the energy available can be calculated by Equation 5.71 for either the crew phase and the standby phase. For the standby phase the eclipse time is taken to size the batteries. Batteries can be sized based on the power requirements for ground operations shown in Table 5.47.

$$E_{req} = P \cdot t \tag{5.71}$$

Table 5.47: Battery requirements.

Parameter	Symbol	Value	Unit
Power requirements crewed flight	P_{crew}	2,484	W
Power requirements standby phase	P_{stb}	341	W
Max energy storage crewed flight	E_{crew}	182,574	Wh
Max energy storage standby phase	\mathbf{E}_{stb}	243	Wh

The batteries chosen with high performance and high readiness are the 100 kWh Lithium-ion batteries of the Tesla S P100D model [55]. Since they are off the shelf, no development costs are to be expected. Radiation and accelerations are expected to provide the biggest complexity for the use of automotive batteries in space. Since they will have to be shielded either way, radiation can be countered. Acceleration is also something that will happen in a Tesla car so will be feasible as well. To provide the 183 kWh of storage the MEV needs, two of these battery packs are implemented in the spacecraft. This means the appropriate margin of 10% on modified off-the-shelf power components is already included [56]. The specifications of the battery pack on the MEV are shown in Table 5.48. Two batteries are installed, so most values are doubled.

Table 5.48: Battery sizing data, most values provided by Tesla test records [55].

Parameter	Symbol	Value	Unit
Available energy storage	E_{avl}	200	kWh
Specific energy battery	\mathbf{e}_{bat}	160	Wh/kg
Mass of battery packs	m_{bat}	1,250	kg
Number of individual Li-ion modules	N_{module}	32	_

The MEV battery will consist of 32 modules of Li-ion battery packs. Their dimensions⁴⁷ have been shown in Fig-

⁴⁷http://www.evwest.com/catalog/product_info.php?products_id=463(Last accessed 12-06-2018)

5.7. Thermal 91

ure 5.48. In order to fit them in the MEV, they are placed at the same level, creating a floor just as high as the 7.87 cm height of the battery. Due to the 5.2 m diameter of the spacecraft, 21.24 m² is available for module placement. The modules, adding all the areas together need 6.62 m² and will be oriented as shown in Figure 5.49. By choosing this spacing, lots of space is still left to implement cooling, wires and connections from the top of the MEV passing through the batteries. The battery-integrated cooling system can be used with minor modification, since the thermal subsystem in section 5.7 ensures that the batteries operate at a temperature of 293 K. This is in line with the users manual of the batteries which state the operational temperature to be between 243 K and 333 K. [57]

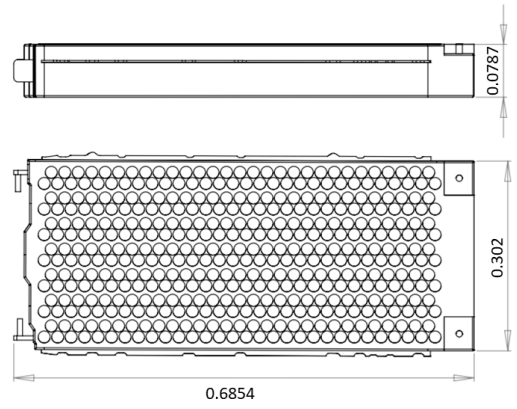


Figure 5.48: A schematic representation of the individual battery module. Dimensions are in meters.

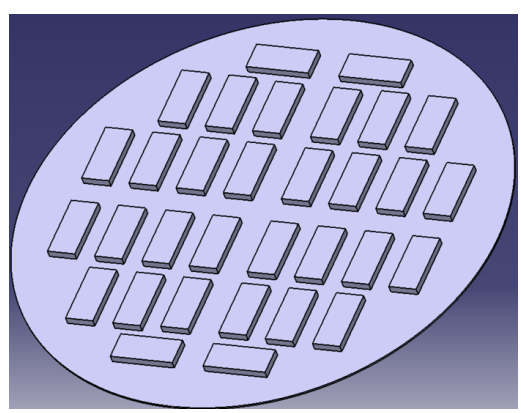


Figure 5.49: A CATIA build of the 32 Li-ion modules on the MEV floor.

5.7. Thermal

The thermal subsystem is sized assuming a human heat output of 110 W per person[11]. It is assumed that all power used by the system, is eventually converted into heat. This results in a total heat production of 3584 W. This is a high estimate, especially for Mars surface operations. However, this turns out to be advantageous: during re-entry, it is permitted to let the internal temperature rise slightly; and in the minutes after landing, the system can bring this temperature back to nominal levels. In fact, after landing, many systems can be powered down, and with less power usage, the thermal system is more effective.

During the re-entry phase, which is not expected to last more than 10 minutes, the air brakes, engines and shielding between the engines, will heat up. These systems will be specifically designed for this "instantaneous heat", whereas the engines are inherently heat resistant. As such, the active thermal system does not specifically have to take into account re-entry. This agrees with the MEV design as proposed by ESA [11], and was further detailed in subsection 5.2.5.

During the uninhabited stay on Mars, the thermal system will be kept running, while other systems are powered down.

5.7.1. Thermal Model

The MEV's thermal system is modelled as follows. The MEV consists of three segments that must be kept at a certain temperature. These are the crewed/cargo section kept at 293 K, the liquid methane tank at 111 K, and the liquid oxygen at 66 K. Each section is assumed to be a cylinder, the dimensions of which are as determined previously.

5.7. Thermal 92

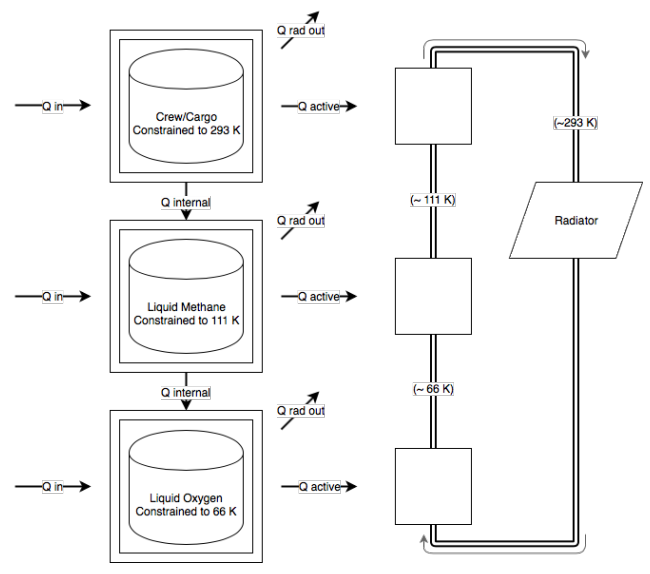


Figure 5.50: Thermal model of the MEV.

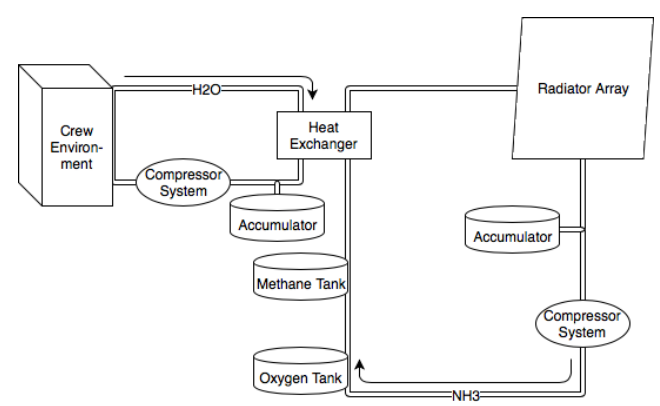


Figure 5.51: Thermal hardware layout of the MEV.

Heat is radiated in from the side of each cylinder as a worst case; this is 586.2 W/m^2 of solar irradiance, as well an albedo factor of 0.33 and a worst case planetary IR 470 W/m^2 [11]. This is the hot case, which is critical for the thermal system: due to the presence of cryogenic propellants and a relatively high peak power compare to the MEV's area.

Each section is insulated by n layers of multi layer insulation (MLI). Thermal heat flow through this insulation material, Q_{ins} is then calculated by Equation 5.72[58].

$$Q_{ins} = \frac{4\sigma T_{avg}^3 A_{ins} \Delta T}{n(2/\epsilon - 1) + 1}$$

$$(5.72)$$

This equation uses the Stefan-Boltzmann constant σ , the insulated area A_{ins} , and the average and difference in temperature over the MLI: T_{avg} and ΔT . The emissivity ϵ is assumed equal to that of aluminium foil, which is 0.05 [59].

The temperature of the outside layer of the MLI in the Sun, T_{sun} , is not known, but is iterated until the heat flow into the MLI (by external radiation) equals the heat flow out of the MLI (by outward radiation and conduction into the ship). Absorption α is taken into account by use of Equation 5.73, where J is the total of incoming radiation in W/m², and radiation outward is calculated by Equation 5.74 [59].

$$Q_{in} = A_{sun} \alpha \sigma J_{sun} \tag{5.73}$$

$$Q_{out} = A_{total} \epsilon \sigma T^4 \tag{5.74}$$

5.7. Thermal 93

The temperature of each section is kept constant. Out of each section, there is a heat flow through the insulation on the shaded side of each cylinder. This uses the same equations as above, but in reversed order. Again, the temperature of the outer layer in the shade, T_{shade} is not yet known; this value is iterated until the heat transfer into the MLI equals the radiation outwards.

There is also heat transfer from the crewed segment to the methane tank, and from the methane tank to the oxygen tank, i.e. from warmer to colder segments. The space between the tanks is not pressurised, so energy is only transferred by radiation, with an area equal to the MEV cross section. All generated power, as stated 3,584 W, is assumed to eventually turn into heat, which is introduced into the crewed segment.

For each segment, the difference between introduced heat and passively outward radiating heat must be taken by the coolant loop, and therefore emitted by the radiator. The coolant loop runs from compressor, by the LOX tanks, then the methane tank, then the crew space heat exchanger, and then finally to the radiator. The temperature of the radiator is then assumed to be equal to the highest temperature of the segments, i.e. 293 K. The radiating power per area can be calculated from this power, from which the required radiator area and mass of the system is determined.

The number of layers of MLI on each segment are optimised for the lowest mass of the combined insulation and active thermal system. This results in a minimum mass, which is advantageous from a mass budget perspective, but also yields improvements in costs and propellant requirements.

MLI weighs 0.018 kg/m^2 per layer [60], and retractable radiators are 5.5 kg/m^2 [61]. Low temperature cryocoolers (lower than 20 K) have a specific mass of 5 kg/W, higher temperature coolers (above 90 K) have a specific mass of 0.35 kg/W, and cooling loops have a mass of 1.2 kg/m^2 [62].

5.7.2. Results

A dissipation capability margin of 50% is deemed appropriate to thermal systems, as well as a 15% margin on radiator surface area [11]. This corresponds to a mass margin of 15% on the radiator area, and approximately 50% on the mass of the rest of the system, such as insulation and coolant loop components, which is included in the results.

From manual iteration, it resulted that the external colour should be white, with $\epsilon = 0.82$ and $\alpha = 0.17$. Most likely, this is because the overall heat production of the electronics and the inward heat flow in full Sun is higher than the ship's outward radiation. This results in the following subsystem characteristics, as seen in the tables below.

		-			
Parameter	Symbol	Crew/Cargo	Methane	Oxygen	Unit
Number of layers	n	2	11	36	_
Sunside temperature	T_{sun}	415	416	416	K
Shade temperature	T_{shade}	98	24	11	K
Insulation mass	m_{ins}	5.9	14.9	52.9	kg
Coolant loop mass	m_{cooler}	182.1	15.4	49.8	kg

Table 5.49: Thermal subsystem characteristics per segment.

Table 5.50: Thermal subsystem characteristics.

Parameter	Symbol	Value	Unit
Radiator area	A_{rad}	10.7	m^2
Radiator mass	m_{rad}	59.0	kg
Coolant loop mass	m_{loop}	12.9	kg
Total mass	m_{total}	536.5	kg

Verification

The workings of this iterative solver have been verified as follows. Firstly, the behaviour to extreme inputs has been verified: Zero-heat flow in yields to a total outward yield flow equal to the heat production of the electrical system. Zero insulation leads to an unfeasibly large radiator design, whereas numbers of MLI layers larger than the optimum lead to smaller radiator design but a suboptimal mass of the thermal system as a whole.

The results have been verified for a simple case with 10 layers of insulation about the entirety of the MEV, using the Excel sheet used for preliminary sizing of the thermal system of the ITV in the Baseline Report [4]. The results are very similar. For MEV dimensions and conditions, Excel sheet yields a radiator size of 10.7 m². When constraining the iterative solver to 10 layer of MLI everywhere, which was assumed during preliminary design, the result is in 9.7 m² of radiator area. Note that, although this area is smaller than the chosen MEV radiator area, the mass of the

insulation this requires is significantly larger.

The assumption that the radiator temperature is equal to the temperature of the crew segment is justified, given that a high end current-tech radiator emissive power of 350 W/m^2 [63] yields a similar radiator area of 10.6 m^2 .

Since the external temperature is an output of the iterative approach, they have been compared to the ISS's manned compartments' external temperatures, of which the shadow side and Sun side are 116 K and 394 K respectively.

Finally, a low end radiator with an emissive power of 100 W/m^2 [63], would yield a radiator area of 37 m^2 . This is slightly larger than the result of scaling ESA's proposed radiator by power generated. ESA does not use the newly developed radiators mentioned above, so scaling results in 32 m^2 .

Validation is not easily done, as no manned spacecraft of this size exist. The ISS is the closest in occupancy and uses over 400 m^2 of radiator panels. However, it is intended for full-time habitation, is positioned closer to the Sun, and has a very large amount of (processing) power for scientific experiments, which would explain the difference in size of the radiators.

Sensitivity analysis

Regarding any sensitivity analysis, it is concluded that this method is very sensitive to the exact values of emissivity and absorptivity, especially to that of multi-layer insulation. Different combinations of these values, whether surfaces with these properties exist or not, may result in mass estimate outliers of 300 kg on one end and over 1500 kg on the other end. It is recommended that for a more detailed sizing of the thermal system, more research is done into combinations of load sensitive MLI and active cooling, for which no consistent value could be found.

However, the system is not very sensitive to a change in incoming heat flow. For a 10% increase in irradiation, the total mass of the thermal system becomes 735 kg, with a relatively heavier insulation and a relatively lighter active coolant system.

In eclipse on full power, the required radiator power reduces with only 3%, meaning that active thermal control should be able to handle this as part of a simple closed control loop.

When the spacecraft is completely powered down and in eclipse, it requires approximately 670 W of interal power to maintain the temperature in the crewed section. Considering a standby power of 340 W, this requires and additional 330 W heater. Even using a worst case inefficient heater, this requires at most 5 kg of the mass budget [64].

5.8. Attitude Determination and Control

The attitude determination and control subsystem is required to properly determine and control the orientation of the vehicle with respect to a given reference frame. The following section will describe the instruments and hardware used to achieve the desired accuracy for reorienting the vehicle. The ADCS will be sized for four modes - the orbit insertion and acquisition mode, on-station mode, slew mode and safe mode [12].

5.8.1. Attitude Determination

The MEV requires an accurate attitude determination system for both the orbital and atmospheric phase. The trade-off performed in the Midterm Report [3] presented multiple option for attitude determination sensors. Due to the complexity of the mission a proper redundancy measures are required especially during the orbit insertion and acquisition mode which is the period during and after the boost while the spacecraft is brought to final orbit and the on-station mode which is used for the vast majority of the mission.

The MEV is equipped with eight Sun sensors and six star trackers. Usually, for the final selection the MEV should have at least two Sun sensors, in case one is blinded, and three star sensors, in case of blockage by natural satellites. Most reference missions such as the Mars Climate Orbiter and the Mars Reconnaissance Orbiter use between six to eight sensors in total including IMUs and horizon sensors. However, the MEV is a bigger vehicle and during some of the operational phases additional obstacles such as asteroid fields and natural satellites might block multiple sensors; this is why a higher redundancy number is chosen. Additionally, horizon sensors such as scanners and fixed heads are used when the MEV approaches lower altitudes near the Mars surface. Lastly, Inertial Measurement Units are used to measure accelerations during the de-orbit phase and the ascent trajectory. A summary of the chosen hardware is presented in Table 5.51 with typical performance characteristics and mass estimations. The total power is an extreme peak power which nominally will not occur. The system will need at most two unobstructed sensors running at the same time to provide an accurate measurement.

Table 5.51: Chosen ADCS Sensors.

Sensor	Typical performance range	Mass [kg]	Power range [W]
3x Inertial Measurement Unit (Gyros	Gyro drift rate = 0.003 deg/hr to 1 deg/hr, Linearity	0.3	~ 10
and Accelerometers)	= 1 to $5 \times 10^{-6} g/g^2$ over range of 20 to 60 g		
8x Sun Sensors	Accuracy = 0.005 deg to 3 deg		-
6x Star Sensor (Scanners and Mappers)	Attitude accuracy = 1 arc sec to 1 arc min 0.0003		-
	deg to 0.01 deg		
2x Horizon Sensors	Attitude accuracy:		
•Scanners/Pipper	0.1 deg to 1 deg (LEO)	0.6	~ 5
•Fixed Head (Static)	<0.1 deg to 0.25 deg	0.6	~ 5
Total		17.5	~ 28

5.8.2. Disturbance Torques

In order to properly control the attitude one needs to estimate the worst-case disturbance toques that are present during the different phases of the mission. Table 5.52 present the estimated inputs for disturbance torques that will be used to calculate the final disturbances.

Table 5.52: Inputs for worst case disturbance torques.

Parameter	Value	Unit	Parameter	Value	Unit
$\overline{I_y}$	296,409.831	kg m ²	cg	3.73	m
$I_{\mathcal{Z}}$	47,596.95	kg m ²	$F_{\mathcal{S}}$	1,367/591	W/m^2
μ	$3.986 \cdot 10^{14} / 4.28 \cdot 10^{13}$	m^3/s^2	c	3.10^{8}	m/s
R	6,771/3,890	m	q	0.6	[-]
θ	30	deg	i	0	deg
$A_{\mathcal{S}}$	213	m^2	D	20	$A \cdot m^2$
c_{pa}	6.5	m	B	$5.13 \cdot 10^{-5} / 6.76 \cdot 10^{-9}$	T
c_{ps}	6.5	m	C_d	1.4	[-]

There are four main disturbances that are expected to act on the MEV during the mission.

Gravity gradient

$$T_g = \frac{3\mu}{2R^3} |I_z - I_y| \sin(2\theta)$$
 (5.75)

where T_g is the torque due to gravity, I_z and I_y are the moments of inertia of the vehicle around the Z- and Y-axes, R is the orbit radius and θ is the maximum deviation of the Z-axis.

Solar radiation

$$T_{sp} = F(c_{ps} - cg)$$
 (5.76)
$$F = \frac{F_s}{C} A_s (1+q) \cos(i)$$
 (5.77)

In Equation 5.76, T_{sp} is the solar radiation pressure, c_{ps} is the location of the centre of solar pressure and cg is the centre of gravity. F is the solar constant, c is the speed of light, in Equation 5.77 A_s is the surface area of the vehicle, q is the reflectance factor and i is the incidence angle.

Magnetic Field

$$T_m = DB$$
 (5.78) $B = \frac{2M}{R^3}$

The magnetic field is calculated with Equation 5.78, where T_m is the magnetic torque, D is the residual dipole of the vehicle and B is the planet's magnetic field. The magnetic field can be calculated using the magnetic moments of Earth and Mars respectively, (M_e and M_m).

Aerodynamic disturbance

$$T_a = F(c_{pa} - cg) \tag{5.80}$$

Equation 5.80 gives the aerodynamic disturbances on the vehicle. T_a is the aerodynamic torque, F is the aerodynamic force, c_{pa} is the centre of pressure and cg is the centre of gravity. The aerodynamic force is a function of density at

the orbit altitude, velocity of the vehicle, the drag coefficient and surface area. The reference cross-sectional area of the vehicle is $213 \,\mathrm{m}^2$ and the density at an altitude of $400 \,\mathrm{km}$ at Earth is $10^{-13} \,\mathrm{while}$ the martian density is only 1.63% of that at an altitude of $200 \,\mathrm{km}$ at LMO.

Table 5.53 presents the final results for the worst-case disturbance torques that the attitude control system should be able to react to.

Table 5.53: Final results for worst-case disturbance torques.

Worst-case disturbance torques	Value [Nm]
Gravity gradient	0.235
Magnetic field	$0.135 \cdot 10^{-6}$
Solar radiation	0.00186
Aerodynamic	$0.22 \cdot 10^{-5}$

As can be seen the highest torque that acts on the MEV is sue to gravity. This can be expected since the solar radiation is lower at Mars compared to Earth as it decreases with the square of the distance. Moreover, the aerodynamic disturbance is also very small due to the thin atmosphere on the Red Planet.

5.8.3. Attitude Control

The main attitude control hardware used on the MEV will be the RCS thrusters capable of inducing motion in six degrees of freedom. A preliminary sizing procedures for the RCS thrusters were applied in subsection 5.1.6. There will be four clusters of five thrusters positioned 10.2 meters as measured from the bottom of the MEV and four clusters of two thrusters located at the bottom of the MEV.

Each thruster will use GOX/GCH_4 as propellant providing 400 N of thrust. The mass of each is estimated to be 1.9 kg which makes the total attitude control system mass to be 53.2 kg.

Initially it was decided that Control Moment Gyros will be beneficial for the attitude control system when passive zero momentum control is used when the MEV is in orbit. However, it was calculated that the RCS thrusters are able to provide full axis stabilisation and control.

Usually, CMGs are capable of providing higher torque levels than the zero momentum wheels for the same power supply. The MEV can be equipped with two Double Gimbal Control Moment Gyroscopes (DGCMG) with unlimited gimbal freedom about each axis. The current technology available on the International Space Station uses four 4,760 Nms DGCMGs which are capable of producing an output torque of 258 Nm [65]. Since the dry mass of the MEV is approximately 66 tonnes it was estimated that only one DGCMG will be enough to provide 3-axis torque of 258 Nm. However, as mentioned, there will not be any DGCMGs on the MEV. This will save approximately 200 kg of the dry mass since each gyro has a mass of 100 kg.

For atmospheric control, the air brakes may be controlled individually to act as rudimentary control surfaces. However, attitude is mostly controlled by the MEV's passive aerodynamic stability, during descent. During ascent, the MEV is passively unstable, but the attitude will be controlled by thrust vectoring actuation. This requires a very accurate and multiply redundant system for the attitude sensors used while in atmosphere.

5.9. Navigation and Guidance Systems

In addition it is required that the MEV can determine its orbital position very accurately at any point in time, as well as determining the characteristics of the orbit. The critical phases for navigation and guidance are the rendezvous phase with the ITV, and the landing phase. Docking with the ITV requires even more accurate positioning, however this positioning is relative to the ITV and can be done with separate hardware. This is further detailed in subsection 5.9.2.

Several Earth-based systems for navigation of interplanetary vehicles exist. They consists of multiple large ground antennas spread around the Earth, which individually determine the difference in time of arrival of incoming radio signals. This is known as Δ Differential One-Way Ranging (Δ DOR). The Deep Space Network (DSN) is NASA's implementation of, which allows an accuracy of 150 m at 1 AU distance, or approximately 400 m at Mars's maximum distance from Earth [12]. In addition, the DSN can provide an two-way accuracy of 2 m in range and and 0.1 mm/s in velocity, which is calculated using the Doppler shift phenomenon [66].

However, an Earth-based system has many drawbacks. Firstly, measurement data is not directly available: it may take up to an hour receive the measurements from Earth, ignoring processing time. Earth-based measurements are

also not continuously available, historically allowing a number of requests in the order of five per day. As such this approach is more appropriate for accurately measuring the ITV's interplanetary trajectory and performing accurate measurements on the MEV's standby orbit, i.e. when waiting for the next ITV.

NASA has developed the Deep-Space Positioning System (DPS), which can determine a spacecraft's position without the use of external infrastructure. It is also a compatible receiver for the abovementioned techniques, so it can use the Earth-based systems to enhance its accuracy. The receiver is small, requiring only 10 W of power and weighing only 5 kg. Unfortunately information on the accuracy is not available.

5.9.1. Landing

For landing specifically, the MEV will need a radar altimeter and a set of pitot tubes and static pressure sensors for airspeed measurements. This allows for accurate true speed computations. Spacecraft altimeters weigh in the order of 2 kg [67] and can be considered to require less than 12 W [68]. Pitot tubes are considerably light and power effective in comparison with the rest of the guidance system; as such their budget usage is currently neglected.

In addition, the MEV will require an optical system to recognise the landing location from a lower altitude. A combination of three-dimensional imaging sensor and a visual range imaging sensors are, in addition to existing ADCS hardware, sufficient to allow for automated pinpoint powered landings [69]. Three dimensional imaging LIDARs are less than 10 kg per package, and uses less than 60 W of power [70].

Once a settlement has been established, a system can be set up to more easily guide landing MEVs, for example to aid with radar beacons or optical lights. This should be considered in a detailed mission design.

5.9.2. Docking

Once the MEV and ITV are within a visual range, docking can be performed with reliance on other hardware. As the ITV and MEV are able to communicate, it is also possible to utilise any sensors the ITV may use. However, it is preferable that the ITV does not need to reorient itself, since the ITV is several orders of magnitude heavier and will therefore require much more RCS propellant. Instead, the MEV should perform most of the manoeuvres during docking.

TriDAR is a combination of triangulation and LIDAR technology. The system has been used on several Space Shuttle mission to the ISS, and allows for automatic recognition of the target vehicle, and can automatically navigate to docking [71]. The Relative Navigation TriDAR Sensor (RNLS TriDAR) requires a power of at most 40 W and is only powered on for a relatively short amount of time⁴⁸. This is only a minimal portion of the power budget. Although the exact mass of RNLS TriDAR is not publicly available, older generation TriDAR packages have a mass of 29 kg. Considering other LIDAR packages are in the range of 10-20 kg, the package for docking positioning can be estimated to be 20 kg at most. An infrared camera for supervision by the crew (less than 1 kg, less than 1 W)⁴⁹ is not included in the budget.

The table below shows a summary. The total power shown is again an extreme peak power, which will never occur, as these sensors are in triplicate for redundancy purposes. Only one of each will run at once, and only during their respective flight phase.

Sensor	Ammount	Mass [kg]	Power[W]
DPS Receiver	3	5	10
Radar Altimeter	3	2	12
3D LIDAR	3	10	60
RNLS TriDAR	1	20	40
Total	10	71	286

Table 5.54: Summary of the budget use of the guidance components.

To conclude, the found masses and power requirements of the ADCS (Table 5.51) and guidance systems (Table 5.54) fall well within the allowed margins.

⁴⁸https://neptec.com/products/docking/(Last accessed 29-06-2018)

⁴⁹http://neptecuk.com/products/(Last accessed 29-06-2018)

5.10. Hardware Block Diagrams

Various block diagrams have been generated for the MEV's systems. It has been split up in multiple diagrams for legibility; these diagrams can be found on the following pages. The diagrams show all hardware the MEV is expected to contain. Similar components have been depicted using a similar icon, a list of which is found below.

- · Control units, including the main Mission Interface Unit, and the subsystem control units are indicated in grey
- · Components and actuators are indicated as rectangles
- · Sensors are indicated as rounded rectangles
- Resource containers, such as electricity and propellants, are indicated as cylinders
- External arrays, which are the solar and radiator systems, are indicated as parallelograms
- · External interfaces are indicated as hexagons
- Pumps are indicated as ovals
- · Valves are indicated as diamonds

The main block diagram can be found in Figure 5.52.

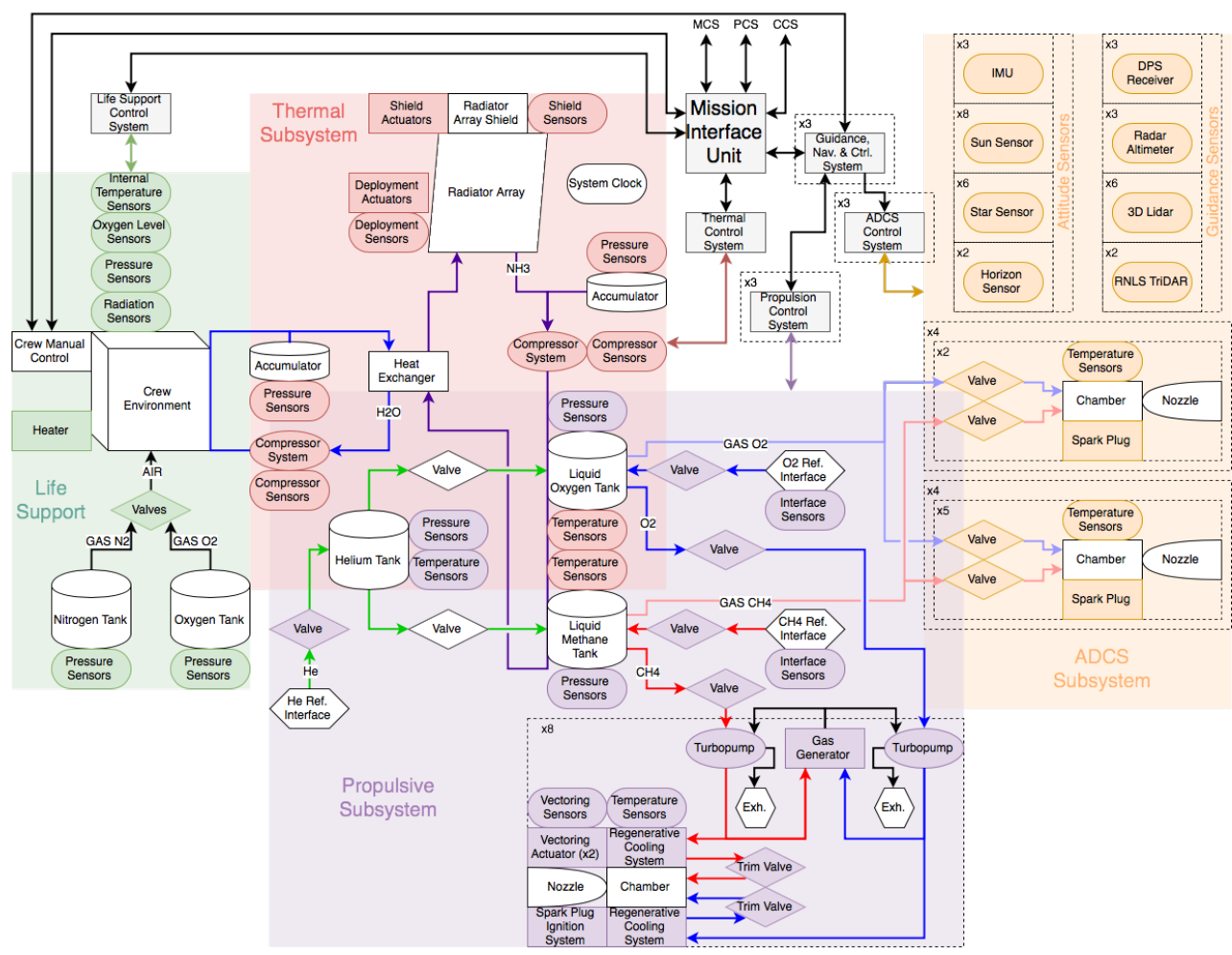


Figure 5.52: Main hardware block diagram.

The main computing unit of the MEV is the Mission Interface Unit (MIU). This section oversees and gives instructions to each control system, i.e. each separate control computer. Although the MIU has integrated redundancy, it consists of only one unit: should the MIU fail, the MEV is still fully operational, although specific functions will have to be operated manually by the crew.

The Life Support Control System controls the crew environment. The green bidirectional arrow indicates it reads sensor data from and sends instruction to the components indicated in green. This system contains a flow of gaseous

nitrogen and oxygen, regulated by valves, to the crew environment to maintain pressure and oxygen level. The crew environment is cooled by the secondary coolant loop, in blue, which utilises water.

The Thermal Control System controls both liquid coolant loops and the radiator. The red bidirectional arrow indicates it reads sensor data from and sends instructions to the components indicated in red. The primary coolant loop cools the propellant tanks and extracts heat from the secondary loop by means of a heat exchanger. It utilises ammonia.

The Guidance, Navigation and Control System controls the trajectory of the MEV. In addition to the built-in redundancy of the computational units, it is implemented in triplicate. It directly controls and monitors the Propulsion Control System and the ADCS Control System, which also are triply redundant.

The Propulsion Control System controls the propellant flow and the main engines. The purple bidirectional arrow indicates it reads sensor data from and sends instructions to the components indicated in purple. It allows refueling of the propellant tanks from the refueling interfaces, which connect to the ITV's tanks while docked. Liquid propellants are pumped to the engines through turbopumps, which are powered by a gas generator using the same propellants. The propellants pass through regenerative cooling before entering the combustion chamber. The pressure in the tanks is maintained by replacing used propellant with helium from a separate tank. The helium can also be refueled from the ITV.

The ADCS Control System controls the sensors, gyros and RCS thrusters. The orange bidirectional arrow indicates it reads sensor data from and sends instructions to the components indicated in orange. The ADCS sensors contain the Deep Space Positioning System (DSPS) transceiver, which is the main source method for accurate positioning in space. It utilises NASA's Deep Space Network Array on Earth to determine its position (by one-way X-band radio/visual imagery) and velocity (by Doppler calculations). Gaseous propellant from the main tanks is used to fire the RCS thrusters.

The MIU also directly communicates with the Mechanical Control System (MCS), Power Control System (PCS), and the Communication Control System (CCS). These subsystems are depicted in separate figures.

The Communication Subsystem utilises two antennas, one main and one backup. A communication diagram is presented in Figure 5.53

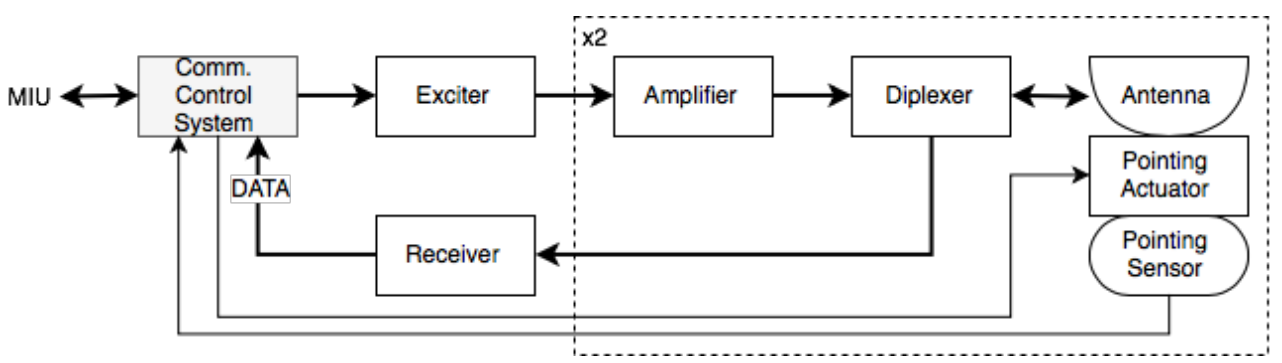


Figure 5.53: Communication subsystem hardware diagram.

The Mechanical Subsystem control the mechanics of the landing gear, air brakes and hatches. It is presented in Figure 5.54. The blue bidirectional arrow indicates it reads sensor data from and sends instructions to the components indicated in blue.

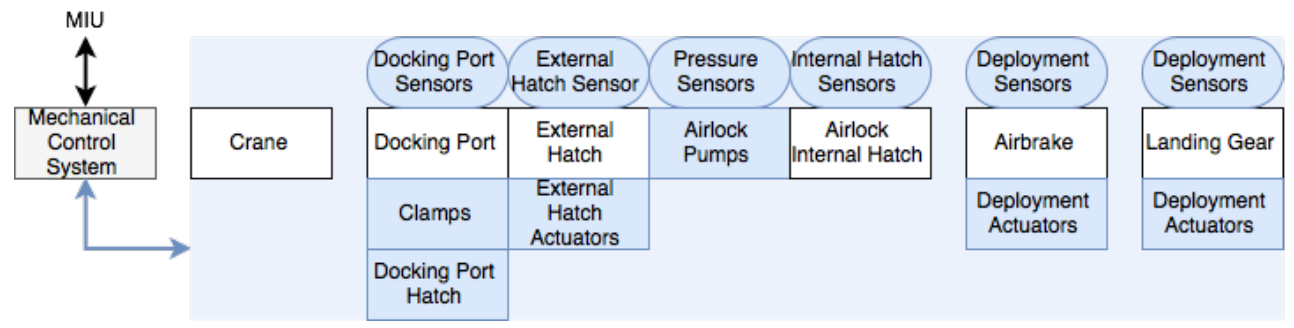


Figure 5.54: Mechanical subsystems hardware diagram.

The Power Subsystem controls the generation and storage of electricity, as depicted in Figure 5.55. The yellow bidirectional arrow indicates it reads sensor data from and sends instructions to the components indicated in yellow. It allows recharging from both the solar array as well as from the ITV, through the Power Link Interface when docked. The Power Bus distributes power to the rest of the components. This is further discussed in subsection 5.10.3.

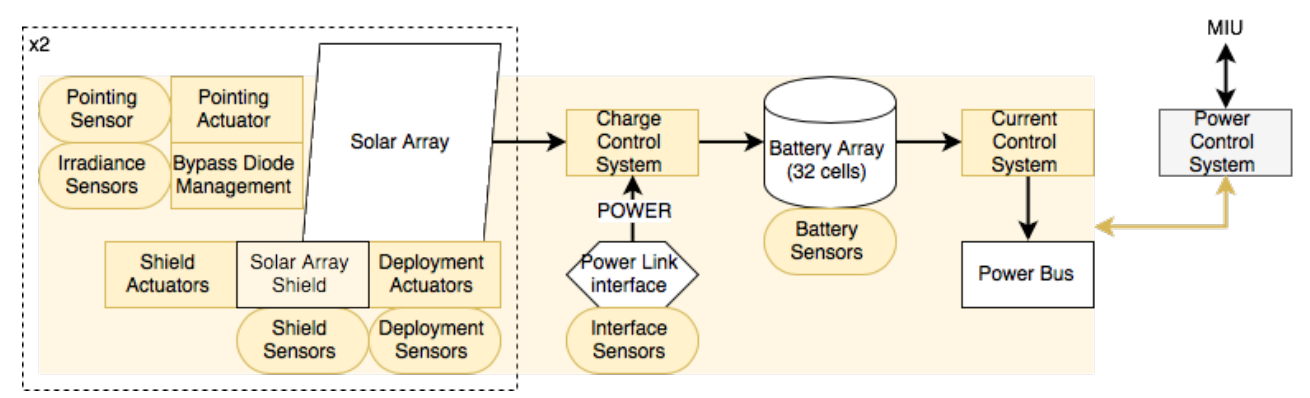


Figure 5.55: Power subsystems hardware diagram.

5.10.1. Communication Flow Diagram

The Communication Flow Diagram depicts the communication traffic between the components of the MEV as well as between the MEV and other mission signals. this diagram remains mostly unchanged from the Midterm Report: the most significant change is due to a clearer distinction between the subsystem control systems. The diagram is depicted in Figure 5.56, and the abbreviations used to describe the links are listed below.

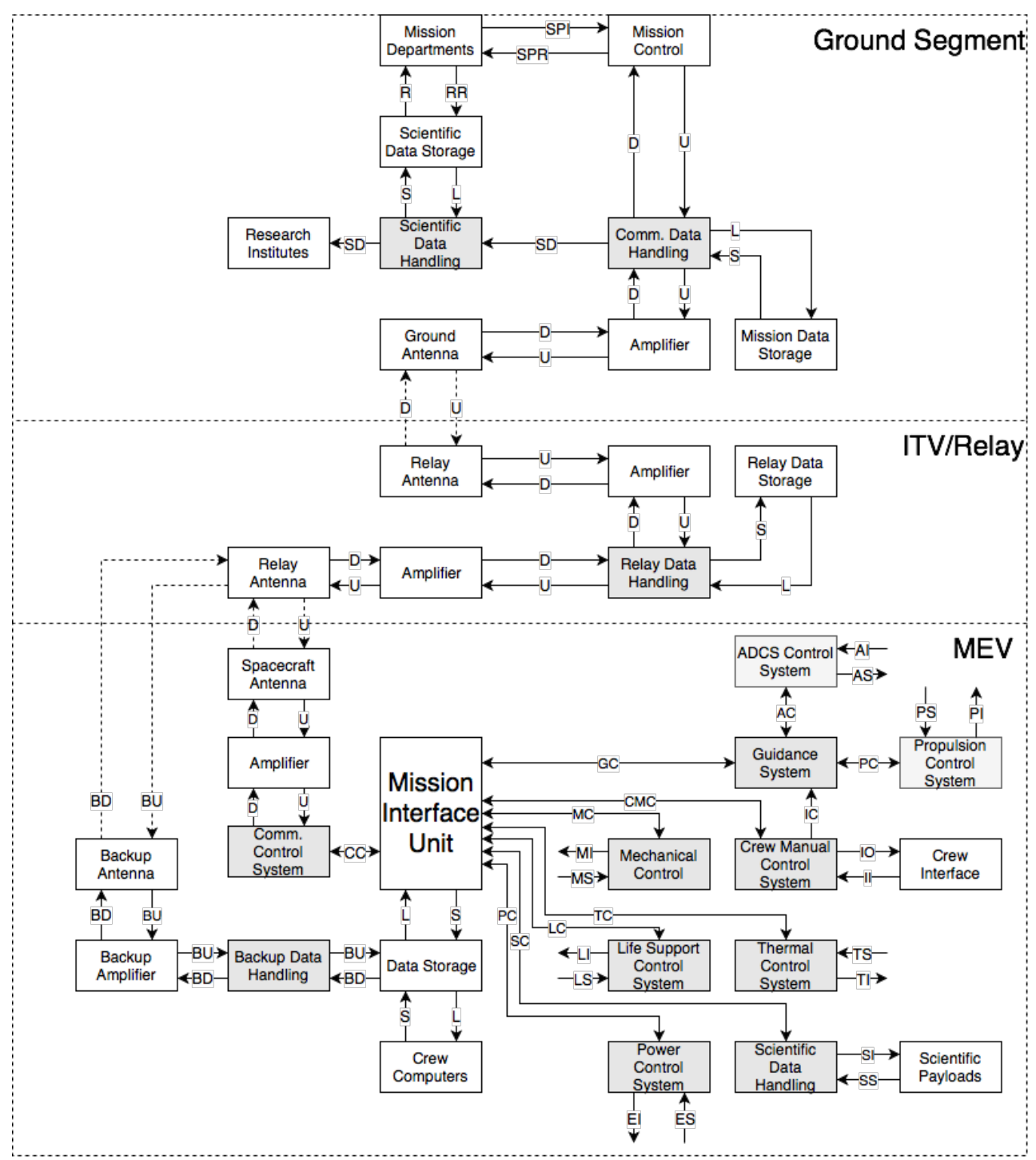


Figure 5.56: Communication flow diagram.

- MEV General Control: The MIU controls each subsystem computer, which means that it sends instructions and reads status reports:
- AC: ADCS Control
- CC: Communication Control
- CMC: Crew Manual Control
- EC: Electrics System Control
- GC: Guidance Control
- LC: Life Support Control
- DC: Direct Control
- IO: Interface Output
- II: Interface Input
- MC: Mechanical Control
- PC: Propulsion Control
- SC: Scientific Control
- TC: Thermal Control

- Communication and Ground Segment: Between the space segments and the ground segments, most notable is the flow of the uplink and downlink:
- **BD:** Backup Downlink
- BU: Backup Uplink
- **D:** Downlink
- L: Load
- R: Research
- RR: Research Results
- S: Save
- **SD:** Scientific Downlink
- **SPI:** Support Information
- SPR: Support Request
- U: Uplink

- Subsystem Control: Each subsystem control computer sends instruction to components such as actuators, and reads incoming sensor data:
- AI: ADCS Instructions
- AS: ADCS Sensor Data
- CI: Communication Instructions
- **CS:** Communication Sensor Data
- EI: Electric System Instructions
- ES: Electric System Sensor Data
- LI: Life Support Instructions
- LS: Life Support Sensor Data
- MI: Mechanical Instructions
- MS: Mechanical Sensor Data
- **PI:** Propulsion Instructions
- PS: Propulsion Sensor Data
- **TI:** Thermal Instructions
- TS: Thermal Sensor Data
- **UD:** Uplink/Downlink

The ground segment contains mission control and the ground antenna array. In addition, it contains all actors that will perform analysis, storage, and research on the scientific data that is produced during the missions. It is important to ensure this data is freely available to the public, which indicated as the Scientific Downlink in the diagram. Information will also be shared to and from Mission Control, which may required additional research and help from the departments of the space agency. For example, Mission Control may require a more accurate trajectory analysis to be done on-site. Finally, any live streaming of, for example the first Mars landing, will be done by a separate streaming service from Mission Control, so this is not included in this diagram.

The MEV requires at least a form of relay to send data back to Earth, as has been determined in the Midterm Report. There are various satellites already in orbit which can act as relay. The ITV can also act as relay in case that is necessary. It is expected that these communication requirements will not add any constraints on the ITV design. The communication data handling systems, in grey, contain functions such as compression and (de)modulation, as is typical for spacecraft communication systems.

Regarding the MEV itself, the Mission Interface Unit handles the incoming data and relays this to the other computers, including the crew systems. The same control systems from the hardware diagram are depicted here, with two additions: Firstly, backup data handling is added explicity with direct access to the data storage. In addition, scientific payloads are shown as well.

5.10.2. Data Handling Block Diagram

The hardware chain-of-command is defined as follows. The Mission Interface Unit (MIU) is the main data handling system, which controls the other flight computers. It is a fail-safe system, which is typically implemented by redundancy of the hardware, or a multi-core solution as will be explained below. Complete failure of the MIU means that

the MEV is still operational, but each subsystem must then be controlled manually. The MIU contains or directly interfaces with the system clock, which is the main reference for timekeeping. Each computer will likely have its own clock as well, which is good for redundancy, but there must be one reliable and accurate reference.

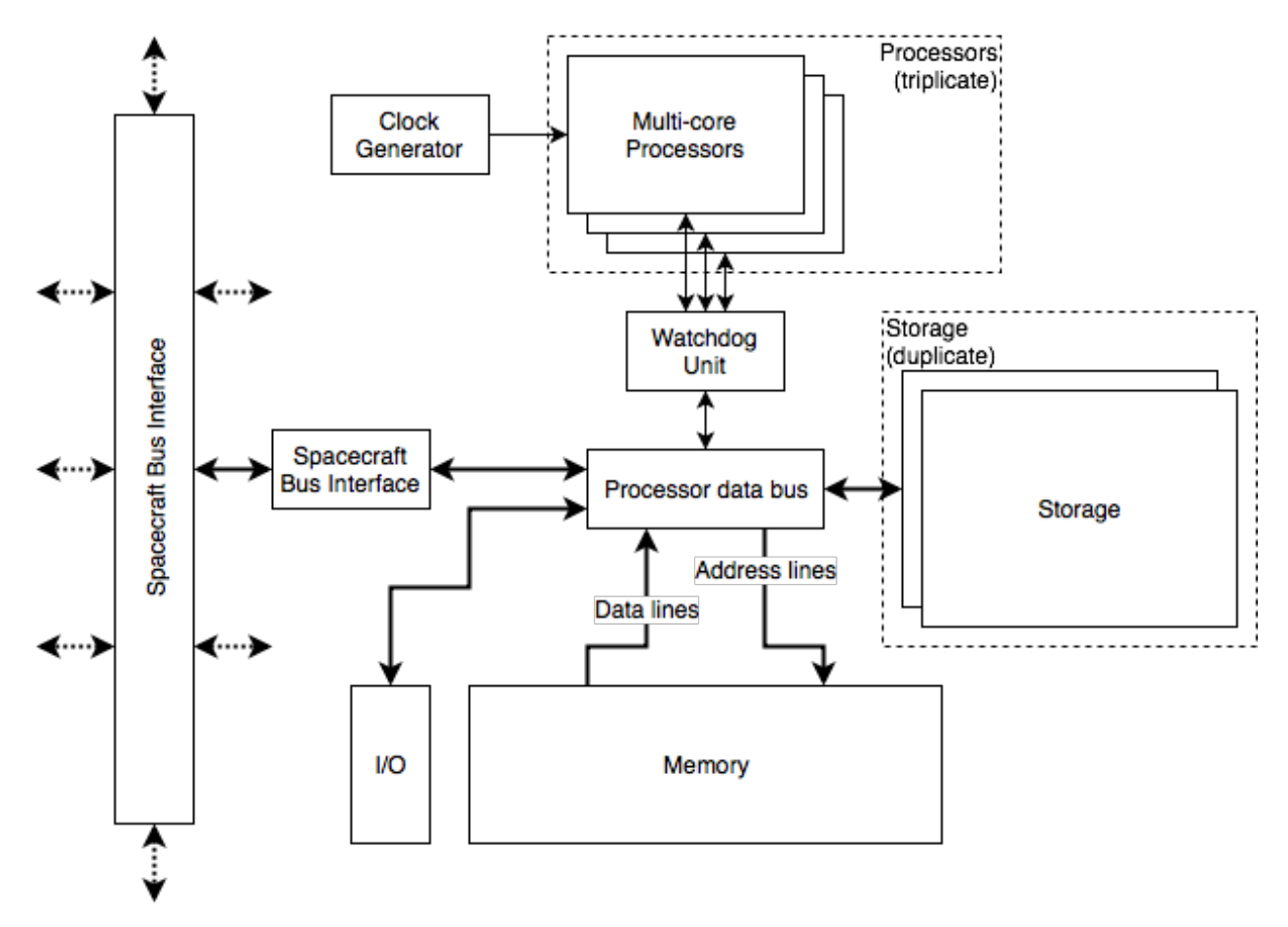


Figure 5.57: Block diagram of a generic data handling module.

A diagram of a typical data handling component is presented in Figure 5.57. It is very similar to the architecture of computers in general, containing processors, memory, storage and specific input/output, depending on the computer. Communication between the specific computers goes via the Spacecraft Bus Interface, which connects all computers. The required directions of communication have been presented in the communication flow diagram and hardware diagram.

The current practice as utilised by SpaceX uses multiple multi-core processors. Each core performs the same computations, and if the results are not the same, the entire processor is ignored altogether. Each processor runs different software, perhaps developed by different programming teams. A watchdog unit determines which of the resulting instructions will be forwarded, in case the processors do not agree. This is likely by majority (in case one processor is faulty) but in a worst-case scenario, the system can still continue with one functioning processor, by continuing to trust the processor that has historically been most often correct.

5.10.3. Electric Block Diagram

Figure 5.58 depicts the electric lines. From the power bus, subsystems have individual lines, which allows a breaker system such that any faults are more easily traceable. Direct current of 28 V is available on each lines; this voltage level was present on the Apollo Lander Modules, due to low transfer losses. Conservative voltage reducers (CVRs) allow a 5 V connection for low power devices, such as simple sensors, where necessary. Specifically, digital reducers have the highest relative efficiency [72], especially when considering the expected cumulative length of all power lines in the MEV.

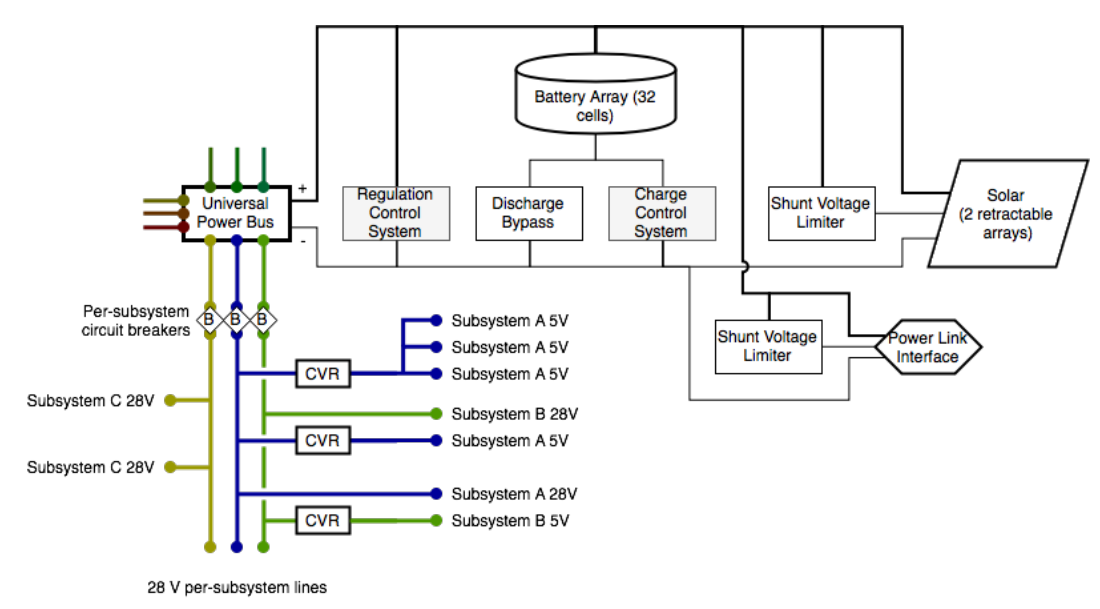


Figure 5.58: Block diagram of the electrical system.

5.11. Embarkment and Disembarkment

Although the design choices for embarkment and disembarkment are not particularly critical with respect to the design of the overall vehicle, the options must be considered to ensure compliance with the requirements. This section looks at both the disembarkment on the Mars surface, as well as the disembarkment from one vehicle onto another.

5.11.1. Docking Port

The ITV and the MEV both require docking ports in order to be able to connect with one another, to allow for the transfer of crew and cargo. The ITV will have two docking ports, while the MEV will only have one. It was decided upon to use the International Berthing and Docking Mechanism (IBDM) which is currently under development by ESA⁵⁰ for both vehicles. It was selected for its androgynous mating, which will add redundancy to the system as two MEVs can dock, as well as for the fact it is designed to facilitate the docking of two spacecraft with considerably different masses [73].

The port has a maximum outer diameter of 1.485 m and passage diameter of 0.8 m⁵⁰ and should have a mass of approximately 325 kg⁵¹. The docking port was developed in accordance with the International Docking System Standard [74], meaning it is also compatible with the International Docking Adaptor which is used on the ISS.

The IBDM has ports to facilitate the transfer of power and data between the MEV and the ITV^{50} . However, it currently has no ability for the transfer of propellant, so additional lines would still have to be added for the fuel and oxidiser transfer. These lines would not pass through the docking port itself, but a separate interface will be loaded just below it to allows for the connection of these lines.

5.11.2. Surface Disembarkment

There are many options for lowering down crew and cargo to the surface of Mars. From this, those that allow only disembarkment (such as slides) have been immediately eliminated. From the remaining options, it was considered that a powered option is necessary, in order to easily transfer heavy cargo.

An elevator down through the MEV was not considered, due to complexity and space requirements on fuel tanks and engine positioning. A extendable elevator on a rail on the outside of the MEV was also not considered, due to interference with the landing gear and air brake design.

To unload passengers and cargo, a deployable crane is chosen with an extending arm, electric motor and cable reaching a distance of 13.3 m from the top of the door to the surface. A typical passenger mass including spacesuit is about 125 kg, and the maximum mass of an ISS cargo transfer bag is 180 kg. These bags may also be up to .5x.5x.4 m

⁵⁰http://wsn.spaceflight.esa.int/docs/Factsheets/27%20IBDM.pdf(Last accessed 19-06-2018)

 $^{^{51}} https://en.wikipedia.org/wiki/International_Berthing_and_Docking_Mechanism (Last accessed 19-06-2018)$

in size⁵². It is assumed that a three point harness is built into the spacesuit.

A suitable electric motor for lifting people is the Atlas Powered Ascender (APA-5)⁵³. This motor is capable of lifting 2,675 N and uses a power of approximately 3.1 Wh per meter traversed while lifting 1,115 N. It is reasonable to assume that the power is proportional to the force lifted, thus to traverse the entire distance with the payload mass of 5,000 kg will use approximately 363 Wh. The mass of this motor including rope is 12 kg.

5.12. Iteration, Safety Factors and Margins

Designing a complex system like the MEV, involves subsystems that are heavily interdependent. For example increasing propellant mass will then increase the structural mass required to carry the extra propellant. This well known effect called the snowball effect in aerospace terms is clearly visible in the design of the MEV. The subsystems that are mostly influenced by a mass change are structures and propulsion. Communication, Thermal, Power and Payload are relatively constant for a changing mass. The interrelations have been shown in Figure 5.59. Iterations during the design process were run by establishing the propellants masses needed for an acceptable descent and ascent profile, the tank masses needed for this much propellant are then established, with the structure calculations then being run with the accelerations and dynamic pressures provided by ascent and descent as well as the dry and wet masses.

As well as dealing with the interdependency of the systems, safety factors and margins must also be considered. Safety factors are applied during the design process different subsystems and vary depending on the load case. Safety factors allow for machining and production imperfections as well as deviation outside of the nominal operating conditions. Safety factors are imposed on the design throughout the different project phases and are imposed also on the final design.

The following safety factors were adopted during the structural design of the MEV:

- A safety factor of 2 is applied to the ultimate strength of all pressure vessels;
- A safety factor of 1.4 is applied to the air brake ultimate strength;
- A safety factor of 2 is applied to the ultimate strength of hull and floor of the MEV;
- A safety factor of 2 is applied to the buckling load.

Margins however are only imposed on the design during different design phases, and vary depending on the phase. Margins are meant to allow for fluctuations in the parameters of the subsystems during the design phases while keeping these parameters under or over a certain limit. During this phase of design the report "Margin philosophy for science assessment studies" from ESA is used to provide margins [75]. This entails using a margin of 10% on power and 15% on cryogenic cooling systems with a further 15% on the radiator. The recommended margin on dry mass when sizing propellant mass is 20%. This value is reduced to 10% in the design of the MEV as many of the structural elements are currently idealised during their sizing and a reduction in there mass is highly guaranteed.

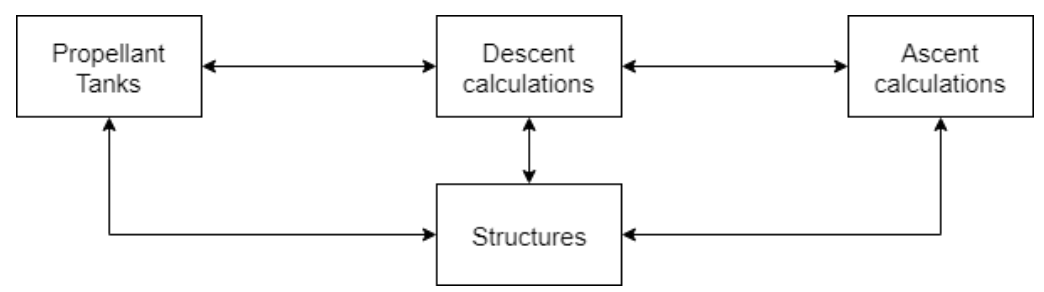


Figure 5.59: Block diagram of the different departments that influence each other when iterating.

During the final phases of the preliminary design a number of revisions of the design were conducted where values were exchanged between the sizing tools designing different subsystems. The different revisions have been listed in Table 5.55. Blue numbers indicate a change over the revision, which are mainly in the structures, air brake and propulsion sections. A number of factors caused significant changes during the revisions. An increase in the air

 $^{^{52} \}texttt{nasa.gov/eps/eps_data/126269-OTHER-001-003.ppt} (Last\ accessed\ 22-06-2018)$

 $^{^{53} \}texttt{https://atlasdevices.com/wp-content/uploads/APA-5-atlas-powered-ascender-fact-sheet.pdf} (Last accessed 22-06-2018) \\$

brake weight during revisions six was a result of a mistake being discovered in the assumptions being used to size the air brakes. Its subsequent decrease in mass in revision eight was due to a change in cross section increasing the MOI and lowering the mass. It should be noted that within each design revision the process of exchanging values between subsystems was carried out until that specific design revision converged to a final value. These iterations were conducted manually and converged for each design revision. The final increase in revision 10 is due to the addition of margins and not a divergence in the design.

Iteration:	1	2	3	4	5	6	7	8	9	Final: 10
Structures	855	855	855	805	804	829	823	816	898	1,674
Air brake	490	490	570	570	560	1,137	1,167	1,067	1,067	1,101
Landing legs	1,500	1,500	1,500	1,500	1,500	1,500	1,500	1,500	1,500	1,500
Thermal	1,500	1,500	846	537	537	537	537	537	590.7	590.7
Airlock	-	-	-	-	-	350	350	350	385	385
ADCS	450	450	450	450	450	450	450	450	450	450
Power	1,293	1,293	1,293	1,293	1,293	1,293	1,293	1,293	1,293	1,293
Propulsion	620	620	827	827	827	827	827	827	909.7	909.7
Communications	58.2	58.2	58.2	58.2	58.2	58.2	58.2	58.2	58.2	58.2
Prop tank	1,100	1,100	655	643	632	637	650	650	715	994.4
Env tank	600	600	470	470	470	580	580	580	638	632.5
Payload	5,000	5,000	5,000	5,000	5,000	5,000	5,000	5,000	5,000	5,000
Dry	13,475	13,475	12,533	12,162	12,140	13,207	13,244	13,137	13,558	14,597.3
Propellant up	11,500	11,500	8,600	7,160	6,720	8,450	8,400	8,350	10,530	12,900
Propellant down	34,000	33,000	35,000	33,500	32,500	35,000	35,000	35,000	37,250	38,450
Propellant RCS	-	-	-	-	-	490	490	490	539	539
Total	58,975	57,975	56,133	52,822	51,360	56,657	56,644	56,487	61,338	65,947.3

Table 5.55: Masses of different subsystems in different revisions.

5.13. General Approach to Sensitivity Analysis

Sensitivity analysis was performed for each subsystem in order to gauge how stable the system is while guaranteeing that each design decision made is valid. Each subsystem was mainly dependent on specific variables that defined the entire system characteristics. Such variables are the dry mass, the propellant mass, velocity etc. Various tools were developed that calculate the entire mass distribution, the propulsion system characteristics, the landing and ascending trajectories as well as the structural characteristics. The main parameters in each subsystem were varied and the entire system change was estimated as a percentage of base value. Some subsystems such as structures showed a high sensitivity to even small changes in the mass of certain components. Additionally, higher range in velocity magnitude might lead to the MEV not being able to land. Each sensitivity analysis is explained after each subsystem and measures for counteracting each severe changes are also given.

5.14. Contingency Management

Contingency management involves the active monitoring of Technical Performance Measurements (TPM) in order to ensure that the Technical Resource Budgets (TRB) are completed within budget. TRB are the technical parameters that determine the success of the project.

For Project Cardinal the parameters include engine mass, engine thrust, structural mass, propellant mass, power system mass, and comm system mass. These parameters, as the name suggests, are technical and and look at masses, thrusts, and watts produced. TPM is the practise of carefully managing and allocating different amounts to these budgets during different phases of the project, to ensure the project is completed successfully [76]. Figure 5.60 shows an example of how contingency management would be put in to action during the detailed design phase of the project.

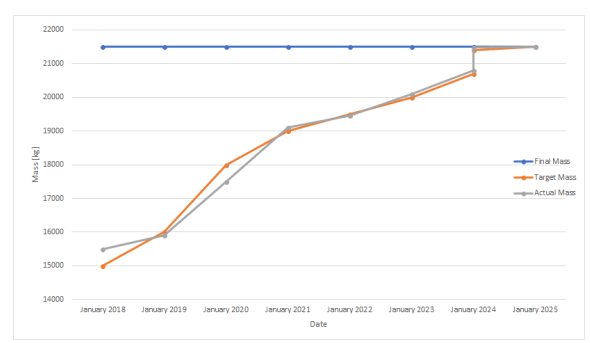


Figure 5.60: An example of contingency management of the NTR engine mass.

Design Overview

The results shown in the previous chapters together form a preliminary design for the MEV. An overview of this design in given in this chapter.

6.1. Configuration & Layout

This section presents a variety of configuration drawings, technical drawings and scale drawings of the MEV and ITV. The drawings can be found in Figure 6.1, Figure 6.2, Figure 6.3, Figure 6.4, and Figure 6.5.

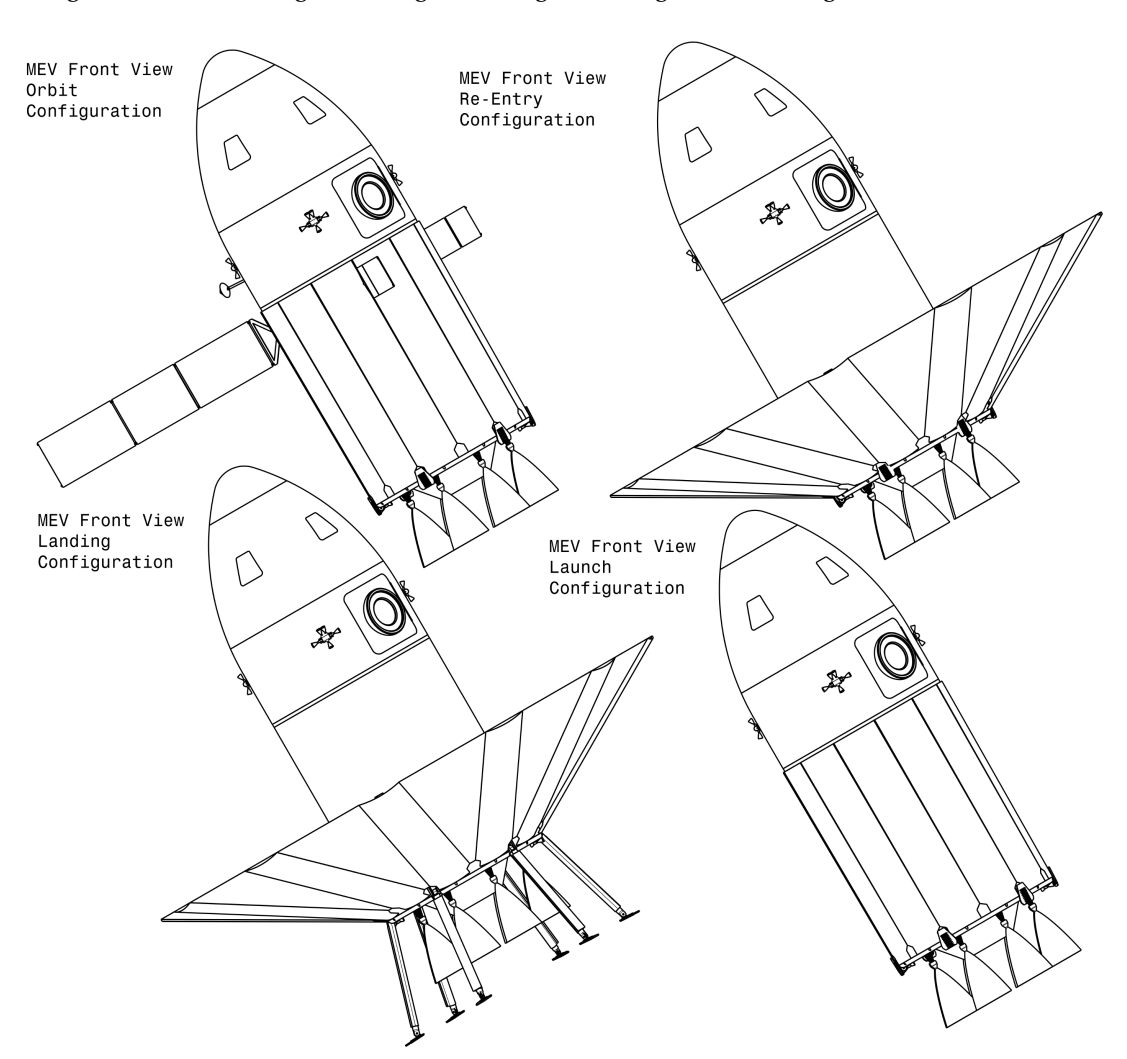


Figure 6.1: MEV in orbit, re-entry, landing and launch configurations.

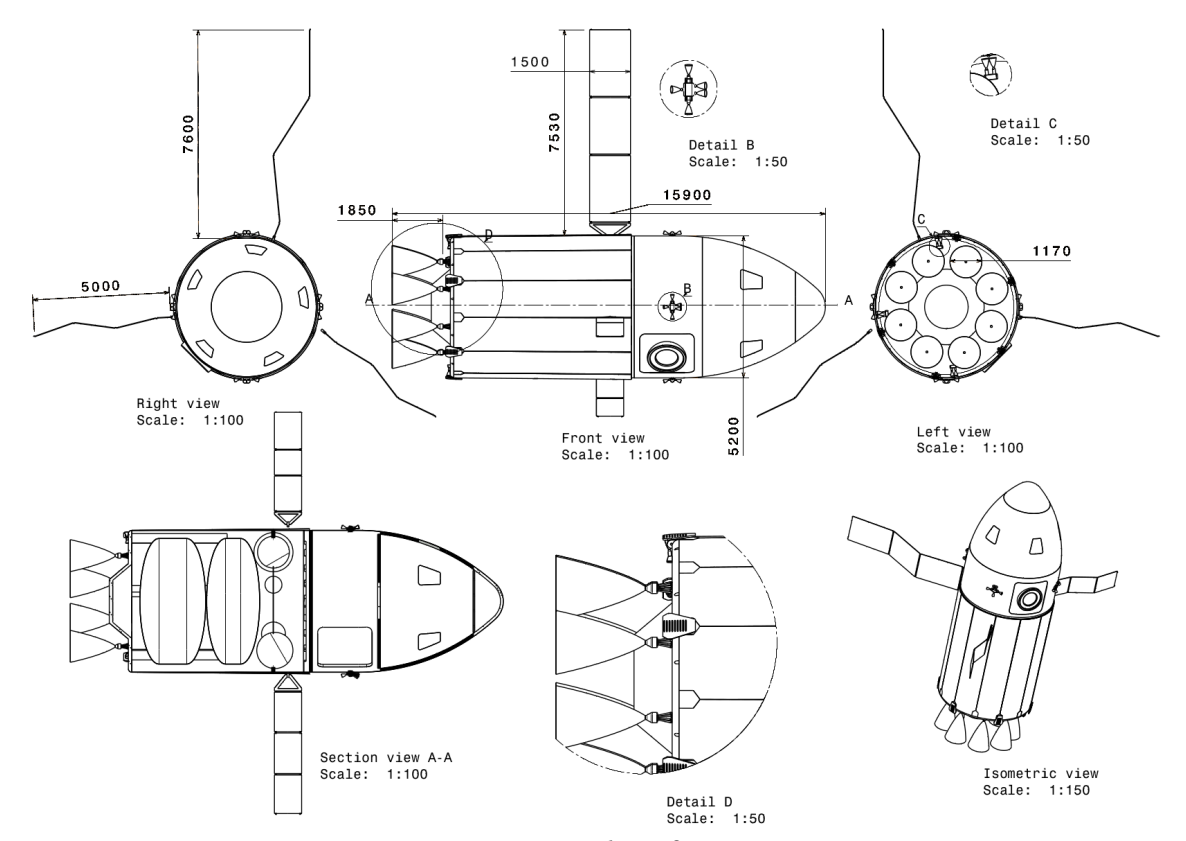


Figure 6.2: MEV in orbit configuration.

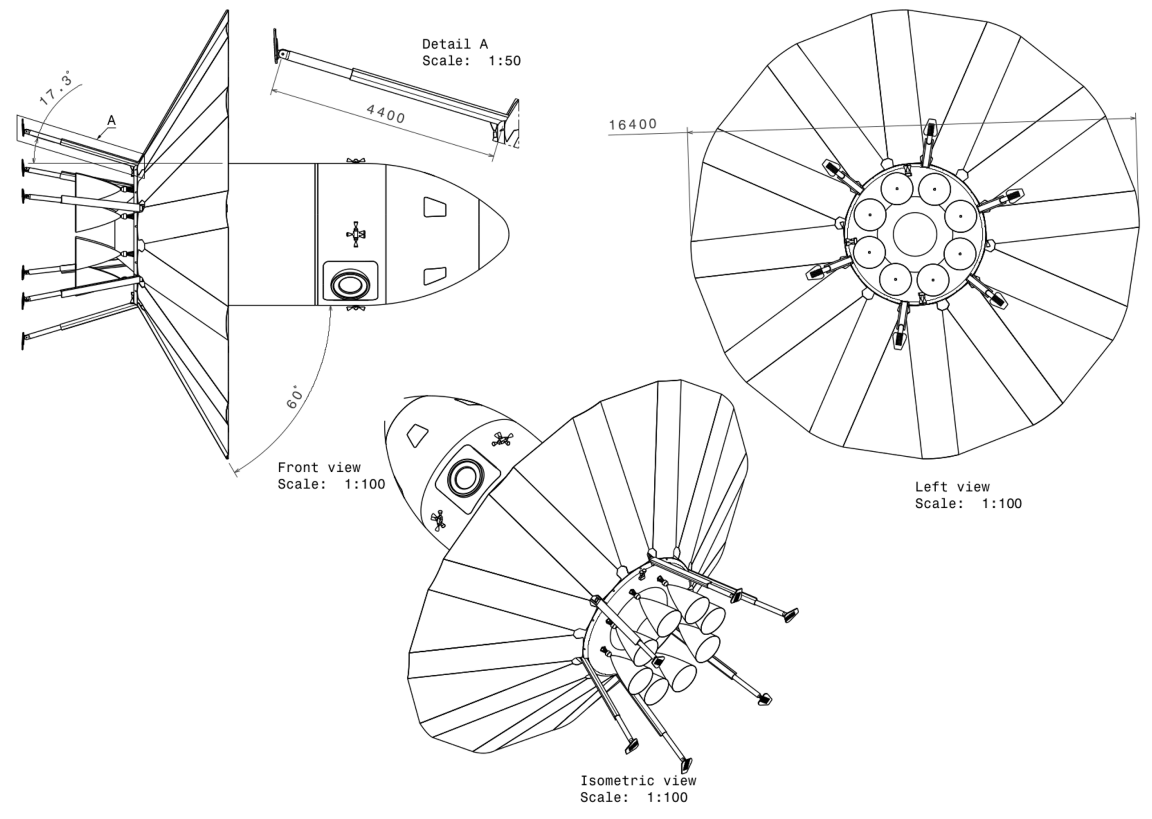


Figure 6.3: MEV landing configuration.

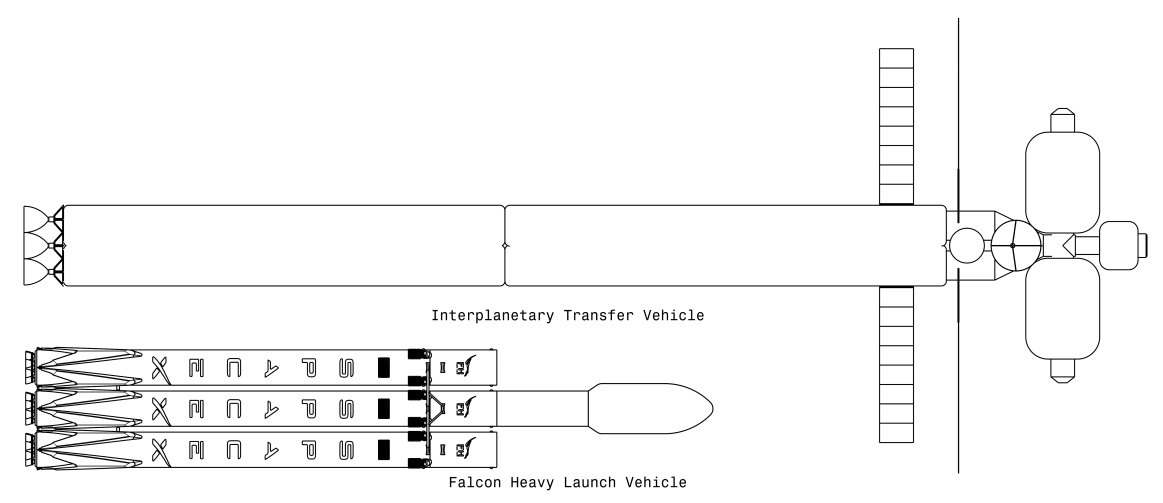


Figure 6.4: ITV scale relative to the SpaceX Falcon Heavy configuration.

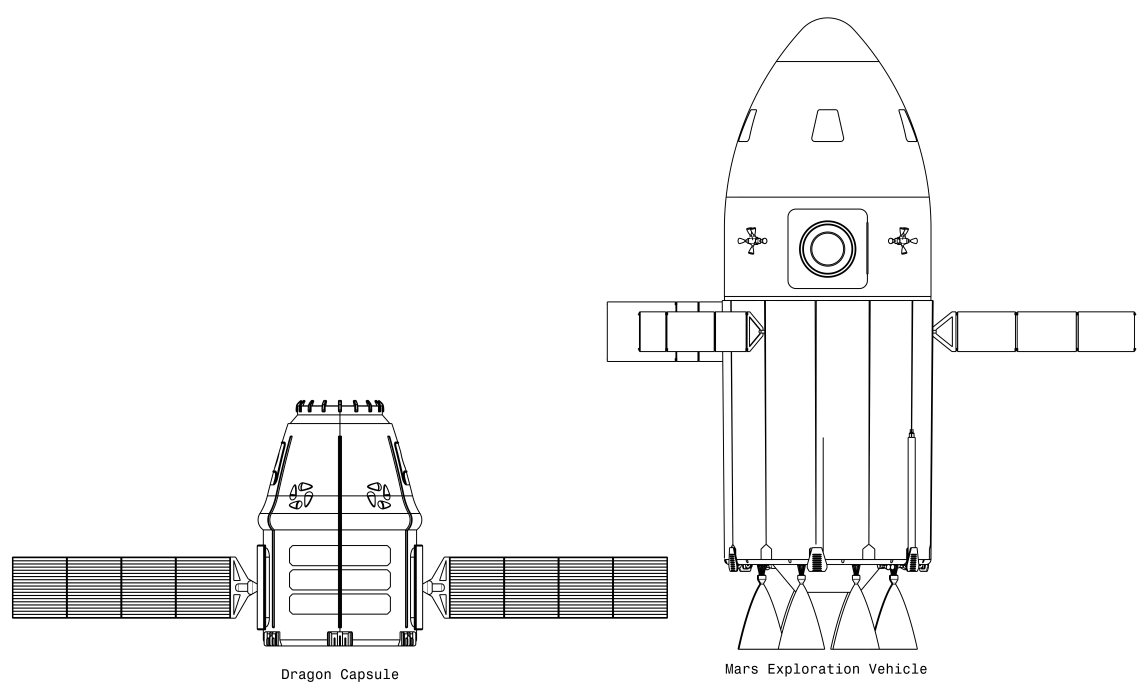


Figure 6.5: MEV scale relative to the SpaceX Dragon capsule.

6.2. System Characteristics

This section presents a summary of the main characteristics of the MEV, which can be found in Table 6.1.

Characteristics	Value	Units
General		
Total wet mass	65,947.3	kg
Dry mass	14,597.3	kg
Payload mass to Mars surface	5,000	kg
Payload mass to Mars orbit	5,000	kg
Height	15.9	m
Diameter	2.6	m
Volume	245.4	m^3
Design dry mass (w/o payload)	9,597.3	kg

Table 6.1: MEV performance and specifications with margins.

Propulsion		
Number of main engines	8	
Main engine propellant	LOX/LCH ₄	_
Main engine injector type	Pintle	_
Main engine igniter type	Spark torch	_
Main engine cooling	Regenerative	_
Main engine material	Niobium C-103	_
Main engine O/F	3.4	-
Main engine mass	104.8 (10 % margin = 115.3)	kg
Main engine I_{sp}	340	s
Main engine max mass flow	14.98	kg/s
Main engine thrust	50,000	N
Main engine chamber pressure	70	bar
Main engine characteristic chamber length	1.016	m
Main engine expansion ratio	276	-
Main engine contraction ratio	7	-
Main engine throat diameter	0.0703	m
Main engine chamber length (cylindrical part)	0.1451	m
Main engine total chamber length	0.2453	m
Main engine height	1.9017	m
Main engine skin thickness	2.0	mm
Main engines propellant mass	51,350	kg
Number of RCS thrusters		
RCS thruster propellant	GOX/GCH_4	-
RCS thruster injector type	Impinging	-
RCS thruster igniter type	Spark torch	-
RCS thruster O/F	3.4	-
RCS thruster mass	1.9 (10 % margin = 2.1)	kg
RCS thruster I_{sp}	313	S
RCS thruster max mass flow	0.13	kg/s
RCS thruster thrust	400	N
RCS thruster chamber pressure	8	bar
RCS thruster characteristic chamber length	1.25	m
RCS thruster expansion ratio	47.3	-
RCS thruster contraction ratio	7	-
RCS thruster throat diameter	0.0194	m
RCS thruster height	0.3663	m
RCS thruster propellant mass	539	kg
Pressure tanks		
Oxidiser tank dry mass	487 (10 % margin = 535.7)	kg
Oxidiser tank height	2.73	m
Oxidiser tank radius	2.3	m
Oxidiser tank skin thickness	4.78	mm
Fuel tank dry mass	417 (10 % margin = 458.7)	kg
Fuel tank height	2.19	m
Fuel tank radius	2.3	m
Fuel tank skin thickness	4.78	mm
Oxygen tank wet mass	74.8 (10 % margin = 82.28)	kg
Oxygen tank height	0.608	m
Oxygen tank radius	0.304	m
Oxygen tank skin thickness	4.0	mm
Nitrogen tank wet mass	251 (10 % margin = 276.1)	kg
Nitrogen tank height	0.85	m
Nitrogen tank radius	0.425	m
Nitrogen tank skin thickness	9.5	mm
Structures		
Structural mass	1,674	kg
Skin mass	581	kg
Stringer mass	81	kg
Floor mass	308	kg

Floor beams mass	705	kg
Air brake mass	1100	
Thermal Control Mass	537 (10 % margin = 590.7)	kg kg
Power	337 (10 % margin = 330.7)	<u></u>
Mass of power system	1,293	ka
-	43	kg
Mass of solar arrays		kg
Power generated	740 (10 % margin = 862.5)	W
Power source	Battery, solar	2
Area of solar panel	8.72	m^2
Power requirements - crewed flight	2,484	kW
Power requirements - standby phase	341	W
Battery mass	1,250	kg
Maximum energy storage needed(crewed phase)	182,574	Wh
Maximum energy storage	200,000	Wh
Specific energy	160	Wh/kg
Number of battery cells	32	
Thermal		
Mass of thermal system	536.5	kg
Radiator area	10.7	m^2
Radiator mass	59	kg
Communication		
Mass of communication system	58.2	kg
Data rates	2.66	Mbit/sec
Transmission power	50	W
Communication subsystem power	116.9	W
Antenna diameter	0.45	m
Antenna efficiency	0.5	-
Amplifier efficiency	0.55	_
Astrodynamics		
ΔV required for ITV mission (Hohmann)	5.7-5.9	km/s
ΔV required for ITV mission (gravity assist)	9.0-11.5	km/s
ΔV required for attitude control	0.3	km/s
ΔV required for orbit circularisation	2.09	km/s
ΔV required for de-orbit burn	0.239	km/s
ΔV required for landing burn	0.726	km/s
ΔV required for launch to LMO	2.263	km/s
ΔV required for orbit insertion burn	1.45	km/s
ΔV required for rendezvous	0.346	km/s
Time of flight (Interplanetary transfer - Hohmann)	260-270	days
Time of flight (Interplanetary transfer - gravity assist)	310-380	days
Time from de-orbit to Entry Interface	6.91	
•		mins
Time from entry to surface Time from surface to orbit	8.67 11.6	mins mins
	76.11	mins
Time required for rendezvous manoeuvre	70.11	1111118
Aerodynamics		
Drag coefficient launch	0.4	-
Drag coefficient descent	1.4	-
Lift coefficient	0.2	-
Centre of pressure	6.5	m
Descent propellant	12,900	kg
Ascent propellant	38,400	kg
Landing angle Φ	89.8	deg
Horizontal distance travelled	1,148.319	km
Angle change of travel Ψ	19.42	deg
Landing velocity	1.8	m/s
Maximum dynamic pressure q_{max}	6,083	Pa
Maximum heat flux ψ_{max}	5	W/cm
Altitude of burn	8.7	km
Air brake effective area	213	m^2
Air brake actual area	243	m^2
Air brake angle	60	deg

Maximum descent acceleration	27.5	m/s^2
Maximum ascent acceleration	20	m/s^2
Landing altitude	-2	km
Attitude determination and control		
Mass ADCS system hardware	75.7	kg
Sun sensors	8	-
Star trackers	6	-
Horizon sensors	2	-
Inertial measurement units	3	-
RCS thrusters	28	-
Controllable air brakes	12	-
Thrust vectoring main engines	8	-
Two-way positioning accuracy	2	m
Two-way velocity accuracy	0.1	mm/s

6.3. RAMS Analysis

In this section, the reliability, availability, maintainability, and safety characteristics will be reviewed. They will be analysed for the whole mission profile of the MEV as described in the general functional flow diagram in Figure 3.5.

6.3.1. Reliability

Since Project Cardinal is creating a system that has never been created before, only rough estimates based on historically similar missions can be made for the reliability. Given the re-entry nature of the vehicle, the Space Shuttle programme is considered to be the most logical mission with respect to comparability. The Space Shuttle programme resulted in a total mission count of 135 missions¹. Out of these 135 system launches, two resulted in a critical failure and loss of life. These are the January 1986 Challenger mission² and the February 2001 Columbia mission³. Considering a similar reliability to that of the Space Shuttle programme for the MEV would result in a reliability of 0.985, as was calculated in the Midterm Report [3]. However, in order to properly compare the MEV with the Space Shuttle, the nature of the Space Shuttle failures should be reassessed. The Columbia failure occurred due to an O-ring failure in one of the solid rocket boosters that was used to launch the Space Shuttle to LEO. This means that the failure did not occur in the Space Shuttle itself. The Challenger mission failed due to a collision with the heat shield of its left wing, causing the heat shield to fail upon re-entry. This is a critical failure that did occur in the Space Shuttle and could also occur in the MEV, meaning that in the comparison, this is the only critical mission failure that is taken into account. Therefore, the reliability of the MEV system for the re-entry and take-off phase will most likely be around 0.9926.

The second part of the MEV reliability that should be considered is the system waiting in orbit for the next ITV. Although the crew will be able to maintain the MEV once they are docked, the system should maintain operational throughout the 1.5 years of orbiting Mars. In Figure 6.6 the relationship of spacecraft reliability with respect to mission duration is shown. Because the MEV will be classed as a large spacecraft, it is expected that reliability will drop significantly when in orbit for longer periods of time. After around 1.5 years after orbit insertion, the reliability has dropped to 0.975 for large (>2,500 kg) satellites. It is assumed that the maintenance of the MEV increases the reliability again with a factor of 0.8, given the assumption of a maintainability efficiency of 80%. After another 1.5 years, the reliability will again decrease with a factor of 0.975. Continuing this iteration, the MEV will have a reliability of 0.965 in 10 years.

 $^{^{1} \}texttt{https://www.space.com/12376-nasa-space-shuttle-program-facts-statistics.html} (Last accessed 14-06-2018) \\ \texttt{accessed 14-06-2018}) \\ \texttt{acce$

²https://www.space.com/31732-space-shuttle-challenger-disaster-explained-infographic.html(Last accessed 14-06-2018)

 $^{^3 \}texttt{https://www.space.com/19436-columbia-disaster.html} (Last accessed \ 18-06-2018)$

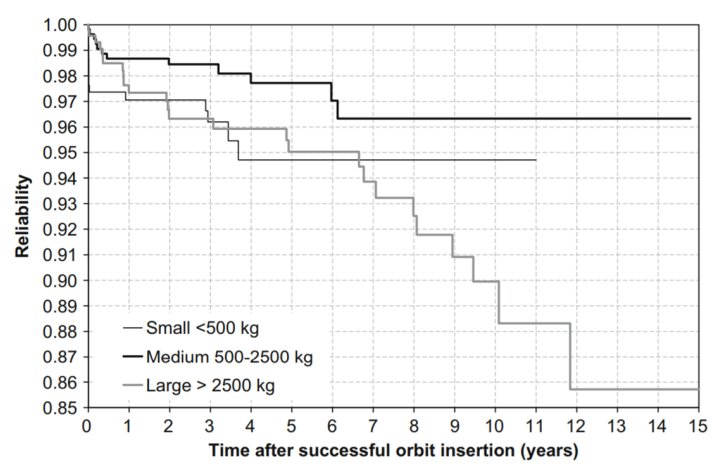


Figure 6.6: Representation of the degradation of reliability over the lifespan of the satellite [77].

The total reliability after 10 years is found to be the multiplication of the landing and ascent reliability times the LMO loiter phase reliability. This results in a reliability after 10 years of 0.9579 for the overall MEV. The reliability of the manned phase is equal to 0.9926.

6.3.2. Availability

As stated in section 4.2, the cost of the system depends highly on the reusability of the system. In order for the system to be the most cost effective, ensuring easier investment as stated in section 3.6, the uptime should be as high as possible. Several design choices have been made to increase this uptime, both for cost effectiveness and safety purposes. The MEV mission profile can be found in Figure 3.1. The availability of the MEV is taken from the point where the MEV is placed in LMO. After solar panel deployment, the batteries of the MEV will slowly recharge. During nominal manned operations, this will take 1.5 years since this is the time between two manned missions. This ensures that the MEV is available at the moment that the ITV with crew arrives at Mars. One MEV can house a crew of up to 10 people. Given that the ITV can house up to 22 people, as described in subsection 3.3.1, there are multiple possibilities to ensure the uptime of the MEV. The first option is to use multiple MEVs such that crew can immediately be transferred to Mars surface. The second option is to recharge the batteries and refill the fuel tanks of a single MEV while docked with the ITV. Although this would increase downtime and therefore overall mission time, the initial investment can be lowered. From the power generation of the ITV in the Midterm Report, it can be calculated that it takes up to 14 hours to recharge the MEV batteries, taking into account eclipse durations and a 90% transfer efficiency. This can be considered insignificant downtime with respect to the overall mission duration of approximately 600 days. For the cargo missions, multiple Mars landings and launches are required. This means that the MEV-Cs do not have 1.5 years to recharge, resulting in recharges on the ITV. The batteries of the MEV are designed to work for three days after landing, meaning that the MEV will be available directly in case non-nominal behaviour of the habitat is observed. Finally, in case of ISRU on the Martian surface, the process of refuelling the MEV at the ITV can be disregarded.

6.3.3. Maintainability

Two types of maintainability can be observed when looking at the mission profile: preventive- and corrective maintenance. Preventive maintenance is comparable with scheduled service in a car or on an aircraft, where after a specific number of kilometres/cycles/flights, the system is given a full check to ensure the quality of the system. Corrective maintenance is more focused on the unexpected events that might occur during the mission. These include random failure that require maintenance outside the scheduled maintenance activities. A breakdown structure of this maintenance is shown in Figure 6.7.

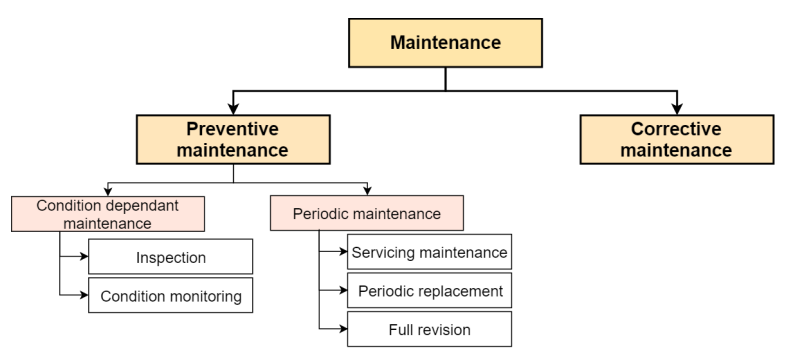


Figure 6.7: Maintainability breakdown diagram [78].

Preventive maintenance is to be carried out at different rates when looking at different subsystems. They have been described below. As can be seen, two groups have been shown: subsystems which are assumed to need maintenance after every flight, and subsystems that require extensive checking but are not expected to need maintenance every flight.

• Frequent maintenance:

- Heat shields: Have to be maintained after every trip to the Mars surface. Parts are included in the ITV cargo to perform this maintenance. An Extra Vehicular Activity (EVA) is required to perform this repair.
- Air brakes: Air brakes need to be checked to make sure they are still fully deployable, because a failure would mean a loss in drag. They also have to be repaired after every trip through the Martian Atmosphere like the heat shields.

• Infrequent maintenance:

- Landing legs: Confirm that all legs are at correct displacement. Inspect weak points (joints, landing feet) for damage. Check that the latches work.
- Airlock: Inspect functionality and accuracy of sensors, inspect propellant lines for cracks and wear, and inspect the closing off of the hatches for leaks;
- Engines/Thrusters: Visual inspection for cracks and signs of wear on Mars surface. Make sure that the gimbal still functions by testing. Visual check to ensure no residue is clogging the nozzle throat;
- Propellant/Environmental tanks: The tanks need to be inspected for cracks and strain, which can be
 done by visual inspection. The content of the tanks should also be checked, to see if it complies with the
 expected content to rule out any leaking or damage to the aluminium liner;
- Power system: The batteries and power control system contain an internal monitoring system. Some parts of the electrical system, such as the breaker system, may be able to be replaced. The extension/retraction mechanism must be monitored carefully, due to the novelty of retractable and shielded solar arrays. Even though the solar panels are shielded on Mars, they should sometimes be checked for sand blocking the panels.
- Thermal system: The internal coolant loops must be monitored for leaks, any repairs may be done on the
 Mars surface on in orbit. The external radiator must be inspected for any impacts, which can be done by
 visual inspection. The extension/retraction mechanism must be monitored carefully, due to the novelty
 of retractable and shielded radiators.
- Skin: Has to be inspected for cracks and signs of wear, which can be done by visual inspection on Mars.

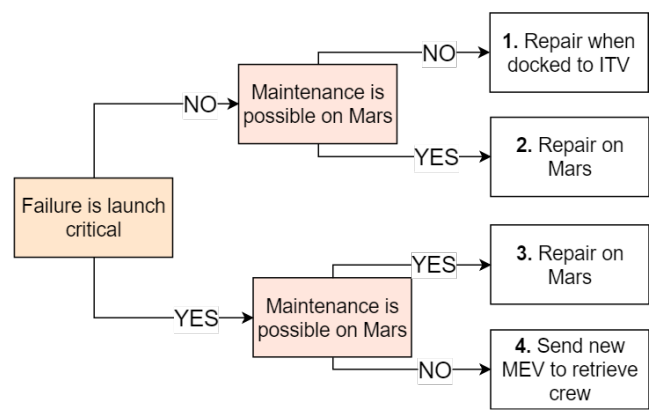


Figure 6.8: Maintainability flow diagram.

Corrective maintenance can be either carried out on Mars or on the ITV. A list of failures (one engine out, damage to sensors etc.) will be made and divided into four categories, which determine the severity and therefore the steps taken when this failure occurs. The first category consists of failures which are not critical for launch, and are therefore not required to be addressed until the MEV is docked with the ITV again, such as damage to an air brake. However, as an EVA in space is more dangerous than an EVA on Mars, an evaluation is done on the accessibility on Mars. If the failure can be repaired on Mars, this is preferred, such as small damage to a landing leg. This is the second category. The third category consists of failures which are critical for launch, and can therefore not wait until arriving back at the ITV. For these failures, it is assessed whether it is possible to repair them on Mars with the available materials and tools. If this is the case, this is preferred, such as a leaking valve or a damaged power line. If this is not the case, the fourth category comes in place, which requires a second MEV to be sent to the Martian surface to retrieve the crew, such as a major crack in the skin. This is illustrated in Figure 6.8.

6.3.4. Safety

To determine all the safety characteristics, all possible failures of the system were listed in Table 6.2. The identifiers of the functions correspond to those described earlier in the functional flow diagram in subsection 3.4.1. It must be noted that the overall strategy for MEV-related contingencies relies on the fact that one ITV can take two MEVs to Mars, which will be done prior to the first manned mission. This means that there are always two MEVs availble in Mars Orbit, even during the first manned mission. Each MEV has multiple redundancies built-in, but in case the used MEV becomes entirely unusable, the second MEV will allow safe recovery of the crew.

Table 6.2: Safety critical functions and redundancy.

Id.	Safety Critical Function	Failure	Implemented Redundancy
2.2/3/4	Perform supply transfer	Reaction between different propellants	Perform separate fuel, oxidiser and
			power transfers
2.5/6.1	Wait for landing window	Missed landing window	Wait for next landing window
2.6	Perform payload transfer	Airlock failure	Ensure reliable system + more system
			checks to check for safe lock
3.6	Close docking cover	Cover not closed properly	Re-dock to the ITV and repair
4.1	Check for sufficient propellant	Not enough propellant	Switch to other ITV
6.2/6	Perform landing burns	Engine failure	Add throttle on remaining engines
6.4	Perform air brake	Air brake does not deploy	Burn more propellant to counter lower
			drag force
6.5	Deploy landing leg	Landing leg does not extend	6 landing legs included
7.3	Enter surface configuration	Landing leg collapses	6 landing legs included
7.3	Enter surface configuration	Tip over of MEV	6 landing legs included
5.2/8.1	Power on MEV	Power outage	Perform EVA or switch to other MEV
5.3	Perform system check (start-up)	Failed start-up	Switch to other MEV
8.7	Wait for launch window	Missed launch window	Wait for next launch window
9.2	Fire engines	Engine failure	Add throttle on remaining engines
9.5	Maintain course	Flight computer failure	Manual take over, assistant guidance from ITV

For manned flight, safety is the most critical aspect. Therefore, a lot of measures are taken to increase the safety of the

MEV. In order to ensure safety of the crew, redundancies are added, such as two X-band antennas and more engines than necessary. Also, an anomalies strategy is obtained where a handbook is adopted with a number of anomalies mentioned. For all these anomalies, a protocol is made, and when an anomaly is not mentioned in the handbook, the system is to be shut down and the anomaly is to be communicated to Earth, in order to find a solution.

6.4. Compliance Matrix

After the Baseline Report, the list of requirements was updated in order to only account for those which met the VALID (Verifiable, Achievable, Logical, Integral and Definitive) criteria. This updated list can be found in Appendix A.

Tables 6.3 to 6.8 provide the compliance matrix of the design requirements. The full requirements list from Appendix A, which includes the requirements on the entire mission profile from Earth's surface to Mars and back again, was assessed. However, as the design of EEV and ITV was beyond the scope of the report, the compliance of requirements related to them was deemed inconclusive. As such the compliance matrix below is focused on the requirements on the MEV, which was the focus of this report. The first column lists the requirement identifier code, the second column the requirement itself, the third lists met/not met, and the fourth and final column provides an explanation as to how the requirement was or was not met. In the Met? column, three symbols are used. ✓ implies the requirement was met, ✗ implies the requirement was not met, and ♣ implies that the depth of design work done so far is insufficient to determine whether or not this criteria has yet been met or not. To conclude a ♣, further analysis is required.

Table 6.3: Compliance Matrix of Technical Requirements.

ID	Requirement	Met?	Explanation
TEC-02	The ITV shall be able to transport a payload from LEO to LMO.	*	Sub-requirements TEC-02.1 and TEC-02.1 need more in-depth analysis.
TEC-02.1	The system shall be able to withstand interplanetary space environment.		TEC-02.1.6 requires more indepth analysis, before this requirement can be concluded.
TEC-02.1.4	The MEV shall withstand sustained dynamic pressure of 50 MPa.	X / √	This number was not predicted accurately. An actual maximum dynamic pressure of 23 kPa was found in section 5.3, which the MEV is capable of withstanding.
TEC-02.1.5	The MEV shall be rated to external temperatures within a range of 150 - 385 K, as shown in section 5.7.	✓	The thermal system will be able to sustain internal temperatures at an even wider temperature range.
TEC-02.1.6	The MEV shall be rated to a sustained radiation dose of 10.2 mrad/hr.	*	The ratings of individual components must be known, therefore further testing during the detailed design stage is required.
TEC-02.2	The ITV shall be able to control its attitude.		As it is not yet know if there is sufficient ΔV , this cannot yet be concluded.
TEC-02.2.1	The system shall be able to determine the ITV's attitude with an accuracy of at most 15 nanoradians.	*	During the detailed design phase, the accuracy of the ADCS system of the ITV must be analysed for this to be concluded.
TEC-02.2.2	The ITV shall have at least 50 m/s ΔV for attitude adjustments.	*	Only the ΔV for the transfer was determined, as the ΔV for attitude adjustments can only be determined when the accurate characteristics of the ITV are known.
TEC-02.3	The ITV shall be able to control its position.	- J -	As shown below, the ITV has sufficient ΔV and position determination accuracy to achieve this.
TEC-02.3.1	The ITV shall be able to determine its position with an accuracy of at most 1 m. $ \\$	1	This accuracy can be achieved by integration of NASA's Deep-Space Positioning System.

TEC-02.3.2	The ITV shall be able to determine its orbit within 1 m accuracy.	✓	This accuracy can be achieved by integration of NASA's Deep-Space
TEC-02.3.3	The ITV shall have at least 5.4 km/s ΔV for interplanetary transfer to Mars.	1	Positioning System. ITV is able to transfer with ΔV of 5.7-5.9 km/s with Hohmann trajectory and 6.5 km/s with gravity
TEC-02.3.4	The ITV shall have re-ignitable propulsion.	✓	assist trajectory. Nuclear thermal rockets are inher- ently re-ignitable.
TEC-02.4	The MEV shall be able to rendezvous with the ITV.	- y -	Sufficient ΔV is provided for manoeuvring, sensors are available and a docking port is present.
TEC-02.4.1	The MEV shall be able to control its attitude.	✓	Sufficient RCS thrusters (subsection 5.1.6).
TEC-02.4.1.1	The MEV shall be able to determine its attitude with an accuracy of at most 7 arcminutes.	✓	Accuracy achieved by integration of star sensors.
TEC-02.4.1.2	The MEV shall have at least 40 m/s ΔV for attitude adjustments.	✓	A sufficient amount of propellant is carried on board to account for attitude adjustments using the RCS thrusters.
TEC-02.4.2	The MEV shall be able to control its position.	✓	Sufficient engine power and position determination possibilities.
TEC-02.4.2.1	The MEV shall be able to determine its position with an accuracy of at most 1 cm.	✓	Accuracy achieved by the docking port visual system.
TEC-02.4.2.2	The MEV shall be able to determine its velocity with an accuracy of at most 1 cm/s.	✓	Accuracy achieved by the docking port visual system.
TEC-02.4.2.3	The MEV shall have at least 20 m/s ΔV for velocity adjustments.	1	A safety factor is added to the amount of ΔV needed to account for velocity adjustments.
TEC-02.4.2.4	The MEV shall have re-ignitable propulsion.	1	The liquid propellant engine with a spark torch igniter is re-ignitable (subsection 5.1.2).
TEC-02.5	The MEV shall be able to dock with the ITV.	- \sqrt -	Compatible docking ports (subsection 5.11.1).
TEC-02.5.1	The system shall allow docked transfer of payload from ITV to MEV.	✓	Capable of fitting through 0.8 m docking port passage.
TEC-02.5.2	The system shall allow docked transfer of propellant from ITV to MEV.	✓	Fuel and oxidiser lines connecting MEV and ITV whilst docked.
TEC-03	The MEV shall be able to transport a payload from LMO to Mars surface.	*	Designed for 5,000 kg payload (section 5.3), but can not be concluded until TEC-03.3 is met.
TEC-03.1	The MEV shall be able to de-orbit.		MEV is capable of precisely de- orbiting at least two times per day (see subsection 5.2.5.
TEC-03.2	The MEV shall be able to re-enter Mars atmosphere.	- J -	The decent trajectory described in subsection 5.2.5 shows re-entry in the mars atmosphere is possible by an injection burn and re-entry using main engines and air brakes.
TEC-03.3	The MEV shall be able to land on Mars.		Capable of withstanding landing loads, but is not know yet if with sufficient accuracy.
TEC-03.3.1	The MEV shall be able to land within 10 m accuracy.	*	Further closed-loop simulations to be done. Currently 600 m accuracy is achieved but model needs optimisation which may increase the accuracy to less than 3 m.

TEC-03.4	The MEV shall have 120 m/s ΔV for travel from Mars orbit to Mars surface.	XI√	The requirement was improperly defined, it is unrealistic to meet exactly 120 m/s and the number should be higher even with aerobraking. The total ΔV required for powered landing is in within 3.8-4.1 km/s. The MEV uses aerobraking and achieves landing (including de-orbit burn) with 965 m/s. Requirement is in principle met but improperly stated during requirement generation phase.
TEC-03.5	The MEV shall allow payload disembarkment without external infrastructure.		On board crane (see subsection 5.11.2).
TEC-03.6	The MEV shall be capable of landing with a nominal velocity of 2 m/s		MEV is capable of landing with a nominal velocity of 1.8 m/s (see subsection 5.2.5.
TEC-04	The system shall be able to transport a payload within an appropriate environment.	*	The system is capable of providing the required environment, but testing is required to shown there is no damage before this can be concluded.
TEC-04.1	The system shall transport the cargo without damage.	*	Meets sub-requirements for damage, however cannot be finalised as an actual mission would have to be performed in order to fully verify this requirement.
TEC-04.1.1	The system shall retain cargo within a temperature range which does not degrade the cargo.	✓	Both the crewed and cargo segment are kept at 293 K by the thermal system.
TEC-04.1.2	The system shall retain cargo within an atmosphere which does not degrade the cargo.	✓	The life support system supports the cargo environment as given in section 5.4.
TEC-04.1.2.1	The system shall retain cargo within an atmospheric composition which does not degrade the cargo.	✓	The life support system supports the cargo environment as given in section 5.4.
TEC-04.1.2.2	The system shall retain cargo within a pressure range which does not degrade the cargo.	✓	The crew and cargo compartment are pressurised to 101,300 Pa (pressure at Earth sea level) see section 5.3.
TEC-04.1.3	The system shall not subject the cargo to accelerations which may damage the cargo.	✓	58.86 m/s ² is the highest acceleration experience during Earth launch. During standard operations 27.5 m/s ² is the highest acceleration experienced.
TEC-04.1.4	The system shall ensure the cargo is not subjected to radiation levels which may degrade the cargo.	✓	Radiation dose inside the is 0.121 mSv for at most three days, which is sufficiently low for high tolerance cargo such as habitat materials. More sensitive cargo should be shielded individually.
TEC-04.2	The system shall transport crew comfortably (note: this implies safely)	* - * -	TEC-04.2.5 and TEC-04.2.5 are mainly focused upon the requirements for the ITV habitats, which were beyond the scope of the design work within this report. As such, either a detailed design must be performed on new habitats, or a analysis of the one selected in subsection 3.3.1 to ensure they are met.

TEC-04.2.1	The system shall retain crew within a comfortable temperature range as defined by Johnson [79].	✓	Both the crewed and cargo segment are kept at 293 K by the ther-
TEC-04.2.2	The system shall retain crew within a comfortable atmosphere.	✓	mal system. The life support system supports the crew compartment as given in section 5.4.
TEC-04.2.2.1	The system shall retain crew within a comfortable atmospheric composition as defined by Belles [80].	✓	The life support system supports the crew compartment as given in section 5.4.
TEC-04.2.2.2	The system shall retain crew within an atmosphere with an oxygen level within a comfortable range as defined by [80].	✓	The life support system supports the crew compartment as given in section 5.4.
TEC-04.2.2.3	The system shall retain crew within a comfortable pressure range as defined by Belles [80].	✓	The crew and cargo compartment are pressurised to 101,300 Pa (pressure at Earth sea level) see section 5.3.
TEC-04.2.3	The system shall not subject crew to acceleration levels above human tolerance.	✓	58.86 m/s ² is the highest acceleration experience during Earth launch. During standard operations 27.5 m/s ² is the highest acceleration experienced ⁴ .
TEC-04.2.3.1	The system shall not subject crew to sustained acceleration above human comfort levels as defined by Kumar and Norfleet [81].	✓	Maximum acceleration at Mars is 27.5 m/s^2 , at Earth the launch acceleration can be reduced to 40 m/s^2 .
TEC-04.2.3.2	The system shall not subject crew to instantaneous acceleration above human safety levels as defined by [81].	✓	Maximum acceleration at Mars is 27.5 m/s^2 , at Earth the launch acceleration can be reduced to 40 m/s^2 .
TEC-04.2.4	The system shall ensure crew is not subjected to radiation above human health levels.	✓	In a worst case scenario without shielding, crew is subjected to 0.03 mrad, out of a 0.5 mrad yearly recommendation for astronauts.
TEC-04.2.5	The system shall provide crew with comfortably sufficient consumables.	*	MEV capable of providing this. The ITV has been sized to carry the required consumable mass, but sufficient habitat analysis to be done to ensure they are incorporateable into the design.
TEC-04.2.5.1	The system shall be able to transport/regenerate sufficient potable water.	*	The MEV is designed to transport sufficient consumables, but further design is needed to ensure there is either sufficient water tanks and recycling on both vehicles.
TEC-04.2.5.2	The system shall be able to transport/regenerate sufficient food.	*	MEV designed to transport food for 3 days, but further analysis is required into the ITV detailed de- sign to ensure this is met.
TEC-04.2.5.3	The system shall be able to transport/regenerate sufficient oxygen.	*	MEV has sufficient tank space, but further design needed to ensure ITV also does.
TEC-04.2.5.4	The system shall be able to transport sufficient hygienic material.	*	Not applicable to MEV design, but a more in depth ITV design re- quired for this.
TEC-04.2.5.5	The system shall be able to transport sufficient clothing.	*	Not applicable to MEV design, but a more in depth ITV design required for this.

 $[\]overline{^{4} \text{http://www.gforces.net/insight-human-tolerance-vertical-axis.html} (Last accessed 21-06-2018)$

TEC-04.2.5.6	The system shall be able to transport sufficient cleaning materials.	*	Not applicable to MEV design, but a more in depth ITV design is re-
TEC-04.2.6	The system shall retain crew within an environment which does not deteriorate psychological health.	*	quired. Not applicable to MEV design, a more in depth ITV design is required. This analysis should include manned trials of the environment on Earth under the supervision of a physiologist.
TEC-04.2.6.1	The system shall provide crew with a personal volume which does not deteriorate psychological health.	✓	The ITV is sized such that it has a habitat with sufficient volume (subsection 3.3.1).
TEC-04.2.6.2	The ITV shall provide crew with entertainment which is sufficient to not deteriorate psychological health.	*	More in-depth analysis of the ITV needed, probably with the input of physiologists and not just aerospace engineers.
TEC-04.2.6.3	Each vehicle shall be able to communicate with Earth Surface.	1	The MEV will be in contact with the ITV or a Mars relay satellite, which will be in contact with Earth.
TEC-04.2.6.4	Each vehicle shall be able to perform bidirectional communication.	1	Link budgets were produced for both up- and downlinks, mean- ing they can perform bidirectional communication.
TEC-04.2.6.5	Each vehicle shall be able to continuously communicate.	✓	The position of the planets and Sun might block the view of Earth with respect to Mars, meaning no communication is possible between the two planets at times. Vehicles are still able to communicate with each other, just not with Earth.
TEC-04.2.6.6	The communication network shall have a bitrate at least sufficient for real-time 1080p30 video transmission.	/	The ITV is capable of sending bitrates of 4.82 Mbps which is sufficient to send real-time 1080p30. The MEV is designed for 720p, but is less heavily dependent on this requirement since it is only used for maximum of three days at a time.
TEC-05	The MEV shall be able to transport a payload from Mars Surface to LMO.	1	Can bring a crew of ten and a cargo of 4,000 kg to 200 km orbit around Mars.
TEC-05.1	The MEV shall allow payload embarkment without external infrastructure.		On board crane which is capable of lowering both crew and cargo bags (subsection 5.11.2).
TEC-05.2	The MEV shall be have at least 4.1 km/s ΔV for launch to LMO.	- y -	Requirement is met but wrongly stated during requirement generation phase (poor requirement definition). The correct should be: "The MEV shall be able to reach LMO with no more than 4.1 km/s ΔV". Total ΔV including insertion burn is 3.95 km/s.
TEC-05.3	The system shall allow docked transfer of payload from the MEV to the ITV.	- , -	A docking port has been designed and the rendezvous of the MEV with the ITV has been determined in subsection 5.2.6.
TEC-06	The ITV shall be able to transport a payload from LMO to LEO.	✓ 	Designed to bring a crew of 10 from LEO to LMO.

TEC-06.1	The ITV shall have ΔV for interplanetary transfer to Earth.	✓	ITV is capable of returning back to
			Earth with a ΔV of 5.9 km/s (sub-
			section 5.2.1).

Table 6.4: Compliance Matrix of General Requirements.

ID	Requirement	Met?	Explanation
GEN-01	All components shall be manufactured on Earth.	✓	The production plan clearly that it is possible to manufacture everything on earth and then transfer it to where it is needed (section 7.3).
GEN-02	All components shall be assembled on Earth [This does not exclude in orbit rendezvous of mission segments].	√	See production plan (section 7.3). It allows for the ITV to be rendezvoused in-orbit.
GEN-03	The system shall not rely on in-situ propellant production during the initial set-up period, 2030-2035.	✓	Sufficient propellant taken with ITV, but MEV propellant chosen for ISRU compatibility.
GEN-04	The first launch of the programme shall be scheduled in 2030.	Х	Due to the transfer windows which are available, the first cargo launch will be in 2028 while the first crewed launch will be in 2033 (section 7.2).
GEN-05	The launch cost per kg to Mars shall not exceed 10,000 USD.	Х	The launch cost per kg is 12,500 USD, taking into account only recurring costs.
GEN-05.1	The launch cost per kg to LEO shall not exceed 1500 USD.	- √ -	1,411 USD/kg for Falcon Heavy Launch ⁵ (section 4.2).
GEN-06	The duration of each mission on Mars surface shall be no shorter than one month, from landing to take-off for returning to Earth.	*	Technically possible, however dependent on external features such as the available transfer windows back to Earth and the capabilities of the surface habitats.
GEN-06.1	The MEV shall be able to remain on the Mars surface for at least one month per mission without loss of functionality.	*	Dependent upon the ability of the habitat to provide it with sufficient power to keep the propellant cryogenic.
GEN-07	The system shall be able to transport a habitat from Earth to Mars.	*	The MEV is designed to transport cargo without crew so could deploy a habitat, but it is dependant upon the size of the habitat, which has yet to be designed.
GEN-07.1	The system shall be able to transport a habitat which can sustain a crew of at least 10 members.	*	The capabilities of the habitat are beyond the scope of this report, and will need further analysis.
GEN-07.2	The system shall be able to transport a habitat which can sustain a crew no shorter than one month.	*	The capabilities of the habitat are beyond the scope of this report, and will need further analysis.

Table 6.5: Compliance Matrix of Regulatory Requirements.

ID	Requirement	Met?	Explanation
REG-01	Ground operations shall adhere to local laws.	*	Too dependant on location of
			ground station and location of
			manufacturing etc., so will be es-
			tablished at a later date.

 $[\]overline{^{5} \texttt{http://www.spacex.com/about/capabilities}} (Last \ accessed \ 01-07-2018)$

REG-02	The system shall adhere to international laws.	*	A proper analysis of the laws is beyond the capabilities of the aerospace engineers, so lawyers should be hired to ensure the laws are adhered to.
REG-03	The system shall comply with the UN Treaty on Outer Space [82].	✓	No intention of placing weapons of mass destruction in space and shall only be used for peaceful purposes.
REG-04	The system shall comply with the COSPAR Planetary Protection Policy ⁶ .	1	Interplanetary contamination has been included in the sustainability approach.
REG-05	The system shall comply with Inter-Agency Space Debris Coordination Committee regulations.	1	As the system is fully reusable, it does not produce any space debris.
REG-06	The habitats shall obey the OSHA and NASA Risk Management and Health Standards [83].	*	Habitats were not yet designed sufficiently in depth to determine this.
REG-07	The system shall comply with NASA Human Rating Certification [1].	*	The ITV and MEV are planned to be refueled with humans on board, which is against current regulation and thus will probably need renegotiation.

Table 6.6: Compliance Matrix of System and Performance Requirements.

ID	Requirement	Met?	Explanation
PRF-01	The design shall be entirely based on technologies and materials	✓	All technologies and materials
	fully available at the current day.		have a TRL of at least 6, which is
			considered as fully available.
PRF-01.1	The system shall only use technology with a NASA technology	- - -	All technology considered has a
	readiness level of at least 6.		TRL of at least 6.
PRF-01.2	The system shall only use materials with a NASA technology		Section 7.3 gives materials for the
	readiness level of at least 6.		main components of the MEV, all
			of which have a sufficient TRL.
PRF-01.3	The system shall only require production methods with a NASA	-	Section 7.3 gives all production
	technology readiness level of at least 6.		methods for the main compo-
			nents of the MEV, all of which have
			a sufficient TRL.
PRF-02	A crew of at least 10 people shall be present on each travel of the	✓	ITV equipped with habitats capa-
	reusable spaceship to Mars.		ble of sustaining up to 12 people
			(subsection 3.3.1.
PRF-03	A crew of at least 10 members shall be present on each travel of	✓	ITV equipped with habitats capa-
	the reusable spaceship to Earth.		ble of sustaining up to 12 people
			(subsection 3.3.1.
PRF-04	The launcher shall be able to bring a payload to a 400 km circular	1	The Falcon Heavy is capable of
	orbit.		launching both EEVs carrying
			crew or cargo and MEVs.

 $Table\ 6.7: Compliance\ Matrix\ of\ Requirements\ on\ Safety,\ Reliability,\ and\ Sustainability.$

ID	Requirement	Met?	Explanation
RMS-03	The MEV shall be reusable for at least 100 Mars launches.	*	This requires more in-depth anal-
			ysis. This number was considered
			for the entirety of the design (e.g.
			fatigue), but estimates will have to
			be made from prototyping.

⁶https://cosparhq.cnes.fr(Last accessed 08-05-2018)

RMS-03.1	The MEV shall facilitate inspection.	*	Further design and analysis is needed to ensure that at least the most critical components of the MEV shall be easily accessible for inspection on Mars.
RMS-03.2	The MEV shall facilitate maintenance.		Planned maintenance both in orbit and on surface (subsection 6.3.3).
RMS-03.3	The MEV shall facilitate refurbishment.		More design and anlysis to ensure components can easily be replaced on Mars, and that sufficient components are available for is.
RMS-05	The manned spaceship used by the programme shall be fully reusable for a minimum of 10 Earth-Mars return trips.	*	More in-depth analysis needed on the ITV.
RMS-06	The system shall only employ non-hazardous materials and propellants.	✓	All material used for design, production and maintenance are non-hazardous for nominal operation.
RMS-07	The systems shall only employ non-toxic materials and propellants.	√	The propellants and materials used do not produce any toxic byproducts that would cause acute exposure in nominal use, however any material or substance used in large enough amounts could induce toxicity.

Table 6.8: Compliance Matrix of Power Requirements.

ID	Requirement	Met?	Explanation
PWR-01	The ITV shall be able to supply a nominal power of at least 27.53	✓	The MEV is designed with 704 m ²
	kW.		solar panels and a set of batter-
			ies in order to supply the 27.53 kW
			power production (section 3.2).
PWR-02	The MEV shall be able to supply a nominal power of at least 2,483	X/ √	The requirement was lowered to
	W when manned for at least seven days.		three days, due to a better land-
			ing/launch trajectory, so batter-
			ies have been sized for only three
			days.
PWR-03	The MEV shall be able to supply a nominal power of at least 341	✓	Two deployable solar panels and a
	W when uncrewed.		battery ensure the MEV is powered
			when in standby mode around
			LMO.

As can be seen from the tables above, additional analysis and design must be done before the requirements can be specified as met/not met. Some of the requirements are also too specific on the cargo being carried, so it can also not yet be stated whether of not these requirements are met.

Only two of the requirements were not met, but neither of these will be that detrimental to the project. The first, **GEN-04**, was not met, as the first launch does not occur in 2030. However, as the first cargo launch actually occurs before this, the schedule is not delayed, but may be a little rushed. The other requirement not met is **GEN-05**, which looks at the cost per kg to Mars. It was calculated to be 12,500 USD/kg which is higher than the requirement of 10,000 USD/kg. This may cause issues with the stakeholders, and selling tickets, however it is believed that once the use of the ISRU is permitted, the reduced propellant needed for the transfer will decrease the cost to meet the requirement.

6.4.1. Driving and Killer Requirements

When the requirements were defined, a number of these requirements were defined to be killer and driving. Driving requirements were defined as those which are driving to the design. They were identified to be as follows:

- * TEC-03: The MEV shall be able to transport a payload from LMO to Mars surface;
- ✓ **TEC-05:** The MEV shall be able to transport a payload from Mars surface to LMO;

- ✓ **GEN-01:** All components shall be manufactured on Earth;
- ✓ **GEN-02:** All components shall be assembled on Earth [This does not exclude in orbit rendezvous of mission segments];
- ✓ **GEN-04:** The first launch of the programme shall be scheduled in 2030;
- ✓ PRF-01: The design shall be entirely based on technologies and materials fully available at the current day;
- ✓ PRF-02: A crew of at least 10 people shall be present on each travel of the reusable spaceship to Mars;
- ✓ PRF-03: A crew of at least 10 members shall be present on each travel of the reusable spaceship to Earth;
- * RMS-03: The MEV shall be reusable for at least 100 Mars launches;
- * RMS-05: The manned spaceship used by the program shall be fully reusable for a minimum of 10 Earth-Mars return trips;
- ✓ RMS-06: The system shall only employ non-hazardous materials and propellants;
- ✓ **RMS-07:** The systems shall only employ non-toxic materials and propellants.

As can be seen, all the driving requirements have either been met or need further in-depth analysis. The payload requirements were important as without them any transport system developed has no purpose, or not the intended purpose. Certain driving requirements are restrictions on the materials, production and scheduling of the system, which restricted the design in some aspects and thus drove the design.

The reusability requirements were important, as reducing the cost and improving the sustainability of the design were important requirements as well; the reusability could also impact the efficiency of the design, such as drop tanks. Lastly hazardous and toxic materials were restricted, which drove the design in many ways, but the most obvious was the RCS thrusters, as hydrazine was considered toxic, and thus GOX/GCH₄ was chosen. Overall these requirements have driven the design in significant ways, while others were just technical requirements with few significant cascading effects. The starred requirements are expected to be met, but the actual completion of these requirements can only be determined during the detailed design phase.

Killer requirements were considered to be those which may drive the project to an unacceptable extent, in the sense that if they are not met the project may no longer be possible. These were identified to be as follows:

- ✓ GEN-01: The system shall not rely on in-situ propellant production during the initial set-up period, 2030-2035;
- * **REG-07:** The system shall comply with NASA Human Rating Certification[1].

As was shown in the compliance matrix above, only **GEN-03** was met. **REG-07** was deemed to still need further analysis. This has two reasons. First, until all aspects of the mission have been designed in the detailed design stage, it cannot be clearly stated that the mission will meet the requirements. Second, NASA frowns upon the refuelling of vehicles whilst crewed. It is not entirely clear whether or not this is a direct requirement of the Human Rating Certification, but it is believed further negotiations will be needed before the requirement can be said to be met. As the mission cannot happen without complying with the Human Rating Certification, a more in-depth analysis has to be done to establish whether the mission is feasible. However, it is believed that with further analysis and negotiations, the Human Rating Certification requirement will be met.

Post-DSE Activities

The DSE only accounts for the preliminary design, however there are many steps to be taken from the preliminary design to the actual product. These steps are further elaborated on in this chapter.

7.1. Project Design and Development Logic

Figure 7.1 shows a flow diagram depicting the steps which must be completed in order for the project to be finished in accurate and timely manner. It contains logic commands G and \bar{G} , which represent the G0 and a No G0 situation respectively.

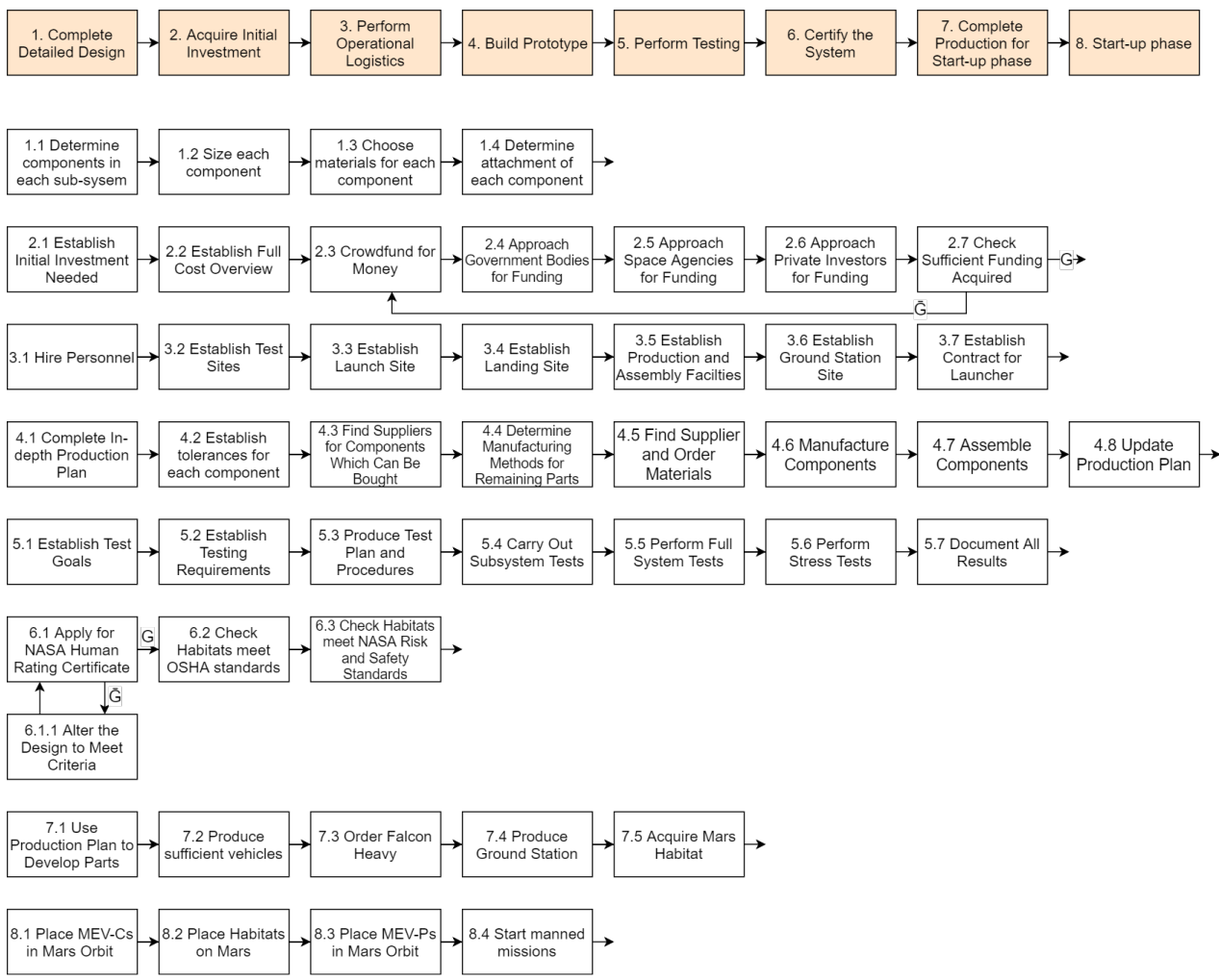


Figure 7.1: Project design and development logic flow diagram.

As this diagram does not fully account for activities which happen in parallel, a breakdown structure is also made for the project design and development logic. This is given in Figure 7.2 below. It provides more depth than the flow

7.2. Project Gantt Chart 126

diagram, and accounts for activities such as constant sourcing of funding, not just the gathering of a sufficient initial investment.

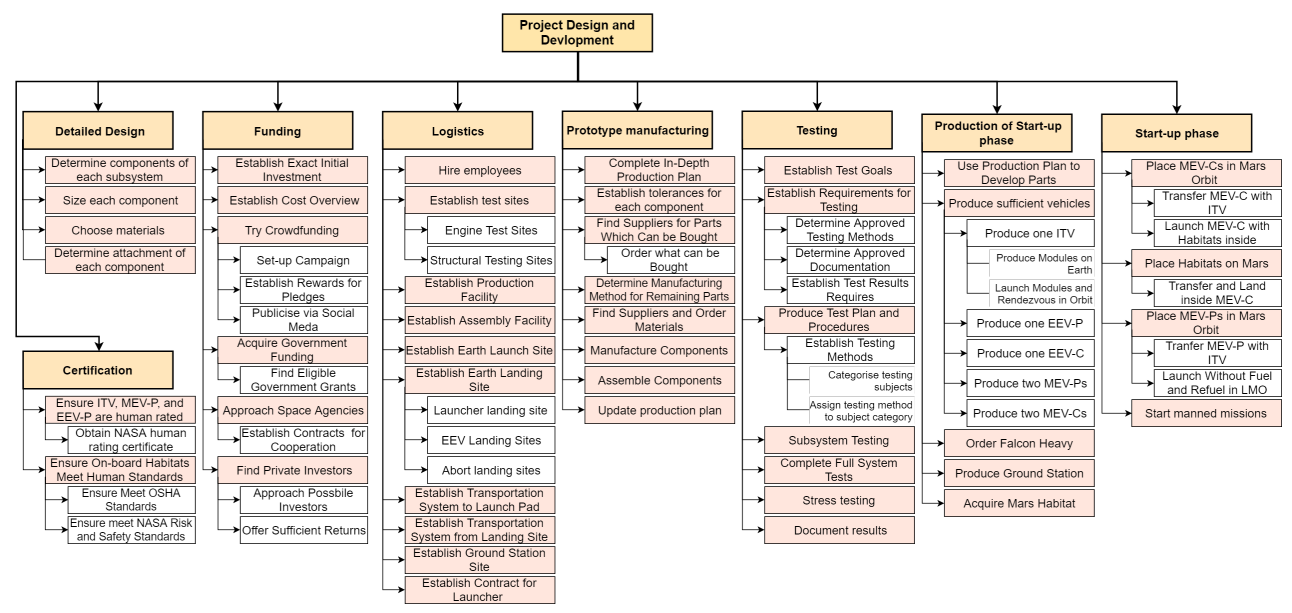


Figure 7.2: Project design and development logic breakdown structure.

7.2. Project Gantt Chart

A Gantt Chart is produced from the activities explained in section 7.1. It spans all the activities needed to finish Project Cardinal in time for the crewed launch window for the Hohmann Transfer to Mars. This time line can also been seen in Figure 3.11. Because the span of the project is very broad, time spans of certain activities may be very inaccurate the further away they are. Deadlines are indicated on the top of the Gantt Chart. They were used as a guideline to fill in the activities needed before the deadline. Figure 7.3 shows the first part of the post-DSE activities, while Figure 7.4 shows the second part.

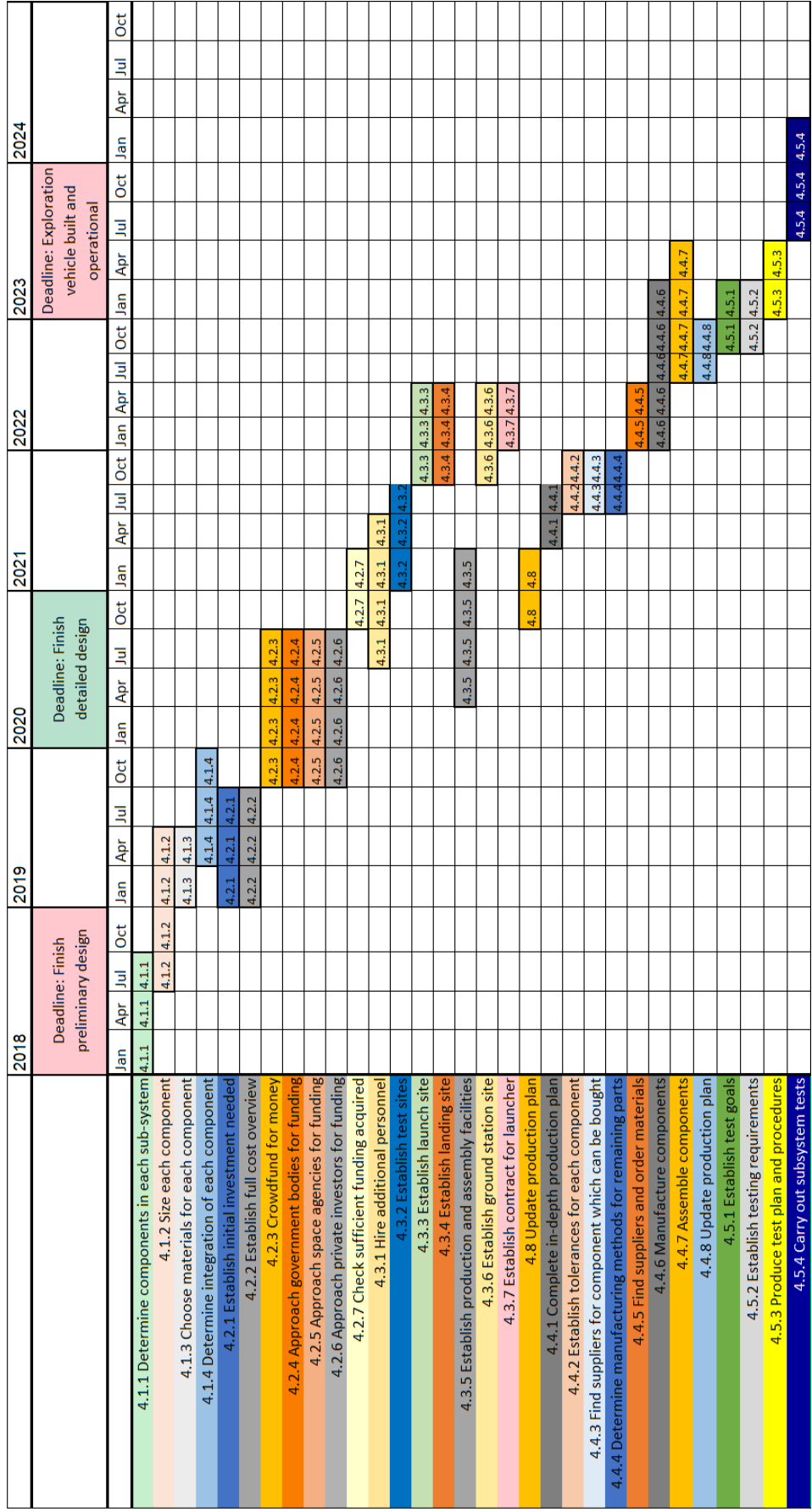


Figure 7.3: First project Gantt Chart.

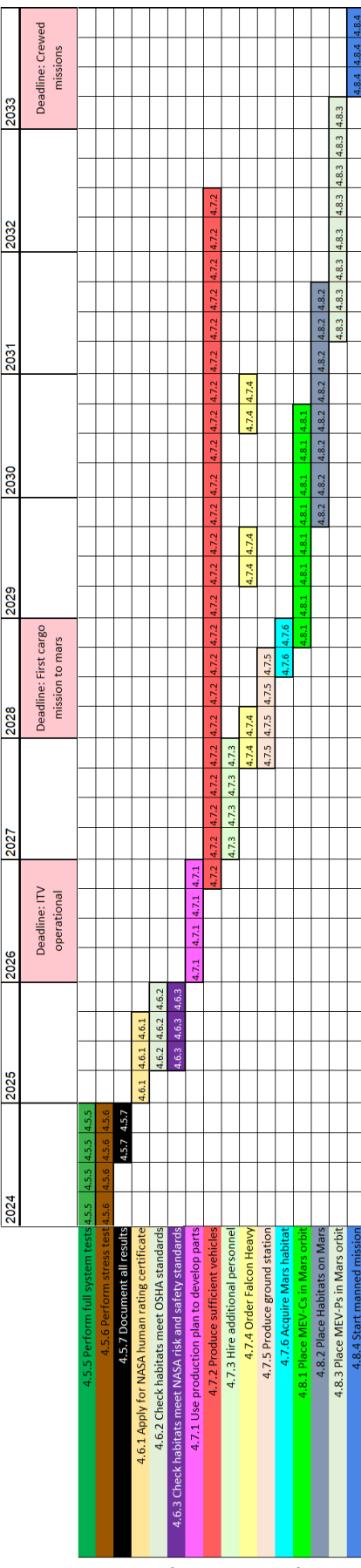


Figure 7.4: Second project Gantt Chart.

7.3. Production Plan

7.3. Production Plan

For the production plan, only the production of the first prototype of the MEV is considered. The subsystem are divided into their different parts and the materials are analysed, after which appropriate manufacturing methods are established. This has been shown in Figure 7.5, with the manufacturing methods in italics. Figure 7.6 represents this breakdown more graphically using the CAD models for the MEV.

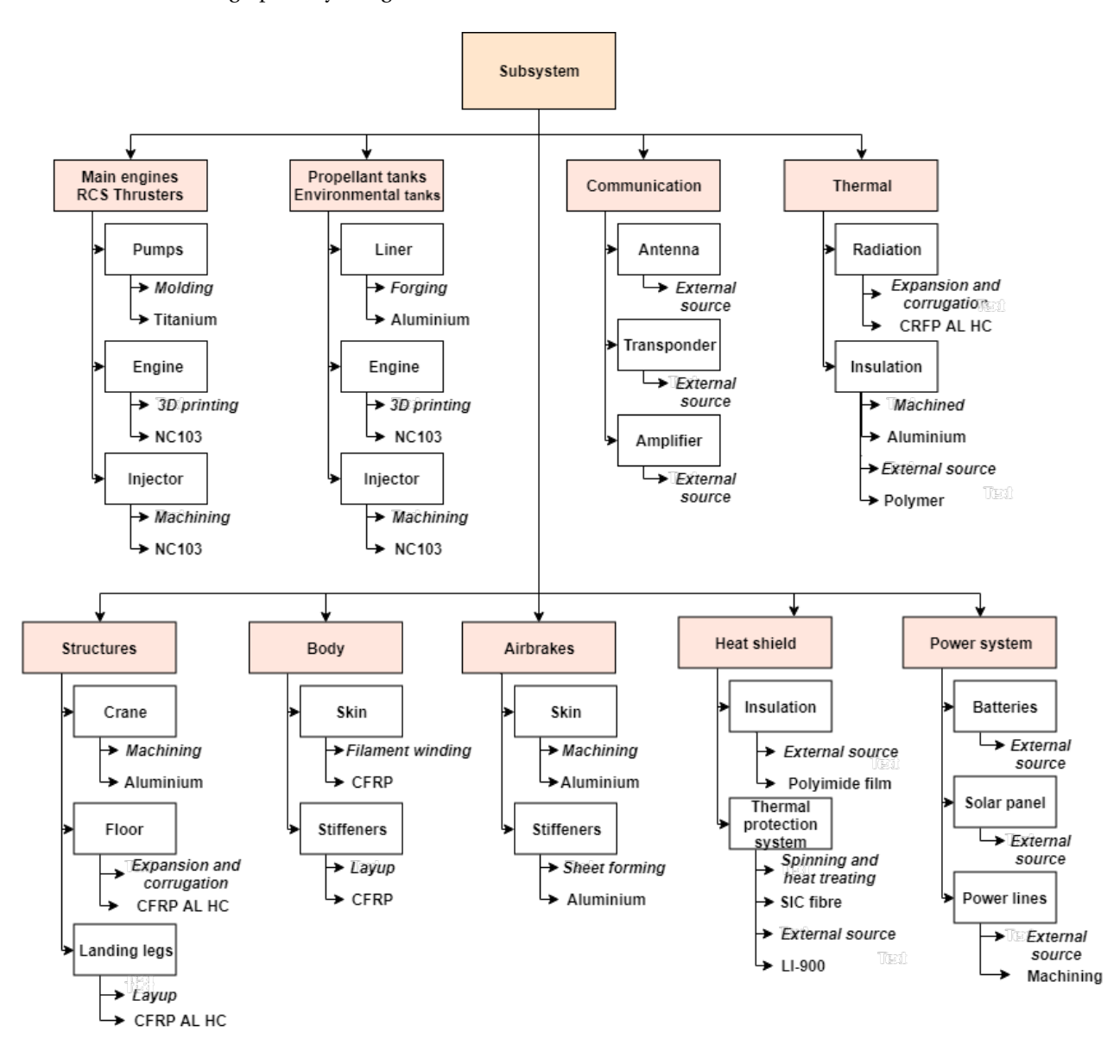


Figure 7.5: Production breakdown structure.

7.3. Production Plan

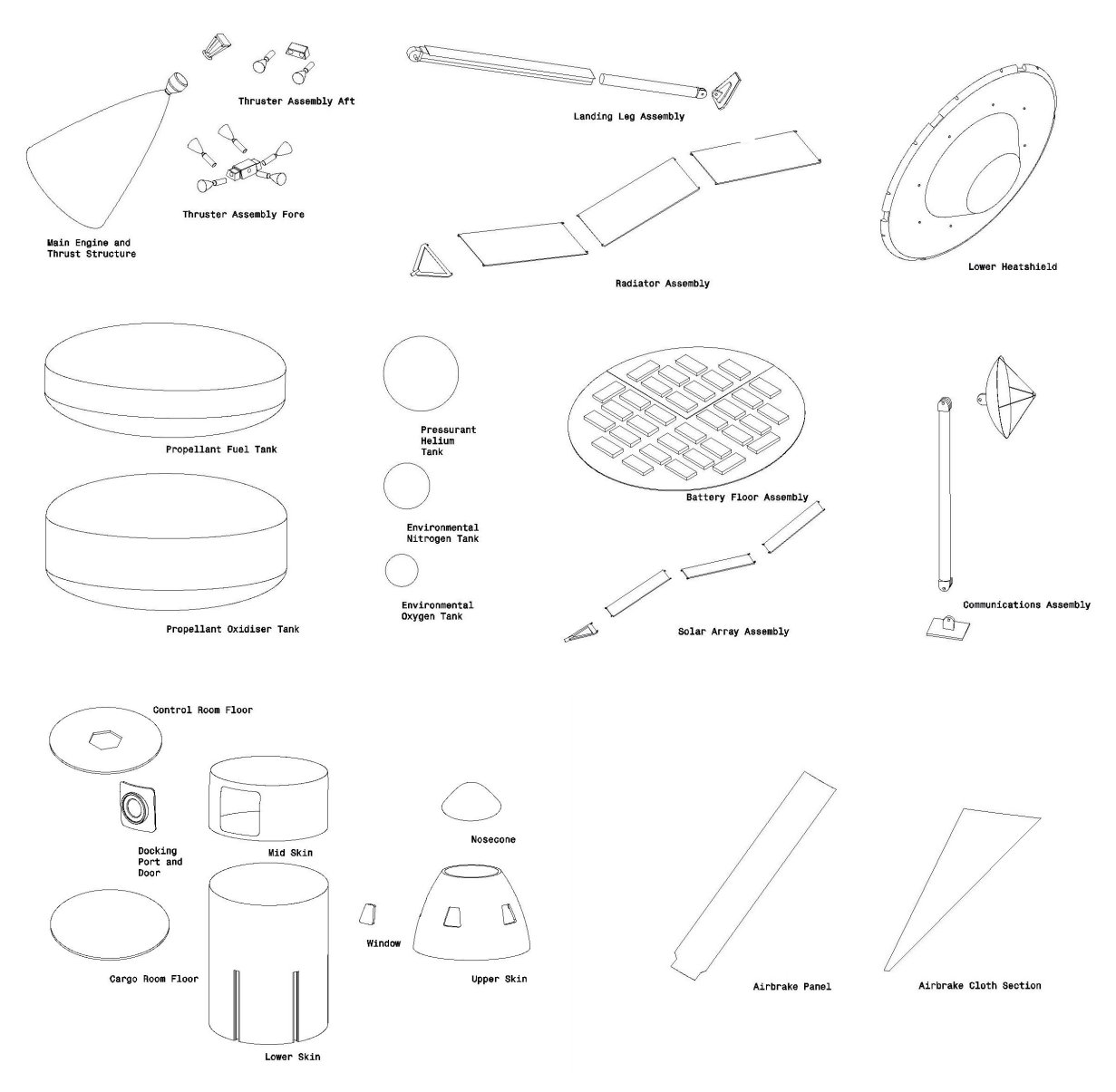


Figure 7.6: Breakdown of assemblies to be produced.

After this, the components are assembled into their respective subsystems, which are then mounted onto their respective floor. These floors are then integrated into the body, after which the last components are mounted to the body. This assembly process is shown in Figure 7.7. Figure 7.8 shows this final assembly process.

7.3. Production Plan

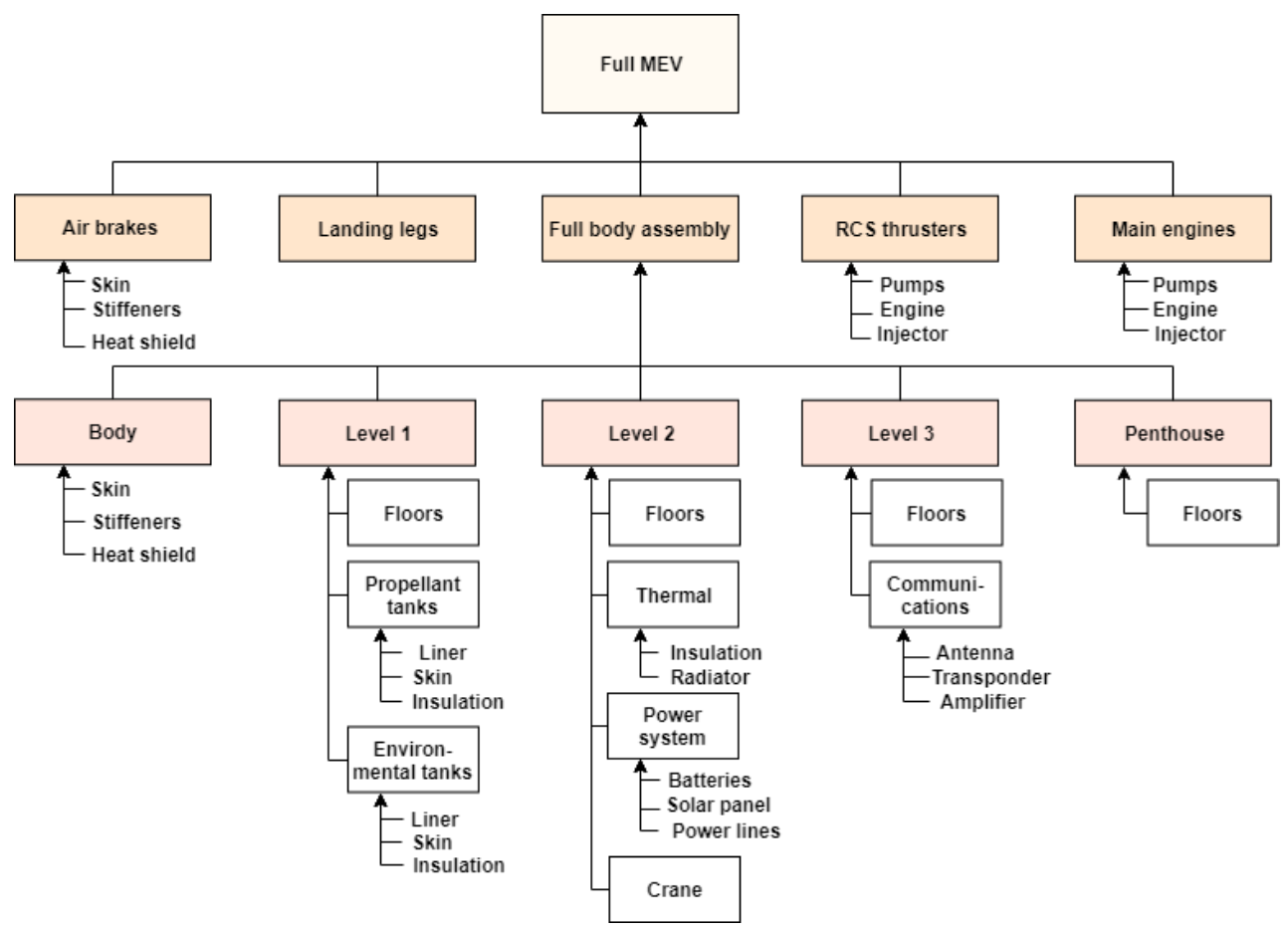
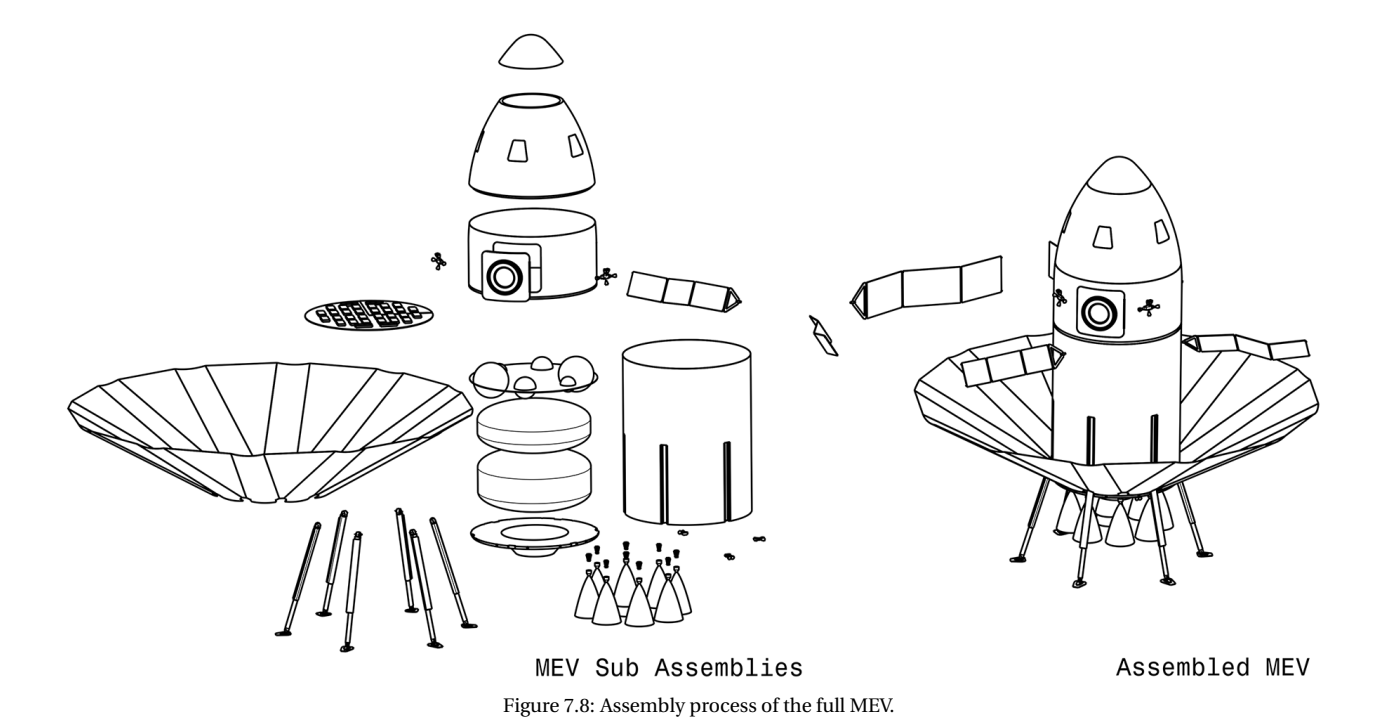


Figure 7.7: Schematic assembly of the MEV from its individual components.



Note that after the production of the prototype, this production plan is subject to change based on the difficulties experienced during the initial production.

7.4. Verification and Validation Procedures

Once the detail design of the MEV and other systems is initiated, a standardised Verification and Validation procedure has to be developed for the future. The design will go through a few phases: the design phase, the prototyping phase, the production phase and the mission phase. The procedures should be able to account for all system phases. The method of determining the accuracy of the design can be determined through a few forms of analytical, numerical, and experimental tests: environmental, integration, qualification and acceptance, and model tests.

7.4.1. Environmental Testing

Most of the environmental tests can not be performed true to the extraterrestrial conditions on Earth, however the environments can be closely simulated. The two main environments are the vacuum of space and the atmosphere of Mars. Ideally the tests would be performed through a launched prototype in space, or through aerodynamic tests in a wind tunnel simulating the atmosphere. The system can only be fully validated through an actual mission, and as such having the initial mission as a cargo mission is a great way to ascertain the validity of the system.

7.4.2. Integration Testing

The ability for all subsystems to work as part of an entire system is arguably more important than their ability to function as a single entity. Integration testing ensures that the system functions properly; this can be accomplished in a few ways: hardware checks and software checks.

Software checks ensure that the computers, programs, and control systems are all communicating and working as designed; a good way to accomplish this is to put in all possible mission variables and check how the system responds, either through physical inputs or through numerical inputs. Hardware checks are done to make sure the physical components work as expected. One way to ensure this is, for example, to ensure the actuators for the air brakes can deploy while under the design loads; another is determining if all sensors work as expected. Once both of these are done then an entire integration test can be done in order to validate the design.

7.4.3. Qualification and Acceptance

It is imperative that the system follows all standards set, whether they are for safety or otherwise. Determining the qualification can be done through a few methods, some involve just checking the ability of the system to run nominally and do nondestructive testing on certain parts afterwards, such as a dye-penetration test to determine cracks or a X-ray interference test to determine residual stresses and delaminations. Finally, destructive testing can be done in order to ascertain the structural ability of the system.

7.4.4. Model Testing

Model testing is rather straightforward, ideally the model would be developed and then a reference mission would be used to verify and validate the model. In some cases an existing reference does not exist or it is impossible to find data for it; one way to overcome this is to verify as much of the model as possible, and then develop the part or subsystem and then test it. After the part is tested, the results can be used to validate the model, and if the model is wrong, then the new data points can be used to fix it.

Conclusions and Recommendations

The preliminary design of the Mars 2030 mission, Project Cardinal, presents a feasible, reusable and cost effective design for a manned Mars Excursion Vehicle, without reliance on in-situ propellant production. This is done as part of the full, intended mission to Mars, and provides a milestone for the design of the mission as a whole.

8.1. Conclusions

The mission need statement for Project Cardinal is to provide a realistic means of transporting people and payload to, and from Mars in order to allow for future settlement and further space exploration. From this mission need statement, requirements have arose, which had to be met in order to fulfil the need.

The design choices and results, as found in the Midterm Report, have been worked out extensively. The mission concept of multiple vehicles, with a tailored re-entry capability for both the EEV and MEV (and none for the ITV), remain the most optimal configuration of a mission of this scope. SpaceX's mission proposal is deemed infeasible by current means without ISRU.

In the compliance matrix, a few requirements have been designated a *symbol, illustrating that more analysis is necessary in order to determine the viability of the requirement. The analysis is planned to be performed during the first stages of the detailed design after the symposium (section 7.2). Certain requirements have not been met, though this is because the initial requirements were deemed wrong, and new correct requirements had to be established, which have all been met.

The iterative approach to the subsystems has proven useful for the concurrent design, which allowed for better time management with the resources available. Difficulty regarding the use of margins and safety factors was overcome by using a centralised approach, however the consistent use of conservative assumptions resulted in a heavy, albeit low risk, design.

Considering the statements above, a realistic means of transporting people and payload to and from Mars is achieved in order to allow for future settling and further space exploration.

8.2. Recommendations

The design of the vehicles, including the MEV, requires more attention before there is a straight-to-metal design. It is expected that this design phase will take several years, when performed by a SpaceX-sized company of professional engineers.

In addition to the detailed design, it is recommended to conduct further research into the current preliminary design. Certain subsystems, such as the structural subsystem, can be analysed further and with greater accuracy. It is expected that the structural design, especially the air brakes, can be made significantly lighter by use of a finite-element analysis and repositioning of the actuators.

One of the requirements of this project prohibited the use of technologies that are not currently readily available. There are many materials and components currently in development that would make the design lighter, more efficient, and cheaper. Some of these characteristics have been described in the report. For example, it has been considered that lithium-ion batteries and solar panels will improve significantly over the course of the next decade, only currently available technology has been implemented. It may be fruitful to investigate how lower TRL subsystems can improve the design in the future.

This includes the possibility of ISRU on Mars. It is concluded that if SpaceX's design proposal is at all feasible, it would work with ISRU only. The current mission layout (EEV, ITV, and MEV) is considered as the most efficient without ISRU, however its efficiency can be improved by allowing for ISRU as less propellant will need to be brought

8.2. Recommendations

from Earth for both the ITV and the MEV.

It must be noted that ISRU at a later stage is considered in the design, i.e. after five years of the mission. The current design is compatible with in-situ methane production, which can allow for higher payload masses for both the MEV and the ITV. In the case ISRU is not assumed available on Mars, it is recommended that further research keeps considering the possibility of ISRU in the future.

Specific recommendations can be made for the design of the descent trajectory. The key driving variable for the trajectory is the dry mass of the MEV, where more mass usually results in more propellant, however for landing the ΔV does not remain the same. In order to maintain around the same ΔV , the thrust to weight ratio must remain more or less constant. A 10% increase in thrust, while keeping all parameters constant, results in a 2.5 tonne drop in propellant mass, which is a significant amount.

Increasing the size of the air brake also lowers the amount of fuel necessary, but increases the mass of the air brakes, which are already quite heavy. Only increasing dry mass will exponentially increase the mass, to the point where a 20% increase reduces the thrust to weight ratio so much it becomes impossible to land, as more propellant is necessary for launch and as a result more propellant is needed for landing, cascading the increase in mass further.

A recommendation for the future would be to increase the thrust to weight ratio, and if possible increase the specific impulse of the MEV; it would not be recommended to increase the air brake size as the structural mass would increase much more, resulting in a potential detrimental effect.

Additionally, during the design process it was found that the ΔV required for a Venus gravity assist transfer will increase from 6.5 to approximately 10 km/s. This does not change the sizing of the MEV but it is recommended to re-design the ITV since it is supposed to carry more fuel and this structural mass. The increase in total wet mass will be somewhere between 35% and 50%. It is necessary to perform further analysis on the fuel tanks and improve the thrust to weight ratio.

Another detail to look at is the nosecone, and in general the shape of the MEV, there are possibly more aerodynamic nosecones, and while drag accounts for a very low amount of the ΔV requirements, propellant could still be saved. Additionally, because the drag is low, then wider nosecones can be considered to allow for more room for volumetric payload, and specifically more space for the passengers. In general a more detailed trade-off can be done between the two configurations.

Further analysis should be performed for the transfer trajectory back to Earth. Based on the operational and logistics diagram it can be seen that it usually takes at least 1 year stay on the the surface of Mars before the next launch window for a transfer to Earth. Usually this stay time can be lowered by constructing optimal ballistic trajectories by varying the ΔV and entering different transfer plane. This analysis is beyond the scope of this report and more research will be performed in the detailed design phase.

Regarding operational life cycle it is necessary to look more critically into each operational phase. It is recommended to develop a detailed cycle of the mission with each possible launch window and production deadlines for separate subsystems. This gives an idea of possible delays and measures to mitigate any risks that might occur related to schedule and cost.

In the detailed design phase the construction of an orbital propellant storage facility around Mars should be analysed in depth. Since later missions may have excess payload capacity available that can be used to store propellant in Mars orbit for later use.

The cargo variant of the MEV will need to be considered extensively in the detailed design phase.

At this time the thermal system is very sensitive as explained in section 5.7. Hence a more detailed sizing of the thermal system is recommended. especially into combinations of load sensitive MLI and active cooling.

Project Cardinal aimed at designing and presenting a realistic, cost-effective and safe mission to Mars which uses reusable vehicles and establishes a future settlement on the red planet. Throughout the 10 weeks in which the team designed the preliminary mission to Mars, with a more in-depth design of the Mars Excursion Vehicle it was proven that such a mission is possible within budget and schedule as long as all requirements are defined properly and each phase of the research and development is strictly planned.

Bibliography

- [1] Office of Safety and Mission Assurance. Human-Rating Requirements for Space Systems. Tech. rep. NASA, 2006.
- [2] Robert M. Zubrin. *Nuclear thermal rockets using indigenous extraterrestrial propellants*. Tech. rep. Martin Marietta Astronautics, 1990.
- [3] Kathleen Blyth et al. Project Cardinal Midterm Report. 2018.
- [4] Kathleen Blyth et al. Mars 2030 Baseline Report. 2018.
- [5] Roger D. Launius. "Space Stations: Base Camps to the Stars". In: (2004).
- [6] Ivan a. Getting. "The global positioning system". In: (1993).
- [7] Assessment of the Socioeconomic Impact of the ESA Participation to the International Space Station (ISS) Programme. Tech. rep. pwc, 2016.
- [8] F. Eilingsfeld and D. Schaetzler. "The Cost of Capital for Space Tourism Ventures". In: 51st IAC 1.4.02 (2000).
- [9] Toby Miller. ""Drowning In Information and Starving For Knowledge": 21st Century Scholarly Publishing". In: *International Journal of Communication* 1 (2007).
- [10] Shufan Wu. Satellite System Engineering–Budget & Margin. Presentation. 2016.
- [11] A. Santovincenzo. Human Missions to Mars. Tech. rep. ESA, 2004.
- [12] James R. Wertz and Wiley J.Larson. Space Mission Analysis and Design. 3rd ed. Torrance, California: Microcosm Press, 2001.
- [13] Dietrich E. Koelle. *Handbook of cost engineering for space transportation systems with transcost 7.0.* Ottobrunn, Germany: TCS-TransCostSystems, 2000.
- [14] James Meredith et al. "A performance versus cost analysis of prepreg carbon fibre epoxy energy absorption structures". In: *Composite Structures* 124 (2015), pp. 206–213. ISSN: 0263-8223.
- [15] P. Lang et al. "Application of test effectiveness in spacecraft testing". In: *Annual Reliability and Maintainability Symposium* 1995 Proceedings. 1995, pp. 486–495. DOI: 10.1109/RAMS.1995.513289.
- [16] R. C. Hibbeler. Mechanics of Materials. 2011.
- [17] Christian Junaedi et al. Compact and Lightweight Sabatier Reactor for Carbon Dioxide Reduction. Tech. rep. NASA, 2011.
- 18] Rodney J Allam. "Improved Oxygen Production Technologies". In: Energy Procedia 1 (2009), pp. 461-470.
- [19] J. Hanova and H. Dowlatabadi. "Strategic GHG reduction through the use of ground source heat pump technology". In: *Environmental Research Letters* 2 (2007), pp. 461–470.
- [20] Fei Chen et al. Planetary Protection Concerns During Pre-Launch Radioisotope Power System Final Integration Activities. Tech. rep. NASA, 2013.
- [21] Dieter K. Huzel and David H. Huang. Modern engineering for deign of liquid-propellant rocket engines. AIAA, 1992.
- [22] Angelo Cervone. *Propulsion and Power Formula Sheet*. Course AE2230-II. 2016.
- [23] B. T. C. Zandbergen. Thermal Rocket Propulsion. 2017.
- [24] S. D. Heister. *Handbook of Atomization and Sprays*. Springer, 2011.
- [25] George P. Sutton. Rocket Propulsion Elements. 7th ed. John Wiley & Sons, 2001.
- [26] Y. Torano, M. Arita, and H. Takahashi. *Current Study Status of the Advanced Technologies for the J-I Upgrade Launch Vehicle LOX/LNG Engine.* Tech. rep. American Institute of Aeronautics and Astronautics, 2001.
- [27] John Hebda. Niobium alloys and high temperature applications. 2001.
- [28] J.K. Partridge. Fractional Consumption OF Liquid Hydrogen and Liquid Oxygen During the Space Shuttle Program. Tech. rep. American Institute of Physics, 2012.
- [29] J. M. Bauer G. A. Dressler. TRW Pintle Engine Heritage and Performance Characteristics. Tech. rep. TRW Inc, 2000.
- [30] R.A. Spores et al. *GPIM AF-M315E Propulsion System*. Tech. rep. Aerojet Rocketdyne, 2013.
- [31] Automated Transfer Vehicle: Europe's Space Freighter. Tech. rep. 2014.
- [32] Steven S. Pietrobon. Analysis of Propellant Tank Masses. Tech. rep. Small World Communications, 2009.
- [33] Simon Box, Christopher M. Bishop, and Hugh Hunt. *Estimating the dynamic and aerodynamic paramters of passively controlled high power rockets for flight simulaton.* Tech. rep. Cambridge rocketry, 2009.
- [34] Rakesh Panwar. Satellite Orbital Decay Calculations. Tech. rep. IPS Radio and Space Services The Australian Space Weather Agency, 1999.
- [35] Arnaud Valeille. On Mars thermosphere, ionosphere and exosphere: 3D computational study of suprathermal particles. Tech. rep. Atmospheric, Space Science, and Scientific Computing University of Michigan, 2009.
- [36] Karl T. Edquist et al. *Aerothermodynamic Design of the Mars Science Laboratory Heatshield.* Tech. rep. American Institute of Aeronautics and Astronautics, 2014.
- [37] NASA. Lecture #1: Stagnation Point Heating. TFAWS Aerothermodynamics. 2010.
- [38] Stephen Whitmore. Appendix to Section 3: Space Shuttle Tile Thermal Protection System. Course MAE 5420. 2017.
- [39] Joseph A. Del Corso et al. *Advanced High-Temperature Flexible TPS for Inflatable Aerodynamic Decelerators.* Tech. rep. American Institute of Aeronautics and Astronautics, 2018.
- [40] Andre Makovsky, Peter Ilott, and Jim Taylor. Deep Space Communications. John Wiley & Sons, Inc., 2016.
- [41] C. G. Justus and R.D. Braun. *Atmospheric Environments for Entry, Descent and Landing (EDL)*. Tech. rep. NASA Marshall Space Flight Center and Georgia Institute of Technology, 2007.
- [42] Falcon 9 Launch Vehicle Payload User's Guide. Tech. rep. Space X, 2015.
- [43] Karen S. Bernstein. Structural Design Requirements and Factors of Safety for Spaceflight Hardware. Tech. rep. NASA, 2011.

BIBLIOGRAPHY 136

- [44] L. M. Calle et al. Corrosion on Mars. Tech. rep. NASA, 2017.
- [45] Kai Beng Yap R.C. Hibbeler. Mechanics for Engineers Statics. Pearson Education South Asia Pte Ltd, 2012.
- [46] *Pyrogel XT*. Tech. rep. aspen aerogels, inc, 2015.
- [47] DuPont KAPTON HN Polyimide Film. Tech. rep. DuPont, 2016.
- [48] $HexWeb^{TM}$ Honeycomb Attributes and Properties. Tech. rep. Hexcel Composites, 1999.
- [49] ECSS Secretariat. Data for selection of space materials and processes. Tech. rep. ESA, 2004.
- [50] Shruti Nambiar and John T. W. Yeow. "Polymer-Composite Materials for Radiation Protection". In: *Applied Materials and Interfaces* (2012).
- [51] Jon Rask et al. Space Faring The Radiation Challenge. Tech. rep. National Aeronautics and Space Administration, 1989.
- [52] Duncan Boyd. Calculate the Uncertainty of NF Measurements. Tech. rep. Microwaves and RF, 1999.
- [53] Pat Beauchamp et al. Solar Power and Energy Storage for Planetary Missions. 2015.
- [54] Patrich Höhn. Design, Construction and Validation of an articulated solar panel for CubeSats. Tech. rep. 2015.
- [55] David Wright and Suraj Nagaraj. *Request for issuance of a new certificate of Conformity 2017 MY Model S AWD*. Tech. rep. Vehicle Programs and Compliance Division Environmental Protection Agency, 2016.
- [56] Margin philosophy for science assessment studies. Tech. rep. ESA, 2012.
- [57] Model S Owner's Manual. Tech. rep. Tesla, 2018.
- [58] Peter Fortescue, Graham Swinerd, and John Stark. Spacecraft Systems Engineering. John Wiley & Sons, New York City, 2011.
- [59] B.T.C. Zandbergen. Spacecraft Design and Sizing. 2017.
- [60] S. Borowski, D. R. McCurdy, and T. W. Packard. Near Earth Asteroid Human Mission Possibbilities Using Nuclear Thermal Rocket Propulsion. Tech. rep. NASA.
- [61] Albert Juhasz and George Peterson. Review of Advanced Radiator Technologies for Spacecraft Power Systems and Space Thermal Control. Tech. rep. NASA, 1994.
- [62] NASA Technology Roadmaps TA 14: Thermal Management Systems. Tech. rep. NASA, 2015.
- [63] Active Thermal Control System (ATCS) Overview. Tech. rep. Boeing, 2013.
- [64] Flexible Heaters Design Guide. 2016.
- [65] Charles Gurrisi et al. "Space Station Control Moment Gyroscope Lessons Learned". In: (June 2018).
- [66] F. Budnik, T.A. Morley, and R.A. Mackenzie. *ESOC's System for Interplanetary Orbit Determination*. Tech. rep. ESA/ESOC, 2004.
- [67] Alex Foessel-Bunting and William Whittaker. *MMW-Scanning Radar for Descent Guidance and Landing Safeguard*. Tech. rep. Carnegie Mellon University.
- [68] John L. MacArthur et al. "Evolution of the Satellite Radar Altimeter". In: John Hopkins APL Technical Digest 10.4 (1989).
- [69] Xiangyu Huang et al. Autonomous Navigation and Control for Pinpoint Lunar Soft Landing. Tech. rep. 2007.
- [70] J. Pereira do Carmo et al. Imaging LIDARs for Space Applications. Tech. rep. ESA.
- [71] F. Blais et al. The NRC-D Laser Tracking System: IIT's Contribution to the International Space Station Project. Tech. rep. National Research Council Canada, 2001.
- [72] D. Eakman et al. Small Spacecraft Power and Thermal Subsystems. Tech. rep. NASA, 1994.
- [73] Marco Caporicci. Human Space Transportation and Logistic Activities at ESA. Tech. rep. 2004.
- [74] International Docking System Standard (IDSS) Interface Definition Document (IDD). Tech. rep. Revision E. 2016.
- [75] SRE-PA & D-TEC staff. Margin philosophy for science assessment studies. Tech. rep. ESA, 2012.
- [76] W. Verhagen. AE3221-I Systems Engineering and Aerospace Design. 2017.
- [77] Gregory F. Dubos, Jean-Francois Castet, and Joseph H. Saleh. "Statistical reliability analysis of satellites by mass category: Does spacecraft size matter?" In: *Acta Astronautica* 67.5 (2010), pp. 584–595.
- [78] R.J. Hamann and M.J.L. van Tooren. "System Engineering & Technical Management Techniques". In: *Lecture Notes AE3-S01* (2006).
- [79] Robert W. Johnson. Criteria for Thermal Regulation for Manned Spacecraft Cabins. Tech. rep. NASA, 1966.
- [80] Frank E. Belles. High Pressure Oxygen Utilization by NASA. Tech. rep. NASA, 1973.
- [81] K. Vasantha Kumar and Wiliam T. Norfleet. *Issues on Human Acceleration Tolerance After Long-Duration Space Flights*. Tech. rep. NASA, 1992.
- [82] United Nations Treaties and Principles On Outer Space, tech. rep. United Nations, 1966.
- [83] Jeffrey Kahn, Catharyn T. Liverman, and Margaret A. McCoy. Health Standards for Long Duration and Exploration Spaceflight: Ethics Principles, Responsibilities, and Decision Framework. Tech. rep. Board on Health Sciences Policy; Institute of Medicine, 2014.
- [84] M. M. Finckenor and K. K. de Groh. Space Environmental Effects. NASA ISS Program Science Office, 2015.
- [85] W. J. Helms and K. M. Pohlkamp. Docking Offset Between the Space Shuttle and the International Space Station and Resulting Impacts to the Transfer of Attitude Reference and Control. Tech. rep. NASA, 2011.
- [86] John G. Furumo. Cold-gas Propulsion for Small Satellite Attitude Control, Station Keeping, and Deorbit. Tech. rep. University of Hawaii, 2013.
- [87] M.E. Polites. An Assessment of the Technology of Automated Rendezvous and Capture in Space. Tech. rep. NASA, 1998.
- [88] Allan R. Klumpp. Rendezvous Guidance Trajectory Shaping. Tech. rep. Jet Propulsion Laboratory, 1987.
- [89] Hiroshi Yamakawa. ISAS Mercury Orbiter Mission Trajecory Design Strategy. Tech. rep. ISAS, 1999.



Requirements

TEC-01.1 The system shall be able to transport a payload from Earth Surface to LEO. The EEV shall allow payload embarkment. The EEV shall withstand sustained dynamic pressure of 11.6 kPa. The EEV shall withstand sustained dynamic pressure of 11.6 kPa. The EEV shall withstand sustained dynamic pressure of 11.6 kPa. The EEV shall be rated to external temperatures within a range of 150 - 385 K. TEC-01.3 The EEV shall be able to entrol its attitude. TEC-01.4.1 The EEV shall be able to ocntrol its attitude adjustments. TEC-01.4.1.2 The EEV shall be able to control its position. TEC-01.4.2.1 The EEV shall be able to control its position. TEC-01.4.2.3 The EEV shall be able to determine its position within 1 cm accuracy. TEC-01.4.3 The EEV shall be able to determine its velocity within 1 cm/s accuracy. TEC-01.4.3 The EEV shall be able to determine its velocity within 1 cm/s accuracy. TEC-01.4.3 The EEV shall have at least 20 m/s ΔV for velocity adjustments. The EEV shall have re-ignitable propulsion. The EEV shall have re-ignitable propulsion. The EEV shall be able to dock with the ITV. The System shall allow docked transfer of fuel from EEV to ITV. The System shall allow docked transfer of payload from EEV to ITV. The System shall allow docked transfer of payload from EEV to ITV. The System shall allow docked transfer of payload from EEV to ITV. The TEC-02.1 The ITV shall be able to external temperatures within a range of 150 - 385 K. The ITV shall be rated to a sustained dynamic pressure of 11.6 kPa. The MEV shall be rated to external temperatures within a range of 150 - 385 K. The CO2.1.4 The MEV shall be rated to external temperatures within a range of 150 - 385 K. The CO2.1.5 The ITV shall be rated to external temperatures within a range of 150 - 385 K. The CO2.1.6 The ITV shall be rated to external temperatures within a range of 150 - 385 K. The ITV shall be rated to external temperatures within a range of 150 - 385 K. The ITV shall be rated to external temperatures within a range of 150 - 385 K. The ITV shall	ted on the e ² . This is the Falcon load mass
TEC-01.2 The EEV shall withstand sustained dynamic pressure of 11.6 kPa. TEC-01.3 The EEV shall be rated to external temperatures within a range of 150 - 385 K. TEC-01.4 The EEV shall be able to rendezvous with the ITV. TEC-01.4.1.1 The EEV shall be able to control its attitude. TEC-01.4.1.2 The EEV shall be able to determine its attitude within 7 arcminutes accuracy. TEC-01.4.2.1 The EEV shall be able to control its position. TEC-01.4.2.2 The EEV shall be able to control its position. TEC-01.4.2.3 The EEV shall be able to determine its velocity within 1 cm accuracy. TEC-01.4.2.1 The EEV shall be able to determine its velocity within 1 cm/s accuracy. TEC-01.4.2.2 The EEV shall be able to determine its velocity adjustments. TEC-01.4.3 The EEV shall be able to determine its velocity adjustments. TEC-01.4.1 The EEV shall be able to determine its velocity adjustments. TEC-01.4.2.1 The EEV shall be able to determine its velocity adjustments. TEC-01.4.2.2 The EEV shall be able to determine its velocity adjustments. TEC-01.4.3 The EEV shall have at least 20 m/s ΔV for velocity adjustments. TEC-01.5 The EEV shall be able to dock with the ITV. TEC-01.5.1 The system shall allow docked transfer of payload from EEV to ITV. TEC-02.1.2 The ITV shall be able to transfer of fuel from EEV to ITV. TEC-02.1.1 The system shall allow docked transfer of payload from LEO to LMO. TEC-02.1.2 The itry shall be able to withstand interplanetary space environment. TEC-02.1.3 The ITV shall be rated to a sustained dynamic pressure of 11.6 kPa. TEC-02.1.3 The ITV shall be rated to a sustained dynamic pressure of 50 MPa. TEC-02.1.4 The MEV shall be rated to external temperatures within a range of 150 - 385 K. TEC-02.1.6 The MEV shall be rated to sustained radiation dose of 10.2 mrad/hr.	e ² . This is the Falcon yload mass
TEC-01.3 The EEV shall be rated to external temperatures within a range of 150 - 385 K. TEC-01.4 The EEV shall be able to rendezvous with the ITV. TEC-01.4.1.1 The EEV shall be able to control its attitude. TEC-01.4.1.1 The EEV shall be able to determine its attitude within 7 arcminutes accuracy. TEC-01.4.1.2 The EEV shall have at least 50 m/s ΔV for attitude adjustments. TEC-01.4.2.1 The EEV shall be able to control its position. TEC-01.4.2.2 The EEV shall be able to determine its position within 1 cm accuracy. TEC-01.4.2.3 The EEV shall be able to determine its velocity within 1 cm/s accuracy. TEC-01.4.3 The EEV shall have at least 20 m/s ΔV for velocity adjustments. TEC-01.5 The EEV shall have re-ignitable propulsion. TEC-01.5.1 The system shall allow docked transfer of payload from EEV to ITV. TEC-01.5.2 The system shall allow docked transfer of payload from EEV to ITV. TEC-02.1 The system shall allow docked transfer of payload from EEV to ITV. TEC-02.1 The system shall be able to withstand interplanetary space environment. TEC-02.1.1 The fairing shall withstand sustained dynamic pressure of 11.6 kPa. TEC-02.1.2 The ITV shall be rated to a sustained radiation dose of 10.2 mrad/hr. TEC-02.1.3 The MEV shall be rated to external temperatures within a range of 150 - 385 K. TEC-02.1.5 The MEV shall be rated to sustained radiation dose of 10.2 mrad/hr.	
TEC-01.4.1 The EEV shall be able to rendezvous with the ITV. TEC-01.4.1.1 The EEV shall be able to control its attitude. TEC-01.4.1.1 The EEV shall be able to control its attitude. TEC-01.4.1.1 The EEV shall be able to determine its attitude within 7 arcminutes accuracy. TEC-01.4.1.2 The EEV shall have at least 50 m/s ΔV for attitude adjustments. TEC-01.4.2.1 The EEV shall be able to control its position. TEC-01.4.2.2 The EEV shall be able to determine its position within 1 cm accuracy. TEC-01.4.2.3 The EEV shall be able to determine its velocity within 1 cm/s accuracy. TEC-01.4.2.3 The EEV shall have at least 20 m/s ΔV for velocity adjustments. TEC-01.5.1 The EEV shall be able to dock with the ITV. TEC-01.5.2 The system shall allow docked transfer of payload from EEV to ITV. TEC-01.5.2 The system shall allow docked transfer of fuel from EEV to ITV. TEC-02.1.1 The fairing shall withstand sustained dynamic pressure of 11.6 kPa. TEC-02.1.2 The ITV shall be rated to external temperatures within a range of 150 - 385 K. TEC-02.1.5 The MEV shall be rated to sustained radiation dose of 10.2 mrad/hr. TEC-02.1.6 The MEV shall be rated to sustained radiation dose of 10.2 mrad/hr. TEC-02.1.1 The MEV shall be rated to sustained radiation dose of 10.2 mrad/hr. TEC-02.1.2 The MEV shall be rated to sustained radiation dose of 10.2 mrad/hr. TEC-02.1.3 The MEV shall be rated to sustained radiation dose of 10.2 mrad/hr.	
TEC-01.4.1.1 The EEV shall be able to control its attitude. The EEV shall be able to determine its attitude within 7 arcminutes accuracy. TEC-01.4.1.2 The EEV shall have at least 50 m/s ΔV for attitude adjustments. TEC-01.4.2.1 The EEV shall be able to control its position. TEC-01.4.2.1 The EEV shall be able to determine its position within 1 cm accuracy. TEC-01.4.2.2 The EEV shall be able to determine its position within 1 cm/s accuracy. TEC-01.4.2.3 The EEV shall have at least 20 m/s ΔV for velocity within 1 cm/s accuracy. TEC-01.4.3 The EEV shall have at least 20 m/s ΔV for velocity adjustments. TEC-01.5 The EEV shall have re-ignitable propulsion. TEC-01.5.1 The system shall allow docked transfer of payload from EEV to ITV. TEC-01.5.2 The system shall allow docked transfer of payload from EEV to ITV. TEC-02.1 The system shall be able to transport a payload from LEO to LMO. TEC-02.1 The system shall be able to withstand interplanetary space environment. TEC-02.1.1 The fairing shall withstand sustained dynamic pressure of 11.6 kPa. TEC-02.1.2 The ITV shall be rated to external temperatures within a range of 150 - 385 K. TEC-02.1.5 The MEV shall withstand sustained dynamic pressure of 50 MPa. TEC-02.1.5 The MEV shall be rated to external temperatures within a range of 150 - 385 K. TEC-02.1.6 The MEV shall be rated to sustained radiation dose of 10.2 mrad/hr. The MEV shall be rated to sustained radiation dose of 10.2 mrad/hr. The MEV shall be rated to sustained radiation dose of 10.2 mrad/hr. The MEV shall be rated to external temperatures within a range of 150 - 385 K. TEC-02.1.6 The MEV shall be rated to sustained radiation dose of 10.2 mrad/hr.	
racy. TEC-01.4.1.2 The EEV shall have at least 50 m/s ΔV for attitude adjustments. TEC-01.4.2.1 The EEV shall be able to control its position. TEC-01.4.2.1 The EEV shall be able to determine its position within 1 cm accuracy. TEC-01.4.2.2 The EEV shall be able to determine its velocity within 1 cm/s accuracy. TEC-01.4.2.3 The EEV shall have at least 20 m/s ΔV for velocity adjustments. TEC-01.4.3 The EEV shall have re-ignitable propulsion. TEC-01.5 The system shall allow docked transfer of payload from EEV to ITV. TEC-01.5.1 The system shall allow docked transfer of fuel from EEV to ITV. TEC-02 The ITV shall be able to transport a payload from LEO to LMO. TEC-02.1 The system shall be able to withstand interplanetary space environment. TEC-02.1.2 The ITV shall be rated to a sustained dynamic pressure of 50 MPa. TEC-02.1.3 The MEV shall be rated to external temperatures within a range of 150 - 385 K. TEC-02.1.6 The MEV shall be rated to sustained radiation dose of 10.2 mrad/hr. TEC-02.1.6 The MEV shall be rated to sustained radiation dose of 10.2 mrad/hr.	_
TEC-01.4.1.2 The EEV shall have at least 50 m/s ΔV for attitude adjustments. Typical ΔV requirement for cold-gas attitu [86]. TEC-01.4.2.1 The EEV shall be able to control its position. TEC-01.4.2.2 The EEV shall be able to determine its position within 1 cm accuracy. TEC-01.4.2.3 The EEV shall have at least 20 m/s ΔV for velocity adjustments. TEC-01.4.3 The EEV shall have re-ignitable propulsion. TEC-01.5 The system shall allow docked transfer of payload from EEV to ITV. TEC-01.5.1 The system shall allow docked transfer of fuel from EEV to ITV. TEC-02.1 The system shall be able to transport a payload from LEO to LMO. TEC-02.1.1 The fairing shall withstand sustained dynamic pressure of 11.6 kPa. TEC-02.1.2 The ITV shall be rated to a sustained radiation dose of 10.2 mrad/hr. TEC-02.1.3 The MEV shall be rated to external temperatures within a range of 150 - 385 K. TEC-02.1.6 The MEV shall be rated to sustained radiation dose of 10.2 mrad/hr.	based on
TEC-01.4.2.1 The EEV shall be able to determine its position within 1 cm accuracy. TEC-01.4.2.2 The EEV shall be able to determine its velocity within 1 cm/s accuracy. The EEV shall have at least 20 m/s ΔV for velocity adjustments. Typical rendezvous ΔV usage [88]. Required for in-orbit manoeuvring and rend TEC-01.5 The EEV shall have re-ignitable propulsion. The EEV shall be able to dock with the ITV. TEC-01.5.1 The system shall allow docked transfer of payload from EEV to ITV. TEC-01.5.2 The system shall allow docked transfer of fuel from EEV to ITV. The system shall be able to transport a payload from LEO to LMO. The system shall be able to withstand interplanetary space environment. TEC-02.1.1 The fairing shall withstand sustained dynamic pressure of 11.6 kPa. TEC-02.1.2 The ITV shall be rated to external temperatures within a range of 150 - 385 K. TEC-02.1.3 The MEV shall withstand sustained dynamic pressure of 50 MPa. TEC-02.1.5 The MEV shall be rated to external temperatures within a range of 150 - 385 K. The MEV shall be rated to sustained radiation dose of 10.2 mrad/hr. The MEV shall be rated to sustained radiation dose of 10.2 mrad/hr. The MEV shall be rated to sustained radiation dose of 10.2 mrad/hr. The MEV shall be rated to sustained radiation dose of 10.2 mrad/hr. The MEV shall be rated to sustained radiation dose of 10.2 mrad/hr. The MEV shall be rated to sustained radiation dose of 10.2 mrad/hr.	de control
TEC-01.4.2.1 The EEV shall be able to determine its position within 1 cm accuracy. TEC-01.4.2.2 The EEV shall be able to determine its velocity within 1 cm/s accuracy. TEC-01.4.2.3 The EEV shall have at least 20 m/s ΔV for velocity adjustments. TEC-01.4.3 The EEV shall have re-ignitable propulsion. TEC-01.5 The EEV shall be able to dock with the ITV. TEC-01.5.1 The system shall allow docked transfer of payload from EEV to ITV. TEC-01.5.2 The ITV shall be able to transport a payload from LEO to LMO. TEC-02 The ITV shall be able to withstand interplanetary space environment. TEC-02.1.1 The fairing shall withstand sustained dynamic pressure of 11.6 kPa. TEC-02.1.2 The ITV shall be rated to a sustained radiation dose of 10.2 mrad/hr. TEC-02.1.3 The MEV shall be rated to external temperatures within a range of 150 - 385 K. TEC-02.1.5 The MEV shall be rated to sustained radiation dose of 10.2 mrad/hr. TEC-02.1.6 The MEV shall be rated to sustained radiation dose of 10.2 mrad/hr.	
TEC-01.4.2.2 The EEV shall be able to determine its velocity within 1 cm/s accuracy. TEC-01.4.2.3 The EEV shall have at least 20 m/s ΔV for velocity adjustments. Typical rendezvous ΔV usage [88]. Required for in-orbit manoeuvring and rend TEC-01.5.1 The system shall allow docked transfer of payload from EEV to ITV. TEC-01.5.2 The system shall allow docked transfer of fuel from EEV to ITV. The system shall be able to transport a payload from LEO to LMO. The system shall be able to withstand interplanetary space environment. TEC-02.1.1 The fairing shall withstand sustained dynamic pressure of 11.6 kPa. TEC-02.1.2 The ITV shall be rated to external temperatures within a range of 150 - 385 K. TEC-02.1.3 The MEV shall withstand sustained dynamic pressure of 50 MPa. TEC-02.1.5 The MEV shall be rated to external temperatures within a range of 150 - 385 K. TEC-02.1.5 The MEV shall be rated to sustained radiation dose of 10.2 mrad/hr. The MEV shall be rated to external temperatures within a range of 150 - 385 K. The MEV shall be rated to sustained radiation dose of 10.2 mrad/hr. The MEV shall be rated to sustained radiation dose of 10.2 mrad/hr. The MEV shall be rated to sustained radiation dose of 10.2 mrad/hr. The MEV shall be rated to sustained radiation dose of 10.2 mrad/hr. The MEV shall be rated to sustained radiation dose of 10.2 mrad/hr. The MEV shall be rated to sustained radiation dose of 10.2 mrad/hr.	
TEC-01.4.2.3 The EEV shall have at least 20 m/s ΔV for velocity adjustments. Typical rendezvous ΔV usage [88]. Required for in-orbit manoeuvring and rend TEC-01.5.1 The system shall allow docked transfer of payload from EEV to ITV. TEC-01.5.2 The system shall allow docked transfer of fuel from EEV to ITV. The system shall be able to transport a payload from LEO to LMO. TEC-02.1 The system shall be able to withstand interplanetary space environment. TEC-02.1.1 The fairing shall withstand sustained dynamic pressure of 11.6 kPa. TEC-02.1.2 The ITV shall be rated to external temperatures within a range of 150 - 385 K. TEC-02.1.4 The MEV shall withstand sustained dynamic pressure of 50 MPa. TEC-02.1.5 The MEV shall be rated to external temperatures within a range of 150 - 385 K. TEC-02.1.6 The MEV shall be rated to sustained radiation dose of 10.2 mrad/hr. The MEV shall be rated to external temperatures within a range of 150 - 385 K. TEC-02.1.6 The MEV shall be rated to sustained radiation dose of 10.2 mrad/hr.	
TEC-01.4.3 The EEV shall have re-ignitable propulsion. TEC-01.5 The System shall allow docked transfer of payload from EEV to ITV. TEC-01.5.2 The system shall allow docked transfer of fuel from EEV to ITV. TEC-02 The ITV shall be able to transport a payload from LEO to LMO. TEC-02.1 The system shall be able to withstand interplanetary space environment. TEC-02.1.1 The fairing shall withstand sustained dynamic pressure of 11.6 kPa. TEC-02.1.2 The ITV shall be rated to external temperatures within a range of 150 - 385 K. TEC-02.1.3 The ITV shall withstand sustained dynamic pressure of 50 MPa. TEC-02.1.4 The MEV shall withstand sustained dynamic pressure of 50 MPa. TEC-02.1.5 The MEV shall be rated to external temperatures within a range of 150 - 385 K. TEC-02.1.6 The MEV shall be rated to sustained radiation dose of 10.2 mrad/hr. TEC-02.1.6 The MEV shall be rated to sustained radiation dose of 10.2 mrad/hr.	
TEC-01.5 The EEV shall be able to dock with the ITV. TEC-01.5.1 The system shall allow docked transfer of payload from EEV to ITV. TEC-01.5.2 The system shall allow docked transfer of fuel from EEV to ITV. The system shall allow docked transfer of fuel from EEV to ITV. The system shall be able to transport a payload from LEO to LMO. TEC-02.1 The system shall be able to withstand interplanetary space environment. TEC-02.1.1 The fairing shall withstand sustained dynamic pressure of 11.6 kPa. TEC-02.1.2 The ITV shall be rated to external temperatures within a range of 150 - 385 K. TEC-02.1.3 The ITV shall be rated to a sustained radiation dose of 10.2 mrad/hr. TEC-02.1.4 The MEV shall withstand sustained dynamic pressure of 50 MPa. TEC-02.1.5 The MEV shall be rated to external temperatures within a range of 150 - 385 K. TEC-02.1.6 The MEV shall be rated to sustained radiation dose of 10.2 mrad/hr.	ezvous.
TEC-01.5.1 The system shall allow docked transfer of payload from EEV to ITV. TEC-01.5.2 The system shall allow docked transfer of fuel from EEV to ITV. THEC-02 The ITV shall be able to transport a payload from LEO to LMO. TEC-02.1 The system shall be able to withstand interplanetary space environment. TEC-02.1.1 The fairing shall withstand sustained dynamic pressure of 11.6 kPa. TEC-02.1.2 The ITV shall be rated to external temperatures within a range of 150 - 385 K. TEC-02.1.3 The ITV shall be rated to a sustained radiation dose of 10.2 mrad/hr. TEC-02.1.4 The MEV shall withstand sustained dynamic pressure of 50 MPa. TEC-02.1.5 The MEV shall be rated to external temperatures within a range of 150 - 385 K. TEC-02.1.6 The MEV shall be rated to sustained radiation dose of 10.2 mrad/hr.	
TEC-01.5.2 The system shall allow docked transfer of fuel from EEV to ITV. In-orbit refueling of the ITV is necessary to receive the ITEC-02. The ITV shall be able to transport a payload from LEO to LMO. TEC-02.1.1 The system shall be able to withstand interplanetary space environment. TEC-02.1.2 The fairing shall withstand sustained dynamic pressure of 11.6 kPa. TEC-02.1.2 The ITV shall be rated to external temperatures within a range of 150 - 385 K. TEC-02.1.3 The ITV shall be rated to a sustained radiation dose of 10.2 mrad/hr. TEC-02.1.4 The MEV shall withstand sustained dynamic pressure of 50 MPa. TEC-02.1.5 The MEV shall be rated to external temperatures within a range of 150 - 385 K. TEC-02.1.6 The MEV shall be rated to sustained radiation dose of 10.2 mrad/hr.	
TEC-02 The ITV shall be able to transport a payload from LEO to LMO. TEC-02.1 The system shall be able to withstand interplanetary space environment. TEC-02.1.1 The fairing shall withstand sustained dynamic pressure of 11.6 kPa. TEC-02.1.2 The ITV shall be rated to external temperatures within a range of 150 - 385 K. TEC-02.1.3 The ITV shall be rated to a sustained radiation dose of 10.2 mrad/hr. TEC-02.1.4 The MEV shall withstand sustained dynamic pressure of 50 MPa. TEC-02.1.5 The MEV shall be rated to external temperatures within a range of 150 - 385 K. TEC-02.1.6 The MEV shall be rated to sustained radiation dose of 10.2 mrad/hr.	each Mars
TEC-02.1 The system shall be able to withstand interplanetary space environment. TEC-02.1.1 The fairing shall withstand sustained dynamic pressure of 11.6 kPa. TEC-02.1.2 The ITV shall be rated to external temperatures within a range of 150 - 385 K. TEC-02.1.3 The ITV shall be rated to a sustained radiation dose of 10.2 mrad/hr. TEC-02.1.4 The MEV shall withstand sustained dynamic pressure of 50 MPa. TEC-02.1.5 The MEV shall be rated to external temperatures within a range of 150 - 385 K. TEC-02.1.6 The MEV shall be rated to sustained radiation dose of 10.2 mrad/hr.	Jucii iviuis.
TEC-02.1.1 The fairing shall withstand sustained dynamic pressure of 11.6 kPa. TEC-02.1.2 The ITV shall be rated to external temperatures within a range of 150 - 385 K. TEC-02.1.3 The ITV shall be rated to a sustained radiation dose of 10.2 mrad/hr. TEC-02.1.4 The MEV shall withstand sustained dynamic pressure of 50 MPa. TEC-02.1.5 The MEV shall be rated to external temperatures within a range of 150 - 385 K. TEC-02.1.6 The MEV shall be rated to sustained radiation dose of 10.2 mrad/hr.	
TEC-02.1.2 The ITV shall be rated to external temperatures within a range of 150 - 385 K. TEC-02.1.3 The ITV shall be rated to a sustained radiation dose of 10.2 mrad/hr. TEC-02.1.4 The MEV shall withstand sustained dynamic pressure of 50 MPa. TEC-02.1.5 The MEV shall be rated to external temperatures within a range of 150 - 385 K. TEC-02.1.6 The MEV shall be rated to sustained radiation dose of 10.2 mrad/hr.	
385 K. TEC-02.1.3 The ITV shall be rated to a sustained radiation dose of 10.2 mrad/hr. TEC-02.1.4 The MEV shall withstand sustained dynamic pressure of 50 MPa. TEC-02.1.5 The MEV shall be rated to external temperatures within a range of 150 - 385 K. TEC-02.1.6 The MEV shall be rated to sustained radiation dose of 10.2 mrad/hr.	
TEC-02.1.3 The ITV shall be rated to a sustained radiation dose of 10.2 mrad/hr. TEC-02.1.4 The MEV shall withstand sustained dynamic pressure of 50 MPa. TEC-02.1.5 The MEV shall be rated to external temperatures within a range of 150 - 385 K. TEC-02.1.6 The MEV shall be rated to sustained radiation dose of 10.2 mrad/hr.	
TEC-02.1.4 The MEV shall withstand sustained dynamic pressure of 50 MPa. TEC-02.1.5 The MEV shall be rated to external temperatures within a range of 150 - 385 K. TEC-02.1.6 The MEV shall be rated to sustained radiation dose of 10.2 mrad/hr.	
TEC-02.1.5 The MEV shall be rated to external temperatures within a range of 150 - 385 K. TEC-02.1.6 The MEV shall be rated to sustained radiation dose of 10.2 mrad/hr.	
385 K. TEC-02.1.6 The MEV shall be rated to sustained radiation dose of 10.2 mrad/hr.	
TEC-02.1.6 The MEV shall be rated to sustained radiation dose of 10.2 mrad/hr.	
THE VELL THE IT V SHAIL BE ABLE to CONTROL IS ACCURACE.	
TEC-02.2.1 The system shall be able to determine the ITV's attitude with an accuracy Measurement requirements for interplaneta	ry transfer
of at most 15 nrad. [66]	ry transier
TEC-02.2.2 The ITV shall have at least 50 m/s ΔV for attitude adjustments. Two way interplanetary attitude control e [89].	stimations
TEC-02.3 The TTV shall be able to control its position.	
TEC-02.3.1 The ITV shall be able to determine its position with an accuracy of at	
most 1 km.	
TEC-02.3.2 The ITV shall be able to determine its orbit within 1 m accuracy. Measurement requirements for interplaneta [66].	ry transfer
TEC-02.3.3 The ITV shall have at least 5.4 km/s ΔV for interplanetary transfer to Mars.	
TEC-02.3.4 The ITV shall have reignitable propulsion.	
TEC-02.4 The MEV shall be able to rendezvous with the ITV.	
TEC-02.4.1 The MEV shall be able to control its attitude.	
TEC-02.4.1.1 The MEV shall be able to determine its attitude with an accuracy of at	
most 7 arcminutes.	
TEC-02.4.1.2 The MEV shall have at least 40 m/s ΔV for attitude adjustments.	

https://www.nasa.gov/mission_pages/shuttle/shuttlemissions/sts118/launch/launch-blog.html(Last accessed 21-06-2018) thtps://web.archive.org/web/20130702201040/http://history.nasa.gov/ap16fj/01_Day1_Pt1.htm(Last accessed 21-06-2018)

TEC-02.4.2	The MEV shall be able to control its position.	
TEC-02.4.2.1	The MEV shall be able to determine its position with an accuracy of at	
	most 1 cm.	
TEC-02.4.2.2	The MEV shall be able to determine its velocity with an accuracy of at	
TEC 02 4 2 2	most 1 cm/s. The MEV shall have at least 20 m/s ΔV for velocity adjustments.	Based on ΔV calculation.
TEC-02.4.2.3 TEC-02.4.2.4	The MEV shall have re-ignitable propulsion.	based on ΔV calculation.
TEC-02.5	The MEV shall be able to dock with the ITV.	
TEC-02.5.1	The system shall allow docked transfer of payload from ITV to MEV.	
TEC-02.5.2	The system shall allow docked transfer of fuel from ITV to MEV.	
TEC-03	The MEV shall be able to transport a payload from LMO to Mars Surface.	
TEC-03.1	The MEV shall be able to de-orbit.	
TEC-03.2 — — — — — — — — — — — — — — — — — — —	The MEV shall be able to re-enter Mars atmosphere.	
TEC-03.3 TEC-03.3.1	The MEV shall be able to land on Mars. The MEV shall be able to land within 10 m accuracy. The MEV shall be able to land within 10 m accuracy.	
TEC-03.3.1	The MEV shall have 120 m/s ΔV for travel from Mars orbit to Mars sur-	Based on AV calculations
110 03.4	face.	bused on Av culculations.
TEC-03.5	The MEV shall allow payload disembarkment without external infras-	
	tructure.	
TEC-03.6	The MEV shall be capable of landing with a nominal velocity of 2 m/s	Common on Mars landers ³ .
TEC-04	The system shall be able to transport a payload within an appropriate	
	environment.	
TEC-04.1.1	The system shall transport the cargo without damage. The system shall retain cargo within a temperature range which does not	Values are specific to cargo
1EC-04.1.1	degrade the cargo.	values are specific to cargo.
TEC-04.1.2	The system shall retain cargo within an atmosphere which does not de-	
120 01.1.2	grade the cargo.	
TEC-04.1.2.1	The system shall retain cargo within an atmospheric composition which	
	does not degrade the cargo.	
TEC-04.1.2.2	The system shall retain cargo within a pressure range which does not de-	
TTT-C 04.1.0	grade the cargo.	
TEC-04.1.3	The system shall not subject the cargo to accelerations which may dam-	
TEC-04.1.4	age the cargo. The system shall ensure the cargo is not subjected to radiation levels	
1EC-04.1.4	which may degrade the cargo.	
TEC-04.2	The system shall transport crew comfortably [note: this implies safely].	
TEC-04.2.1	The system shall retain crew within a comfortable temperature range as	
	defined by [79].	
TEC-04.2.2	The system shall retain crew within a comfortable atmosphere.	
TEC-04.2.2.1	The system shall retain crew within a comfortable atmospheric compo-	
TEC-04.2.2.2	sition as defined by [80]. The system shall retain crew within an atmosphere with an oxygen level	
TEC-04.2.2.2	within a comfortable range as defined by [80].	
TEC-04.2.2.3	The system shall retain crew within a comfortable pressure range as de-	
	fined by [80].	
TEC-04.2.3	The system shall not subject crew to acceleration levels above human	
	tolerance.	
TEC-04.2.3.1	The system shall not subject crew to sustained acceleration above hu-	
TEC 04 2 2 2	man comfort levels as defined by [81].	
TEC-04.2.3.2	The system shall not subject crew to instantaneous acceleration above human safety levels as defined by [81].	
TEC-04.2.4	The system shall ensure crew is not subjected to radiation above human	
	health levels.	
TEC-04.2.5	The system shall provide crew with comfortably sufficient consumables.	
TEC-04.2.5.1	The system shall be able to transport/regenerate sufficient potable water.	
TEC-04.2.5.2	The system shall be able to transport/regenerate sufficient food.	
TEC-04.2.5.3	The system shall be able to transport/regenerate sufficient oxygen.	
TEC-04.2.5.4	The system shall be able to transport sufficient hygienic material.	
TEC-04.2.5.5 TEC-04.2.5.6	The system shall be able to transport sufficient clothing. The system shall be able to transport sufficient cleaning materials.	
TEC-04.2.6	The system shall retain crew within a environment which does not dete-	Psychological healthcare is a field of research on its own
	riorate psychological health.	and outside the scope of this project.
TEC-04.2.6.1	The system shall provide crew with a personal volume which does not	,
	deteriorate psychological health.	
TEC-04.2.6.2	The ITV shall provide crew with entertainment which is sufficient to not	The exact psychological requirements are beyond the
TTPO CA O C	deteriorate psychological health.	scope of this report.
TEC-04.2.6.3	Each vehicle shall be able to communicate with Earth Surface.	By extension, each vehicle can communicate with each
TEC-04.2.6.4	Each vehicle shall be able to perform bidirectional communication.	other.
110-04.2.0.4	Each vehicle shan be able to perform blunectional communication.	

 $[\]overline{^3{\tt https://www.seis-insight.eu/en/public-2/the-insight-mission/landing} (Last accessed 20-06-2018)}$

TEC-04.2.6.5	Each vehicle shall be able to continuously communicate.	
TEC-04.2.6.6		High quality video connection is deemed a requirement for the psychological health of the crew.
TEC-05	The MEV shall be able to transport a payload from Mars Surface to LMO.	
TEC-05.1	The MEV shall allow payload embarkment without external infrastruc-	
L	ture.	
TEC-05.2	The MEV shall be have 4.1 km/s ΔV for launch to LMO.	
TEC-05.3	The system shall allow docked transfer of payload from the MEV to the	
	ITV.	
TEC-06	The ITV shall be able to transport a payload from LMO to LEO.	
TEC-06.1	The ITV shall have ΔV for interplanetary transfer to Earth.	
TEC-06.2	The system shall allow docked transfer of payload from the ITV to the	
	EEV.	
TEC-07	The EEV shall be able to transport a payload from LEO to Earth surface.	
TEC-07.1	The EEV shall be able to de-orbit.	
TEC-07.2	The EEV shall be able to re-enter Earth atmosphere.	
TEC-07.3	The EEV shall be able to land on Earth.	
TEC-07.3.1	The EEV shall be able to land within 10 m accuracy.	
TEC-07.4	The EEV shall have 280 m/s ΔV for travel from Earth orbit to Earth sur-	Based on ΔV . calculations
	face.	
TEC-07.5	The EEV shall allow payload disembarkment.	

Identifier	Requirement	Rationale
GEN-01	All components shall be manufactured on Earth.	
GEN-02	All components shall be assembled on Earth.	
GEN-03	The system shall not rely on in-situ propellant production during the ini-	
	tial set-up period, 2030-2035.	
GEN-04	The first launch of the programme shall be scheduled in 2030.	
GEN-05	The launch cost per kg to Mars shall not exceed 10,000 USD.	
GEN-05.1	The launch cost per kg to LEO shall not exceed 1,500 USD.	
GEN-06	The duration of each mission on Mars surface shall be no shorter than	
	one month, from landing to take-off for returning to Earth.	
GEN-06.1	The MEV shall be able to remain on the Mars surface for at least one	
	month per mission without loss of functionality.	
GEN-07	The system shall be able to transport a habitat from Earth to Mars.	
GEN-07.1	The system shall be able to transport a habitat which can sustain a crew	
L	of at least 10 members.	
GEN-07.2	The system shall be able to transport a habitat which can sustain a crew	
	no shorter than 1 month.	

Identifier	Requirement	Rationale
REG-01	Ground operations shall adhere to local laws.	
REG-02	The system shall adhere to international laws.	
REG-03	The system shall comply with the UN Treaty on Outer Space [82].	Main legal document regarding space activities.
REG-04	The system shall comply with the COSPAR Planetary Protection Policy ⁴ .	
REG-05	The system shall comply with Inter-Agency Space Debris Coordination	
	Committee regulations.	
REG-06	The habitats shall obey the OSHA and NASA Risk Management and	
	Health Standards [83].	
REG-07	The system shall comply with NASA Human Rating Certification [1].	In order to ensure certified safety levels for human
		flight.

Identifier	Requirement	Rationale
PRF-01	The design shall be entirely based on technologies and materials fully	
	available at the current day.	
PRF-01.1	The system shall only use technology with a NASA technology readiness	
	level of at least 6.	
PRF-01.2	The system shall only use materials with a NASA technology readiness	
	level of at least 6.	
PRF-01.3	The system shall only require production methods with a NASA technol-	
	ogy readiness level of at least 6.	
PRF-02	A crew of at least 10 members shall be present on each travel of the	
	reusable spaceship to Mars.	

⁴https://cosparhq.cnes.fr(Last accessed 08-05-2018)

PRF-03	A crew of at least 10 members shall be present on each travel of the
	reusable spaceship to Earth.
PRF-04	The launcher shall be able to bring a payload to a 400 km circular orbit.
PRF-04.1	The launcher shall have at least 9.3 km/s DeltaV with an EEV payload.
PRF-04.2	The launcher shall have at least 9.3 km/s DeltaV with an MEV payload.
PRF-04.3	The launcher shall have at least 9.3 km/s DeltaV with a fueler payload.

Identifier	Requirement	Rationale
RMS-01	The launcher segment of the programme shall be fully reusable for a	More specific launcher requirements are not listed, due
	minimum of 100 flights.	to the decision to use a launcher service.
$\overline{R}\overline{MS}$ - $\overline{0}1.\overline{1}$	The launcher shall be able to de-orbit.	
RMS-01.1.1	The launcher shall have re-ignitable propulsion.	
RMS-01.1.2	The launcher shall be able to control its attitude.	
RMS-01.2	The launcher shall be able to re-enter Earth atmosphere.	
$\overline{R}\overline{MS}$ - $\overline{0}1.\overline{3}$	The launcher shall be able to land on Earth.	
RMS-02	The EEV shall be reusable for at least 100 Earth launches.	
RMS-03	The MEV shall be reusable for at least 100 Mars launches.	
RMS-03.1	The MEV shall facilitate inspection.	
RMS-03.2	The MEV shall facilitate maintenance.	
RMS-03.3	The MEV shall facilitate refurbishment.	
RMS-04	The fairing shall be reusable for at least 100 flights.	
RMS-05	The manned spaceship used by the programme shall be fully reusable for	
	a minimum of 10 Earth-Mars return trips.	
RMS-06	The system shall only employ non-hazardous materials and propellants.	
RMS-07	The systems shall only employ non-toxic materials and propellants.	

Identifier	Requirement	Rationale
PWR-01	The ITV shall be able to supply a nominal power of at least 156.36 kW.	Based on habitat calculations.
PWR-02	The system shall be able to supply a nominal power of at least 79 kW to	
	the habitat.	
PWR-03	The system shall be able to store at least 55.2 kWh of net suppliable en-	
	ergy.	